



**University of
Reading**

Novel Dendritic Fuel and Lubricant Additives

A thesis submitted in part fulfilment of the degree of
Doctor of Philosophy

Clare Louise Higgins

Department of Chemistry

Supervised By: Professor Wayne Hayes and Dr Sorin Filip

December 2015

Declaration of Original Authorship

I confirm that the research described in this thesis is my own work and that the use of all materials from other sources has been properly and fully acknowledged.

Clare Louise Higgins

Acknowledgements

Firstly I would like to thank my supervisors Professor Wayne Hayes and Dr Sorin Filip for the opportunity to undertake this PhD. I would like to thank Wayne in particular for his support and guidance throughout my University career and for always pushing me to achieve my best. I am grateful for your constant belief in me that I could get through this PhD when I doubted that I could.

I have been privileged to work alongside some very talented chemists in the Hayes Research Group over the years and their support and friendship has been invaluable. I would like to thank everyone who has been part of the team, past and present, for making Lab 204 such an enjoyable place to work. I would also like to thank my friends from the rest of the department who have been there every step of the way. The countless coffees, cakes and ciders were much appreciated!

I would like to thank the staff in the Department of Chemistry, particularly Martin and Nick for running the mass spectrometry samples and Professor Howard Colquhoun for assisting me with the computer modelling. Also thank you to Gez and Phil in the stores for dealing with the daily shopping list of equipment and orders.

I would also like to thank the Analytical department at the BP Technology Centre, Pangbourne for allowing me use the thermal analysis equipment during this project. I truly value the support you have given me over the years and thank you for always welcoming me back with open arms. This really is the end of an era.

I also thank BP and the BBSRC for funding this research.

Finally, I would like to thank my family for their unwavering support in everything I do. Without their constant encouragement and belief in me, I would be far from where I am today. I would like to dedicate this thesis to them because believe me when I say, they have been through the trials and tribulations of this journey just as much as I have!

“Nothing in life is to be feared. It is to be understood.”

Marie Curie

Synopsis

Oxidation processes have a detrimental effect on hydrocarbon based materials such as fuels, lubricants, polymers and foodstuffs. Antioxidants are known to interrupt oxidation processes by predominantly reacting with radical species. The development of such stabilisers is discussed in **Chapter 1**. The use of dendritic architectures in antioxidant development is a relatively 'young' area of research. This unique class of macromolecule consists of a well-defined, branched structure which can potentially bear a high loading of antioxidant under an excellent degree of structural control.

Dendritic architectures are the focus of this thesis and **Chapter 2** discusses the synthesis of a series of antioxidant functionalised polyester dendrons *via* the growth of the AB₂ monomer *bis*(MPA). The intention was to provide a high degree of sterically hindered phenolic end groups for enhanced oxidative stabilisation properties in addition to good solubility within a hydrocarbon matrix and good thermal stability with a resistance to volatilisation at high temperatures. It was revealed that these new branched antioxidants provided superior thermal and oxidative stability properties in comparison to the small molecule antioxidants currently used in the industry.

Alternative functional core monomers were also investigated in **Chapter 3**. The functionalisation of glycerol and triethanolamine (TREN) with antioxidant moieties plus solubilising alkyl chains to yield a series of first generation polyester antioxidants is discussed. Once again, superior thermal and oxidative properties were revealed in comparison to the current industry antioxidants Irganox L135 and Irganox L57.

The incorporation of a diphenylamine derivative into the same branching unit as the hindered phenol was investigated in **Chapter 4** with the aim of targeting synergistic antioxidant properties. Excellent oxidative stabilities were observed, when compared to a 1:1 blend of Irganox L135 and Irganox L57, whereby an impressive 52% increase in oxidation induction time was observed. The enhanced stabilities were attributed to interesting structure-activity relationships from which it was concluded that the close contact of both amine and phenol functionalities was key in accessing improved antioxidant capabilities.

A radical scavenging assay was investigated in **Chapter 5** with the aim to understand structure-activity relationships of new sterically hindered phenolic antioxidants. It was revealed that complex mechanistic pathways, in addition to solvent effects, limited the use of this assay. Therefore, further refinement of this potentially time-saving spectroscopic assay is required in order to render it usable in fuel and lubricant development.

List of Abbreviations

A·	Antioxidant radical
ABTS	2,2'-Azino- <i>bis</i> -3-ethylbenzthiazoline-6-sulfonic acid
ADMET	Acyclic diene metathesis
AIBN	Azobisisobutyronitrile
ARP	Antiradical power
BHA	Butylated hydroxyanisole
BHT	Butylated hydroxytoluene
<i>rac.</i> BINAP	(±)2,2'- <i>Bis</i> (diphenylphosphino)-1,1'-binaphthalene
Bis(MPA)	2,2'- <i>Bis</i> (hydroxymethyl)propionic acid
CDCl ₃	Chloroform (deuterated)
CuAAC	Copper-catalyzed azide-alkyne cycloaddition
d	Doublet
DCC	N, N'-Dicyclohexylcarbodiimide
DCU	N,N'-Dicyclohexylurea
DI	Direct Injection
DMAP	4-(Dimethylamino)pyridine
DMP	2,2-Dimethoxypropane
DMSO-d ₆	Dimethyl sulfoxide (deuterated)
DPE-Phos	Bis[(2-diphenylphosphino)phenyl]ether
DPF	Diesel Particulate Filters
DPPH	1,1-Diphenyl-2-picryl-hydrazyl
DPPHH	1,1-Diphenyl-2-picrylhydrazine
DPTS	4-(Dimethylamino)pyridinium-4-toluenesulfonate
DSC	Differential Scanning Calorimetry
EC ₅₀	Efficient Concentration
ESI	Electron Spray Ionisation
FT-IR	Fourier Transform Infra-red
HAT	Hydrogen Atom Transfer
HBA	Hydrogen bond acceptor
HDPE	High density polyethylene
HOO·	Hydroperoxide radical
LMWPE	Low molecular weight polyethylene
M ⁿ⁺	Transition metal ion
m/z	Mass/charge ratio
NMR	Nuclear Magnetic Resonance
OEM	Original Equipment Manufacturer
OIT	Oxidation Induction Time
OOT	Oxidation Onset Temperature
PAMAM	Poly(amidoamine)
PFI	Port Fuel Injection
PG	Propyl gallate
ppm	Parts per million
q	Quartet
quin	Quintet
R·	Alkyl radical
R _f	Retention Factor

ROMP	Ring opening metathesis polymerization
ROO·	Alkyl peroxy radical
ROOH	Hydroperoxide
s	Singlet
SCR	Selective Catalytic Reduction
sex	Sextet
SPLET	Sequential proton-loss electron-transfer
t	Triplet
TBHQ	<i>Tert</i> -butylhydroquinone
TEC	Thiol-ene coupling
<i>tert</i>	Tertiary
T _g	Glass transition temperature
TGA	Thermogravimetric Analysis
THF	Tetrahydrofuran
TLC	Thin Layer Chromatography
TREN	Triethanolamine
TsOH	<i>p</i> -Toluene sulfonic acid
UV-Vis	Ultraviolet-visible
ZDDP's	Zinc dialkyldithiophosphates

Contents

Chapter 1: Introduction

1.1	Introduction to the Combustion Engine.....	1
1.2	Fuel and Lubricant Composition.....	3
1.2.1	Gasoline.....	3
1.2.2	Diesel.....	3
1.2.3	Biofuels.....	4
1.2.4	Lubricants.....	5
1.3	Degradation Processes.....	5
1.3.1	Mechanism of Oxidation.....	6
1.3.1.1	Initiation.....	6
1.3.1.2	Propagation.....	7
1.3.1.3	Chain Branching.....	8
1.3.1.4	Termination.....	8
1.4	Antioxidants.....	9
1.5	Dendritic Macromolecules	22
1.6	Conclusion.....	30
1.7	Aims of Research.....	30
1.8	References.....	32

Chapter 2: Synthesis and Analysis of a Series of Novel Dendritic Phenolic Antioxidants

2.1	Introduction.....	39
2.2	Results and Discussion.....	41
2.2.1	Synthesis and Characterisation.....	42
2.2.2	Thermal Stability Studies.....	53
2.2.3	Oxidative Stability Studies.....	55
2.3	Conclusions and Future Work.....	60
2.4	Experimental.....	60
2.4.1	Purification and Characterisation.....	61
2.4.2	Thermal and Oxidative Analysis	61
2.4.3	Synthetic Methods.....	62
2.5	References.....	67

Chapter 3: Investigating a Series of Alternative Core Monomers for Dendritic Antioxidants

3.1	Introduction.....	70
3.2	Results and Discussion.....	72
3.2.1	Glycerol.....	72
3.2.2	Nitrogen Centered Core Monomers.....	79

3.3	Conclusions.....	86
3.4	Experimental.....	86
3.5	References	92

Chapter 4: Investigating the Synergy Between Diphenylamine Derivatives and Hindered Phenolic Antioxidants

4.1	Introduction.....	95
4.2	Results and Discussion.....	98
4.2.1	Synthesis, Characterisation and Testing –Series 1.....	98
4.2.2	Synthesis, Characterisation and Testing –Series 2.....	109
4.2.3	Synthesis, Characterisation and Testing –Series 3.....	117
4.3	Conclusions.....	123
4.4	Experimental.....	123
4.5	References.....	141

Chapter 5: From Food to Petroleum Analysis: The Development of a Screening Assay for New Antioxidants Using the Stable Radical DPPH

5.1	Introduction.....	143
5.2	Results and Discussion.....	147
5.2.1	Radical Scavenging Analysis Using Alcoholic Solvents.....	148
5.2.2	Radical Scavenging Analysis Using Hydrocarbon Reaction Mediums.....	153
5.2.3	Efficient Concentration Analysis.....	158
5.3	Conclusions.....	166
5.4	Experimental.....	167
5.5	References.....	170

Chapter 6: Conclusions and Future Perspectives

6.1	Conclusions.....	174
6.2	Future Perspectives	177
6.3	References.....	181

Chapter 1

Introduction

Abstract

This chapter outlines the detrimental effects of oxidation processes on hydrocarbon based materials with particular focus on fuels, lubricants and polymers. Antioxidants, such as sterically hindered phenol and diphenylamine derivatives, are known to interrupt oxidation processes by predominantly reacting with radical species. The development of such stabilisers is discussed with a focus on improving the structural characteristics to prevent additive migration within the bulk material. Volatilisation is a type of migration process and is a significant problem encountered with fuel and lubricant additive chemistry as a result of the high temperatures experienced within an engine. Antioxidant immobilisation, through various polymerisation techniques, is reported in the literature and provides a route to introducing higher molecular weights and enhanced thermal stabilities. An alternative approach to immobilisation is the use of dendritic architectures. This unique class of macromolecule consist of a well-defined, branched structure which can potentially bear a high loading of antioxidants under an excellent degree of structural control.

1.1 Introduction to the Combustion Engine

In the late 19th century, the rise of the oil industry prompted an interest in developing an internal combustion engine with the hope of providing more power to automotive vehicles and machinery. It was realised that chemical energy within a fuel can be accessed *via* combustion to provide mechanical power.^[1] Many inventors proposed an array of possible designs, however, the first internal combustion engine using liquid fuel, to be built and sold, was claimed by Nikolaus Otto.^[1] Further developments to this engine design were most notably from Dugald Clerk, James Robson and Karl Benz, in the late 1880s, who all developed two-stroke combustion engines. In the early 1890s Rudolf Diesel described a new form of engine based around the direct injection of the fuel into the cylinder.^[1] Based on these designs, automotive engines are now generally divided into either spark-ignition for gasoline or compression ignition for diesel. Since these first internal combustion engines were introduced, the technology behind the automotive industry has changed dramatically and was controlled predominantly by customer

demand for more speed and power. Today, in terms of consumer preference, not much has changed; there is still an inclination for increased power and performance but more important, in the light of decreasing petroleum stocks and environmental concerns, is greater efficiency, extended engine life and lower emissions.^[2]

The majority of modern motor vehicles rely on a four-stroke combustion engine typically consisting of a piston within a cylinder equipped with two or four valves, one or two for the controlled delivery of the air to the cylinder and the others to permit the exhaust fumes to be expelled after combustion.^[3] The fuel is delivered directly into the combustion chamber by injectors, which operate as fast acting valves (direct injection, DI, engines), or, in the slightly older port fuel injection (PFI) technology, the fuel is delivered through inlet valves. To highlight the inner workings of a typical cylinder a schematic representation of a typical compression engine cylinder found in an automobile is shown in **Figure 1.1**.

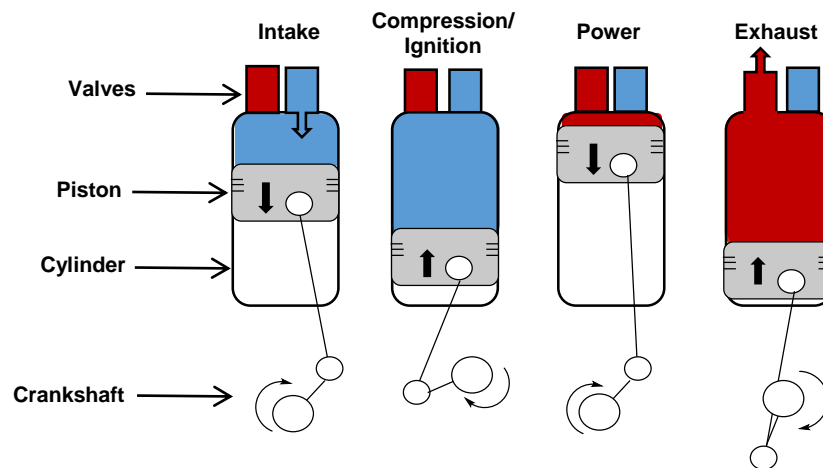


Figure 1.1 Schematic representation of a cylinder combustion cycle which consists of four stages: intake, compression/ignition, power and exhaust.

This basic four stroke principle of intake, compression/ignition, combustion and exhaust is a fundamental process of any automobile. In the PFI engines, the basic process begins with the fuel being drawn into the cylinder through the intake valve. The intake and exhaust valves close and the piston assembly compresses the fuel. In a gasoline engine a spark plug is used to ignite the fuel whereas in a diesel engine the fuel autoignites and causes an increase in pressure within the cylinder. The pressure drives the piston downwards and gives power to the vehicle. As the piston moves upwards, the exhaust valve opens and the cycle begins again.^[3] Engines are assembled from many different components, all playing an important role while subjected to harsh conditions such as

temperature, pressure and mechanical forces. Engine volumetric capacities have actually decreased over the years but the power output has actually increased. Consequently, this has put huge pressure on the components in the engine and hence with the endless developments of new engine technologies, the chemistry of fuels and lubricants also needs to remain in line.

1.2 Fuel and Lubricant Composition

Fuels and lubricants are derived from crude oil and are complex mixtures of hydrocarbon compounds, the ratios of which can be altered to tailor specific characteristics such as volatility and viscosity.

1.2.1 Gasoline

The spark ignition engine has remained a popular choice for personal automotive transport for many years and the fuel designed for this engine is gasoline. Gasoline is a careful formulation of hydrocarbons and additives which is now, more than ever, strongly controlled by emission regulations. A typical formulation consists of 30-60% saturated hydrocarbons with chain lengths in the region of C₄-C₁₂.^[4] These hydrocarbons are given an octane rating between 0 and 100 which indicates the degree of compression it can withstand before igniting. The standards used to assign these ratings are heptane and 2,2,4-trimethylpentane (iso-octane) which have octane ratings of 0 and 100, respectively, whereby the higher the rating, the higher the compression capability and resistance to autoignition. Aromatic compounds are another major component, they have high octane values and are typically used at 25-35%, however, toxic compounds such as benzene have caused significant limitations on their use.^[4] Alkenes, in particular olefins, are used at 10-15% and are typically clean burning. Other unsaturated hydrocarbons found in gasoline formulations include dienes, alkynes and polycyclic aromatics, however, these compounds are often only used in trace amounts.^[4] Performance enhancing additives are also incorporated into the formulation to improve a property of the fuel or the performance of the engine. They are used at low levels, typically <2500 ppm and include antioxidants, metal deactivators, ferrous and copper corrosion inhibitors, anti-wear additives and deposit control additives.

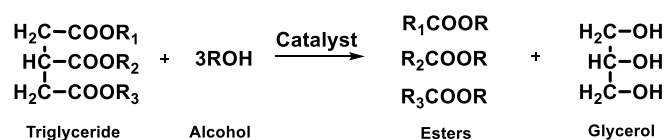
1.2.2 Diesel

In contrast to gasoline, which is spark-ignited, diesel fuel is ignited by the heat of compression within the engine. This difference in the ignition process reveals some

significant variances in their chemical composition and physical properties. Diesel consists of many aliphatic hydrocarbons containing carbon chain lengths of C₈-C₁₂ with boiling points in the range of 130-370 °C.^[5] Compared to gasoline, the fractions of hydrocarbons are typically heavier in a diesel formulation. The ignition quality of diesel is determined by the cetane number and the standards used to assign this rating are hexadecane and 2,2,4,4,6,8,8-heptamethylnonane which have cetane numbers of 100 and 15, respectively.^[6] Long chain, unbranched, saturated hydrocarbons have high cetane numbers with a good ignition quality whereas branched hydrocarbons and aromatics have low cetane numbers with a poor autoignition quality.^[6] Combustion emissions from diesel engines lacking after treatment systems such as diesel particulate filters (DPF) and selective catalytic reduction (SCR), are considered one of the major sources of air pollution and can cause health problems. Such emissions include particulate matter, nitrogen oxides, carbon monoxide and unburnt hydrocarbons which can cause acid rain, photochemical smog and ozone depletion.^[5] Hence, the search for alternative, more environmentally friendly fuels is required.

1.2.3 Biofuels

The uncertainties surrounding petroleum availability and concerns of harmful environmental pollution have encouraged researchers to investigate alternative fuels. There are two global, biorenewable fuels that have the potential to replace gasoline and diesel fuel. The term 'biofuel' refers to solid, liquid or gaseous fuels that are predominantly produced from biomass and they offer a number of advantages including sustainability, reduction of greenhouse gas emissions, agriculture and security of supply.^[7,8] Bioethanol is one such fuel and is produced almost entirely from food crops. Biodiesel is another alternative and besides being a renewable resource it has a number of other distinct advantages. These include biodegradability, low toxicity and reduced exhaust emissions.^[9] Biodiesel is derived from the transesterification of vegetable or animal oils and is composed of saturated and unsaturated long-chain esters (**Scheme 1.1**).



Scheme 1.1 Transesterification reaction for producing biodiesel from a vegetable or animal derived triglyceride.

The use of vegetable oils in diesel engines is nearly as old as the diesel engine itself whereby the inventor of the diesel engine, Rudolf Diesel, reportedly used peanut oil as a fuel for demonstration purposes.^[6] Other common sources of biodiesel include soybean oil, sunflower oil, corn oil, rapeseed oil and castor oil.^[9] Unfortunately, biodiesel also has some undesirable characteristics which include oxidative instability and poor low temperature properties.^[10,11] These performance characteristics highlight the need for more advanced additives to enhance the stabilisation of these new alternative fuels.

1.2.4 Lubricants

Lubricating oil is also derived from crude oil, however, it is less volatile and more viscous than gasoline or diesel. Lubricants are introduced into the engine to predominantly prevent friction and wear between surfaces and are typically comprised of 80% base oil and 20% performance additives. Base oils can be classified as natural or synthetic and are rated depending on the ratio of saturates, aromatics and sulfur content. The typical environments under which a lubricant performs can vary dramatically, however extreme conditions, including oxidative stress, chemical contamination, high temperatures and mechanical shear pressures, are usually common place. With the development of more powerful engines^[3], automotive lubricants are subjected to even more extreme environments than ever before and can suffer from degradation. An understanding of such degradation processes is thus fundamental and the chemistry underpinning the performance of enhancing additives requires continuous development.

1.3 Degradation Processes

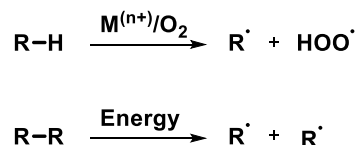
The earliest documented examples of the deterioration of modern hydrocarbon materials followed the discovery of rubber by European explorers in the Amazonian forests. On the voyage back to Europe its rebounding behaviour that made it so interesting was lost and it was believed it had perished during the journey.^[12] This deterioration is nowadays referred to as 'ageing' or 'fatigue' and has a significant impact on the properties of the material. Petroleum based products, such as those described previously, in addition to other industrial products such as plastics, cooking oil, cosmetics and processed foods are subjected to degradation resulting from mechanical, oxidative, heat and light stress.^[13] Oxidative degradation is the dominant degradation process and understanding the mechanisms behind the process is essential for the development of effective stabilisation.

1.3.1 Mechanism of Oxidation

The self-accelerating oxidation of hydrocarbons was the subject of significant research in the early 20th century where various proposals were suggested on the mechanism and products associated with the degradation process.^[14–16] Booser and Fenske investigated the oxidation characteristics of a series of hydrocarbons, including 1-methylnaphthalene, hexadecane and phenanthrene, in an effort to understand the mechanisms of the deterioration of lubricating oil.^[17] It was not until a few years later that Bolland and Gee, from the Natural Rubber Producers Research Association, experimentally established the chain mechanism of this process using ethyl linoleate. The fundamentals outlined in this series of papers have not been revised significantly since their proposal in the 1940s.^[18,19] The self-accelerating oxidation of hydrocarbon based materials is more commonly termed ‘autoxidation’ and can be defined as the reaction of organic substances with molecular oxygen under mild conditions.^[20,21] Originally, the autoxidation mechanism was only proposed for polymers that contained an activated allylic C-H bond, such as those found in rubbers, however, it has since been universally adapted to explain the oxidative degradation of most hydrocarbon materials. The general autoxidation mechanism consists of a four-step, free-radical chain reaction consisting of initiation, propagation, chain-branching and termination.

1.3.1.1 Initiation

Initiation begins with the generation of a free-radical species *via* a number of possible pathways. An initial consideration was the simple cleavage of the hydrocarbon to form two radicals, a process which can be initiated through heat, light or mechanical shear stress. The activation energy of this process, however, is large and so was unlikely to be the main source of free-radicals, even in a high temperature engine. Alternatively, hydrocarbon bonds can cleave through the reaction with oxygen to produce alkyl radicals (R \cdot) (**Scheme 1.2**).^[21,22] This process is typically catalysed by traces of transition metal ions (Mⁿ⁺) such as cobalt, iron, vanadium, chromium, copper and manganese.^[20,22–25] Traces of these transition metals can originate from polymer synthesis or are often found in the components of engine parts.

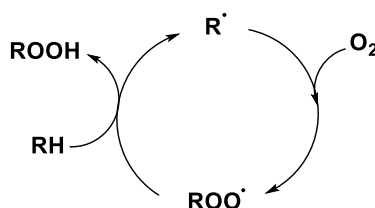


Scheme 1.2 Initiation of autoxidation through the generation of alkyl radicals (R[·]).

The site of oxygen attack is determined by the strength of the C-H bond. The ease of the homolytic cleavage of alkyl hydrogens follows the order of phenyl, primary, secondary, tertiary, allylic and benzylic.^[22,24] Under ambient temperatures the rate of initiation is very slow with a rate constant of between 10⁻⁹–10⁻¹⁰ mol⁻¹s⁻¹.^[22] At elevated temperatures, the selectivity of the process is reduced and the reaction rate increases.

1.3.1.2 Propagation

Propagation is where the radical species, generated from the initiation stage, stabilise themselves by reacting with another species. Propagation occurs through the irreversible reaction of the alkyl radical (R[·]), formed during initiation, with oxygen to form an alkyl peroxy radical (ROO[·]) (**Scheme 1.3**). In comparison to the initiation stage, this reaction is fast and has a very high rate constant of 10⁷–10⁹ mol⁻¹s⁻¹.^[26] Bell and co-workers investigated the reactions of alkyl radicals associated with the low temperature oxidation of paraffins and revealed the activation energy of the combination of an alkyl radical with oxygen to be very low at *ca.* 4–8 kJmol⁻¹.^[27] The rate of reaction of the carbon-centred radicals depends on the carbon substituents and the stabilisation of the peroxy radical (ROO[·]) dictates that tertiary alkyl radicals react faster with oxygen than primary alkyl radicals. The newly formed peroxy radical (ROO[·]) can then abstract a hydrogen atom from another hydrocarbon molecule to form a hydroperoxide (ROOH) and a new alkyl radical (R[·]). This process therefore generates a continuous propagation chain (**Scheme 1.3**) reaction causing the oxidation of many hydrocarbon molecules.

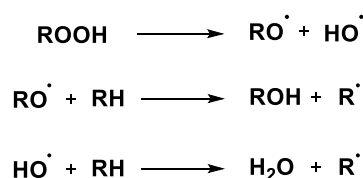


Scheme 1.3 Continuous generation of alkyl radicals (R[·]) to form a propagation chain.

The oxidation process can hence be self-accelerating if the diffusion of oxygen within the material is a non-limiting factor.^[28]

1.3.1.3 Chain Branching

Chain branching is a significant stage in the oxidation process as it is here where the physical characteristics of the bulk matrix (i.e. an engine lubricating oil, a hydrocarbon fuel, a polymer or a foodstuff) begin to change. This process begins with the cleavage of a hydroperoxide into an alkoxy radical. This reaction has a high activation energy and hence only occurs at increased temperatures. It has been reported that as the temperature increases above 100 °C the hydroperoxide concentration decreases.^[29] The resulting radicals can undergo a series of chemical reactions as outlined in **Scheme 1.4**.

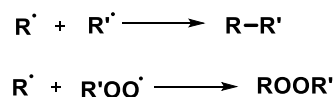


Scheme 1.4 Decomposition of hydroperoxides (ROOH) to generate further primary oxidation products in the form of alkyl radicals (R[·]) in addition to secondary oxidation products including alcohols, aldehydes, ketones and water.

Hydroxy and alkoxy radicals are so reactive that they abstract hydrogen atoms in a non-selective manner therefore forming further initiator alkyl radicals. The decomposition of hydroperoxides has been reported over many years whereby the major degradation products are lower molecular weight aldehydes and ketones, however, the generation of alcohols and water has also been observed.^[28-34] These compounds can contribute to a change in the properties of the material. For example a hydrocarbon based lubricant may experience, at this stage, an increase in volatility and an increase in polarity.^[35]

1.3.1.4 Termination

The oxidation process eventually slows to a standstill before the hydrocarbon is completely consumed and this final stage is referred to as termination. This is where two radical species combine (**Scheme 1.5**) to produce various compounds such as alcohols, acids, aldehydes, ketones, carboxylic acids and longer chain hydrocarbons.



Scheme 1.5 Examples of possible radical termination reactions.

Over time, at high temperatures, the viscosity of the oil increases. This is thought to be a result of the reactive species formed in the oxidation process reacting further to form a complex mixture of oligomers and polymers. Once the viscosity of the oil has increased to the point where diffusion of oxygen is limited, termination reactions dominate.

In terms of lubricant chemistry, the oxidation process is particularly detrimental. Oligomers which are still fully soluble in the oil cause an increase in viscosity. When these species continue to react, through polycondensation reactions, their molecular weights increase and solubility limits are reached. This causes immiscibility between the oligomers and the lubricant which leads to the formation of 'sludge'.^[36] Volatile components of the oil, either produced during oxidation or from the base oil itself, are readily lost through evaporation when the temperatures of the engine increase. This also results in a viscosity increase and the volume of the lubricant is reduced. In addition to the formation of sludge, the metal surfaces of the engine components can be found to be coated with lacquers or deposits. These varnish-like deposits have been found to consist of carbon and complex carbonised organic components and can cause an accumulation and aggregation of wear debris, soot and acids.^[36] These deposits not only reveal the failure of the material but can also block and inhibit key components in the engine leading to reduced power, increased fuel usage and at time failure of the engine. There are a series of preventative measures which can be introduced to the material to reduce the effects of the oxidation process. The most effective preventative measures include the trapping of catalytic impurities through the use of 'metal deactivators' or by the destruction of alkyl and alkyl peroxy radicals and hydroperoxides through the use of 'antioxidants'.

1.4 Antioxidants

Antioxidants are important additives whose role it is to preserve the chemical and physical properties of many different organic materials during transportation, storage, processing and service conditions.^[37] Antioxidants can be divided into a number of groups, however two types have proved to be particularly effective and are termed primary or secondary antioxidants.^[35,38] Primary antioxidants, also referred to as 'radical

scavengers', function by intercepting and stabilising free radicals such as alkyl peroxy radicals (ROO^\cdot) hence interrupting the propagation chain. These specialised compounds are typically reductive in nature with relatively weak O-H and N-H bonds and sterically hindered phenols and aromatic amines represent this class of antioxidant.^[39] A large number of primary antioxidants have been developed and tested in a range of substrates. Key examples of phenolic antioxidants are presented in **Figure 1.2** that are typically used in polymers, fuels or lubricants.

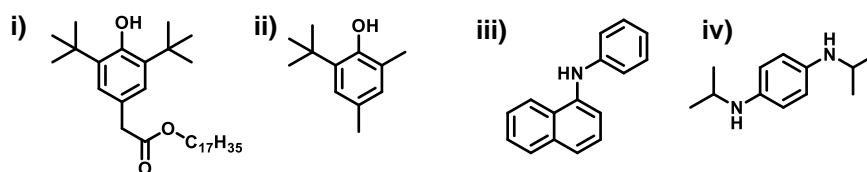
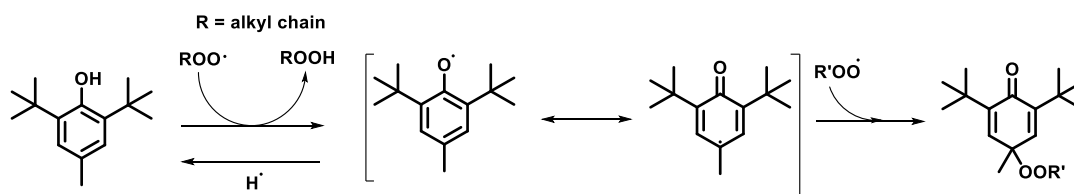


Figure 1.2 Examples of some common primary antioxidants used to stabilise fuels, lubricants and polymers: **i)** Irganox L135, **ii)** 2,4-dimethyl-6-*tert*-butylphenol, **iii)** phenyl- α -naphthylamine, **iv)** Ethanox 4702.

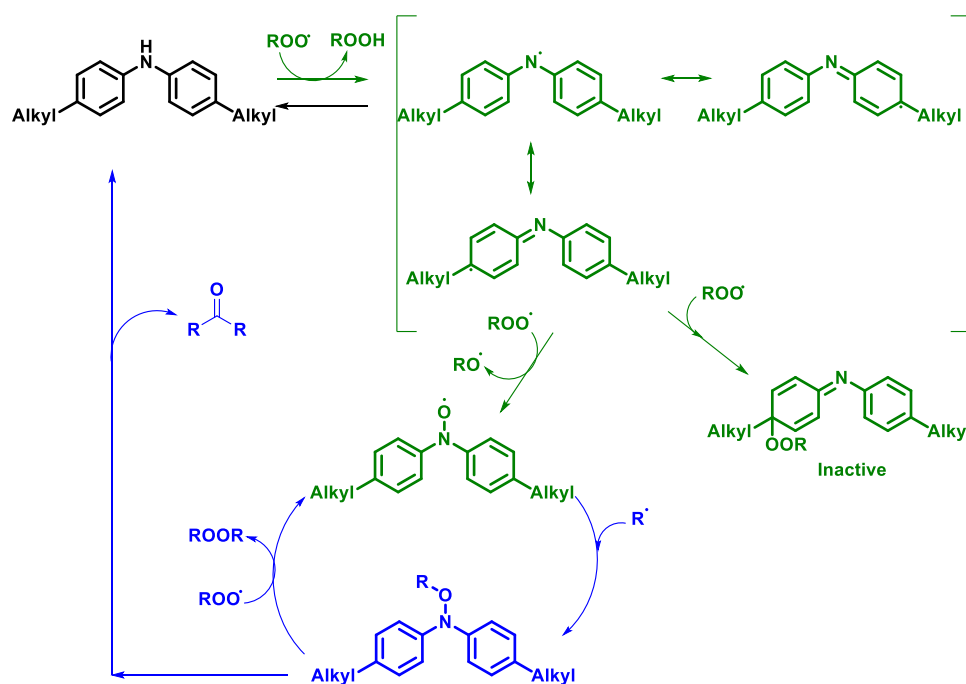
The effectiveness of this class of antioxidant was revealed early on and hydroquinones and phenols were reported as intercepting alkyl peroxy radicals to give a much more stable radical hence leading to a termination of the chain mechanism.^[40–42] As previously discussed, the reaction of alkyl radicals with oxygen is very fast and subsequent abstraction of hydrogen from the substrate by an alkyl peroxy radical is the rate determining step. Alkyl peroxy radicals are typically present at high concentrations in the oxidising system hence the main requirement of a primary antioxidant is to neutralise these species. It is known that the efficiency of this type of antioxidant depends in their rate of reaction with alkyl peroxy radicals (ROO^\cdot) and the reactivity of the generated antioxidant radical (A^\cdot).^[43–45] The antioxidant radical is stabilised through steric hindrance and resonance structures (**Scheme 1.6**).



Scheme 1.6 The radical scavenging mechanism of a sterically hindered phenol.

The steric hindrance is provided by the two *tert*-butyl moieties in the *ortho* position and prevent the phenoxyl radical from attacking other hydrocarbons. The resonance structure can further combine with a second alkyl peroxy radical to form the alkyl peroxide which

is stable at temperatures $<120\text{ }^{\circ}\text{C}$.^[22,35] Typically one phenolic antioxidant can eliminate two radical species; this ratio is referred to as the stoichiometric value. In contrast to phenolic antioxidants, aromatic amines operate *via* a much more complex radical scavenging mechanism. The reaction of diphenyl amines is dependent on the temperature whereby at relatively low temperatures of $<120\text{ }^{\circ}\text{C}$ the interaction with peroxy radicals is the dominant reaction and a similar hydrogen abstraction pathway to sterically hindered phenols is followed.^[35] This initial process is highlighted in green in **Scheme 1.7** and in the temperature region described, one diphenylamine can eliminate four peroxy radicals. At temperatures $>120\text{ }^{\circ}\text{C}$, a catalytic cycle has been proposed which gives access to an enhanced stabilisation mechanism. This secondary process is highlighted in blue in **Scheme 1.7**.



Scheme 1.7 Proposed radical scavenging mechanism of aromatic amine antioxidants.^[22,35]

The nitroxyl radical can react with a secondary alkyl radical and subsequent thermal decomposition regenerates the original diphenylamine.^[46] This gives rise to high stoichiometric values, examples of which are shown in **Table 1.1**.

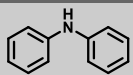
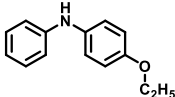
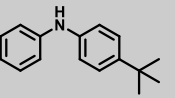
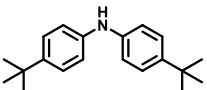
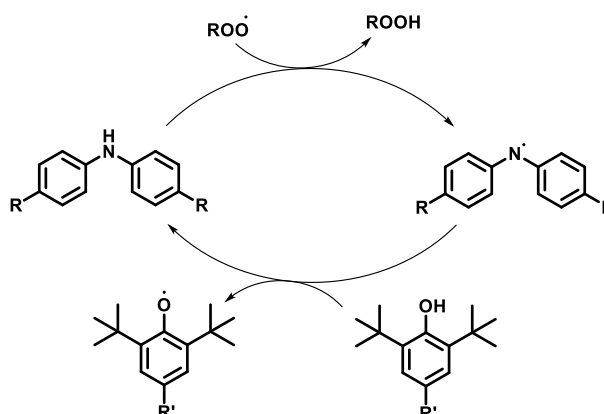
Structure	Stoichiometric Value
	41
	36
	53
	52

Table 1.1 Stoichiometric values for a range of diphenylamine derivatives, analysed in a paraffin oil at 130 °C.^[47]

A further stoichiometric enhancement is observed when two or more antioxidant species are present at the same time. This phenomena is referred to as synergism and three types were defined^[48] by Scott - *homosynergism*, *heterosynergism* and *autosynergism*. A process can only be classified as true synergism if the combined use of two or more antioxidants provides a greater stabilisation than the individual antioxidants. Homosynergism is the most commonly exploited type, especially in the fuels and lubricants industry, and is experienced when two antioxidants acting by the same mechanism interact. A common example is the combination of a hindered phenol and a diphenylamine, and it has been reported that this synergism works so well as a result of a regeneration cycle depicted in **Scheme 1.8**.^[35,38]



Scheme 1.8 Mechanism of regeneration between a diphenylamine and a sterically hindered phenol.

Secondary antioxidants are another class of important antioxidants. Their function is to prevent the formation of free radicals by decomposing unstable hydroperoxides before

their homolytic cleavage, into non-radical, less reactive alcohols. Organosulfur, organophosphorous or a combination of both, such as zinc dialkyldithiophosphates (ZDDPs), are well-known secondary antioxidants (**Figure 1.3**). Recent developments in additive chemistry, however, has revealed a shift away from secondary antioxidants in an attempt to reduce sulfur, phosphorous and ash emissions. The presence of phosphorous in fuels and lubricants is a particular problem because it is a known catalyst poison and hence severely affects the performance of exhaust after treatment systems.

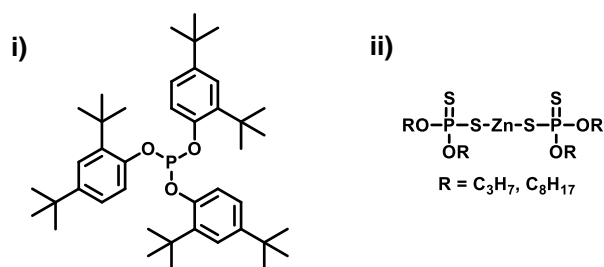


Figure 1.3 Examples of some typical secondary antioxidants: **i)** tris(2,4-di-*tert*-butylphenyl) phosphite (Irgafos 168), **ii)** zinc dialkyldithiophosphates.^[13]

Significant research effort has been targeted at understanding and improving the antioxidant capabilities of primary antioxidants. Sterically hindered phenols have been a popular topic of research in comparison to aromatic amines possibly as a result of their more simplistic radical scavenging mechanism. The majority of the commercially available sterically hindered phenols are based on different derivatives of BHT-like functionalities possessing a variety of substituents. Even though these antioxidants revealed sufficient stabilisation during their early applications, instability and volatility issues at high temperatures have led the additive industry to examine natural antioxidants as an alternative. An example of this progression has been observed in the stabilisation of biodiesel. As discussed, biodiesel is derived from fats and oils and is particularly susceptible to oxidative degradation in comparison to a traditional fuel or lubricant. A number of studies have investigated the biodiesel stabilisation effects of both synthetic and natural antioxidants.^[10,49-52] Santos and co-workers reported a comparison of the thermal stabilities of a series of common synthetic antioxidants and known natural antioxidants (**Figure 1.4**).^[51]

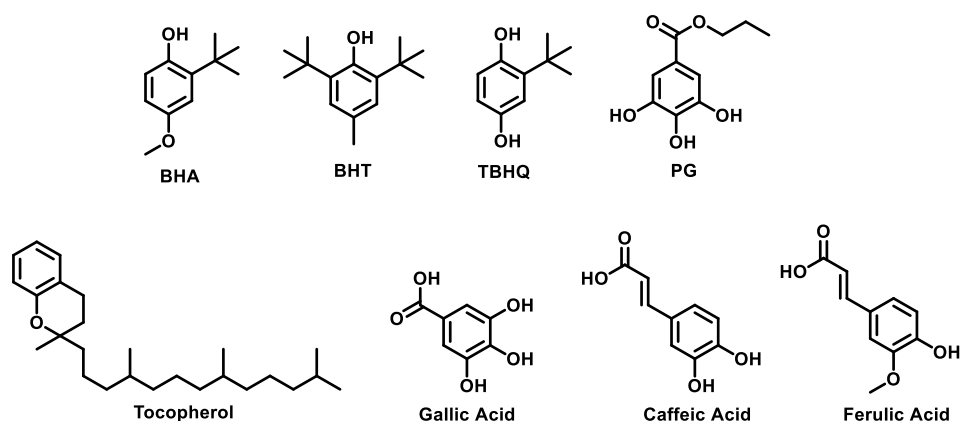


Figure 1.4 A series of synthetic antioxidants, butylated hydroxyanisole (BHA), butylated hydroxyl toluene (BHT), *tert*-butylhydroquinone (TBHQ) and propyl gallate (PG) for comparison against a series of naturally occurring antioxidants, tocopherol, gallic acid, caffeic acid and ferulic acid.

Each antioxidant was subjected to thermogravimetric analysis and results for the synthetic antioxidants revealed initial decomposition temperatures to be less than 110 °C. The low thermal stability of these synthetic antioxidants highlighted the implications of using them for high temperature applications within an engine. In comparison, a significant increase in thermal stability was revealed for the naturally occurring antioxidants with the tocopherol exhibiting the best stability with an initial degradation temperature of 200 °C. Interestingly, an earlier study by Dunn analysed the oxidative stability properties of a similar range of antioxidants in a biodiesel blend.^[10] Oxidation onset temperature analysis and phase separation studies revealed that even though the natural antioxidant, tocopherol, showed a good physical compatibility with the biodiesel it actually provided the least oxidative stability in comparison to BHT and BHA. These two studies highlight the importance of being able to tailor antioxidants to suit the individual and diverse array of applications requiring stabilisation.

Particular effort has been focussed on developing the optimal balance of properties including solubility, volatility, extractability, toxicity and production cost. As discussed, natural antioxidants have shown potential as more thermally stable antioxidants, however very little is known about their structure-activity relationships. The natural hindered phenol, α -tocopherol, is the major active component in Vitamin E (**Figure 1.5**). It has been revealed that this natural phenol can provide a much higher oxidative stability to polyolefins than other commercially available synthetic antioxidants and Burton and Ingold reported that the reactivity of α -tocopherol towards alkyl peroxy radicals in styrene at 30 °C was nearly 250 times greater than BHT.^[53]

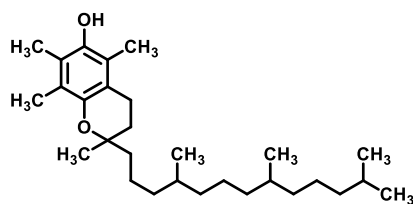


Figure 1.5 Structure of α -tocopherol, the active component in Vitamin E.

Ingold previously alluded to the effects of ring substituents on the rate of reaction between hindered phenols and peroxy radicals.^[54] In this study, they reported that the reaction was accelerated by a *para* oxygen and by the presence of methyl groups instead of *tert*-butyl groups in the 2- and 6- positions. Penketh also agreed with this finding and reported that BHA had an average antioxidant rating of 205 in petroleum when compared to the reference compound BHT which had a rating of 70.^[55]

Many of the reported correlations between the structure and activity of α -tocopherol were carried out at ambient temperatures. It has, however, been reported that the optimal structure of an antioxidant varies according to the conditions it will be subjected to. For example, more hindered phenols are reportedly better than the less hindered derivatives for the long term stabilisation of polyolefins. A more recent investigation took this proposal into account and was carried out by Breese and co-workers.^[56] The key structural characteristics of α -tocopherol were investigated by analysing a series of model compounds each possessing the three structural characteristics - an aliphatic tail, *ortho* substituents and a *para* oxygen (**Figure 1.6**).

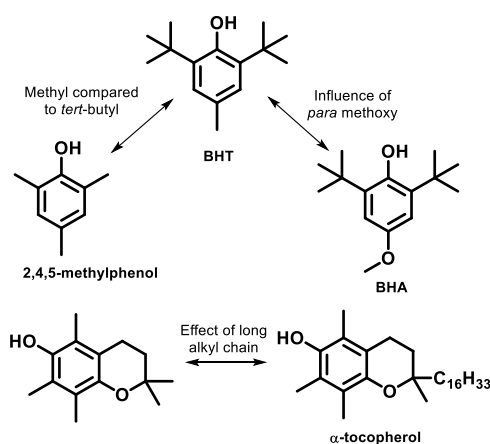


Figure 1.6 Chemical structures of the model compounds investigated by Breese and co-workers.^[56]

Studies investigating antioxidant efficiency typically blend antioxidants into polymer samples. Breese and co-workers, however, used the liquid hydrocarbon squalane as a

model for polypropylene which allowed faster and cheaper sample preparation. In this report they dissolved the antioxidant samples in squalane and analysed the oxidation induction time (OIT) of the sample at 190 °C, using differential scanning calorimetry (DSC). By studying a series of model compounds it was revealed that the key structural difference between α -tocopherol and BHT was the oxygen atom *para* to the active hindered hydroxyl. A 94% increase in antioxidant activity was observed for BHA with the *para* oxygen in comparison to the analogous compound BHT which had no *para* oxygen. It was noted, however, that the radical scavenging stoichiometric value of the hindered phenol may be reduced in this structural configuration, hence as an alternative it was proposed that an oxygen in the *ortho* position would provide the same efficiency as the *ortho* and *para* positions are electronically equivalent. Unfortunately, the effect of methyl *versus tert*-butyl substitution was not evaluated as the model compound 2,4,5-methyl phenol proved to be too volatile under the OIT conditions used. A number of other studies have reported the effect of substituents on the antioxidant activity of phenolic antioxidants, most notably a series of publications presented by Kajiyama and Ohkatsu.^[57-60] A wide range of phenolic derivatives were described and the effect of *ortho*, *meta* and *para* substituents on antioxidant activity was investigated. Antioxidant activity was, however, analysed using an oxygen absorbance method whereby styrene was autoxidised using an azobisisobutyronitrile (AIBN) initiator. Consequently this study did not address the issue of understanding antioxidant performance under extreme high temperature conditions.

Although the synthetic and natural antioxidants discussed provide protection against the damaging effects of energetic free radicals formed within the oxidation process, they suffer from some serious drawbacks. Migration is a term that describes a range of physical processes and interactions involving the materials surroundings and its constituents which include the rate of additive diffusion, additive solubility and volatilisation.^[61] These limitations are predominantly attributed to the antioxidants molecular size hence various approaches have been used to access higher molecular weight antioxidants. Attention was therefore drawn towards macromolecular structures and the manufacturers of plastics, where migration is a significant problem, have effectively abandoned the use of BHT in favour of less volatile antioxidants such as Irganox 1010.^[13] This macromolecular antioxidant not only had a higher molecular

weight but also provided a greater number of antioxidant functionalities per molecule (**Figure 1.7**).

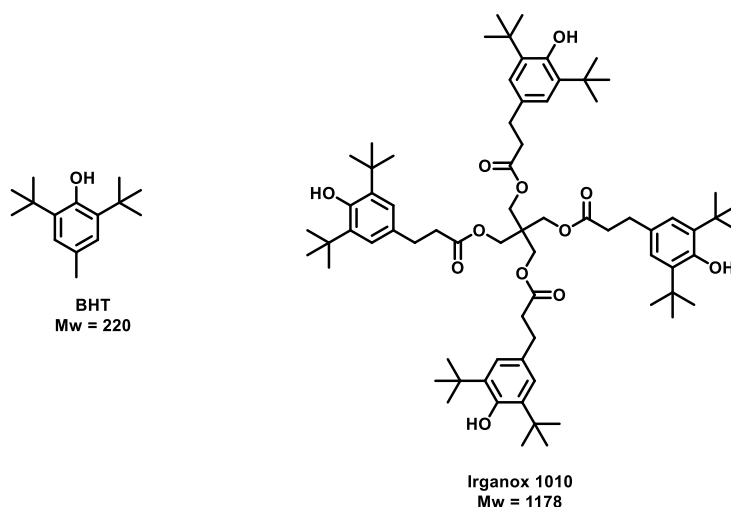


Figure 1.7 The structure of BHT compared to Irganox 1010.

Even though these higher molecular weight antioxidants provided some alleviation of the limitations previously experienced, to access applications in ever more extreme environments, for example in an engine where components are subjected to high temperatures, pressures and mechanical shear, more advanced systems are required. It has been reported that even high molecular weight antioxidants, such as Irganox 1010, leach and migrate from a polymer matrix under such conditions leading to a reduction in oxidative stability and premature aging.^[62-64] Antioxidant immobilisation therefore represents one route to enhanced long-term stability by attempting to reduce antioxidant mobility.^[13,61] A number of different approaches to this have been reported and have revealed improved migration resistance, thermal stability and processability, one example of which is the covalent bonding of the antioxidant to the polymer matrix itself.

Munteanu and Csunderlik reported the synthesis of three monomeric antioxidants bearing the same antioxidant moiety but different polymerisable groups (**Figure 1.8**).^[65]

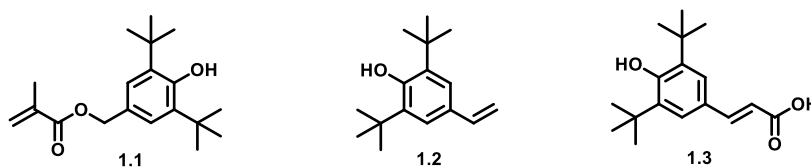
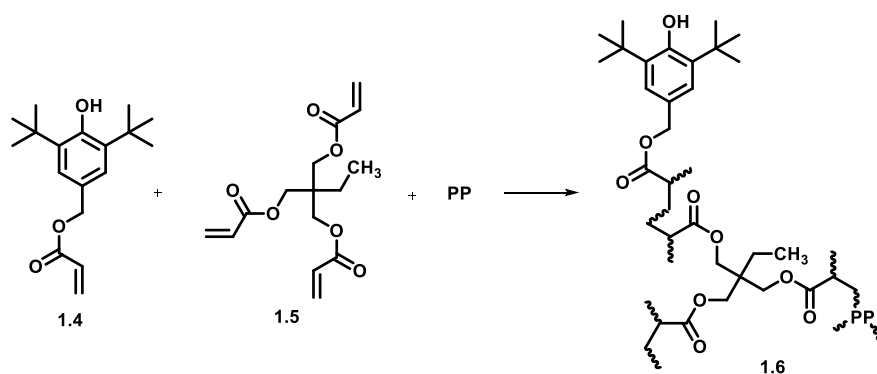


Figure 1.8 Monomeric antioxidants bearing methacrylate (**1.1**), styrene (**1.2**) and cinnamic acid (**1.3**) polymerisable groups.

Each antioxidant monomer was grafted on to low molecular weight polyethylene (LMWPE) and high density polyethylene (HDPE). Since antioxidants function as free radical scavengers it was proposed, in early literature, that they would prevent free-radical-initiated polymerisations.^[66] With this in mind various attempts to protect the phenolic hydroxyl were reported, however, it was revealed this was unnecessary.^[66] Munteanu and Csunderlik reported that their grafting reactions yielded a mixture of grafted polyethylene, unreacted monomeric antioxidant and the antioxidant homopolymer. Although this approach was not able to ensure 100% antioxidant binding to the polyethylene, antioxidant action was, however, preserved revealing greater polyethylene stabilisation over time in accelerating aging analysis.

An improved approach to antioxidant grafting was reported by Al-Malaika and Suharty whereby acrylic functionalised phenolic antioxidants were grafted onto polypropylene using a trifunctional co-agent, trimethylol propane triacrylate (**Scheme 1.9**).^[67]



Scheme 1.9 Grafting of acrylic functionalised phenolic antioxidant with the coagent trimethylol propane triacrylate and polypropylene as reported by Al-Malaika and Suharty.^[67]

In the presence of trimethylol propane triacrylate (**1.5**), the competing grafting reactions, such as antioxidant homopolymerisation, were dramatically reduced to less than 10% which equated to over 90% of antioxidant grafting efficiency. Crucially, no adverse modifications to the physical characteristics (molar mass and solubility) of the polymer were reported, however, no mechanical data was examined. Alternative polymerisable functionalities have also been reported by Kim and co-workers who revealed the synthesis of polymeric hindered phenol antioxidants containing maleimide functionalities. This series of monomers were successfully grafted onto LMWPE (**Figure 1.9**).^[68]

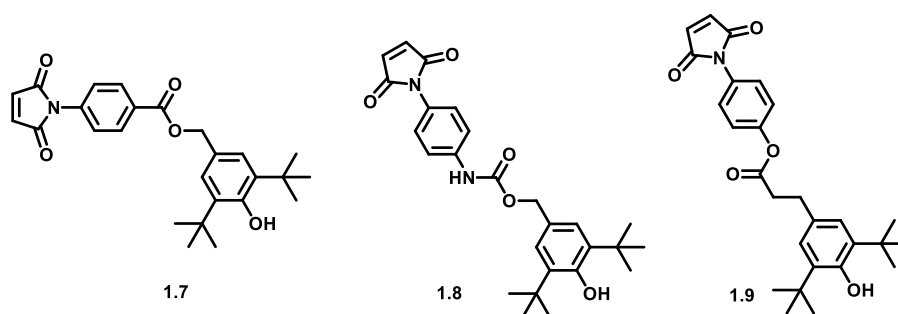
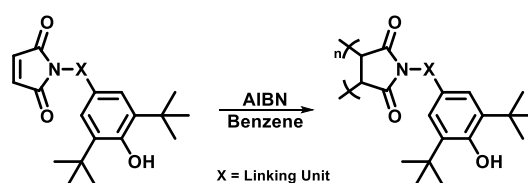


Figure 1.9 A series of monomeric phenolic antioxidants containing a polymerisable maleimide functionality.

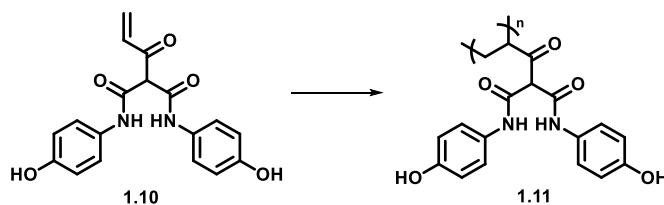
The grafting reactions described have shown some potential in increasing oxidative stability to the polymer matrix and have overcome a number of migration issues, however this method is not suitable for non-polymer matrices such as fuels, lubricants or food. An alternative immobilisation of antioxidants has also been achieved by the polymerisation of monomer bound antioxidants either through free-radical polymerisation or by ring opening metathesis polymerisation (ROMP). Dale, in 1978, reported maleimide functionalised phenols for use in foodstuffs.^[69] It was proposed that the molecular weight could be tuneable through radical polymerisation. The molecular weight could hence be increased to a level which prevented absorption into the cells in the body, therefore reducing potential toxicity issues associated with many synthetic antioxidants. Kim and co-workers also reported the radical polymerisation of their maleimide functionalised phenols (**1.7-1.9**) previously presented in **Figure 1.9 (Scheme 1.10)**. The functionalised polymaleimides exhibited high thermal stabilities in the range of 210-350 °C which was above the targeted polymer processing conditions. In addition, these polymers were soluble in chloroform, acetone, ethyl acetate, tetrahydrofuran and dichloromethane but their solubility in non-polar solvents was not disclosed.



Scheme 1.10 Synthesis of polymeric phenolic antioxidants from monomeric maleimide functionalities.

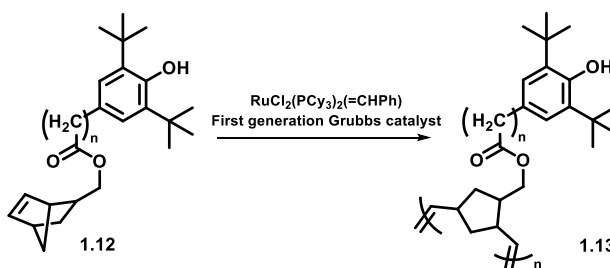
Shehata and Farouk reported the synthesis of acrylic-based polymeric antioxidants (**Scheme 1.11**).^[70] They observed that when the acrylic-based polymeric antioxidants were blended into a styrene butadiene rubber, excellent stability properties were

revealed when compared to a commercial antioxidant, *N*-isopropyl-*N*-phenyl-*p*-phenylenediamine. Mechanical properties of the unaged styrene butadiene rubber were unaffected by the addition of the polymeric antioxidants and all of the elastomeric properties of the polymer were retained for a much longer time period under aging conditions.



Scheme 1.11 Example synthesis of acrylic-based polymeric antioxidants, *via* solution polymerisation, as reported by Shehata and coworkers.^[70]

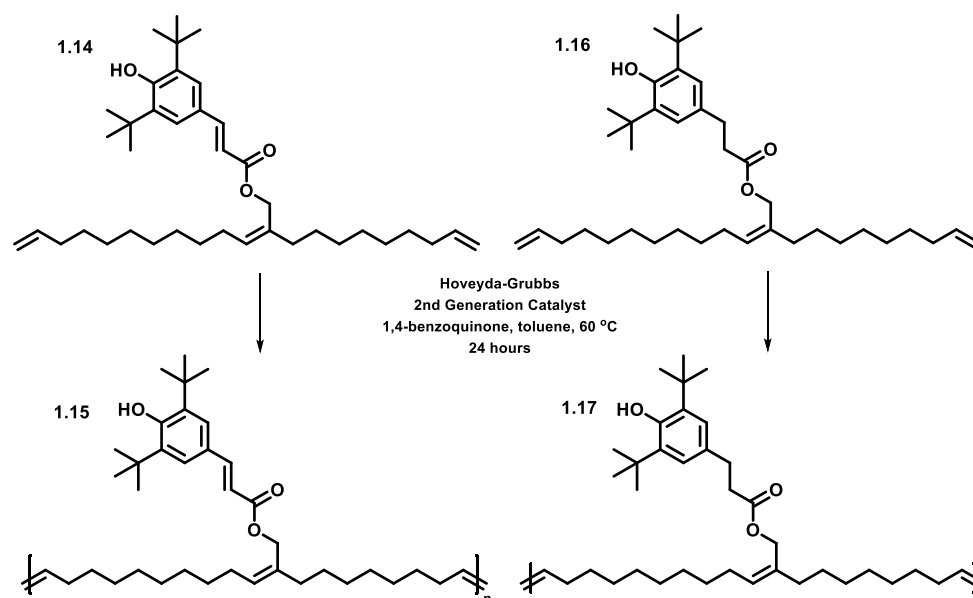
Free radical polymerisation does, however, come with its own limitations in particular when a peroxide is used as the radical initiator as it has been reported that sterically hindered phenols can be consumed by the peroxide species. Ring opening metathesis provides an alternative route to the polymerisation of monomer bound antioxidants.^[71] The ruthenium catalysts, introduced by Grubbs and co-workers, have shown a high tolerance to a broad variety of functional groups in addition to a high level of control over polymer architecture.^[72] A series of sterically hindered phenol functionalised norbornene derivatives were reported by Xue and co-workers by employing the so-called ‘Grubbs’ reaction (**Scheme 1.12**).^[71]



Scheme 1.12 Synthesis of polymeric norbornene derivatised phenolic antioxidants *via* ROMP where $n=0$ or 2 .^[71]

The radical scavenging capability of the polymeric antioxidants were analysed using a stable radical assay. Results revealed that when $n=2$, the radical scavenging capability was greater than when $n=0$, therefore providing an insight into the structure-activity relationships of phenolic antioxidants.

Acyclic diene metathesis (ADMET) polymerisation also presents a feasible route to polymeric antioxidants and such methodology has recently been reported by Beer and co-workers (**Scheme 1.13**).^[73] ADMET polymerisation of α,ω -dienes affords a strictly linear, unsaturated polyethylene backbone and precise functionality placement can be achieved along the backbone.



Scheme 1.13 Synthesis of polymeric antioxidants *via* ADMET polymerisation as reported by Beer and co-workers. 3,5-di-*tert*-butyl-4-hydroxy-cinnamic acid (**1.14**, **1.15**) and 3-(3,5-di-*tert*-butyl-4-hydroxy-phenyl)propionic acid (**1.16**, **1.17**) derivatives are shown.^[73]

Evaluation of the antioxidant efficiency was achieved through the addition of the polymeric antioxidants to polypropylene. The commercial antioxidant Irganox 1010, a widely used stabiliser for polypropylene, was used as a comparison. Equimolar amounts of the sterically hindered phenols were applied to ensure comparable results and the oxidation induction time was initially analysed at 185 °C, using differential scanning calorimetry. Results revealed that the 3,5-di-*tert*-butyl-4-hydroxy-cinnamic acid polymer (**1.15**) did not provide sufficient oxidative stability to the polypropylene sample in comparison to Irganox 1010 and it was proposed the conjugated double bond, present in 3,5-di-*tert*-butyl-4-hydroxy-cinnamic acid, was responsible for this loss in performance. The 3-(3,5-di-*tert*-butyl-4-hydroxy-phenyl)propionic acid polymer derivative (**1.17**) did, however, increase the oxidation induction time to such an extent that the analysis temperature had to be raised to 200 °C for the data to be gathered in a sensible time frame. At this higher temperature comparable concentrations of the 3-(3,5-di-*tert*-butyl-

4-hydroxy-phenyl)propionic acid polymer (**1.17**) and Irganox 1010 revealed oxidation induction times of 34 minutes and 41 minutes, respectively. This study not only highlighted the structural relevance of a conjugated double bond on antioxidant activity but it also provided a positive conclusion that as a result of the higher molecular weight and good compatibility with polypropylene, enhanced long term stabilisation could be expected from the 3-(3,5-di-*tert*-butyl-4-hydroxy-phenyl)propionic acid polymer.

Some additional immobilisation techniques have revealed the attachment of primary antioxidants to polymeric additives such as nanoparticles and nanotubes.^[74,75] Gao and co-workers^[75] presented the immobilisation of a sterically hindered phenol onto the periphery of nano-silica particles. The particles were blended into polypropylene and a greater oxidation induction time was observed for the bound antioxidant in comparison to its low molecular weight equivalent. Single-walled carbon nanotubes were functionalised with BHT derivatives by Lucente-Schultz and co-workers.^[74] It was reported that not only efficient radical scavenging but also reduced cell toxicity was achieved in comparison to their low molecular weight derivatives therefore making these materials potentially suitable for therapeutic medical devices.

Even though these approaches to antioxidant immobilisation have shown promising results particularly in the stabilisation of polyolefins, there are, however, limitations associated with these methodologies. Such limitations include high costs from expensive starting materials, phase separation and poor solubility within the polymer matrix. Therefore, in an attempt to target more cost effective and higher molecular weight antioxidants possessing both solubility within a hydrocarbon matrix and whilst possessing a high degree of functionality, attention has been drawn towards more structurally controlled and branched architectures such as dendritic macromolecules.

1.5 Dendritic macromolecules

The synthesis of polymers with highly controlled molecular architectures has gained increasing importance as a result of the rising demand for speciality polymers that possess novel properties.^[76] Dendritic chemistries have been applied to many areas of science and has been shaped by collaborations between biologists, inorganic, organic, physical and polymer chemists in addition to contributions from other areas of chemistry such as analytical, industrial and theoretical.^[77] Dendrons, dendrimers and hyperbranched polymers are all classified as dendritic macromolecules. One of the

intriguing properties of their architecture is the large number of end groups that may be modified to afford macromolecules with tailored chemical and physical properties. Flory was the first to introduce the concept of hyperbranched polymers, however at the time of this report the studies were purely theoretical in nature.^[78] Synthetic investigations on hyperbranched polymers^[79] was, however, carried out in the late 1970s which revealed irregularly branched macromolecules with polydispersity both in terms of molecular weight characteristics and branching factors. Focus was quickly directed to highly branched ‘starburst’ and ‘arboreal’ structures, independently reported by Tomalia^[80,81] and Newkome^[82-84], which are now more commonly referred to as ‘dendrimers’. These new dendrimers were similar to hyperbranched polymers in that they consisted of three structural regions: a central core, layered branching units and terminal groups. However, when all of the branched end groups were fully reacted, these structures afforded a highly and perfectly branched, mono-disperse spherical polymer. A schematic representation of the key structural features of a dendrimer is shown in **Figure 1.10**.

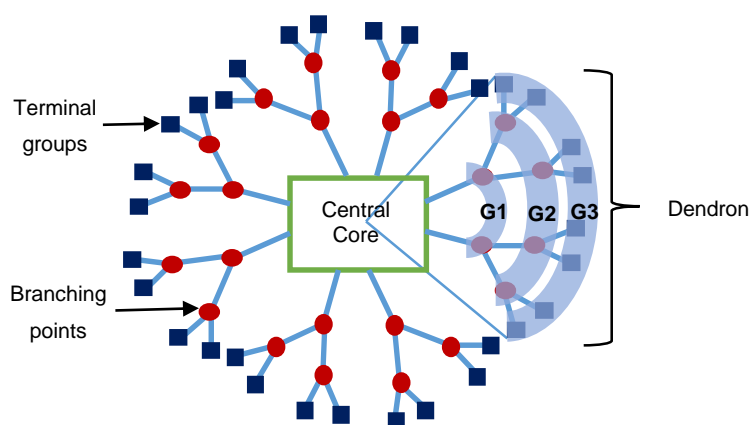
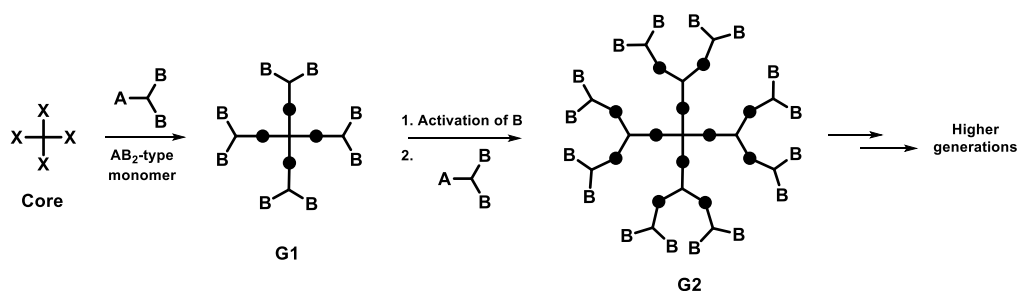


Figure 1.10 A schematic representation of the structural characteristics of a dendrimer.

Dendrimers are constructed in a step-wise manner by repeatable synthetic steps with each repetitive cycle creating an additional layer of branches or ‘generations’. Two major synthetic approaches have successfully emerged and are referred to as either a divergent or convergent approach.

In 1981, Denkewalter^[85,86] reported the first globular polymers prepared by a repetitive stepwise process originating from a polyfunctional core; a process which is now referred to as ‘divergent growth’. The drawback to this report was that the products obtained were poorly characterised and it was believed they were highly contaminated with unwanted structures therefore rendering them far from what would now be described as a true

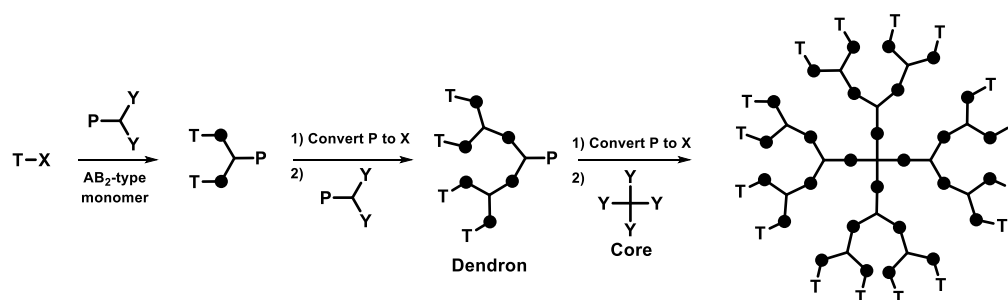
dendrimer.^[87] The potential of the divergent growth approach, however, was realised by both Tomalia^[80] and Newkome^[82] who used building blocks and synthetic steps that preserved a high degree of symmetry about the branching points. The key feature of divergent growth involves the dendrimer being grown radially outwards from a central polyfunctional core by the addition of typically AB_x type monomers in a series of coupling and activation processes.^[88–91] The molecular size and the number of chain ends increase with each new generation in proportion to the functionality of the AB_x monomer. A schematic representation of this growth method is shown in **Scheme 1.14**.



Scheme 1.14 Dendritic growth *via* the divergent approach.^[91]

A limitation associated with the divergent growth strategy is that the number of chain ends increases rapidly at each stage of the growth process. This leads to a number of potential problems as the growth progresses. Firstly, any incomplete reaction of the terminal groups can lead to imperfections in the subsequent generation, with the probability of these imperfections increasing with the increasing growth. Secondly, in order to obtain a monodisperse higher generation dendrimer, a large excess of reagent is required to prevent side reactions and ensure full conversion of all terminal groups. Even though the divergent approach has proven successful for a range of dendrimer syntheses,^[80,82,92,93] it still remains a relatively uncontrolled process.

In an attempt to overcome the limitations associated with the divergent approach, Hawker and Fréchet^[90,94] developed an alternative 'convergent' growth where their initial reports demonstrated the synthesis of dendritic polyethers based on the 3,5-dihydroxybenzyl alcohol monomer. By exploiting the symmetrical nature of dendrimers, the convergent approach initiates growth from the chain ends and repetition of the coupling and activation proceeds towards a focal point to afford larger and larger dendritic fragments or 'dendrons'. The final reaction required the attachment of these fragments to a polyfunctional core.^[87,88,91] A schematic representation of this growth method is shown in **Scheme 1.15**.



Scheme 1.15 Dendritic growth *via* a convergent approach where T represents a terminal group, X/Y are reactive groups and P is a protected group.^[91]

Unlike the divergent approach, generation growth using convergent methodology involves coupling reactions at a predetermined and constant number of reactive sites of a monomer rather than at an ever increasing number of sites associated with a growing dendrimer. This approach, therefore, leads to a greater degree of control over the purity and structural integrity of both the individual dendrons and the final dendrimer. A limitation of this approach, however, is the requirement that increasingly larger dendrons must be used for generational growth, leading to potential steric problems at the final coupling stage. Nevertheless, the convergent growth approach has been utilised in the synthesis of a range of dendrimers possessing various functionalities including polyesters,^[95,96] polyamines,^[97,98] polyethers,^[99] polyphenylenes^[100] and polyetherketones^[101]. Considering the large number of steps involved in the synthesis and purification of higher generation dendrimers, it is desirable to simplify the preparation. Hence, with the advent of new chemical techniques and improved synthetic methodologies dendrimers can now be prepared more efficiently and in shorter reaction times than ever before. As first described by Kolb and co-workers^[102], a particular framework of highly efficient chemical reactions (yields >99%) classed as ‘click’ chemistry has recently opened up the field of dendrimer synthesis. ‘Click’ chemistry is a term used to describe a chemical reaction which joins together small units to generate substances quickly and reliably in high yield. Some of the more successful ‘click’ chemistry reactions, in terms of dendrimer synthesis, include copper-catalysed azide-alkyne cycloaddition (CuAAC)^[103], UV initiated thiol-ene coupling (TEC)^[104] and the Diels-Alder reaction^[105]. These robust reactions are highly selective, known to proceed in a variety of solvents and have simple, non-chromatographic purification methods. From an industrial point of view these are all desirable properties when considering a scalable process.

A highly controlled architecture is not the only advantage dendrimers have over linear macromolecules. Some unique viscosity and solubility characteristics have also been realised from a number of dendrimer studies.^[100,106,107] When a dendrimer is in solution, the volume occupied by a single molecule increases slowly with generation whereas its mass increases rapidly.^[108] This growth pattern, associated with dendrimers, determines the solution properties and causes a deviation from the properties of linear molecules especially those with high molecular weights. This deviation has been measured using the physical parameter of intrinsic viscosity. In contrast to linear polymers, the intrinsic viscosity of dendrimers does not increase with molecular mass but reaches a maximum at a certain dendrimer generation.^[92,109] It is believed that a gradual transition in overall shape, from a more extended arrangement for lower generation dendrimers to a compact globular shape for higher generation dendrimers, causes the deviation in physical behaviour of dendrimers from those of linear macromolecules.^[108]

Among the large number of innovative multi-functional polymers reported in the literature, those based on 2,2-bis(hydroxymethyl)propionic acid (*bis*(MPA)) as the building block have gained significant interest. *Bis*(MPA) is a commercially available, simple, pro-chiral molecule with a molecular weight of 134.06 g mol⁻¹ and features two hydroxyl moieties and one carboxylic group (**Figure 1.11**).

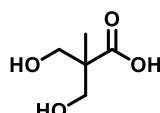
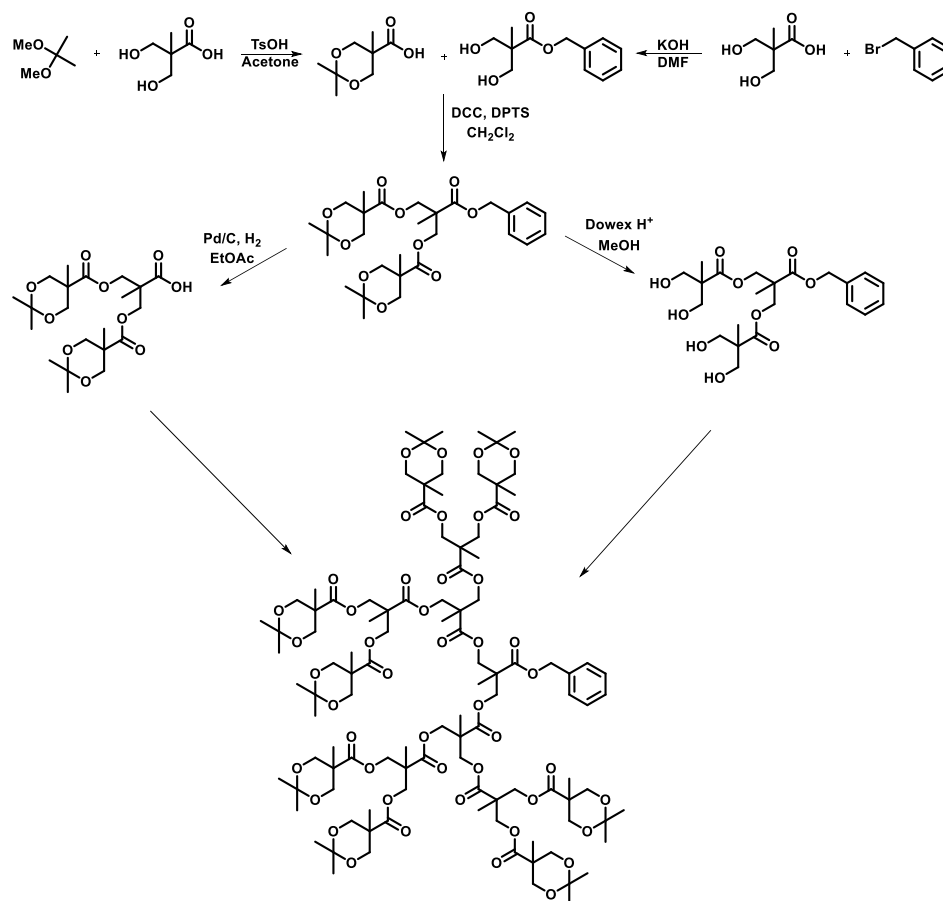


Figure 1.11 The structure of 2,2-bis(hydroxymethyl)propionic acid (*bis*(MPA)).

A variety of novel polymeric scaffolds have been developed using the single AB₂ monomer, *bis*(MPA).^[110,111] The first indication of the usefulness of *bis*(MPA) as a monomer for the synthesis of highly complex polymers was reported by Hult and co-workers.^[112] A series of esterification reactions were employed to reach up to generation 4 *via* a convergent growth approach. The large number of growth and deprotection steps, however, prompted development of a slightly improved strategy hence a ‘double-stage’ convergent approach was reported.^[88] This approach saw the focal point of each single dendron coupled in a divergent manner to the outside of another dendron or dendrimer which had been prepared independently by convergent or divergent growth. This method was used to prepare a fourth generation tridendron dendrimer based on 2,2-

bis(hydroxymethyl)propionic acid (*bis*(MPA)). If a strictly convergent or divergent process was used to synthesise this dendrimer seven synthetic steps and three purifications would be required. By using a combination of both growth procedures, the synthetic steps are reduced to six with only two purification steps. The synthetic route to one of *bis*(MPA) dendrons is shown in **Scheme 1.16**.



Scheme 1.16 Double-stage convergent approach for the synthesis of the fourth generation monodendron based on *bis*(MPA).^[88]

Further improvement to the synthesis of these polyester dendrons was realised by Fréchet and co-workers who exploited the inexpensive anhydride activated benzylidene protected *bis*(MPA).^[113] Iterative esterification and hydrogenolysis deprotection yielded a monodisperse fifth generation dendrimer possessing 96 terminal hydroxyl groups. Even though some impressive macromolecules have been generated using these growth procedures, the esterifications typically rely on the use of the coupling agent *N,N'*-dicyclohexylcarbodiimide (DCC) which requires toxic catalysts such as 4-(dimethylamino)pyridine (DMAP) and lengthy purification procedures. Very recently,

Malkoch and co-workers presented an approach to polyester dendrimers which was described as novel, efficient, scalable and sustainable and eliminated the use of DCC and toxic catalysts.^[114] The approach was based on fluoride-promoted esterification using imidazolid-activated *bis*(MPA) monomers, and a sixth generation *bis*(MPA) dendrimer was generated possessing an impressive 192 terminal hydroxyl moieties. Using this protocol the time taken to synthesise and isolate the sixth generation dendrimer macromolecule was less than one day which highlights the incredible advances in dendrimer synthesis.

Although the homofunctional dendrimers described can offer a large degree of peripheral functionality, an interest in multi-functional systems has driven the chemistry of *bis*(MPA) dendrimers towards the development of more complex materials. The first heterofunctional *bis*(MPA) dendrimer was reported by Fréchet and co-workers in 2002 where they were termed 'bow-tie' dendrimers (**Figure 1.12**) (also referred to as 'Janus' dendrimers).^[115]

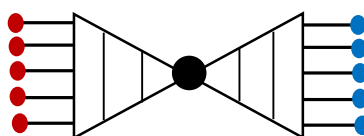


Figure 1.12 Schematic representation of a heterofunctional, 'bow-tie' dendrimer, consisting of a central core, generational growth and different terminal functionalities.

Heterofunctional dendrimer architecture gives access to both a high degree of functionality and tailored solubility while maintaining a well-defined structure. This poses an interesting application for antioxidant immobilisation whereby the diffusion and phase-separation issues observed previously for polymeric antioxidants could be targeted. Rissanen and co-workers have reported a series of bisfunctionalised 'Janus' molecules based on the *bis*(MPA) monomer, an example of which is presented in **Figure 1.13**.^[116-118]

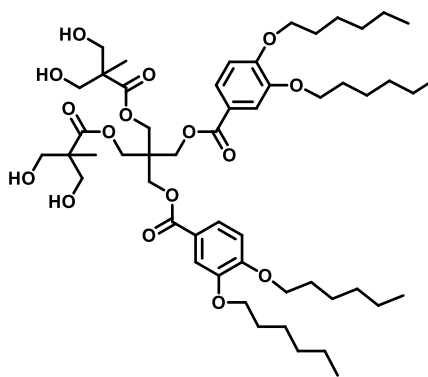


Figure 1.13 Example of a 'Janus' dendrimer reported by Rissanen and co-workers bearing *bis*(MPA) and 3,4-bis-hexyloxybenzoic ester terminal groups.

The series of amphiphilic Janus dendrimers were analysed for their thermal behaviour and were of particular interest because of their two distinct terminal groups of significantly different polarity. It was revealed, using thermogravimetric analysis, that the degradation temperatures ranged from 241-308 °C. This is a promising result and it would be interesting to see if through the functionalisation of the hydroxyl end groups with sterically hindered phenol derivatives the thermal stability remains in this higher temperature range. In terms of antioxidant immobilisation, dendritic chemistry has revealed very few examples of being used for such an application. There have been no examples in the literature of a 'true' dendrimer being functionalised with antioxidant moieties, possibly a result of the many synthetic steps to reach the higher generations and functionalities. One example was reported, however, by Bergenudd and co-workers.^[119] In this case a *bis*(MPA) hyperbranched polymer was functionalised with a sterically hindered phenol derivative. A hyperbranched polymer contains a mixture of linear and fully branched AB_x repeating units and from an industrial point of view are a good, cost-effective alternative to dendrimers.^[120] They can be produced on a large scale at a reasonable cost and still present some of the properties associated with dendrimer architectures even though irregularity is present within the structure.^[121] Several methods can be used to synthesise hyperbranched polymers including the self-condensation of AB_2 monomers. Aliphatic hyperbranched polyesters have been studied extensively and the esterification is usually carried out in the bulk using an acid catalyst. This class of macromolecule has also been industrially developed by Perstorp Speciality Chemicals with applications ranging from radiation-curable resins, binders, lubricants and thermoset plastics.

Bergenudd and co-workers reported^[119] the synthesis and analysis of three hyperbranched antioxidants based on the hyperbranched polyester Boltorn[®] which is a commercial product from Perstorp Speciality Chemicals. Boltorn[®] is based on a pentaerythritol core and *bis*(MPA) monomers. A core molecule is typically used to control the polycondensation and prevent the formation of insoluble cross-linked polymeric materials.^[121] Boltorn[®] has a large number of hydroxyl end groups which can be chemically modified to meet the desired properties. Second, third and fourth generation Boltorn[®] was modified with 3-(3,5-di-*tert*-butyl-4-hydroxy-phenyl) propionic acid and then blended into both squalane and polypropylene. The oxidation induction time was analysed and results revealed that all three generations provided superior oxidative stability to squalane in comparison to the commercial antioxidant Irganox 1010. Interestingly, insignificant stability was achieved in polypropylene blends and it was proposed the hyperbranched antioxidants had low mobility within the polymer matrix. This reveals an opportunity to develop this concept further by targeting solubility through the introduction of alkyl chains into the dendritic architecture.

1.6 Conclusion

An introduction to the oxidative degradation pathway of hydrocarbon based materials has been discussed. Antioxidants, predominantly sterically hindered phenol and diphenylamine derivatives, have revealed excellent oxidative stability properties. However, the low molecular weight of these discrete compounds has caused significant migration issues, most notably within polyolefins. A solution to this problem, referred to as antioxidant immobilisation, has been discussed whereby polymeric antioxidants have been developed to not only provide enhanced stability to a material but also reduced volatility at high temperatures. An array of polymer architectures have been reported, however, these come at a cost by often requiring expensive starting materials and catalysts. In addition, poor dispersion within a hydrocarbon matrix has been encountered. Dendritic macromolecules provide an alternative route to antioxidant immobilisation by using relatively cheap starting materials to produce highly functionalised, well-defined and disperse architectures. In comparison to the polymeric antioxidant immobilisation methods described, dendritic antioxidants remain a relatively new area of research and hence is the focus of this thesis.

1.7 Aims of the research

Dendritic macromolecules present an interesting architecture which is well-defined whereby a high degree of functionality can be accessed through the iterative growth of branching units surrounding a central core. Using these unique structural characteristics, higher molecular weight antioxidants can therefore be targeted with select functionalities.

The initial aim of this project was to develop a series of antioxidant functionalised polyester dendrons synthesised through the growth of the AB₂ monomer *bis*(MPA). The intention was to provide a high degree of sterically hindered phenolic end groups for enhanced oxidative stabilisation properties, good solubility within a hydrocarbon and good thermal stability with a resistance to volatilisation at high temperatures (**Chapter 2**).

Alternative functional core monomers were also investigated with a focus on low cost and commercial availability. Hence, glycerol and triethanolamine (TREN) were targeted and subsequently functionalised with antioxidant moieties and solubilising alkyl chains to yield a series of first generation polyester antioxidants (**Chapter 3**).

Through the enhancement of the hindered phenolic polyester dendrons, synthesised in **Chapter 2**, it was envisaged that by incorporating a diphenylamine derivative into the same branching unit as the hindered phenol, synergistic antioxidant properties could be targeted (**Chapter 4**).

The literature has highlighted numerous studies into the structural and functional characteristics of hindered phenols, however the analysis procedures reported do not often correlate hence comparison of results remains problematic. A radical scavenging assay, which is easily accessible, was therefore investigated with the aim to understand structure-activity relationships of new sterically hindered phenolic antioxidants (**Chapter 5**).

1.8 References

- 1 J. B. Heywood, in *Internal Combustion Engine Fundamentals*, McGraw-Hill College, 1988, pp. 1–37.
- 2 KPMG International, *The Transformation of the Automotive Industry: The Environmental Regulation Effect*, 2010.
- 3 T. J. Wallington, E. W. Kaiser and J. T. Farrell, *Chem. Soc. Rev.*, 2006, **35**, 335–347.
- 4 B. Hamilton and R. J. Falkner, in *Fuels and Lubricants Handbook: Technology, properties, performance and testing.*, ed. G. Totten, ASTM International, 2003, pp. 63–88.
- 5 N. Ribeiro, A. C. Pinto, C. M. Quintella, G. O. Da Rocha, L. S. G. Teixeira, L. L. N. Guarieiro, M. D. C. Rangel, M. C. C. Veloso, M. J. C. Rezende, R. Serpa da Cruz, A. M. De Oliveira, E. A. Torres and J. B. De Andrade, *Energy and Fuels*, 2007, **21**, 2433–2445.
- 6 G. Knothe, R. O. Dunn and M. O. Bagby, in *Fuels and Chemical from Biomass*, eds. B. C. Saha and J. Woodward, ACS Symposium Series: American Chemical Society, Washington DC, 1997, pp. 172–208.
- 7 A. Demirbas, *Prog. Energy Combust. Sci.*, 2007, **33**, 1–18.
- 8 A. Demirbas, in *Biofuels*, Springer, London, 2009, pp. 87–101.
- 9 A. S. M. A. Haseeb, M. A. Fazal, M. I. Jahirul and H. H. Masjuki, *Fuel*, 2011, **90**, 922–931.
- 10 R. O. Dunn, *Fuel Process. Technol.*, 2005, **86**, 1071–1085.
- 11 G. Knothe, *Fuel Process. Technol.*, 2007, **88**, 669–677.
- 12 N. Grassie and G. Scott, *Polymer Degradation and Stability*, Cambridge University Press, New York, 1985.
- 13 A. Dhawan, V. Kumar, V. S. Parmar and A. L. Cholli, in *Antioxidant Polymers: Synthesis, Properties, and Applications*, eds. G. Cirilo and F. Lemma, John Wiley and Sons, Hoboken, NJ, USA, 2012, pp. 385–425.
- 14 H. N. Stephens, *J. Am. Chem. Soc.*, 1928, **50**, 568–571.
- 15 A. Farmer and E. Sundralingam, *J. Chem. Soc.*, 1942, 121–139.
- 16 A. Farmer and E. Sundralingam, *J. Chem. Soc.*, 1943, 125–133.
- 17 E. R. Booser and M. R. Fenske, *Ind. Eng. Chem.*, 1944, **44**, 1850–1856.

- 18 J. L. Bolland and G. Gee., *Trans. Faraday. Soc.*, 1946, **42**, 236–243.
- 19 J. L. Bolland, *Proc. R. Soc. A Math. Phys. Eng. Sci.*, 1946, **186**, 218–236.
- 20 C. E. Frank, *Chem. Rev.*, 1950, **46**, 155–169.
- 21 J. Betts, *Q. Rev. Chem. Soc.*, 1971, **25**, 265–288.
- 22 G. Aguilar, G. Mazzamaro and M. Rasberger, in *Chemistry and Technology of Lubricants*, eds. R. Mortier, M. Fox and S. Orszulik, Springer Science and Business Media, London, 3rd edn., 2010.
- 23 L. Bateman, *Q. Rev. Chem. Soc.*, 1954, **8**, 147–167.
- 24 J. Dong and C. Migdal, in *Lubricant Additives*, ed. L. Rudnick, CRC Press, 2nd edn., 2009.
- 25 T. Colclough, *Ind. Eng. Chem. Res.*, 1987, **26**, 1888–1895.
- 26 E. T. Denisov and I. V. Khudyakov, *Chem. Rev.*, 1987, **87**, 1313–1357.
- 27 E. R. Bell, J. H. Raley, F. F. Rust, F. H. Seubold and W. E. Vaughan, *Discuss. Faraday Soc.*, 1951, **10**, 242–249.
- 28 X. Maleville, D. Faure, A. Legros and J. C. Hipeaux, *Lubr. Sci.*, 1996, **9**, 3–60.
- 29 R. K. Jensen, S. Korcek, L. R. Mahoney and M. Zinbo, *J. Am. Chem. Soc.*, 1979, **101**, 7574–7584.
- 30 J. L. Bolland, *Trans. Faraday. Soc.*, 1948, **44**, 669–677.
- 31 L. Bateman and A. L. Morris, *Trans. Faraday. Soc.*, 1953, **49**, 1026–1032.
- 32 E. J. Harris, *Proc. R. Soc. London A*, 1939, **173**, 126–146.
- 33 A. D. Walsh, *Trans. Faraday. Soc.*, 1945, **42**, 269–279.
- 34 K. U. Ingold, *Chem. Rev.*, 1961, **61**, 563–589.
- 35 J. Dong and C. A. Migdal, in *Lubricant Additives Chemistry and Applications*, ed. L. R. Rudnick, CRC Press Taylor and Francis, London, 2nd edn., 2009, pp. 4–50.
- 36 P. C. Hamblin and P. Rohrbach, *Lubr. Sci.*, 2001, **14**, 3–23.
- 37 G. Scott, *Br. Polym. J.*, 1983, **15**, 208–223.
- 38 J. Brown, in *Lubricants and Lubrication*, eds. T. Mang and W. Dresel, John Wiley and Sons, 2007, pp. 88–118.

- 39 E. T. Denisov and I. B. Afanas'ev, *Oxidation and Antioxidants in Organic Chemistry and Biology*, Taylor & Francis, Florida, 2005.
- 40 C. D. Lowry Jr, G. Egloff, J. C. Morrell and C. G. Dryer, *Ind. Eng. Chem*, 1933, **25**, 804–808.
- 41 J. L. Bolland and P. Ten Have, *Discuss. Faraday Soc.*, 1947, **2**, 252–260.
- 42 J. L. Bolland and P. Ten Have, *Trans. Faraday. Soc.*, 1947, **43**, 201–210.
- 43 J. I. Wasson and W. M. Smith, *Ind. Eng. Chem.*, 1953, **45**, 197–200.
- 44 D. S. Davies, H. L. Goldsmith, A. K. Guta and G. R. Lester, *J. Chem. Soc*, 1956, 4926–4933.
- 45 A. F. Bickel and E. C. Kooyman, *J. Chem. Soc*, 1956, 2215–2221.
- 46 R. K. Jenson, S. Korcek, M. Zinbo and J. L. Gerlock, *J. Org. Chem.*, 1995, **60**, 5396–5400.
- 47 T. A. B. M. Bolsman, A. P. Blok and J. H. G. Frijns, *J. R. Netherlands Chem. Soc.*, 1978, **97**, 310–312.
- 48 G. Scott, *Synergism and Antagonism*, Elsevier, New York, 1965.
- 49 R. Dinkov, G. Hristov, D. Stratiev and V. Boynova Aldayri, *Fuel*, 2009, **88**, 732–737.
- 50 W. W. Focke, I. van der Westhuizen, A. B. L. Grobler, K. T. Nshoane, J. K. Reddy and A. S. Luyt, *Fuel*, 2012, **94**, 227–233.
- 51 N. A. Santos, A. M. T. M. Cordeiro, S. S. Damasceno, R. T. Aguiar, R. Rosenhaim, J. R. Carvalho Filho, I. M. G. Santos, A. S. Maia and A. G. Souza, *Fuel*, 2012, **97**, 638–643.
- 52 D. Lomonaco, F. J. N. Maia, C. S. Clemente, J. P. F. Mota, A. E. Costa and S. E. Mazzetto, *Fuel*, 2012, **97**, 552–559.
- 53 G. W. Burton and K. U. Ingold, *J. Am. Chem. Soc.*, 1981, **103**, 6472–6477.
- 54 J. A. Howard and K. U. Ingold, *Can. J. Chem.*, 1963, **41**, 2800–2806.
- 55 G. E. Penketh, *J. Appl. Chem.*, 1957, **7**, 512–521.
- 56 K. D. Breese, J. F. Lamèthe and C. DeArmitt, *Polym. Degrad. Stab.*, 2000, **70**, 89–96.
- 57 T. Kajiyama and Y. Ohkatsu, *Polym. Degrad. Stab.*, 2001, **71**, 445–452.
- 58 T. Kajiyama and Y. Ohkatsu, *Polym. Degrad. Stab.*, 2002, **75**, 535–542.
- 59 T. Matsuura and Y. Ohkatsu, *Polym. Degrad. Stab.*, 2000, **70**, 59–63.

- 60 Y. Ohkatsu and T. Nishiyama, *Polym. Degrad. Stab.*, 2000, **67**, 313–318.
- 61 S. Al-Malaika and S. Issenhuth, in *Polymer Durability*, ed. R. Clough, Advances in Chemistry American Chemical Society, Washington DC, 1996, pp. 425–439.
- 62 S. Beißmann, M. Stiffinger, K. Grabmayer, G. Wallner, D. Nitsche and W. Buchberger, *Polym. Degrad. Stab.*, 2013, **98**, 1655–1661.
- 63 G. Dörner and R. Lang, *Polym. Degrad. Stab.*, 1998, **62**, 431–440.
- 64 N. Haider and S. Karlsson, *Biomacromolecules*, 2000, **1**, 481–487.
- 65 D. Munteanu and C. Csunderlik, *Polym. Degrad. Stab.*, 1991, **34**, 295–307.
- 66 J. A. Kuczkowski and J. G. Gillick, *Rubber Chem. Technol.*, 1984, **57**, 621–651.
- 67 S. Al-Malaika and N. Suharty, *Polym. Degrad. Stab.*, 1995, **49**, 77–89.
- 68 T. H. Kim and D. R. Oh, *Polym. Degrad. Stab.*, 2004, **84**, 499–503.
- 69 US 4078091, Dynapol, J. Dale, S. Ng, 1978.
- 70 A. B. Shehata, A. Nasr and T. Farouk, *Polym. Plast. Technol. Eng.*, 2005, **44**, 1281–1295.
- 71 B. Xue, K. Ogata and A. Toyota, *Polymer.*, 2007, **48**, 5005–5015.
- 72 M. R. Buchmeiser, *Chem. Rev.*, 2000, **100**, 1565–1604.
- 73 S. Beer, I. Teasdale and O. Brueggemann, *Eur. Polym. J.*, 2013, **49**, 4257–4264.
- 74 R. M. Lucente-Schultz, V. C. Moore, A. D. Leonard, B. K. Price, D. V Kosynkin, M. Lu, R. Partha, J. L. Conyers and J. M. Tour, *Artif. Cells Blood Substitutes Immobil. Biotechnol. Cells Blood Substit Immobil.*, 2009, **131**, 3934–3941.
- 75 X. Gao, X. Meng, H. Wang, B. Wen, Y. Ding, S. Zhang and M. Yang, *Polym. Degrad. Stab.*, 2008, **93**, 1467–1471.
- 76 N. Bikales, *Polym. J.*, 1987, **19**, 11–20.
- 77 R. Haag and F. Vögtle, *Angew. Chem. Int. Ed. Engl.*, 2004, **43**, 272–273.
- 78 P. J. Flory, in *Principles of Polymer Chemistry*, Cornell University Press, Ithaca, New York, 1952, pp. 347–398.
- 79 E. Buhleier, W. Wehner and F. Vogtle, *Synthesis.*, 1978, 155–158.
- 80 D. A. Tomalia, H. Baker, J. Dewald, M. Hall, G. Kallos, S. Martin, J. Roeck, J. Ryder and P. Smith, *Polym. J.*, 1985, **17**, 117–132.

- 81 D. Tomalia, J. R. Baker, J. Dewald, M. Hall, G. Kallos, S. Martin, J. Roeck, J. Ryder and P. Smith, *Macromolecules*, 1986, **19**, 2466–2468.
- 82 G. R. Newkome, Z. Yao, G. R. Baker and V. K. Gupta, *J. Org. Chem.*, 1985, **50**, 2003–2004.
- 83 G. R. Newkome, Z. Yao, G. R. Baker and M. J. Saunders, *J. Am. Chem. Soc.*, 1986, **18**, 849–850.
- 84 G. R. Newkome, G. R. Baker, M. J. Saunders, P. S. Russo, V. K. Gupta, Z. Yao, J. E. Miller and K. Bouillion, *J. Chem. Soc. Chem. Commun.*, 1986, 752.
- 85 US 4,410,688, Allied Corporation. R. Denklewater, J. Kolc, W. Lukasavage, 1981.
- 86 US 4,289,872, Allied Corporation, R. Denklewater, J. Kolc, W. Lukasavage, 1979.
- 87 J. M. J. Fréchet, C. J. Hawker and K. L. Wooley, *J. Macromol. Sci. Part A*, 1994, **31**, 1627–1645.
- 88 H. Ihre, A. Hult, J. M. J. Fréchet and I. Gitsov, *Macromolecules*, 1998, **31**, 4061–4068.
- 89 M. Malkoch, E. Malmström and A. Hult, *Macromolecules*, 2002, **35**, 8307–8314.
- 90 C. J. Hawker and J. M. J. Fréchet, *J. Am. Chem. Soc.*, 1990, **112**, 7638–7647.
- 91 S. Nummelin, M. Skrifvars and K. Rissanen, in *Topics in Current Chemistry*, Springer-Verlag, Berlin, 2000, vol. 210, pp. 1–67.
- 92 D. A. Tomalia, A. M. Naylor and W. A. Goddard, *Angew. Chem. Int. Ed.*, 1990, **29**, 138–175.
- 93 E. M. M. D. B. den Berg and E. W. Meijer, *Angew. Chemie Int. Ed. English*, 1993, **32**, 1308–1311.
- 94 C. J. Hawker and J. M. J. Fréchet, *J. Chem. Soc. Chem. Commun.*, 1990, 1010–1013.
- 95 T. M. Miller, E. W. Kwock and T. X. Neenan, *Macromolecules*, 1992, **25**, 3143–3148.
- 96 C. J. Hawker and J. M. J. Fréchet, *J. Chem. Soc. Perkin Trans. I*, 1992, 2459–2469.
- 97 P. M. Bayliff, J. Feast and D. Parker, *Polym. Bull.*, 1992, **29**, 265–270.
- 98 T. M. Miller and T. X. Neenan, *Chem. Mater.*, 1990, **2**, 346–349.
- 99 K. L. Wooley, C. J. Hawker and J. M. J. Fréchet, *J. Am. Chem. Soc.*, 1991, **113**, 4252–4261.

- 100 T. M. Miller, T. X. Neenan, R. Zayas and H. E. Bair, *J. Am. Chem. Soc.*, 1992, **114**, 1018–1025.
- 101 A. Morikawa, M. Kakimoto and Y. Imai, *Macromolecules*, 1993, **26**, 6324–6329.
- 102 H. C. Kolb, M. G. Finn and K. B. Sharpless, *Angew. Chem. Int. Ed.*, 2001, **40**, 2004–2021.
- 103 P. A. Ledin, F. Friscourt, J. Guo and G.-J. Boons, *Chem. Eur. J.*, 2011, **17**, 839–846.
- 104 K. L. Killops, L. M. Campos and C. J. Hawker, *J. Am. Chem. Soc.*, 2008, **130**, 5062–5064.
- 105 G. Franc and A. K. Kakkar, *Chem. Eur. J.*, 2009, **15**, 5630–5639.
- 106 K. L. Wooley, C. J. Hawker, J. M. Pochan and J. M. J. Fréchet, *Macromolecules*, 1993, **26**, 1514–1519.
- 107 K. L. Wooley, J. M. J. Fréchet and C. J. Hawker, *Polymer (Guildf.)*, 1994, **35**, 4489–4495.
- 108 A. W. Bosman, H. M. Janssen and E. W. Meijer, *Chem. Rev.*, 1999, **99**, 1665–1688.
- 109 T. H. Mourey, S. R. Turner, M. Rubinstein, J. Hawker and K. L. Wooley, *Macromolecules*, 1992, **25**, 2401–2406.
- 110 A. Carlmark, E. Malmström and M. Malkoch, *Chem. Soc. Rev.*, 2013, **42**, 5858–5879.
- 111 S. García-Gallego, A. M. Nyström and M. Malkoch, *Prog. Polym. Sci.*, 2015, **48**, 85–110.
- 112 H. Ihre, A. Hult and E. Söderlind, *J. Am. Chem. Soc.*, 1996, **118**, 6388–6395.
- 113 H. Ihre, O. L. Padilla De Jesús and J. M. J. Fréchet, *J. Am. Chem. Soc.*, 2001, **123**, 5908–5917.
- 114 S. García-Gallego, D. Hult, J. V. Olsson and M. Malkoch, *Angew. Chem. Int. Ed.*, 2015, **54**, 2416–2419.
- 115 E. R. Gillies and J. M. J. Fréchet, *J. Am. Chem. Soc.*, 2002, **124**, 14137–14146.
- 116 T. Tuuttila, M. Lahtinen, J. Huuskonen and K. Rissanen, *Thermochim. Acta*, 2010, **497**, 109–116.
- 117 T. Tuuttila, M. Lahtinen, N. Kuuloja, J. Huuskonen and K. Rissanen, *Thermochim. Acta*, 2010, **497**, 101–108.
- 118 J. Ropponen, S. Nummelin and K. Rissanen, *Org. Lett.*, 2004, **6**, 2495–2497.

- 119 H. Bergenudd, P. Eriksson, C. DeArmitt, B. Stenberg and E. Malmström Jonsson, *Polym. Degrad. Stab.*, 2002, **76**, 503–509.
- 120 E. Malmström, M. Johansson and A. Hult, *Macromolecules*, 1995, **28**, 1698–1703.
- 121 C. R. Yates and W. Hayes, *Eur. Polym. J.*, 2004, **40**, 1257–1281.

Chapter 2

Synthesis and Analysis of a Series of Novel Dendritic Phenolic Antioxidants

Abstract

Antioxidants are essential for providing organic compounds with protection against oxidative degradation. Current antioxidants, particularly those designed for use in hydrocarbon media, suffer from a variety of limitations including high volatility and poor solubility. In order to overcome these issues, a series of dendritic antioxidants have therefore been designed and synthesised. Using 2,2-*bis*(hydroxymethyl)propionic acid (*bis*(MPA)) as the branching unit, a divergent synthetic approach was employed to yield a range of dendritic polyesters, using *N,N'*-dicyclohexylcarbodiimide as the coupling reagent. A hindered phenolic, 3-(3,5-di-*tert*-butyl-4-hydroxyphenyl)propionic acid, was appended to the hydroxyl terminated polyesters to provide the antioxidant functionality. The thermal stability, assessed by thermogravimetric analysis (TGA), revealed that all of the functionalised dendrons have increased thermal stability when compared to 2,6-di-*tert*-butyl-4-methylphenol (BHT). Antioxidant ability was evaluated using differential scanning calorimetry (DSC) and when blended into a lubricant base oil, at 0.5% w/w, an increase in antioxidant performance was observed when compared to current industrial antioxidants.

2.1 Introduction

With a constant effort to reduce worldwide automotive emissions and meet the ever tightening environmental legislation controlling Original Equipment Manufacturers (OEMs), current fuel and lubricant additives need to be advanced or replaced.^[1-3] Significant pressure on fuel suppliers is being applied by the Government and Legislative Bodies to reduce emissions and also consumer behaviour is changing towards more environmentally friendly preferences.^[1-3] The requirement for enhanced fuel and engine efficiency is also a growing demand, both of which can be improved through the use of additives which serve to protect the fuel and engine from degradation.

The oxidative degradation of organic materials has been studied for many years and materials derived from petroleum, such as gasoline, diesel and lubricants, are particularly susceptible as a result of harsh conditions within a combustion engine.^[4-7] High temperatures and pressures in the presence of air and metal contaminants all contribute to the acceleration of oxidative degradation.^[8,9] The oxidation process of liquid hydrocarbons was first proposed by Bolland and Gee in 1946 who described a free radical pathway.^[10,11] Since then, the mechanism of oxidation has been investigated extensively and these studies highlighted a complex process where by-products are formed such as acids, alcohols, aldehydes, ketones and higher molecular weight hydrocarbons.^[8,9,12-16] Collectively, these by-products cause discolouration, increased viscosity and eventual physical failure of both the petroleum based product and the combustion engine. The rate of this detrimental process can be decreased if alkyl peroxy radicals, produced in the oxidative process, are scavenged efficiently.^[17] Additives such as antioxidants are introduced into hydrocarbon materials in order to extend their lifetime.^[8,9,11,16] A class of compounds described as hindered phenolics have been studied comprehensively for their radical scavenging ability in petroleum based-products.^[17-22] It has been found that phenolic antioxidants act by interrupting the reported^[10] radical pathway by providing a more labile proton when compared to the hydrocarbon species. This scavenging mechanism is highlighted in **Figure 2.1** for the antioxidant BHT and shows that phenolic antioxidants can directly remove a number of radicals from the oxidation chain reaction. This is achieved by both liberation of a hydrogen radical and through radical coupling processes, consequently inhibiting the oxidation pathway.^[9]

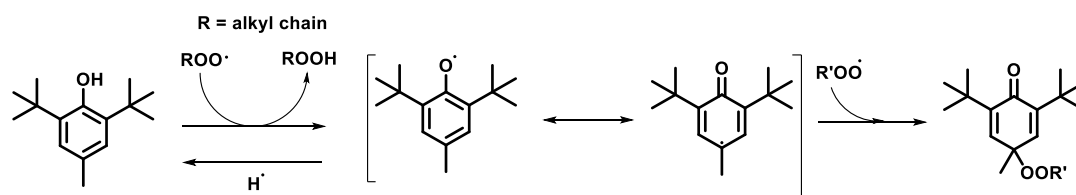


Figure 2.1 Proposed mechanism of radical scavenging of BHT.

There are many examples of both synthetic and natural hindered phenols (**Figure 2.2**) demonstrating varying methods to connect BHT-like functionalities and a number of studies have been dedicated to determine structure-activity relationships.^[23-28]

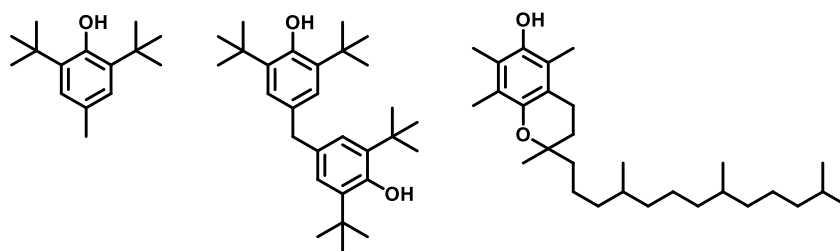


Figure 2.2 Examples of synthetic and natural phenolic antioxidants: BHT, 4,4'-methylenebis(2,6-di-tert-butylphenol) and α -tocopherol from vitamin E.

Antioxidants are, however, eventually consumed either through chemical loss, from their antioxidant action, or physical loss.^[16,29,30] Physical loss is influenced by factors such as volatilisation and precipitation out of the hydrocarbon matrix and often adding a larger amount of the antioxidant at the start would compensate for this loss.^[16,29,30] This, however, has its own disadvantages in that antioxidants often have limited solubility in hydrocarbons and are also relatively expensive. In order to overcome the current issues facing hydrocarbon additives, a series of phenolic-based analogues were prepared with an increasing number of antioxidant units. A branched alkyl chain was also incorporated to aid solubility in hydrocarbon media such as base oils. The structure of the analogues was based on a dendritic design whereby a central linker can be extended to increase the number of reactive end group functionalities. The antioxidant potencies were evaluated using a series of thermal and oxidative tests including thermogravimetric analysis (TGA) and differential scanning calorimetry (DSC).

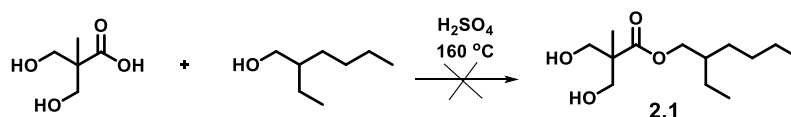
2.2 Results and Discussion

Aliphatic polyesters are the focus of this chapter as it was anticipated that an aliphatic core will have better solubility in a hydrocarbon medium than a fully aromatic structure. The proposed use for these compounds is incorporation into fuels or lubricants and it was hypothesised the additional oxygen provided by the polyester moieties could aid cleaner fuel combustion. The design of a series of antioxidant functionalised dendrons was inspired by an aliphatic hyperbranched polyester, Boltorn[®]. This hyperbranched polyester was first developed by Hult and co-workers with a structure based around bis(MPA) and to date its primary use has been in the coatings industry.^[31-34] Boltorn[®] is of particular interest because of its ability to access a range of molecular weights with a large number of hydroxyl end groups which can be chemically modified to meet a range

of properties such as antioxidant capability. With these targets in mind, a more structurally controlled antioxidant functionalised dendron was designed with *bis*(MPA) as the central core. A branched alkyl chain was introduced to the central core to aid solubility in a hydrocarbon medium and higher molecular weight generations were accessed through further reaction with *bis*(MPA).

2.2.1 Synthesis and Characterisation

A series of branched polyester hydroxyl linkers were synthesised using a divergent approach, with initial attempts utilising Fischer esterification methodology. Direct esterification was proposed as a potential route to a first generation hydroxyl linker to avoid the use of the multiple steps required in protection chemistry. Fischer esterification involved reacting *bis*(MPA) with 2-ethylhexanol as the solvent in the presence of concentrated sulfuric acid at a temperature of 160 °C (**Scheme 2.1**).

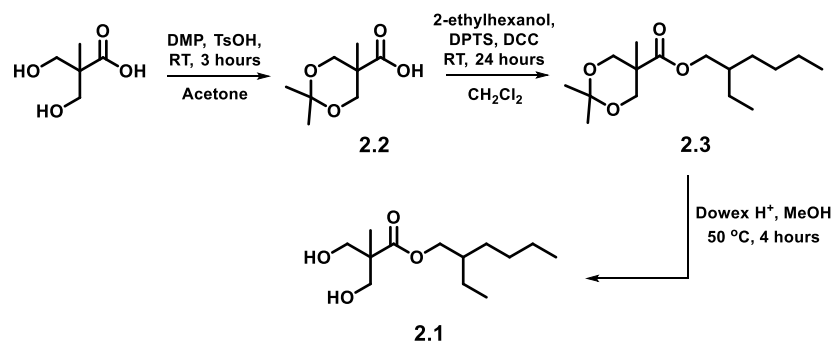


Scheme 2.1 Fisher esterification of *bis*(MPA) and 2-ethylhexanol.

This methodology is a well-established route for forming ester linkages and has been applied to industrial scale processes, however, the desired product **2.1** for this reaction was not achieved. The polyesterification of *bis*(MPA) to produce highly branched polymers has been studied and through using concentrated sulfuric acid as the catalyst and a temperature of 140 °C a range of hyperbranched polymers, derived from *bis*(MPA), have been successfully synthesised by Malmström and co-workers.^[34,35] *Bis*(MPA) possesses both acidic and alcoholic functionalities allowing it to homopolymerise in the esterification process. Therefore, an alternative approach was developed to utilise protection chemistry to prevent polyesterification, an approach often taken in the controlled synthesis of dendrimers.^[36-39]

The synthetic procedure used to reach the first generation hydroxyl linker is summarised in **Scheme 2.2**. Synthesis originated with the successful protection of the 1,3-diol moiety of *bis*(MPA) with an acetonide group (**2.2**). This was achieved by reaction of *bis*(MPA) with 2,2-dimethoxypropane (DMP) and a catalytic amount of *p*-toluene sulfonic acid

(TsOH) in acetone. This reaction was carried out at room temperature and afforded high yields (*ca.* 80%).



Scheme 2.2 Synthesis of the first generation hydroxyl linker based upon bis(MPA).

Protection of the 1,3-diol was confirmed through IR spectroscopic analysis (**Figure 2.3**) whereby the alcoholic -OH stretch at 3364 cm^{-1} was not evident in the spectrum of the acetonide protected *bis*(MPA).

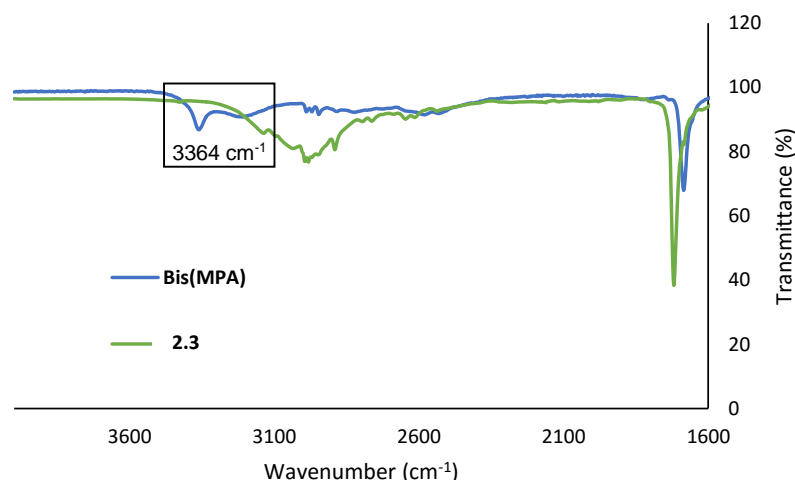


Figure 2.3 Overlay of FTIR spectra to show the protection of bis(MPA) with an acetonide group to yield 2.2.

A Steglich esterification approach, using *N,N'*-dicyclohexylcarbodiimide (DCC) as the coupling agent, was employed for the synthesis of 2.3 and all further esterifications reported in this chapter.^[40] Initial reactions utilised 4-dimethylaminopyridine (DMAP) as the catalyst, common to many esterification reactions of this type, however yields obtained *via* this approach were typically low (*ca.* 40%). An alternative esterification catalyst, 4-(dimethylamino)pyridinium-4-toluenesulfonate (DPTS) (**Figure 2.4**), was first reported by Moore and Stupp.^[41] The advantages of using DPTS were probed by

studying the esterification of simple compounds. It was noted that when solely using the traditional catalyst DMAP, significant amounts of the inactive acyl urea formed but upon introduction of an acid catalyst, TsOH, the acyl urea formation was suppressed.^[41] The optimal ratio of DMAP to TsOH was subsequently found to be 1:1 and the compound DPTS can accurately deliver this ratio to the reaction medium.^[41]

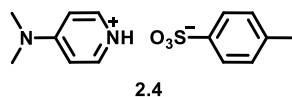


Figure 2.4: 4-(Dimethylamino)pyridinium-4-toluenesulfonate **2.4** - DPTS catalyst.

The DPTS catalyst was synthesised following the method described by Moore and Stupp but with the modification of substituting the solvent benzene for toluene. Using DPTS at 60 mol% the yield of the ester **2.3** improved from *ca.* 40% to 90%. ¹H NMR spectroscopic analysis confirmed the formation of the desired ester linkage as the methylene proton resonances, evident at 3.5 ppm for the 2-ethylhexanol starting material, were subjected to a downfield shift to 4.07 ppm in **2.3** as a result of the electron withdrawing effect of the newly formed ester bond. ¹³C NMR spectroscopic analysis also confirmed the generation of the desired ester moiety as a characteristic ester carbonyl ¹³C resonance was observed at 174 ppm. DCC mediated coupling has also been shown to provide a successful route to esterification under mild conditions with functional group compatibility. Alternative esterification methods were investigated for the synthesis of **2.3** which included anhydride coupling and acyl chloride activation of the carboxylic acid, however in these cases the yields were poor (<50%).

To yield the first generation hydroxyl linker **2.1**, the acetonide group was removed easily to regenerate the diol moiety. This was achieved by stirring the protected diol (**2.3**) in methanol in the presence of an acidic Dowex 50W-X8 resin at 50 °C. The reaction was monitored closely by thin layer chromatography and complete deprotection was seen within a few hours. Deprotection was confirmed using ¹³C NMR spectroscopy whereby the characteristic acetonide ¹³C resonance at 98 ppm was no longer observed (**Figure 2.5**). Furthermore, FTIR spectroscopic analysis revealed the reappearance of the characteristic hydroxyl absorption at 3411 cm⁻¹. The FTIR spectra also revealed a prominent alkyl absorbance at 2933 cm⁻¹ from the alkyl chain attached in the previous esterification step.

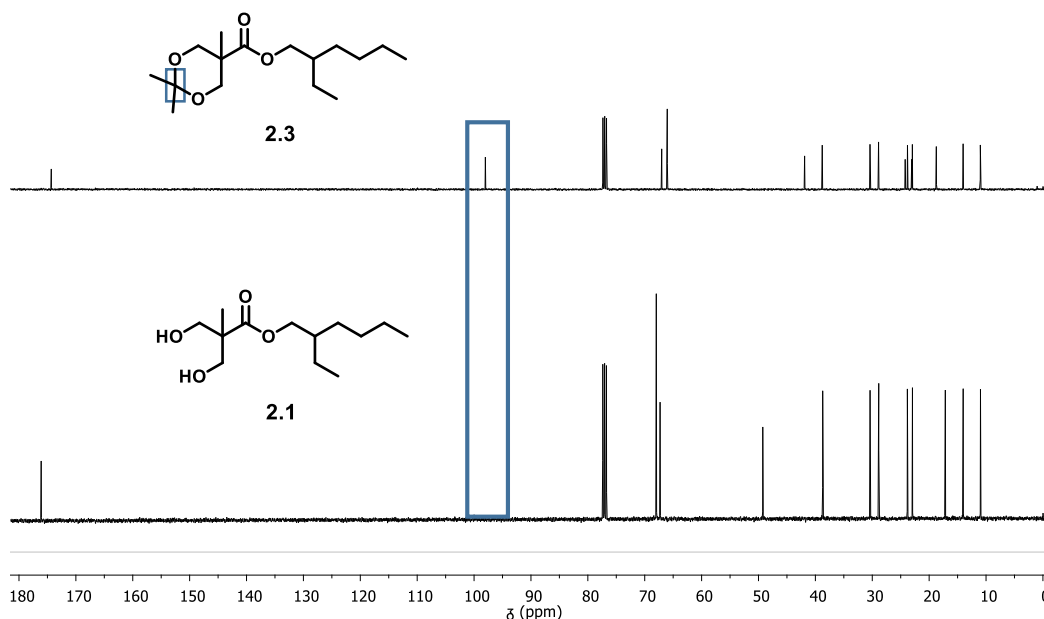
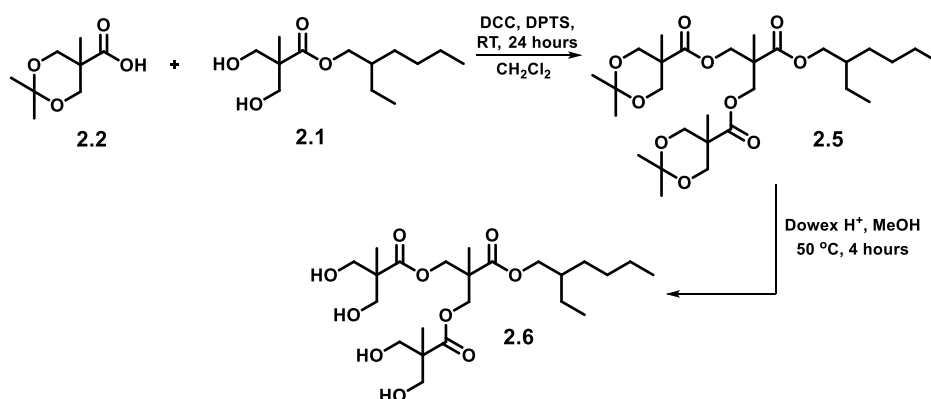


Figure 2.5 ^{13}C NMR spectra of **2.3** and **2.1** to reveal the disappearance of the acetonide resonance at 98 ppm indicating that deprotection was complete.

Using the first generation hydroxyl linker **2.1**, higher generation hydroxyl terminated polyesters could be accessed using the same protection and deprotection strategy outlined previously. The second generation polyester hydroxyl linker **2.6** was generated by the route shown in **Scheme 2.3**. DCC mediated coupling was utilised again to esterify **2.1** and **2.2** to produce the diacetonide triester **2.5**. Successful synthesis of the triester **2.5** was confirmed by ^{13}C NMR spectroscopic analysis where the characteristic tertiary carbon resonance, from the acetonide protecting group, was apparent at 98.1 ppm. In addition, using ^1H NMR spectroscopy, the triplet assigned to the terminal hydroxyl protons at 3.09 ppm was not evident and a new singlet at 4.33 ppm corresponding to the newly attached methylene protons from the protected *bis*(MPA) was present. Deprotection of **2.5**, using Dowex 50W-X8 resin, yielded the hydroxyl terminated second generation linker in good yield (*ca.* 70%). ^1H NMR spectroscopic analysis revealed successful deprotection with the observation of a multiplet at 3.22 ppm assigned to the terminal hydroxyl protons. FTIR spectroscopic analysis also revealed a hydroxyl stretch at 3261 cm^{-1} to reinforce that the deprotection had been achieved.



Scheme 2.3 Synthesis of the second generation hydroxyl linker **2.6**.

In addition, the increase in hydrogen bonding from first (**2.1**) to second (**2.6**) generation esters was also evident, whereby a shift in the hydroxyl stretch was observed from 3384 cm^{-1} to 3261 cm^{-1} (**Figure 2.6**).

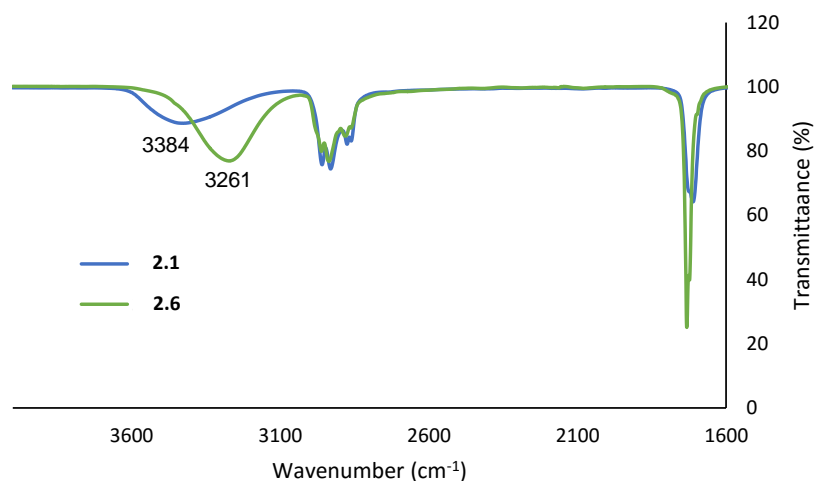
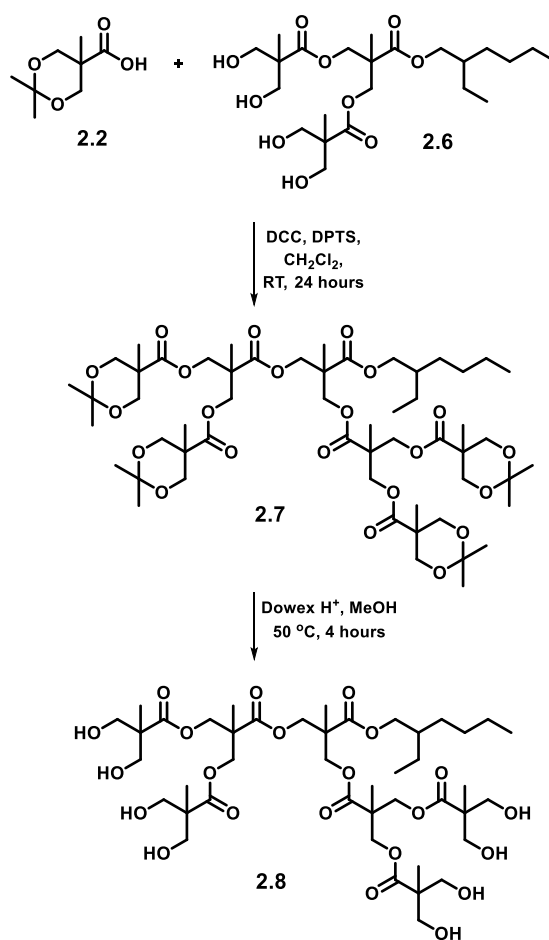


Figure 2.6 FTIR spectroscopy overlay showing an increase in hydrogen bonding from first (**2.1**) to second (**2.6**) generation esters.

A final generation of hydroxyl linker **2.8** was synthesised following **Scheme 2.4**. Again, DCC mediated coupling was employed to yield the hepta-ester **2.7**. At this stage, a large excess of **2.2** was required to ensure complete reaction of all four of the terminal hydroxyl units leading to solubility issues in the reaction medium used and thus the yield was significantly lower, at *ca.* 40%, than previous reactions of this kind.



Scheme 2.4 Synthesis of the third generation polyester hydroxyl linker **2.8**.

Complete reaction of the terminal hydroxyl moieties to yield **2.7** was observed by FTIR spectroscopic analysis which revealed the absence of the hydroxyl stretch, evident in the spectra of **2.6** at 3261 cm^{-1} . Successful coupling of the acetonide protected *bis*(MPA) (**2.2**) was further confirmed by use of ^{13}C NMR spectroscopy by the presence of the tertiary carbon resonance at 98.1 ppm in the spectrum. As observed previously, the acetonide protecting group could be removed in good yield (*ca.* 80%), in this case affording the hydroxyl terminated third generation hepta-ester **2.8**. The insolubility of **2.8** in CDCl_3 unfortunately renders comparison of the ^1H NMR resonances difficult as a result of the differences in chemical shift between CDCl_3 and DMSO-d_6 . In DMSO-d_6 a triplet was, however, evident at 4.65 ppm which integrated to 8 protons as expected for the terminal hydroxyl functionalities. In addition, FTIR spectroscopic analysis demonstrated the re-appearance of the hydroxyl stretch at 3286 cm^{-1} in addition to mass spectrometric analysis confirming the molecular weight $[\text{M}+\text{Na}]^+$ ($\text{C}_{43}\text{H}_{74}\text{O}_{22}$) $m/z = 965.4564$ (Calc.

965.4564). In summary, three generations of hydroxyl terminated bis(MPA) polyesters have been synthesised successfully in good yield.

The antioxidant functionality was then introduced in a divergent approach utilising the proven DCC mediated coupling route. The sterically hindered phenol 3-(3,5-di-*tert*-butyl-4-hydroxy-phenyl)-propionic acid was chosen as the terminal unit in order to provide antioxidant functionality to the hydroxyl linkers of the *bis*(MPA)-based ester dendrons (**Figure 2.7**).

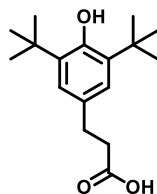
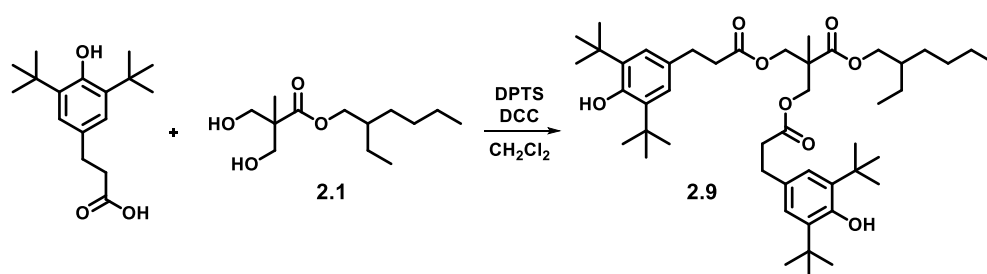


Figure 2.7 Structure of sterically hindered phenolic 3-(3,5-di-*tert*-butyl-4-hydroxy-phenyl)-propionic acid, used for its antioxidant capabilities.

As highlighted previously, sterically hindered phenols have been shown to provide excellent antioxidant in a range of applications from the natural environment to food, plastics and lubricants. 3-(3,5-Di-*tert*-butyl-4-hydroxy-phenyl)-propionic acid was chosen for a number of chemical characteristics in addition to its commercial availability. The sterically hindered phenol possesses an acid moiety making it suitable for DCC esterification, it also possesses a two carbon chain linker between the aromatic ring and the acidic functionality which was believed to aid the solubility of the final compound in a hydrocarbon-based medium. 3-(3,5-Di-*tert*-butyl-4-hydroxy-phenyl)-propionic acid was coupled to the hydroxyl chain ends of the first generation hydroxyl linker (**2.1**), as shown in **Scheme 2.5**, to obtain the desired diphenol (**2.9**) in good yield (*ca.* 75%). The product was purified by flash column chromatography to yield a viscous, colourless oil.



Scheme 2.5 Attachment of antioxidant functionality to the first generation hydroxyl linker.

^1H NMR spectroscopic analysis revealed the successful coupling of the antioxidant functionality to the first generation hydroxyl linker **2.1** as shown in **Figure 2.8**. The singlet observed at 5.08 ppm was assigned to the phenolic protons and has an integral of 2H to confirm full reaction of the terminal 1,3-diol from the first generation linker. In addition, a downfield shift of the *bis*(MPA) methylene resonances to 4.23 ppm is observed and the previously seen doublets, as a result of splitting from the terminal hydroxyls, coalesce to a singlet (highlighted in green in **Figure 2.8**).

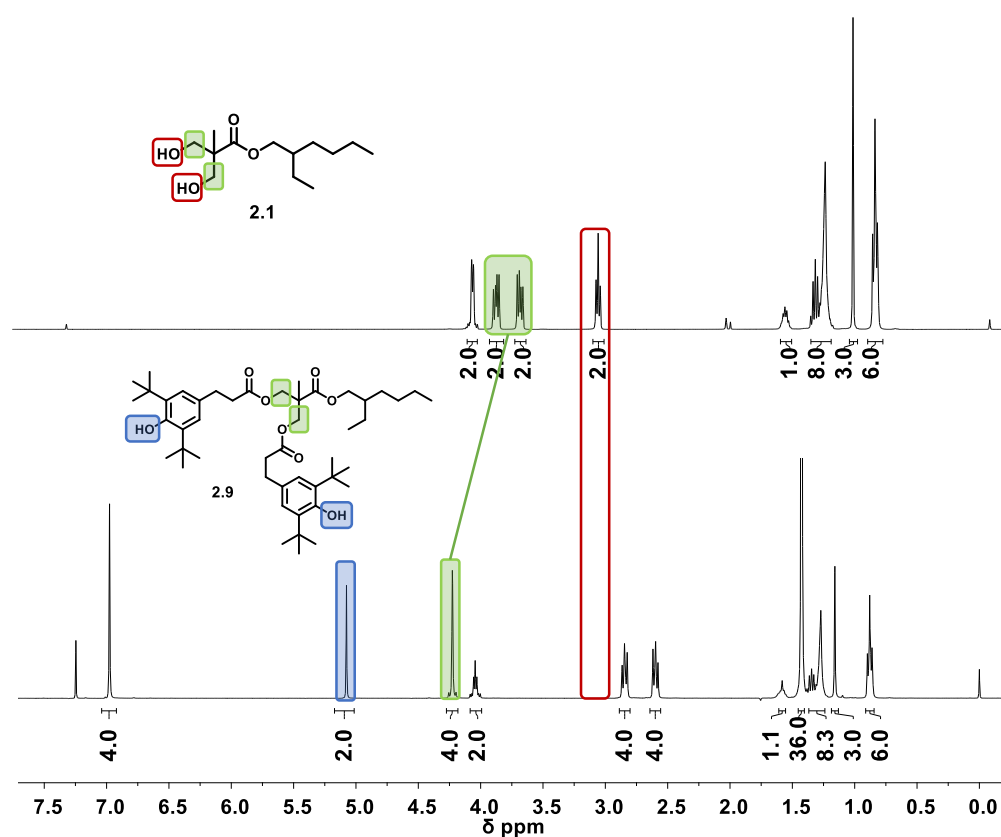
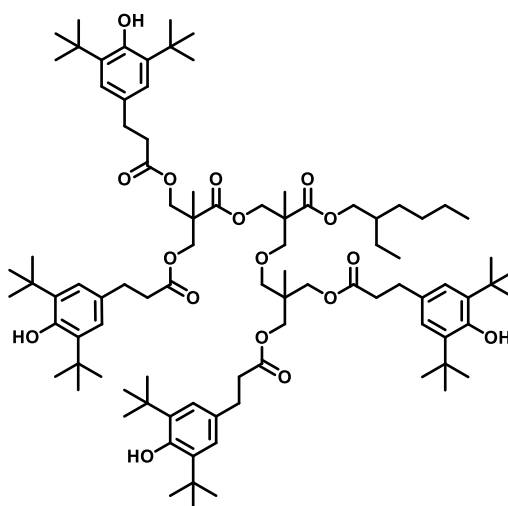


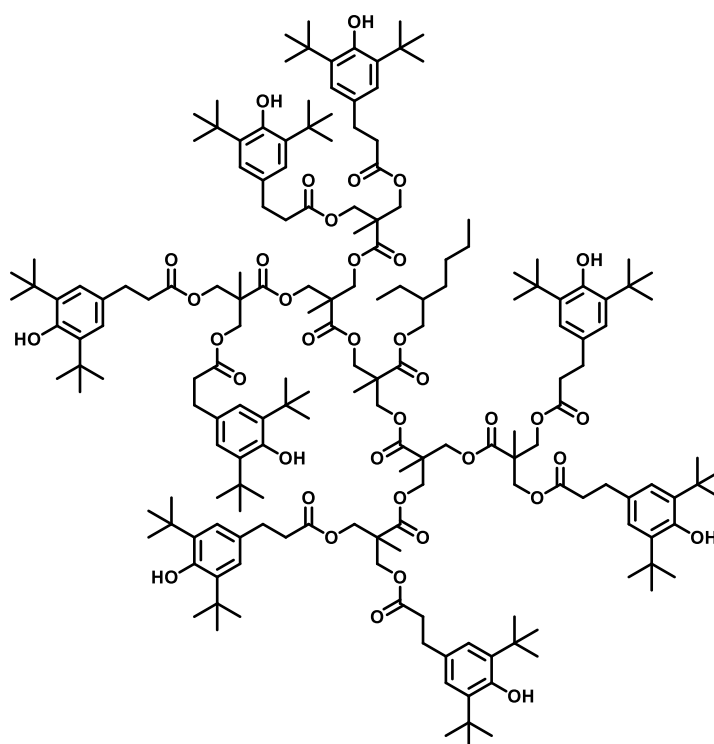
Figure 2.8 ^1H NMR spectra displaying coupling of antioxidant functionality to the first generation hydroxyl linker.

The second and third generation polyester hydroxyl linkers were subject to the same synthetic route as described for the first generation ester to yield the respective tetra- (**2.10**) and octa- (**2.11**) phenolic esters (**Figure 2.9**). The second generation tetraphenol **2.10** was obtained as a low melting point glassy solid (m.p 42 °C). ^{13}C NMR spectroscopic analysis revealed the successful addition of the antioxidant end groups to the hydroxyl linker **2.6** by the presence of a resonance at 152.2 ppm corresponding to the aromatic carbon adjacent to the phenolic functionality. In addition, new resonances were evident

between 120 and 140 ppm corresponding to the aromatic carbon atoms. Further confirmation by ^1H NMR spectroscopic analysis shows, when integrated with respect to the terminal methyl protons of the solubilising alkyl chain, a singlet at 1.42 ppm corresponding to 72 protons of the eight *tert*-butyl groups on the antioxidant unit. Furthermore, the broad multiplet evident at 3.21 ppm, observed in the second generation hydroxyl linker (**2.6**), was not visible indicating complete reaction of the hydroxyl end groups.



2.10



2.11

Figure 2.9 Structures of the second generation (**2.10**) and third generation (**2.11**) antioxidants, respectively.

The third generation octaphenol **2.11** required an adapted synthesis to generate successfully the desired product. An alternative solvent was used to overcome the insolubility of the third generation hydroxyl linker in dichloromethane. Dimethylacetamide was found to be one of the few compatible solvents and DCC and DPTS were used as described previously. The purification of the octaphenol **2.11** proved to be challenging with initial precipitation into water to remove the dimethylacetamide, followed by dissolution in dichloromethane and multiple washings with sodium hydroxide to remove the excess 3-(3,5-di-*tert*-butyl-4-hydroxy-phenyl)-propionic acid. Flash column chromatography was then used to remove traces of the *N,N'*-dicyclohexylurea (DCU) by-product from the esterification process, however, a second pass over the column was required to remove the trace impurities. The octaphenol **2.11** was yielded as a white solid in yield of only *ca.* 15%. The lengthy purification process suggests that impurities and solvent are easily trapped within the large structure of the compound. Entrapment of small molecules within dendritic structures has been reported in the literature most notably by Meijer and co-workers.^[42,43] This work described that once small molecules were trapped within the dendritic structure, diffusion out into the surrounding environment was extremely slow. The low yield of the octaphenol **2.11** was attributed to the bulkiness surrounding the hydroxyl end groups of the third generation hydroxyl linker (**2.8**) which could potentially inhibit the successful coupling using DCC. An alternative method of esterification, such as acyl chloride activation of the 3-(3,5-di-*tert*-butyl-4-hydroxy-phenyl)-propionic acid, may actually improve the yield in this case by reducing the bulkiness of the coupling reagents and also preventing the formation of unwanted by-products such as DCU. Confirmation of the successful isolation of **2.11** was determined by ¹H NMR spectroscopy (**Figure 2.10**). By integrating the methylene protons adjacent to the ester linkage of the solubilising alkyl chain (a singlet at 1.41 ppm, 2 protons) with respect to the protons of the *tert*-butyl groups of the antioxidant terminal units (a singlet at 1.41 ppm, 144 protons) complete conversion of the terminal hydroxyl moieties was ascertained.

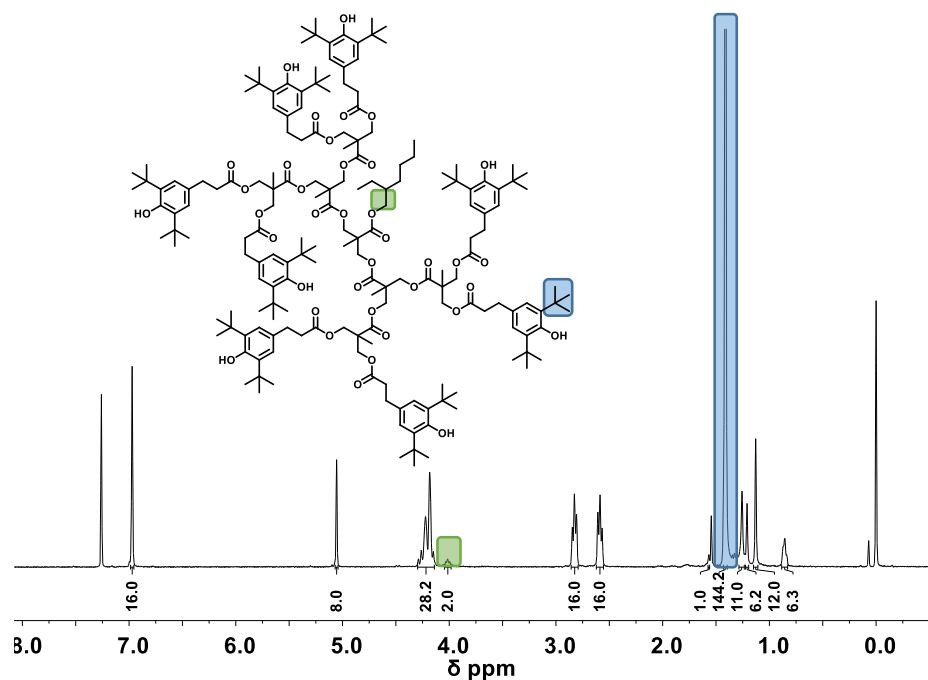


Figure 2.10 ^1H NMR spectra for generation 3 octaphenol **2.11**.

FTIR spectroscopic analysis also confirmed complete reaction of all of the hydroxyl end groups. The broad absorbance at 3287 cm^{-1} in the third generation hydroxyl linker **2.8** was suppressed in the third generation octaphenol **2.11**. In addition, a new absorbance was observed at 3642 cm^{-1} in accordance with the coupled phenolic functionalities.

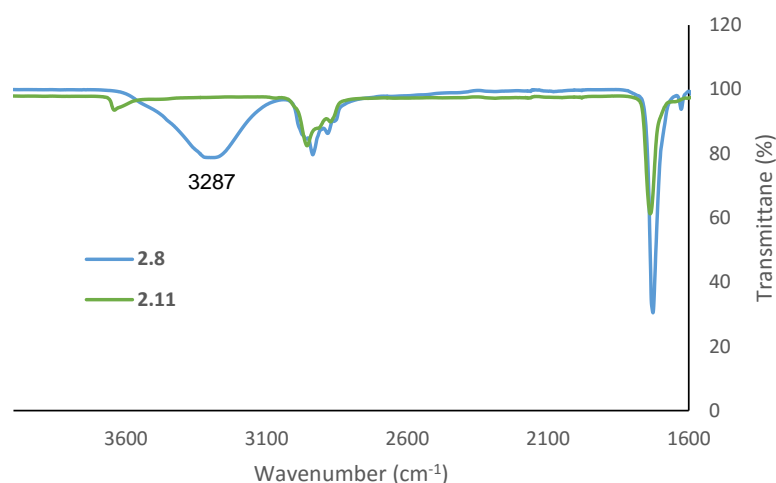


Figure 2.11 Overlay of the FTIR spectra of **2.8** and **2.11** to show complete consumption of the hydroxyl end groups.

Thermal analysis of all of the dendritic antioxidants (**2.9**, **2.10** and **2.11**) by differential scanning calorimetry revealed a glass transition temperature (T_g) for each compound at

-6.17 °C, 23.37 °C and 43.83 °C, respectively. The differences in the glass transition temperatures correspond well with the physical appearance of each generation, ranging from a viscous oil (**2.9**) to a powder (**2.11**), and an increase of *ca.* 20 °C was recorded for each generational increase in molecular weight (767.10>1506.10>3026.00).

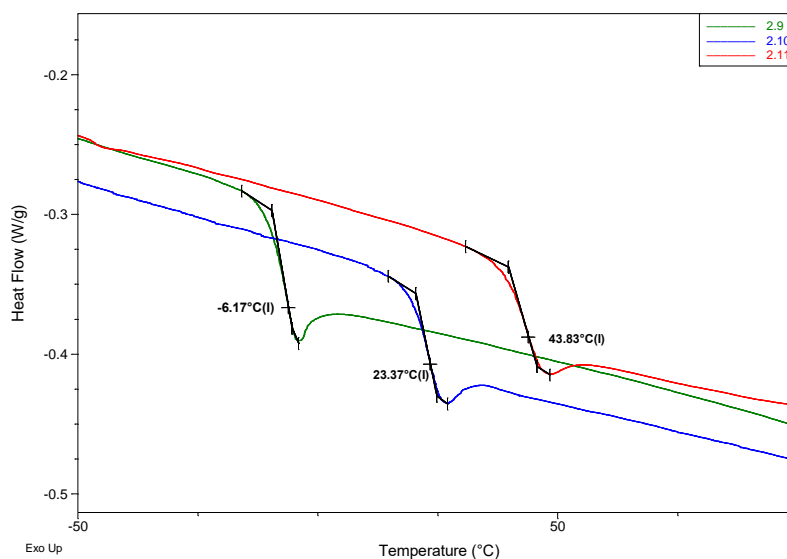


Figure 2.12 A DSC thermogram overlay for the first (**2.9**), second (**2.10**) and third (**2.11**) generation polyphenols showing the mid-point glass transition (T_g).

In summary, three generations of antioxidant functionalised polyester dendrons have been synthesised successfully. The synthetic pathway used to generate the first (**2.9**) and second generation (**2.10**) dendrons was scaled up to 100 g which shows potential for use in industry.

2.2.2 Thermal Stability Studies

Thermogravimetric analysis was used to probe the thermal stability characteristics of the synthesised generational series of antioxidants **2.9-2.11**. One of the key issues of current antioxidants, as discussed, is volatilisation from the bulk material and it was postulated that by increasing the molecular weight of the antioxidant this effect could be reduced. Analysis was carried out under a nitrogen atmosphere and the samples were heated gradually at 10 °C/minute from ambient temperature to 500 °C. The thermal stability of the diphenol **2.9** was compared to three commercial antioxidants, BHT (**Figure 2.1**), Irganox L135 and Irganox L57. Irganox L135 is a phenolic antioxidant and Irganox L57 is an octylated diphenylamine which is designed to work at higher temperatures (**Figure 2.13**).

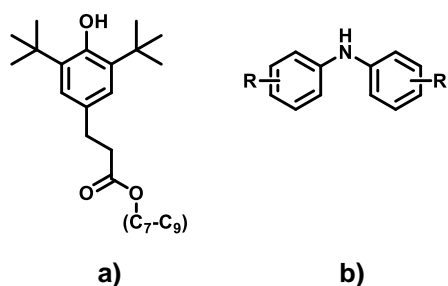


Figure 2.13 Commercial antioxidants a) Irganox L135 and b) L57.

The thermogravimetric analysis traces are shown in **Figure 2.14**. A significant increase in the thermal stability of **2.9** when compared to all three commercial antioxidants was observed. The most significant increase in thermal stability was observed when compared to BHT and examination of molecular weight alone reveals that BHT ($M_w = 220.36$) is nearly 4 times smaller than **2.9** ($M_w = 767.10$) meaning it is much more susceptible to volatilisation, hence complete consumption was seen at *ca.* 150 °C.

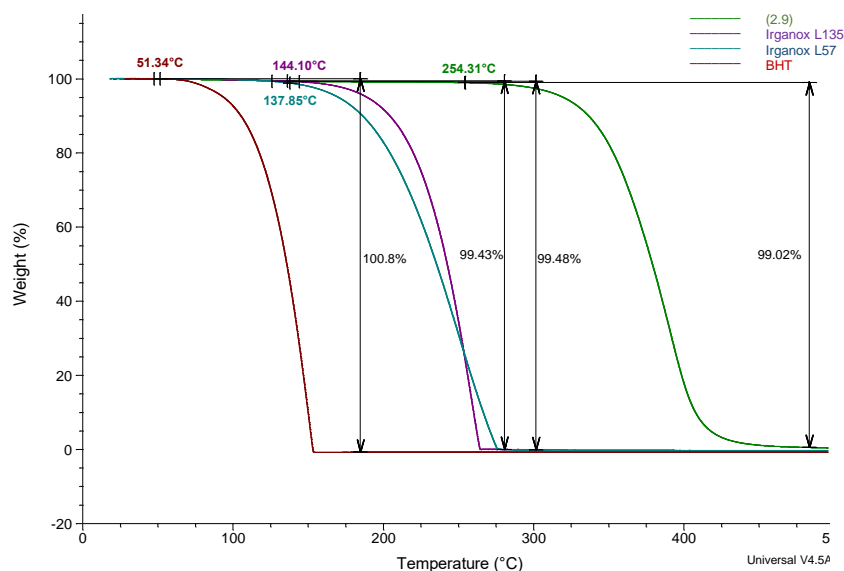


Figure 2.14 Thermogravimetric analysis of **2.9** when compared to BHT, Irganox L135 and Irganox L57.

The first generation diphenol **2.9** also revealed a thermal stability of *ca.* 100 °C higher than both Irganox L135 (Average $M_w = 390.61$) and L57 (Average $M_w = 337.55$). This result again highlights that the large molecular weight of the diphenol **2.9** is contributing to the observed enhanced thermal stability properties.

The polyphenols **2.10** and **2.11** were also analysed and revealed a one-step degradation, however loss of residual entrapped solvent (*ca.* 10%) was observed at *ca.* 100 °C (**Figure 2.14**). A slight increase in the stability was observed between each generation, most likely a result of increasing bulkiness.

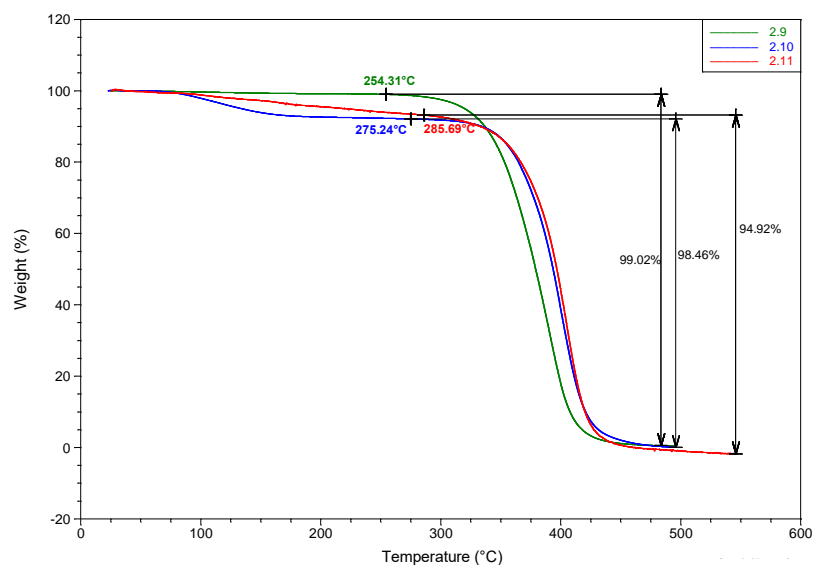


Figure 2.15 Thermogravimetric analysis of polyphenol dendrons **2.9**, **2.10** and **2.11**.

The thermogravimetric data shows that the design of these dendritic compounds has successfully increased bulk and reduced the effect of physical loss of the antioxidant through volatilisation. It can therefore be assumed that these new antioxidants will be present in a hydrocarbon medium for an increased amount of time at high temperatures, consequently providing prolonged stability to the material.

2.2.3 Oxidative Stability Studies

To further assess the antioxidant potential of the polyphenols they were blended into a synthetic lubricant base oil, Durasyn 164. Durasyn 164 is a polyalphaolefin, hydrogenated hydrocarbon base oil composed of dec-1-ene trimers typically used in lubricating oils. At this stage it was found that both the first generation (**2.9**) and second generation (**2.10**) were soluble in the hydrocarbon, however, the third generation (**2.11**) was insoluble and hence analysis of this polyphenol was not possible. The commercial antioxidants Irganox L135 and Irganox L57 were once again used as a comparison and samples were prepared by blending of 0.5% w/w of each antioxidant in 50 mL of lubricant base oil; gentle heating and magnetic stirring was required to ensure a fully homogenous blend.

The blends were analysed using pressurised differential scanning calorimetry (PDSC). DSC is a technique that monitors the heat effects associated with phase transitions and chemical reactions as a function of temperature. Oxidation induction time (OIT) and oxidation onset temperature (OOT) are two DSC methods used to probe the effect of antioxidants on the stability of an oil sample. OIT was analysed by following a standard dynamic procedure where the sample is heated at a defined constant heating rate under oxidising conditions until a reaction begins. Typically, 2 mg of sample was added to an aluminium crucible and the DSC cell was pressurised to 100 psi with cylinder air. The temperature was raised to 50 °C and held isothermally for 5 minutes then ramped at 20 °C/min to 210 °C and held isothermally until the oxidation of the sample was induced. The time of onset of the exotherm minus the time taken to reach 210 °C is then recorded. An example of a typical oxidation induction time trace is shown in **Figure 2.16**.

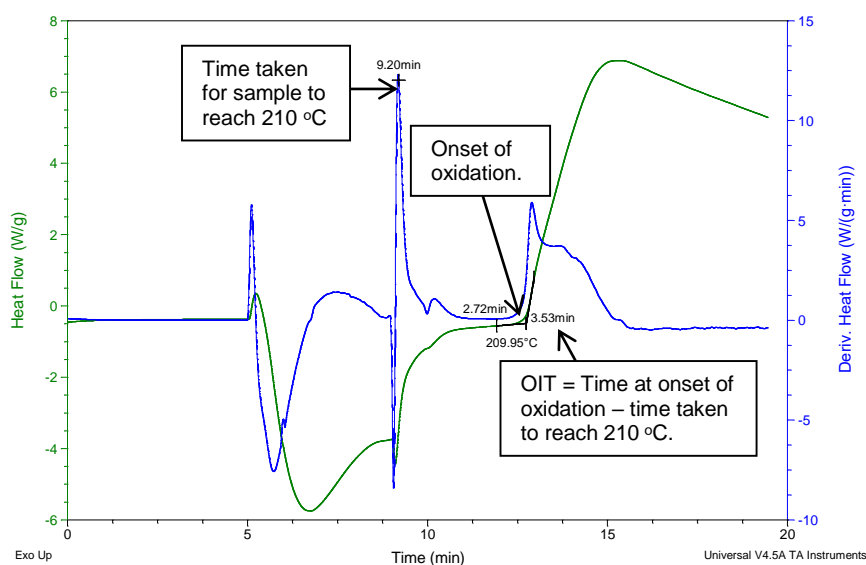


Figure 2.16 An example of a typical oxidation induction time trace.

The time taken for the sample to reach 210 °C can be determined from the derivative heat flow trace highlighted in blue in **Figure 2.16**. The thermal profile of the sample being analysed is shown in green and a large exotherm is seen to start at around 12 minutes indicating the material is undergoing oxidation. The OIT can hence be calculated by subtracting the time taken for the sample to reach 210 °C from the time of the onset of the exotherm. The results for each oil blend are shown in **Figure 2.17**.

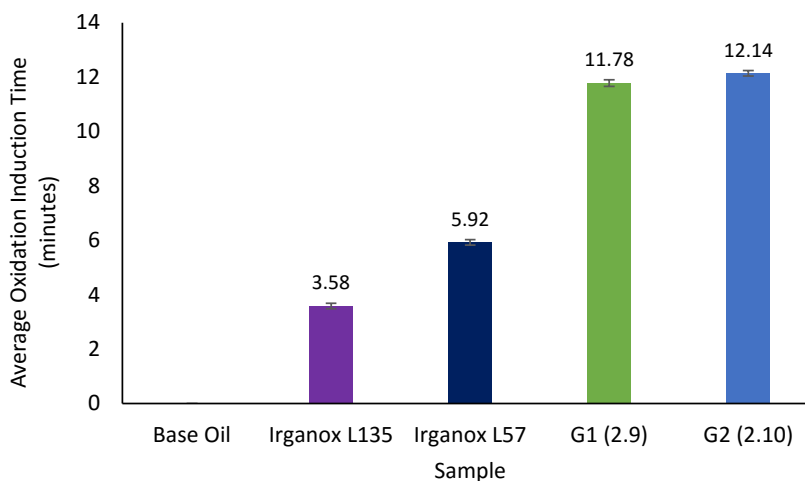


Figure 2.17 Average Oxidation Induction Time of 0.5% w/w antioxidant-base oil samples run in duplicate.

Oxidation induction time analysis has shown that primarily the presence of **2.9** and **2.10** in the base oil has increased greatly the stability of the sample (*ca.* 229%) (**Figure 2.17**). The induction time has been increased from <3 minutes for the unblended base oil to *ca.* 12 minutes for the blended samples. Secondly **2.9** and **2.10** have shown superiority to both of the commercial antioxidants, Irganox L135 and Irganox L57. Interestingly, there was not a significant difference between the results for **2.9** and **2.10** even though the number of active phenolic end groups has doubled between the two dendrons. This trend suggests that possibly increasing the number of active end groups is not the only answer for improved antioxidant ability. As discussed previously, often a larger amount of antioxidant is added to the material to overcome the issues of physical and chemical loss, however, this is not always feasible as a result of poor solubility and the expense associated with such specialised compounds. To investigate the benefits of this new series of antioxidants further, a normalisation test was carried out where additional blends were generated with respect to the number of moles of Irganox L135 which possesses only one active phenolic. The number of moles of the first and second generation were then either halved or quartered corresponding to their respective 2 and 4 active phenolic groups (**Table 1**). The results from these blends are shown in **Figure 2.18** and compared to the original 0.5% w/w blends.

Sample	Mw	Number of phenolic functionalities	Number of mmols	Mass required for the oil blend
Irganox L135	390.61	1	0.64	0.2500 g
2.9	767.09	2	0.32	0.2455 g
2.10	1506.08	4	0.16	0.2410 g

Table 2.1 Calculations to determine amount of 2.9 and 2.10 required when compared to Irganox L135.

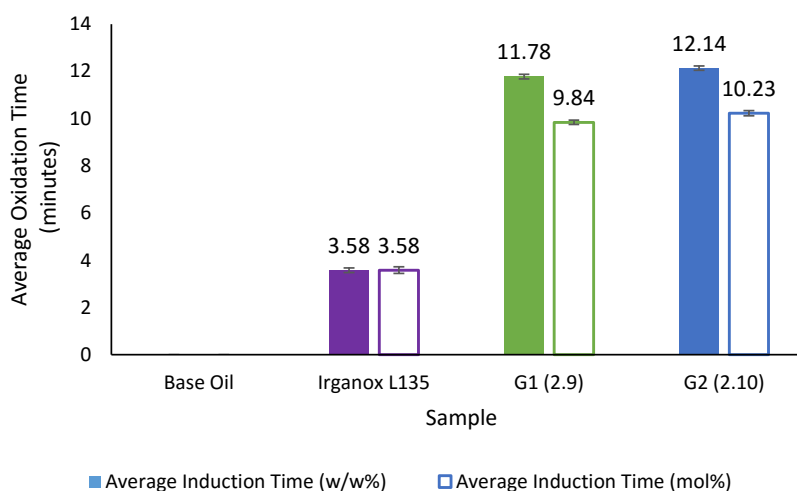


Figure 2.18 Average Oxidation induction time comparison of w/w and mol% oil blends run in duplicate.

The results in **Figure 2.18** are very promising as it shows that even though there has been a slight drop in induction time, the dendrons **2.9** and **2.10** still perform much better than Irganox L135. This could be significant when applied to an industrial process as any small saving on the amount of antioxidant required could have a substantial impact on the overall costs of the product or process.

Oxidation onset temperature (OOT) analysis was also performed. A smaller amount of sample is required for this test, using only 0.5 mg of sample in an aluminium crucible. The cell was pressurised to 500 psi with cylinder air with a flow of 60 mL/min. The temperature was raised to 50 °C and allowed to stabilise before heating at 50 °C/min to

350 °C. The temperature at which the oxidation exotherm occurs is reported and a typical trace is shown in **Figure 2.19**.

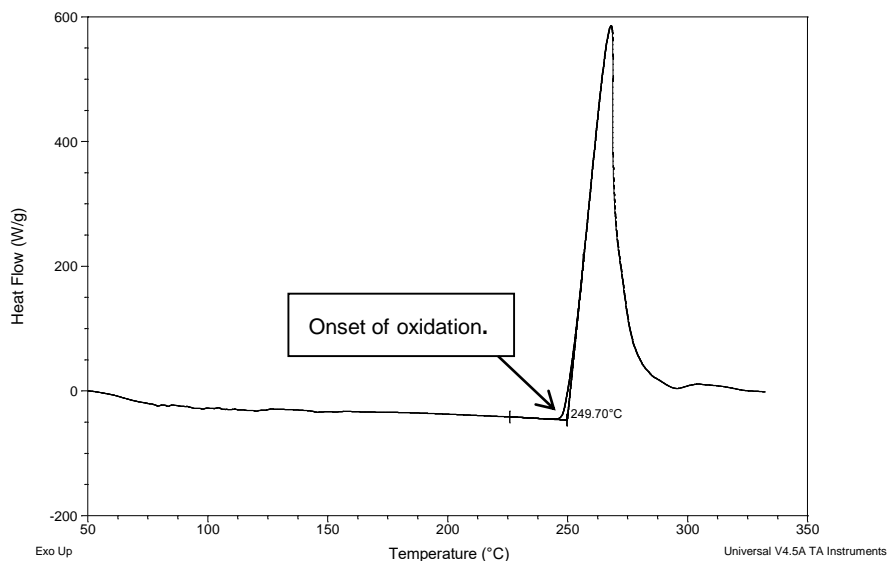


Figure 2.19 An example of a typical trace showing oxidation onset temperature.

The OOT results for each oil blend are shown in **Figure 2.20** where again, a significant increase in temperature was observed when **2.9** and **2.10** were incorporated into the blend when compared to the base oil in isolation. This data shows that the onset of oxidation can be delayed through the use of **2.9** and **2.10**.

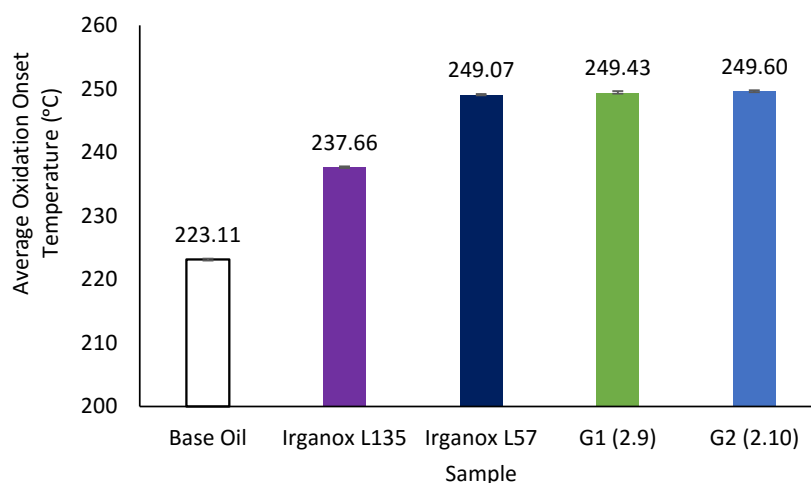


Figure 2.20 Average Oxidation Onset Temperature of 0.5% w/w antioxidant-base oil samples run in duplicate.

Most significantly, these novel antioxidant dendrons reveal a performance comparable to Irganox L57. As described previously, this competitor is an aromatic amine designed to

work at much higher temperatures than the hindered phenolic compounds. This shows that not only have these compounds provided increased oxidative stability to the sample but they are capable of performing in a temperature region that was not predicted from this class of compound.

2.3 Conclusions and Future Work

A synthetic pathway has been developed to access a series of antioxidant terminated polyester dendrons. The antioxidant dendrons **2.9** and **2.10** (first and second generations, respectively) were scaled up successfully to 100 g and have shown superior thermal stability when compared to the industry standard BHT. Dendrons **2.9** and **2.10** were also soluble in a base oil and when blended at 0.5% w/w increased oxidative stability was observed in comparison to two current commercial antioxidants. In particular they exceeded the performance of the high temperature antioxidant, Irganox L57, which is a very promising result. This study would further benefit from investigations into the effect of these novel compounds in other petrochemical products such as diesel and biodiesel. There is also scope to further improve the dendritic structures described. In particular, the solubility of the polyphenols could be improved further through the use of a 'bow-tie' dendritic structure as described in **Chapter 1**. The heterofunctionality of bow-tie dendrimers would allow the incorporation of the same number of solubilising groups to antioxidant functionalities thereby improving the solubility of the higher generation phenols in a hydrocarbon medium.

2.4 Experimental

Reagents and solvents were purchased from Sigma Aldrich and used without further purification with the exception of 3-(3,5-di-*tert*-butyl-4-hydroxy-phenyl)-propionic acid which was purchased from Alfa Aesar. All solvents were dried and freshly distilled prior to use. Tetrahydrofuran (THF) was distilled under a nitrogen atmosphere from sodium and benzophenone. Dichloromethane was distilled under a nitrogen atmosphere from calcium hydride.

2.4.1 Purification and Characterisation

Thin layer chromatography (TLC) was performed on aluminium sheets coated with Merck silica gel 60 F₂₄. Spots were visualised under ultra-violet light (254 nm) with potassium permanganate as the visualising agent. Column chromatography was performed using Merck silica gel 60 (40-63 μm particle size) and a mobile phase as specified. Melting points were recorded using a Stuart MP10 melting point apparatus.

¹H NMR and ¹³C NMR spectra were recorded using either CDCl₃ or DMSO-d₆ as solvent on either a Bruker Nanobay 400 or Bruker DPX 400 operating at 400 MHz for ¹H NMR or at 100 MHz for ¹³C NMR. Infrared (IR) spectroscopic analysis was carried out using a Perkin Elmer 100 FT-IR instrument with a diamond ATR sampling attachment with samples either as solids or oils. Mass spectrometry analysis was carried out on a Thermo-Fisher Scientific Orbitrap XL LC-MS. Samples were prepared as methanol solutions (1 mg/mL) and were ionised using electrospray ionisation (ESI) and the parent mass ions are quoted.

2.4.2 Thermal and Oxidative Analysis

Thermogravimetric analysis (TGA) was performed using a TA instrument TGA 2950. TGA was carried out under a nitrogen atmosphere from ambient temperature to 500 °C at a rate of 10 °C/min using a sample of approximately 10 mg.

Pressurised differential scanning calorimetry (PDSC) was carried out at the BP Technology Centre, Pangbourne. Oxidation induction time (OIT) was performed using a TA instrument Q10 (0010-0141) or Q20 (0020P-0137). The industry standard CEC L-085-99 method was followed whereby 2 mg of sample was added to an aluminium crucible. The cell was pressurised to 100 psi with cylinder air and the temperature was raised to 50 °C and held isothermally for 5 minutes. The temperature was then ramped at 20 °C/min to 210 °C and held isothermally until the oxidation of the sample was induced. The time of onset of the exotherm minus the time taken to reach 210 °C is reported in this method. PDSC oxidation onset temperature (OOT) was performed using a TA instrument 2910. An in-house method was used whereby 0.5 mg of sample was added to an aluminium crucible. The cell was pressurised to 500 psi with cylinder air with a flow of 60 mL/min. The temperature was raised to 50 °C and allowed to stabilise before heating at 50 °C/min to 350 °C. The temperature at which the oxidation exotherm occurs is reported in this method.

2.4.3 Synthetic Methods

Preparation of 2,2,5-trimethyl-1,3-dioxane-5-carboxylic acid (2.2)

2,2-Bis(hydroxymethyl)propanoic acid (bis(MPA)) (10.00 g, 74.55 mmol), 2,2-dimethoxypropane (13.8 mL, 111.83 mmol) and *p*-toluene sulfonic acid (*p*-TsOH) (0.71 g, 3.73 mmol) were dissolved in acetone (50 mL). The reaction was stirred at room temperature for 2 hours. The catalyst was neutralised with 1.0 mL of NH₃/EtOH (50:50). The solvent was removed *in vacuo* and the resulting residue was dissolved in dichloromethane (200 mL) and extracted with two portions of water (40 mL). The organic phase was dried over magnesium sulfate (MgSO₄), filtered and then evaporated to yield 10.32 g (80%) of **2.2** as a white powder. IR (ATR) ν/cm^{-1} : 2984, 1719, 1072, 825, 717. ¹H NMR (400 MHz/CDCl₃)/ppm, δ = 1.21 (s, 3H, -CH₃), 1.42 (s, 3H, -CH₃), 1.45 (s, 3H, -CH₃), 3.68 (d, 2H, J=12.0 Hz, -CH₂O, *equatorial*), 4.20 (d, 2H, J=12.0 Hz, -CH₂O, *axial*); ¹³C NMR (100 MHz/CDCl₃)/ppm, δ = 18.4, 21.8, 25.4, 41.7, 65.9, 98.4, 180.0. Found [M+H]⁺ (C₈H₁₄O₄) m/z = 175.0964 (Calc. 175.0965).

Preparation of the first generation acetonide (2.3) and general esterification procedure

2-Ethylhexan-1-ol (7.30 mL, 46.97 mmol), 2,2,5-trimethyl-1,3-dioxane-5-carboxylic acid (**2.2**) (9.00 g, 51.67 mmol) and DPTS (60%) were dissolved in dry dichloromethane (40 mL). The solution was stirred at room temperature for 30 minutes. To the solution, *N,N'*-dicyclohexylcarbodiimide (DCC) (12.60 g, 61.06 mmol) dissolved in dry dichloromethane (40 mL) was added over 15 minutes. The reaction was left overnight at room temperature under a nitrogen atmosphere. The reaction mixture was filtered to remove the white *N,N'*-dicyclohexylurea (DCU) precipitate and the filtrate was concentrated. The crude product was dissolved in dichloromethane and washed sequentially with 0.5M HCl and saturated NaHCO₃. The organic phase was dried over MgSO₄, filtered and the solvent was removed *in vacuo* to yield a pale yellow oil. Hexane was added to the crude product and the resulting white precipitate was filtered off. The solvent was once again removed *in vacuo* and the resulting oil was purified by flash column chromatography on silica eluting with hexane/ethyl acetate (95:5) (R_f = 0.23) to afford 9.50 g (71%) of **2.3** as a thin colourless oil. IR (ATR) ν/cm^{-1} : 2934, 1735, 1158, 1080, ¹H NMR (400 MHz/CDCl₃)/ppm, δ = 0.90 (s, 3H, -CH₃), 1.21 (s, 3H, -CH₃), 1.30 (m, 6H, -CH₂), 1.39 (s, 3H, -CH₃), 1.43 (s, 3H, -CH₃), 1.61 (m, 1H, -CH) 3.63 (d, 2H,

$J=12.0$ Hz, $-\text{CH}_2\text{O}$), 4.07(m, 2H, $-\text{CH}_2$), 4.17 (d, 2H, $J=12.0$ Hz, $-\text{CH}_2\text{O}$); ^{13}C NMR (100 MHz/ CDCl_3)/ppm, $\delta = 11.0, 14.0, 18.7, 23.0, 23.8, 24.2, 28.9, 30.4, 38.8, 41.9, 66.0, 67.0, 98.0, 174.3$. Found $[\text{M}+\text{H}]^+$ ($\text{C}_{16}\text{H}_{30}\text{O}_4$) $m/z = 287.2222$ (Calc. 287.2223).

Preparation of the first generation hydroxyl linker (2.1) and general procedure for removal of acetonide protecting group

The first generation acetonide (**2.3**) (2.5 g) was dissolved in methanol (30 mL) and DOWEX 5W-X8 resin (*ca.* 2 g) was added. The solution was stirred at 50 °C and monitored by TLC analysis, using hexane/ethyl acetate (80:20) as the eluent, until the deprotection was complete. The resin was filtered off and the filtrate was concentrated *in vacuo* to yield 2.02 g (94%) of **2.1** as a colourless viscous oil. IR (ATR) ν/cm^{-1} : 3458, 2694, 1722, 1042. ^1H NMR (400 MHz/ CDCl_3)/ppm, $\delta = 0.90$ (m, 6H, $-\text{CH}_3$), 1.08 (s, 3H, $-\text{CH}_3$), 1.36 (m, 8H, $-\text{CH}_2$), 1.60 (m, 1H, $-\text{CH}$) 3.08 (t, 2H, $J=16.0$ Hz, $-\text{OH}$), 3.72 (m, 2H, $-\text{CH}_2\text{O}$), 3.88 (m, 2H, $-\text{CH}_2\text{O}$), 4.09 (m, 2H, $-\text{CH}_2$); ^{13}C NMR (100 MHz/ CDCl_3)/ppm, $\delta = 11.0, 14.0, 17.2, 22.9, 23.8, 28.9, 38.7, 49.2, 67.3, 68.0, 176.1$. $[\text{M}+\text{H}]^+$ ($\text{C}_{13}\text{H}_{27}\text{O}_4$) $m/z = 247.1909$ (Calc. 247.1910).

Preparation of the second generation acetonide (2.5)

2,2,5-Trimethyl-1,3-dioxane-5-carboxylic acid (**2.2**) (4.88 g, 28.01 mmol), first generation hydroxyl linker (**2.1**) (3.00 g, 12.18 mmol), DPTS (60%) and DCC (5.78 g, 28.01 mmol) were allowed to react according to the general esterification procedure. The crude product was purified by flash column chromatography on silica eluting with hexane/ethyl acetate (90:10) ($R_f = 0.05$) increasing polarity to (80:20) to afford 4.60 g (70%) of **2.5** as a colourless oil. IR (ATR) ν/cm^{-1} : 2966, 1734, 1079, 831. ^1H NMR (400 MHz/ CDCl_3)/ppm, $\delta = 0.89$ (m, 6H, CH_3), 1.16 (s, 6H, CH_3), 1.29-1.42 (m, 23H, CH_2 and CH_3), 1.59 (m, 1H, CH), 3.63 (d, 4H, $J=12$ Hz, CH_2), 4.05 (m, 2H, CH_2), 4.16 (d, 4H, $J=12$ Hz, CH_2), 4.33 (s, 4H, CH_2); ^{13}C NMR (100 MHz/ CDCl_3)/ppm, $\delta = 10.9, 14.0, 17.8, 18.5, 22.4, 23.7, 24.8, 28.9, 30.3, 38.7, 42.0, 46.8, 65.3, 65.9, 67.6, 98.1, 172.6, 173.5$. Found $[\text{M}+\text{Na}]^+$ ($\text{C}_{29}\text{H}_{50}\text{O}_{10}\text{Na}$) $m/z = 581.3295$ (Calc. 581.3296).

Preparation of the second generation hydroxyl linker (2.6)

The second generation acetonide (**2.5**) (3.9 g) was dissolved in methanol (40 mL). Using the general procedure for removal of the acetonide protective group a yield of 2.32 g (70%) of **2.6** was obtained as a waxy solid. (m.p 38-40 °C) IR (ATR) ν/cm^{-1} : 3284, 2940,

1733, 1240, 1115, 1044. ^1H NMR (400 MHz/ CDCl_3)/ppm, δ = 0.90 (m, 6H, $-\text{CH}_3$), 1.05 (s, 6H, $-\text{CH}_3$), 1.31 (m, 11H, $-\text{CH}_3$, $-\text{CH}_2$), 1.59 (m, 1H, $-\text{CH}$), 3.22 (m, 4H, $-\text{OH}$), 3.71 (m, 4H, $-\text{CH}_2$), 3.83 (m, 4H, $-\text{CH}_2$), 4.07 (m, 2H, $-\text{CH}_2$), 4.27 (d, 2H, $J=12$ Hz, $-\text{CH}_2$), 4.45 (d, 2H, $J=12$ Hz, $-\text{CH}_2$); ^{13}C NMR (100 MHz/ CDCl_3)/ppm, δ = 10.9, 14.0, 17.1, 18.2, 22.9, 23.7, 28.9, 30.4, 38.7, 46.5, 49.7, 64.8, 67.8, 68.1, 173.1, 175.2. Found $[\text{M}+\text{H}]^+$ ($\text{C}_{23}\text{H}_{43}\text{O}_{10}$) m/z = 479.2836 (Calc. 479.2851).

Preparation of the third generation acetonide (**2.7**)

2,2,5-Trimethyl-1,3-dioxane-5-carboxylic acid (**2.2**) (9.43 g, 54.16 mmol), second generation hydroxyl linker (**2.6**) (4.32 g, 9.03 mmol), DPTS (60%) and DCC (11.18 g, 54.16 mmol) were allowed to react according to the general esterification procedure. The crude product was purified by flash column chromatography on silica eluting with hexane/ethyl acetate (70:30) increasing polarity to (50:50) (R_f = 0.28) to afford 5.95 g (60%) of **2.7** as a white solid. IR (ATR) ν/cm^{-1} : 2937, 1723, 1079, 830. ^1H NMR (400 MHz/ CDCl_3)/ppm, δ = 0.89 (t, 6H, $J=12$ Hz, $-\text{CH}_3$), 1.15 (s, 12H, $-\text{CH}_3$), 1.27 (m, 16H, $-\text{CH}_3$), 1.35 (s, 13H, $-\text{CH}_3$ and $-\text{CH}_2$), 1.41 (s, 12H, $-\text{CH}_3$), 1.60 (m, 1H, $-\text{CH}$), 3.62 (d, 8H, $J=12$ Hz, $-\text{CH}_2$), 4.03 (m, 2H, $-\text{CH}_2$), 4.15 (d, 8H, $J=12$ Hz, $-\text{CH}_2$), 4.26 (m, 4H, $-\text{CH}_3$), 4.31 (m, 8H, $-\text{CH}_3$); ^{13}C NMR (100 MHz/ CDCl_3)/ppm, δ = 10.9, 14.1, 17.7, 18.5, 22.2, 22.9, 23.7, 25.1, 28.9, 30.3, 38.7, 42.0, 46.7, 46.8, 64.9, 66.0, 67.9, 98.1, 171.9, 172.1, 173.5. Found $[\text{M}+\text{Na}]^+$ ($\text{C}_{55}\text{H}_{90}\text{O}_{22}\text{Na}$) m/z = 1125.5800 (Calc. 1125.5824).

Preparation of the third generation hydroxyl linker (**2.8**)

The third generation acetonide (**2.7**) (3.83 g) was dissolved in methanol (40 mL). Using the general procedure for removal of the acetonide protective group a yield of 3.03 g (79%) of **2.8** was obtained as a white powder. IR (ATR) ν/cm^{-1} : 3278, 2934, 1727, 1119, 1043. ^1H NMR (400 MHz/ DMSO-d_6)/ppm, δ = 0.85 (m, 6H, $-\text{CH}_3$), 1.01 (s, 12H, $-\text{CH}_3$), 1.17 (s, 6H, $-\text{CH}_3$, $-\text{CH}_2$), 1.20 (s, 3H, $-\text{CH}_3$), 1.26 (m, 8H, $-\text{CH}_2$), 1.56 (m, 1H, $-\text{CH}$), 3.46 (m, 16H, $-\text{CH}_2$), 3.99 (m, 2H, $-\text{CH}_2$), 4.11 (m, 12H, $-\text{CH}_2$), 4.65 (t, 8H, $J=12$ Hz, $-\text{OH}$); ^{13}C NMR (100 MHz/ DMSO-d_6)/ppm, δ = 10.7, 13.8, 16.7, 16.9, 17.1, 22.3, 23.2, 28.2, 29.7, 38.0, 46.2, 46.3, 50.2, 63.6, 64.5, 65.8, 171.8, 172.0, 174.0. Found $[\text{M}+\text{H}]^+$ ($\text{C}_{43}\text{H}_{75}\text{O}_{22}$) m/z = 943.4751 (Calc. 943.4745).

Preparation of first generation diphenol (**2.9**)

3-(3,5-Di-*tert*-butyl-4-hydroxyphenyl)propanoic acid (3.40 g, 12.17 mmol), first generation hydroxyl linker (**2.1**) (1.00 g, 4.059 mmol), DPTS (60%) and DCC (2.51 g, 12.17 mmol) were allowed to react according to the general esterification procedure. The crude product was purified by flash column chromatography on silica eluting with hexane/ethyl acetate (90:10) ($R_f = 0.38$) to afford 2.34 g (75%) of **2.9** as a viscous colourless oil. IR (ATR) ν/cm^{-1} : 3644, 2957, 1734, 1435, 1135, 756. ^1H NMR (400 MHz/ CDCl_3)/ppm, $\delta = 0.88$ (m, 6H, - CH_3), 1.16 (s, 3H, - CH_3), 1.33 (m, 8H, - CH_2), 1.43 (s, 36H, - CH_3), 1.61 (m, 1H, -CH), 2.60 (t, 4H, $J = 16$ Hz, - CH_2), 2.85 (t, 4H, $J = 16.0$ Hz, - CH_2), 4.04 (m, 2H, - CH_2), 4.23 (s, 4H, - CH_2), 5.08 (s, 2H, -OH), 6.98 (s, 4H, -ArCH). ^{13}C NMR (100 MHz/ CDCl_3)/ppm, $\delta = 11.0, 14.0, 17.7, 22.9, 23.7, 28.9, 30.3, 30.9, 34.3, 36.2, 38.7, 46.4, 65.5, 67.3, 124.7, 130.8, 135.9, 252.2, 172.7, 172.9$. Found $[\text{M}+\text{H}]^+$ ($\text{C}_{47}\text{H}_{75}\text{O}_8$) $m/z = 767.5462$ (Calc. 767.5462).

Preparation of second generation tetraphenol (**2.10**)

3-(3,5-Di-*tert*-butyl-4-hydroxyphenyl)propanoic acid (4.36 g, 15.67 mmol), second generation hydroxyl linker (**2.6**) (1.50 g, 3.13 mmol), DPTS (60%) and DCC (3.23 g, 15.67 mmol) were allowed to react according to the general esterification method. The crude product was purified by flash column chromatography on silica eluting with hexane/ethyl acetate (90:10) ($R_f = 0.13$) to afford 3.39 g (72%) of **2.10** as a colourless glassy solid (m.p 42 °C). IR (ATR) ν/cm^{-1} : 3646, 2958, 1739, 1435, 1121, ^1H NMR (400 MHz/ CDCl_3)/ppm, $\delta = 0.87$ (m, 6H, - CH_3), 1.13 (s, 6H, - CH_3), 1.22 (s, 3H, - CH_3), 1.31 (m, 8H, - CH_2), 1.42 (s, 72H, - CH_3), 1.57 (m, 1H, -CH), 2.59 (t, 2H, $J = 16$ Hz, - CH_2), 2.83 (t, 2H, $J = 16$ Hz, - CH_2), 4.01 (m, 2H, - CH_2), 4.18 (s (br), 8H, - CH_2), 4.25 (s (br), 4H, - CH_2), 5.06 (s, 4H, -OH), 6.98 (s, 8H, -ArCH). ^{13}C NMR (100 MHz/ CDCl_3)/ppm, $\delta = 11.0, 14.0, 17.7, 18.2, 22.9, 23.7, 28.9, 30.3, 30.9, 34.3, 36.2, 38.7, 46.4, 65.5, 67.3, 68.1, 124.7, 130.8, 135.9, 252.2, 173.1, 175.2$. Found $[\text{M}+\text{Na}]^+$ ($\text{C}_{91}\text{H}_{138}\text{O}_{18}$) $m/z = 1541.9775$ (Calc. 1541.9883).

Preparation of third generation octaphenol (**2.11**)

3-(3,5-Di-*tert*-butyl-4-hydroxyphenyl)propanoic acid (1.48 g, 5.30 mmol), third generation hydroxyl linker (**2.8**) (0.50 g, 0.53 mmol), DPTS (60%) and DCC (1.09 g, 5.30 mmol) were allowed to react according to the general esterification method with the exception of dimethylacetamide which was used as the solvent (30 mL). The crude

reaction was purified by precipitation into water followed by the general washing procedure and flash column chromatography on silica eluting with chloroform/methanol (99.5:0.5) to afford 0.24 g (15%) of **2.11** as a white powder. IR (ATR) ν/cm^{-1} : 3640, 2954, 1736, 1435, 1120, ^1H NMR (400 MHz/ CDCl_3)/ppm, δ = 0.85 (m, 6H, - CH_3), 1.13 (s, 12H, - CH_3), 1.21 (s, 6H, - CH_3), 1.26 (s, 11H, - CH_2), 1.41 (s, 142H, *tert*-butyl - CH_3), 1.54 (m, 1H, -CH), 2.59 (t, 2H, $J=16$ Hz, - CH_2), 2.83 (t, 2H, $J=16$ Hz, - CH_2), 4.18 (m, 2H, - CH_2), 4.22 (m, 28H, - CH_2), 5.06 (s, 8H, -OH), 6.97 (s, 16H, -ArCH). ^{13}C NMR (100 MHz/ CDCl_3)/ppm, δ = 10.9, 14.1, 17.7, 22.9, 30.3, 30.8, 34.3, 36.1, 46.4, 65.0, 124.7, 130.8, 135.9, 152.2, 171.9, 172.5. Found $[\text{M}+\text{Na}]^+$ ($\text{C}_{179}\text{H}_{266}\text{O}_{38}$) m/z = 3046.8690 (Calc. 3046.8882).

2.5 References

- 1 Deloitte, *Global Automotive Consumer Study Exploring consumers' mobility choices and transportation decisions*, 2014.
- 2 PriceWaterhouseCoopers, *The automotive industry and climate change: Framework and Dynamics of the CO₂ Revolution*, 2007.
- 3 KPMG International, *The Transformation of the Automotive Industry: The Environmental Regulation Effect*, 2010.
- 4 A. Farmer and E. Sundralingam, *J. Chem. Soc.*, 1942, 121–139.
- 5 A. Farmer and E. Sundralingam, *J. Chem. Soc.*, 1943, 125–133.
- 6 J. L. Bolland, *Proc. R. Soc. A Math. Phys. Eng. Sci.*, 1946, **186**, 218–236.
- 7 C. E. Frank, *Chem. Rev.*, 1950, **46**, 155–169.
- 8 R. M. Mortier and S. T. Orszulik, *Chemistry and Technology of Lubricants*, Springer, Netherlands, 1997.
- 9 T. Mang and W. Dresel, *Lubricants and Lubrication*, Wiley-VCH, Weinheim, 2nd edn., 2007.
- 10 J. L. Bolland and G. Gee., *Trans. Faraday. Soc.*, 1946, **42**, 236–243.
- 11 E. T. Denisov and I. B. Afanas'ev, *Oxidation and Antioxidants in Organic Chemistry and Biology*, Taylor & Francis, Florida, 2005.
- 12 E. R. Booser and M. R. Fenske, *Ind. Eng. Chem.*, 1944, **44**, 1850–1856.
- 13 F. R. Mayo, *Accounts Chem. Res.*, 1968, **1**, 193–201.
- 14 G. Karavalakis, S. Stournas and D. Karonis, *Fuel*, 2010, **89**, 2483–2489.
- 15 S. Schober and M. Mittelbach, *Eur. J. Lipid Sci. Technol.*, 2004, **106**, 382–389.
- 16 H. Zweifel, *Stabilisation of Polymeric Materials*, Springer-Verlag, Berlin, 1998.
- 17 K. U. Ingold, *Chem. Rev.*, 1961, **61**, 563–589.
- 18 R. O. Dunn, *Fuel Process. Technol.*, 2005, **86**, 1071–1085.
- 19 R. Dinkov, G. Hristov, D. Stratiev and V. Boynova Aldayri, *Fuel*, 2009, **88**, 732–737.
- 20 W. W. Focke, I. van der Westhuizen, A. B. L. Grobler, K. T. Nshoane, J. K. Reddy and A. S. Luyt, *Fuel*, 2012, **94**, 227–233.

- 21 D. Lomonaco, F. J. N. Maia, C. S. Clemente, J. P. F. Mota, A. E. Costa and S. E. Mazzetto, *Fuel*, 2012, **97**, 552–559.
- 22 N. A. Santos, A. M. T. M. Cordeiro, S. S. Damasceno, R. T. Aguiar, R. Rosenhaim, J. R. Carvalho Filho, I. M. G. Santos, A. S. Maia and A. G. Souza, *Fuel*, 2012, **97**, 638–643.
- 23 K. D. Breese, J. F. Lamèthe and C. DeArmitt, *Polym. Degrad. Stab.*, 2000, **70**, 89–96.
- 24 Y. Ohkatsu and T. Nishiyama, *Polym. Degrad. Stab.*, 2000, **67**, 313–318.
- 25 T. Matsuura and Y. Ohkatsu, *Polym. Degrad. Stab.*, 2000, **70**, 59–63.
- 26 T. Kajiyama and Y. Ohkatsu, *Polym. Degrad. Stab.*, 2001, **71**, 445–452.
- 27 T. Kajiyama and Y. Ohkatsu, *Polym. Degrad. Stab.*, 2002, **75**, 535–542.
- 28 A. Torres de Pinedo, P. Peñalver and J. C. Morales, *Food Chem.*, 2007, **103**, 55–61.
- 29 N. C. Billingham and P. Garcia-Trabajo, *Polym. Degrad. Stab.*, 1995, **48**, 419–426.
- 30 H. Bergenudd, P. Eriksson, C. DeArmitt, B. Stenberg and E. Malmström Jonsson, *Polym. Degrad. Stab.*, 2002, **76**, 503–509.
- 31 WO 93/17060, Perstorp AB, A. Hult, E. Malmström, M. Johansson, K. Soerensen, 1993,
- 32 M. Johansson, T. Glauser, A. Jansson, A. Hult, E. Malmström and H. Claesson, *Prog. Org. Coatings*, 2003, **48**, 194–200.
- 33 M. Johansson, E. Malmström and A. Hult, *Prog. Org. Coatings*, 2003, **48**, 619–624.
- 34 E. Malmström, M. Johansson and A. Hult, *Macromolecules*, 1995, **28**, 1698–1703.
- 35 E. Malmström and A. Hult, *Macromolecules*, 1996, **29**, 1222–1228.
- 36 P. R. Ashton, D. W. Anderson, C. L. Brown, A. N. Shipway, J. F. Stoddart and M. S. Tolley, *Chem. Eur. J.*, 1998, **4**, 781–795.
- 37 H. Ihre, A. Hult, J. M. J. Fréchet and I. Gitsov, *Macromolecules*, 1998, **31**, 4061–4068.
- 38 S. M. Grayson and J. M. J. Fréchet, *Chem. Rev.*, 2001, **101**, 3819–3867.
- 39 H. Ihre, O. L. Padilla De Jesús and J. M. J. Fréchet, *J. Am. Chem. Soc.*, 2001, **123**, 5908–5917.
- 40 B. Neises and W. Steglich, *Angew. Chem. Int. Ed.*, 1978, 522–524.
- 41 J. S. Moore and S. I. Stupp, *Macromolecules*, 1990, **23**, 65–70.

- 42 J. F. Jansen, E. M. M. de Brabander-van den Berg and E. W. Meijer, *Science (80-.)*, 1994, **266**, 1226–1229.
- 43 F. G. A. Jansen, E. W. Meijer and E. M. M. de Brabander-van den Berg, *J. Am. Chem. Soc.*, 1995, **117**, 4417–4418.

Chapter 3

Investigating a series of alternative core monomers for dendritic antioxidants

Abstract

Antioxidant immobilisation techniques have been described in the opening chapters of this thesis and it has been revealed that through the use of dendritic macromolecules, enhanced thermal and oxidative stabilities can be achieved. This chapter reports two alternative core monomers in the form of glycerol and triethanolamine (TREN) derivatives, which were used to synthesise an alternative range of antioxidant functionalised macromolecules. When blended into a lubricant base oil at 0.5% w/w, the oxidation induction times were seen to be greater than the current industry antioxidants, Irganox L135 and Irganox L57. It was observed, in the case of the glycerol-based series, that a solubilising unit was required to ensure good dispersity within the hydrocarbon medium in order to provide enhanced stabilisation properties. However, if the number of solubilising moieties was greater than the number of antioxidant moieties the oxidation induction time was seen to decrease. The functionalised TREN antioxidant derivatives also revealed some excellent oxidation induction times, however poor solubility in the hydrocarbon medium was a significant issue. Again, a solubilising unit was introduced and dissolution within the hydrocarbon was achieved while still maintaining an oxidation induction time greater than the current industry standards.

3.1 Introduction

Chapter 2 reported the use of the *bis*(MPA) monomer in the synthesis of a series of polyester dendrons. The multi-functionality of this monomer promoted a controlled architectural growth allowing both solubilising and functional end-groups to be incorporated. The literature has also revealed the great versatility of using this monomer to produce many other functional macromolecules for a diverse array of applications,^[1,2] however, a number of alternative and inexpensive monomers can be exploited. Glycerol

(1,2,3-propanetriol) (**Figure 3.1**) has recently emerged as an important industrial chemical.

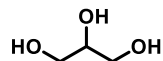


Figure 3.1 Structure of 1,2,3-propanetriol, commercially known as glycerol.

Over the last decade, biodiesel has been realised as a viable fuel alternative and glycerol is the major by-product from its production.^[3,4] Biodiesel production generates about 10% (w/w) of crude glycerol and, with the world biodiesel market continuously increasing, it has been predicted that by 2016 around 4 billion gallons of glycerol will be produced per year.^[4] This surplus has prompted the industry to search for new applications where glycerol can be used as a low-cost feedstock for functional derivatives. Uses in areas such as fuels, chemicals, automotives, pharmaceuticals and detergents have been established.^[3] Glycerol has also been used for a number of years as a monomer in the synthesis of dendritic macromolecules. In particular, biological applications have been targeted such as drug delivery systems and tissue engineering.^[5-8]

Another interesting class of dendritic macromolecules are poly(amidoamines), which are more commonly referred to as PAMAM dendrimers and were first described by Tomalia and co-workers in the 1980s.^[9] This class of dendritic macromolecule are often described as being the most intensively investigated as they were the first dendrimer family to be synthesised, characterised and commercialised.^[10] PAMAM dendrimers are particularly unique because they can be designed to mimic the structural architecture of globular proteins hence, a range of biomedical applications have been proposed such as drug delivery, molecular encapsulation and gene therapy.^[11,12] PAMAM dendrimers typically consist of an ethylenediamine core, however, more recently triethanolamine (TREN) cores (**Figure 3.2**) have been reported.^[13,14] It has been suggested that a TREN core allows greater flexibility to the branching units in comparison to other cores such as *bis*(MPA) or glycerol which can be advantageous for certain applications.

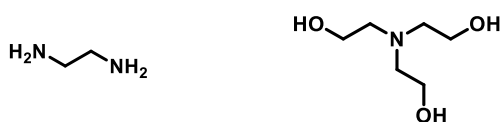


Figure 3.2 Structure of ethylenediamine and triethanolamine (TREN).

More recently, Ottaviani and co-workers^[15] reported a series of PAMAM dendrimers with a TREN core which revealed some interesting copper (II) binding characteristics. The

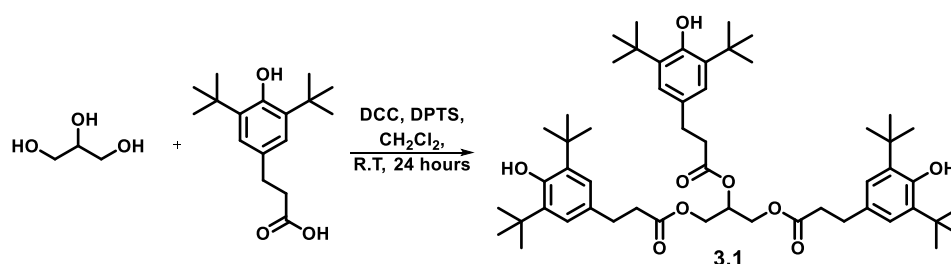
transition metal binding ability of the TREN core has been known for a number of years^[16–18] and could be particularly relevant in the design of oxidation inhibitors. It has been reported that traces of transition metal ions play a significant role in the catalysis of the oxidation process.^[19–21] The oxidative stability of a material could potentially be increased by introducing an antioxidant with both radical scavenging and metal chelation properties.

Herein, the synthesis of a series of first generation, antioxidant functionalised polyesters is described whereby glycerol or TREN derivatives were utilised as the core monomer. Solubilising alkyl chains were introduced to the core monomers to aid better dispersion within a hydrocarbon medium. When blended into a lubricant base oil and subjected to accelerated oxidative conditions, enhanced stabilisation properties were revealed when compared to current industrial antioxidants.

3.2 Results and Discussion

3.2.1 Glycerol

Glycerol consists of two primary alcohols and one secondary alcohol, both differing in reactivity, which can be exploited to introduce different functionalities onto the periphery of the core. Initial synthesis, however, began by exhaustively coupling all three hydroxyl moieties with 3-(3,5-di-*tert*-butyl-4-hydroxyphenyl)propionic acid, using *N,N'*-dicyclohexylcarbodiimide (DCC) mediated esterification to generate the first generation triphenol **3.1** (**Scheme 3.2**).



Scheme 3.1 Synthesis of the triphenol **3.1** from the reaction between glycerol and 3-(3,5-di-*tert*-butyl-4-hydroxyphenyl)propionic acid.

The triphenol (**3.1**) was yielded as a glassy solid with a low melting point of *ca.* 40 °C and its synthesis was confirmed by ¹H NMR spectroscopic analysis (**Figure 3.3**).

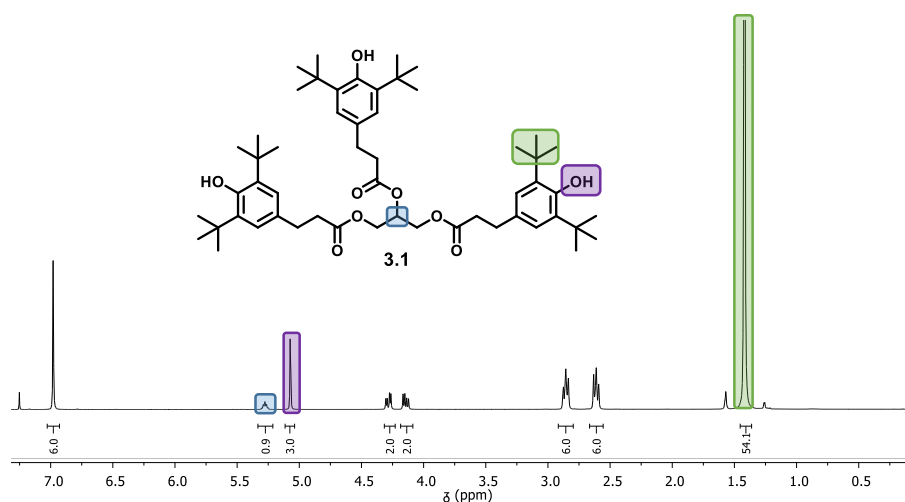
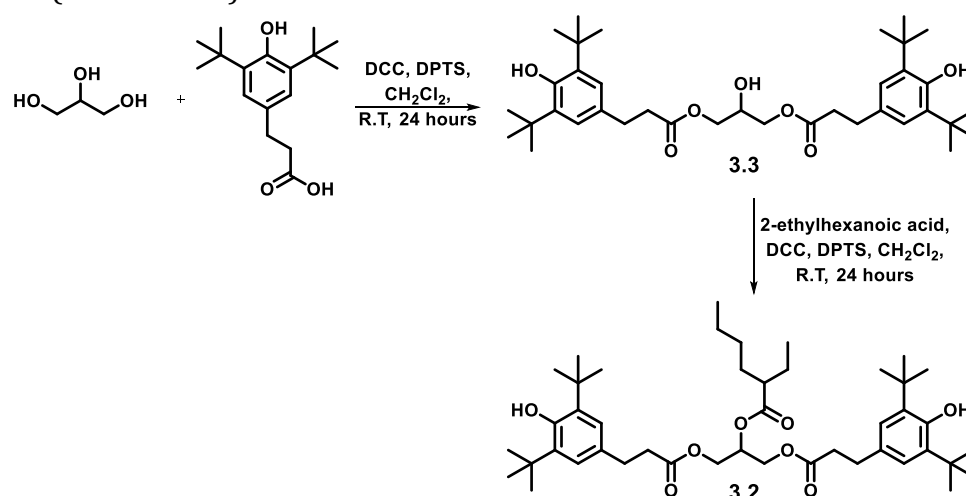


Figure 3.3 ^1H NMR spectroscopic analysis of triphenol **3.1**.

^1H NMR spectroscopic analysis revealed successful coupling of all three phenolic moieties to the glycerol core. The methyne glycerol proton resonance, observed at 5.28 ppm integrated to *ca.* 1 proton, as expected, with respect to the *tert*-butyl proton resonance at 1.42 ppm which integrated to 54 protons. In addition, a singlet resonance at 5.07 ppm was also observed, representing the three phenolic hydroxyl protons.

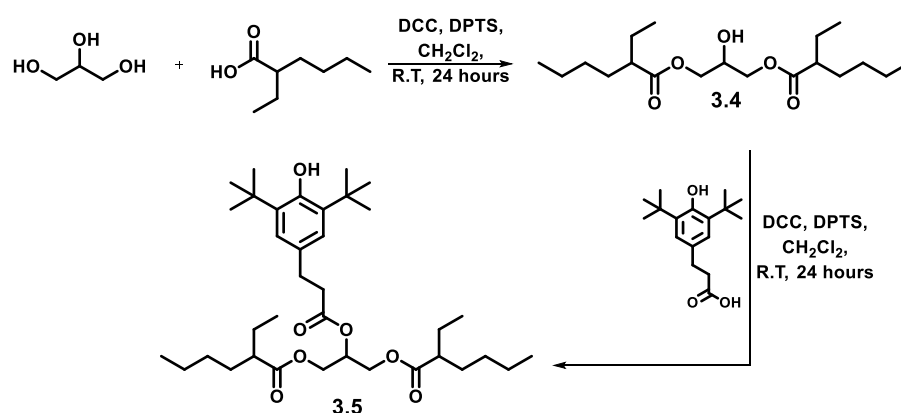
The difference in reactivity of the primary and secondary alcoholic moieties of the glycerol was then exploited to introduce a solubilising alkyl chain with the aim to improve dissolution within a hydrocarbon medium. To generate the diphenol (**3.2**), the primary alcohol moieties were first reacted with two equivalents of 3-(3,5-di-*tert*-butyl-4-hydroxyphenyl)propionic acid whereby the reaction was monitored closely by thin layer chromatography. The diester (**3.3**) was thus generated with one free hydroxyl moiety in a *ca.* 45% yield (**Scheme 3.3**).



Scheme 3.2 Synthesis of the diester (**3.3**), followed by the reaction of the remaining secondary hydroxyl to yield the diphenol (**3.2**).

Successful synthesis of the diester **3.3** was confirmed by ^1H NMR spectroscopic analysis. A significant upfield shift of the methyne glycerol proton, from 5.28 ppm in the triphenol **3.1** to 4.00 ppm in the diester **3.3** was observed. An additional resonance was also observed for the unreacted secondary hydroxyl proton at 2.20 ppm. The remaining hydroxyl moiety was reacted in another DCC mediated esterification with 2-ethylhexanoic acid. Subsequently, the diphenol **3.2** was generated as a viscous, colourless oil. The attachment of the alkyl moiety was confirmed by ^{13}C NMR spectroscopic analysis whereby additional alkyl carbon resonances were observed in the region of *ca.* 11-25 ppm. A second ester carbonyl carbon resonance was also observed at 175.5 ppm confirming that a new ester linkage had been formed between the glycerol secondary hydroxyl and 2-ethylhexanoic acid.

The final reaction scheme of the glycerol series saw the incorporation of two alkyl moieties onto the glycerol monomer. Here, the primary hydroxyl moieties were first reacted with 2-ethylhexanoic acid to yield the diester (**3.4**), where the secondary hydroxyl remained unreacted (**Scheme 3.4**).



Scheme 3.3 Synthesis of the diester (**3.4**) followed by reaction of the remaining secondary hydroxyl moiety to yield the monophenol (**3.5**).

Synthesis of the diester (**3.4**) was confirmed by FTIR spectroscopic analysis (**Figure 3.4**) whereby a hydroxyl stretch was observed at 3499 cm^{-1} in addition to a carbonyl ester absorbance at 1736 cm^{-1} . This analysis therefore confirmed the ester linkages had been achieved while preserving the secondary hydroxyl moiety intact. ^1H NMR spectroscopic analysis confirmed that the correct ratio of alkyl chains to free hydroxyls was achieved by revealing a hydroxyl resonance at 2.58 ppm which integrated to 1 proton with respect

to the 12 protons observed at 0.90 ppm representing the methyl protons of the alkyl chain.

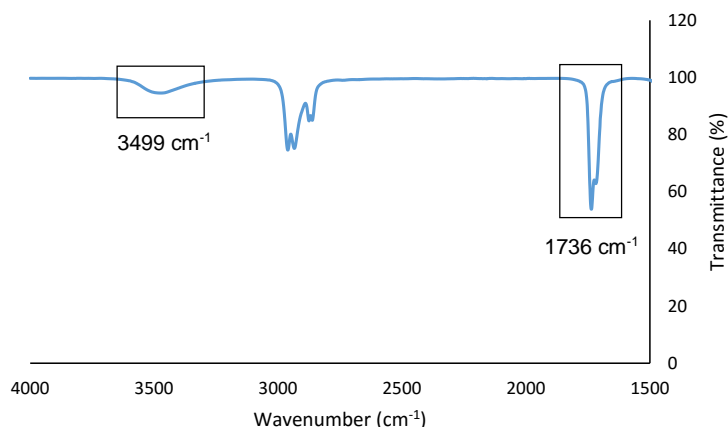


Figure 3.4 FTIR spectroscopic analysis of the diester **3.4**.

The remaining secondary hydroxyl moiety was reacted with 3-(3,5-di-*tert*-butyl-4-hydroxyphenyl)propionic acid to yield the monophenol (**3.5**). Successful addition of the sterically hindered phenol was confirmed using ^{13}C NMR spectroscopic analysis where a second ester carbonyl carbon resonance was observed at 172.1 ppm in addition to a new resonance with a high intensity at 30.3 ppm representing the *tert*-butyl carbons of the newly appended phenolic moiety. ^1H NMR spectroscopic analysis (**Figure 3.5**) further confirmed the formation of the monophenol (**3.5**).

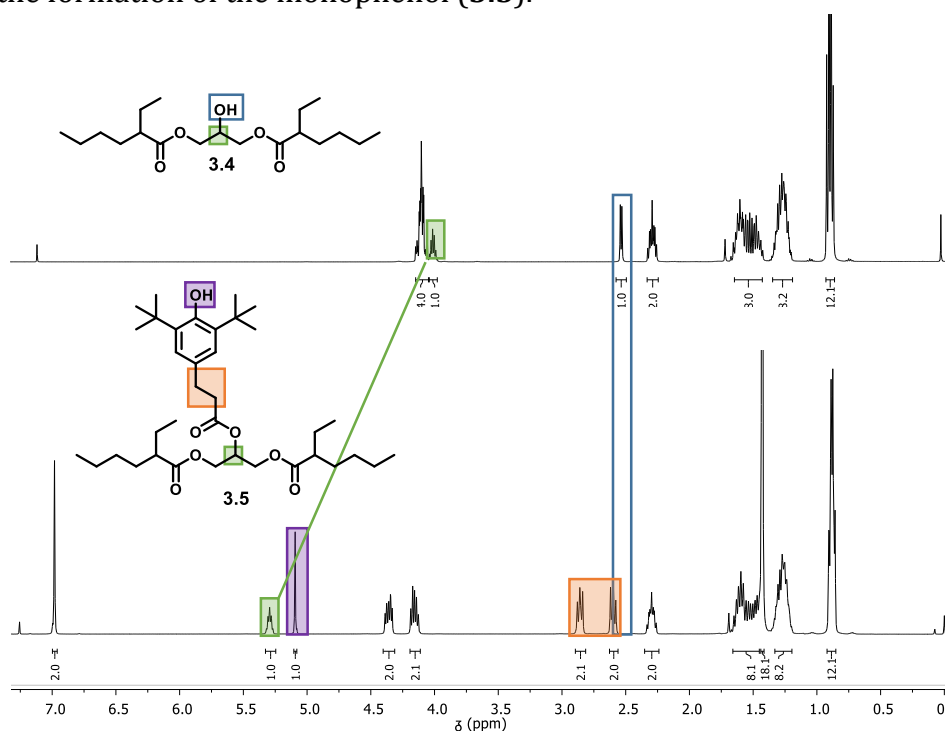


Figure 3.5 ^1H NMR spectroscopic analysis of the monophenol **3.5**.

The analysis in **Figure 3.5** revealed an upfield shift of the methyne glycerol proton from 4.09 ppm to 5.30 ppm as a result of the newly formed ester linkage on the secondary alcohol. The loss of the hydroxyl resonance at 2.57 ppm was also noted and a new resonance was revealed at 5.09 ppm which represented the phenolic hydroxyl proton and integrated to 1 with respect to the quaternary glycerol proton.

The mono-, di- and tri-phenol glycerol derivatives **3.1**, **3.2** and **3.5** were blended into the synthetic lubricant base oil, Durasyn 164, at 0.5% w/w as described in **Chapter 2**. Current commercial antioxidants were used as a comparison, where Irganox L135 is a phenolic antioxidant and Irganox L57 is an aromatic amine antioxidant (**Figure 3.6**).

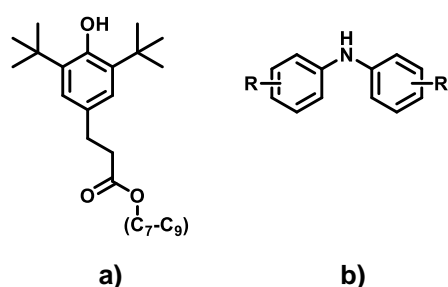


Figure 3.6 Commercial antioxidants a) Irganox L135 and b) Irganox L57 wherein R and R' can be an alkyl chain of varying length and degree of branching.

The blends were analysed using pressurised differential scanning calorimetry where oxidation induction time (OIT) and oxidation onset temperature (OOT) were the two assessment methods used. Oxidation induction time analysis revealed that the presence of **3.1**, **3.2** or **3.5** in the base oil increased the oxidative stability by a greater amount than the current commercial antioxidants (**Figure 3.7**).

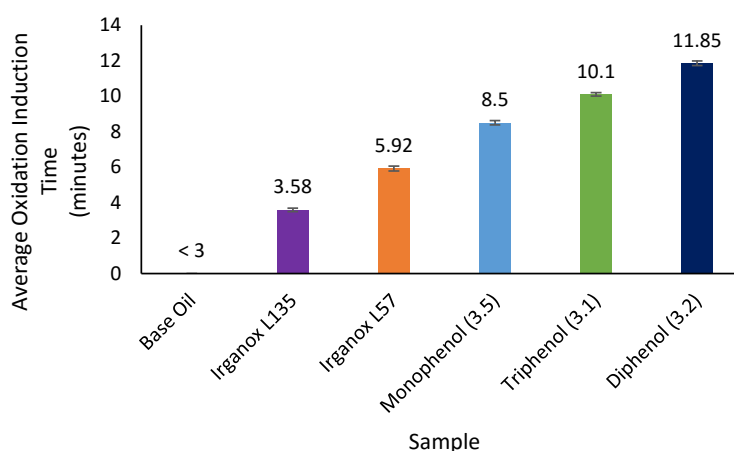


Figure 3.7 Average Oxidation induction time analysis of the glycerol series **3.1**, **3.2** and **3.5** (tested in duplicate).

By initially comparing the two monophenols, Irganox L135 and **3.5**, it was noted that by increasing the molecular weight the induction time increased. Irganox L135 and the monophenol **3.5** are structurally similar in that they both contain one active phenolic moiety in addition to solubilising functionalities which promote good dispersion within the hydrocarbon medium. The average molecular weight of Irganox L135 is *ca.* 390 whereas the molecular weight of **3.5** is *ca.* 605. This increase in molecular weight may contribute to a reduction in volatility, hence, a greater induction time was observed for the monophenol **3.5**. These results also reiterated the findings from **Chapter 2** whereby a series of polyester dendrons were revealed to provide a greater oxidative stability to a lubricant base oil than the small molecule alternatives. In addition, structure-activity relationships were investigated by comparing the triphenol **3.1** and the diphenol **3.2**. It was expected that the triphenol **3.1** would provide the greatest oxidative stability to the lubricant base oil in comparison to the diphenol **3.2** as a result of the extra active phenolic functionality. This, however, was not observed and instead the diphenol **3.2** provided the greatest stability with an oxidation induction time of *ca.* 12 minutes in comparison to *ca.* 10 minutes for the triphenol **3.1**. This induction time was also much greater than both of the commercially available antioxidants Irganox L135 and L57 and it was proposed that the diphenol **3.2** had the most effective balance between active functionalities, molecular weight and solubility. The triphenol **3.1** required prolonged heating and agitation to ensure full dissolution in the hydrocarbon whereas the diphenol **3.2** reached homogeneity more rapidly.

Oxidation onset temperature was also analysed and revealed that all three phenolic glycerol derivatives were capable of providing greater oxidative stability to the lubricious base oil than Irganox L135 (**Figure 3.8**). The diphenol **3.2**, in particular, was observed to be performing in a high temperature region alongside the aromatic amine, Irganox L57.

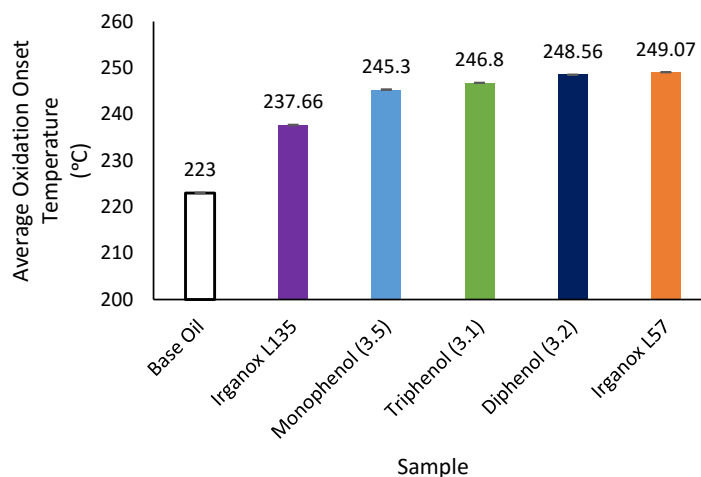


Figure 3.8 Average Oxidation onset temperature analysis of the glycerol series **3.1**, **3.2** and **3.5** (tested in duplicate).

The structures of the three antioxidant functionalised glycerol polyesters are summarised in **Table 3.1** whereby the number of active antioxidant groups and number of solubilising groups are compared.

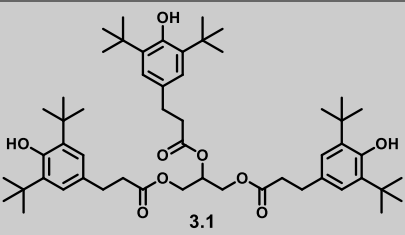
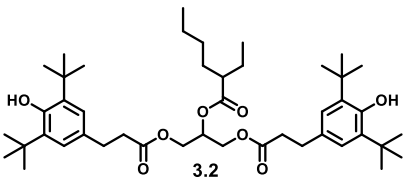
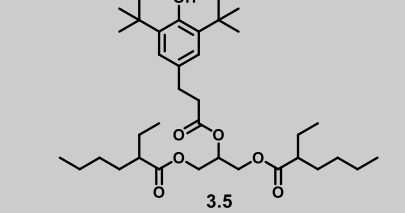
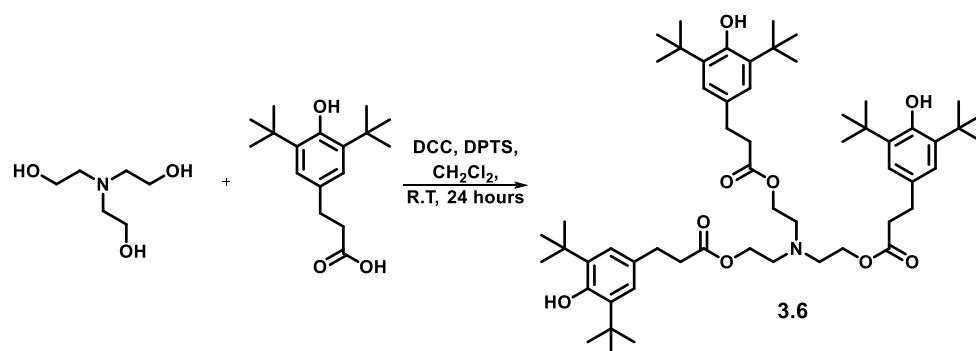
Structure	Antioxidant Active Groups	Solubilising Groups	OIT (minutes)	OOT (°C)
	3	0	10.10	246.80
	2	1	11.85	248.56
	1	2	8.50	245.3

Table 3.1 Summary of the three antioxidant functionalised glycerol polyesters **3.1**, **3.2** and **3.5**.

In conclusion, the oxidative stability analysis revealed the importance of having the correct ratio of active functionality to solubilising groups. Too little active functionality, in the case of the monophenol **3.5**, resulted in a reduced stability. Nevertheless, this stability was still an improvement in comparison to the commercially available antioxidants. Solubility was also revealed to be a key factor when targeting enhanced oxidative stabilities and the best antioxidant properties and dispersion was observed for the diphenol **3.2**. The triphenol **3.1** may theoretically be able to provide the greatest stability, however, the solubility in the hydrocarbon medium was poor and hence the radical scavenging process was thought to be hindered. The solubility could be improved by introducing an alkyl chain linker between the glycerol core monomer and the 3-(3,5-di-*tert*-butyl-4-hydroxyphenyl)propionic acid. This would ensure that while improving solubility within the hydrocarbon, the number of active functionalities is not reduced.

3.2.2 Nitrogen-centred core monomers

The second series of core monomers saw the use of triethanolamine and triisopropanolamine which provided a nitrogen at the centre of the macromolecule. It was envisaged that the nitrogen core may have been able to provide some additional activity such as transition metal chelation. Triethanolamine has been reported as an effective copper chelator in the literature.^[16-18] Triethanolamine was first reacted with 3-(3,5-di-*tert*-butyl-4-hydroxyphenyl)propionic acid in a DCC mediated esterification to afford the triphenol **3.6** (Scheme 3.5).

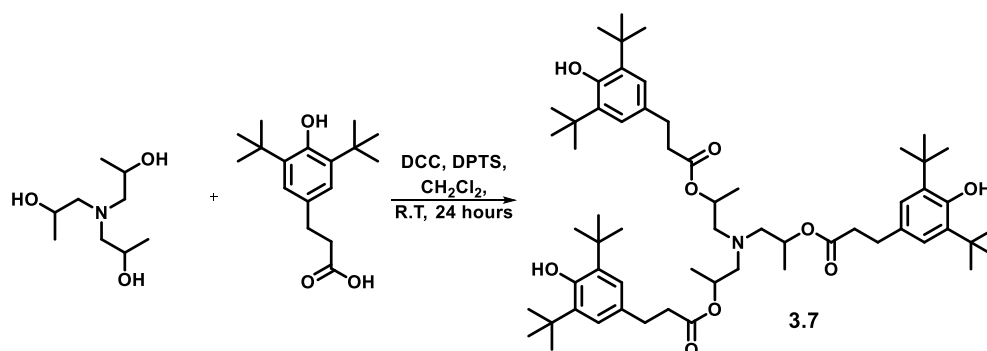


Scheme 3.4 Synthesis of the triphenol **3.6** from the reaction of triethanolamine with 3-(3,5-di-*tert*-butyl-4-hydroxyphenyl)propionic acid.

Successful coupling of the 3-(3,5-di-*tert*-butyl-4-hydroxyphenyl)propionic acid to the triethanolamine was achieved and confirmed using ¹H NMR spectroscopic analysis. The analysis revealed a singlet resonance at 5.06 ppm which was characteristic to the phenolic hydroxyl proton. When this singlet resonance was integrated with respect to the

resonance observed for the methylene protons adjacent to the nitrogen core a ratio of 3:6 (phenol:methylene) was revealed. Mass spectrometric analysis also revealed the expected molecular weight of 930.6458.

Triisopropanolamine was also used as the central core monomer and it was proposed that the methyl moieties of the core would provide additional stability to both the ester functionalities and the nitrogen core in addition to improving the solubility of the final triphenol. This was once again achieved through reaction with 3-(3,5-di-*tert*-butyl-4-hydroxyphenyl)propionic acid using a DCC mediated coupling reaction (**Scheme 3.6**).



Scheme 3.5 Synthesis of the triphenol **3.7** from the reaction of triisopropanolamine with 3-(3,5-di-*tert*-butyl-4-hydroxyphenyl)propionic acid.

In comparison to the triethanolamine core, triisopropanolamine revealed a more complex ^1H NMR spectrum (**Figure 3.9**) which was a consequence of the stereogenic centre adjacent to the ester linkage in the triphenol **3.7**.

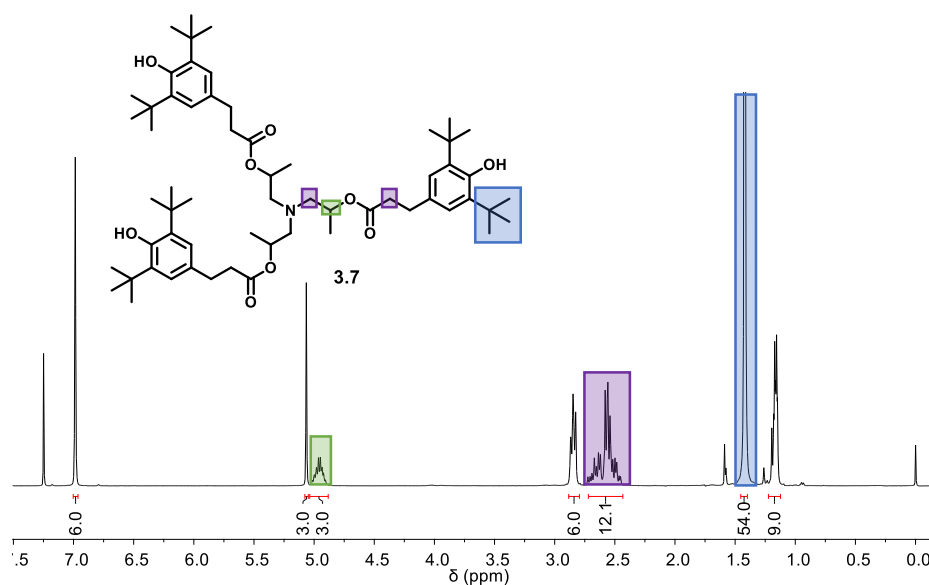


Figure 3.9 ^1H NMR spectroscopic analysis of the triphenol **3.7**.

Primarily, the synthesis of the triphenol **3.7** was confirmed by the singlet resonance observed at 1.42 ppm which integrated to 54 protons, which was expected for the six *tert*-butyl moieties. This integration was carried out with respect to the methyne proton resonance observed at 4.95 ppm which integrated to 3 protons. A complex multiplet was observed in the range of 2.4 ppm to 2.7 ppm which resulted from the splitting of the methylene protons adjacent to the nitrogen core and the chiral carbon. The stereogenic centres gave rise to different conformational isomers or rotamers which were not separable on the ^1H NMR analysis time-scale. In addition, the resonance associated with the methylene protons of 3,5-di-*tert*-butyl-4-hydroxyphenylpropionic acid were also observed in the same ppm range which further complicated the analysis. Mass spectrometric analysis confirmed the expected molecular weight was achieved whereby ($\text{C}_{60}\text{H}_{93}\text{NO}_9$) $m/z = 972.6924$.

The triphenols **3.6** and **3.7** were blended into the synthetic lubricant base oil, Durasyn 164, at 0.5% w/w as previously described and oxidation induction time and oxidation onset temperatures were analysed. Oxidation induction time analysis (**Figure 3.10**) once again revealed enhanced oxidative stabilities in comparison to the commercially available antioxidants.

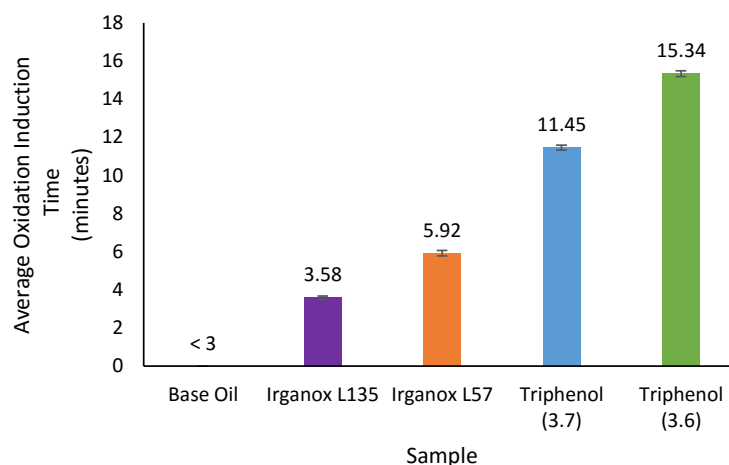
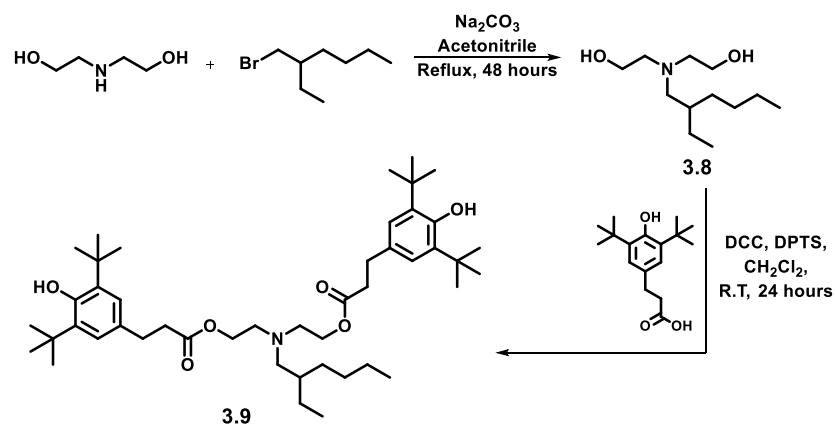


Figure 3.10 Average Oxidation induction time analysis of triphenols **3.6** and **3.7** (tested in duplicate).

The triphenol **3.6**, derived from the triethanolamine core, revealed an excellent oxidation induction time of *ca.* 15 minutes. This was an unexpected result as complete homogeneity of the triphenol in the lubricious base oil was not achieved. A much longer heating time over a few hours compared to *ca.* 30 minutes and a higher temperature of 70 °C compared

to 50 °C was required in order to produce the blend. At room temperature, precipitation of the antioxidant (**3.6**) was observed on the bottom of the sample container. It was therefore proposed that the large induction time may be attributed to the chemical properties of the core monomer. The nitrogen possesses a lone pair of electrons which may contribute to the radical scavenging process. Secondly, as mentioned, triethanolamine is known to chelate transition metal ions which are reported to catalyse the oxidation process. If the transition metal species can be removed from the chain reaction, the rate of degradation would be reduced. It is unknown from the scope of this work whether the triethanolamine is still capable of chelation after functionalisation with sterically hindered phenols and further studies would need to be carried out to confirm this hypothesis. The triisopropanolamine triphenol **3.7** revealed a good induction time of *ca.* 11 minutes, however, this wasn't as high as the triphenol **3.6** (*ca.* 15 minutes). This data indicates that the triethanolamine contributes to the capabilities of the antioxidant. A third proposal as to why the triphenol **3.6** revealed such a large induction time in comparison to the triphenol **3.7** is the flexibility of the triethanolamine core. It was proposed that once soluble in the lubricious base oil, the triphenol **3.6** had more flexibility around the phenolic linkages and potentially a good dispersion was achieved. The saturation point of **3.6** in Durasyn 164 may have been reached at the 0.5% w/w concentration. In comparison, the triphenol **3.7** possesses methyl groups that contribute steric hindrance around the central nitrogen and also cause a more rigid structure. Oxidation onset temperature also revealed enhanced stability properties where the triphenols **3.6** and **3.7** afforded oxidation onset temperatures of 251.14 °C and 244.70 °C, respectively.

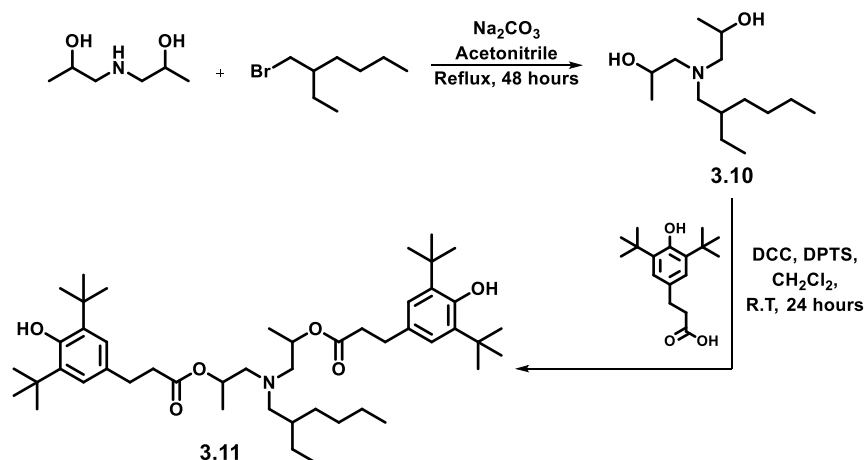
In an attempt to overcome the solubility issues encountered with the triphenols **3.6** and **3.7**, an alternative synthetic approach was targeted to allow incorporation of a solubilising alkyl chain. The synthesis was achieved by reacting diethanolamine with 2-ethylhexyl bromide to afford the diol **3.8**. DCC mediated esterification was subsequently used, as previously described, to couple the 3-(3,5-di-*tert*-butyl-4-hydroxyphenyl)propionic acid to the core to afford the diphenol **3.9** in *ca.* 70% yield.



Scheme 3.6 Incorporation of a solubilising alkyl chain onto diethanolamine to afford the diol **3.8** followed by the DCC coupling of 3-(3,5-di-*tert*-butyl-4-hydroxyphenyl)propionic acid to yield the diphenol **3.9**.

Successful synthesis of the diol **3.8** was revealed by ^1H NMR spectroscopic analysis whereby the methyl protons of the newly appended alkyl chain revealed a resonance at 0.88 ppm and integrated to 6 protons with respect to the 4 methylene protons adjacent to the nitrogen core which revealed a resonance at 3.61 ppm. In addition, a broad singlet was observed at 2.85 ppm which was characterised to the remaining hydroxyl protons. FTIR spectroscopic analysis further confirmed the presence of the hydroxyl moieties by a broad absorbance at 3334 cm^{-1} . Synthesis of the diphenol **3.9** was confirmed using ^{13}C NMR spectroscopic analysis. The analysis revealed the successful formation of the ester linkages between the diol **3.8** and 3-(3,5-di-*tert*-butyl-4-hydroxyphenyl)propionic acid by revealing a resonance at 173.1 ppm which is characteristic to carbonyl carbons. In addition, aromatic carbon resonances were also observed in the region of *ca.* 125-150 ppm. FTIR spectroscopic analysis confirmed the complete reaction of both hydroxyl moieties by revealing a new absorbance at 3642 cm^{-1} , which is characteristic to phenolic hydroxyls, and the broad hydroxyl absorbance from the diol **3.8** was no longer observed at 3334 cm^{-1} . A carbonyl absorbance was also noted at 1730 cm^{-1} further confirming the formation of ester linkages.

For a comparison against the triisopropanolamine core monomer, diisopropanolamine was also functionalised and the diphenol **3.11** was yielded *via* the pathway shown in **Scheme 3.8**.



Scheme 3.7 Incorporation of a solubilising alkyl chain onto diisopropanolamine to afford the diol **3.10** followed by the DCC coupling of 3-(3,5-di-*tert*-butyl-4-hydroxyphenyl)propionic acid to yield the diphenol **3.11**.

The synthesis of the intermediate diol **3.10** was confirmed using ^1H NMR spectroscopic analysis and revealed a similar spectrum to the intermediate diol **3.8**, however an additional resonance at 1.14 ppm was observed for the methyl protons adjacent to the hydroxyl moieties. It was also noted that the stereogenic centres adjacent to the hydroxyl moieties gave rise to more complex splitting patterns as a result of the conformational isomers. Synthesis of the diphenol **3.11** could once again be confirmed using ^{13}C NMR spectroscopic analysis whereby the ester carbonyl resonance was observed at 172.7 ppm. In addition, an intense resonance at 30.3 ppm was also observed which was characterised to the 4 *tert*-butyl moieties of the 3-(3,5-di-*tert*-butyl-4-hydroxyphenyl)propionic acid.

The diphenols **3.9** and **3.11** were blended into the synthetic lubricant base oil, Durasyn 164, at 0.5% w/w and once again the oxidation induction time and oxidation onset temperatures were analysed. An initial observation was that both **3.9** and **3.11** were fully soluble in the lubricious base oil with minimal heating required. Oxidation induction time analysis (**Figure 3.11**) revealed excellent oxidation induction times, once again, for both diphenols **3.9** and **3.11**.

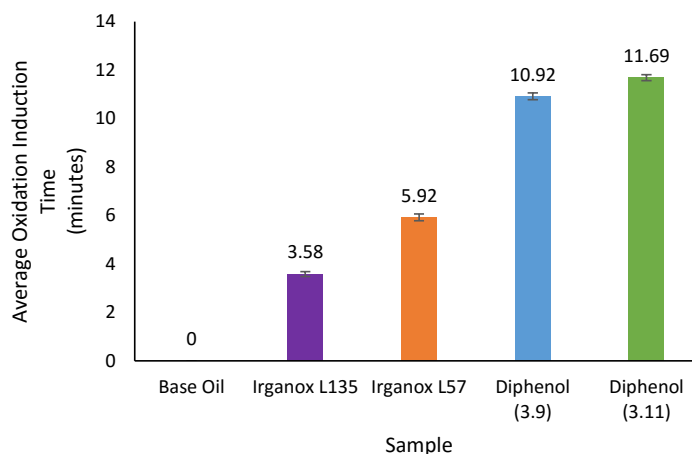


Figure 3.11 Average Oxidation induction time analysis of diphenols **3.9** and **3.11** (tested in duplicate). Interestingly, the more sterically hindered diphenol **3.11** revealed the larger induction time at *ca.* 12 minutes in comparison to the diphenol **3.9** which had an induction time of *ca.* 11 minutes. This is the opposite result to the triphenol derivatives (**3.6** and **3.7**) which would indicate that the additional steric hindrance may actually contribute to an enhanced oxidative stability. Comparison of the diphenol **3.11** and the triphenol **3.7** revealed that the replacement of the one active phenolic moiety for a solubilising alkyl chain had little to no effect on the oxidation induction time. This once again highlights the importance of balancing functionality with solubility.

Additionally, the oxidation induction time analysis has also revealed that the diphenols **3.9** and **3.11**, which contain a nitrogen core, performed in the same time region, of approximately 10-12 minutes, as the glycerol diphenol **3.2**. This would suggest that the nitrogen core is not having any additional effect on the antioxidant capabilities of the phenols. Instead it can be concluded that the benefits of using a core monomer can lead to higher molecular weights and hence reduced volatility in addition to tailored solubility characteristics. Another perspective to consider is that the presence of the solubilising alkyl chain may have disrupted the metal chelating characteristics that are known for triethanolamine. Chelation is a structurally sensitive process and it is quite possible that the structural adaptation involved in the synthesis of the diphenols **3.9** and **3.11** resulted in unfavourable metal binding. Finally, oxidation onset temperature analysis revealed very similar results of 245.41 °C and 245.89 °C for the diphenols **3.9** and **3.11**, respectively which again agreed with the analysis of the glycerol diphenol **3.2**.

3.3 Conclusions

In conclusion, a series of alternative core monomers were investigated for their use in the synthesis of dendritic phenolic antioxidants. The series of glycerol-based antioxidants revealed some interesting structure-activity relationships and highlighted the need to consider a balance between both solubility and functionality when designing new antioxidant macromolecules. This was observed from the comparison between the diphenol (**3.2**) and the triphenol (**3.1**) whereby the diphenol (**3.2**), which had improved solubility, revealed the higher induction time of *ca.* 12 minutes. A series of nitrogen core monomers were also investigated and the triphenols **3.6** and **3.7** revealed some excellent oxidation induction times in the region of *ca.* 12-15 minutes, however solubility in the lubricious base oil was an issue. As an alternative, the diphenols **3.9** and **3.11** were synthesised to include a solubilising alkyl chain and these again revealed oxidation times in the region of *ca.* 10-12 minutes. It was therefore concluded that the central core monomer does not necessarily contribute to the antioxidant capabilities but instead promotes an increase in molecular weight and hence reduced volatility. In addition, solubilising alkyl chains can be introduced easily to a core monomer and enhanced antioxidant properties are targeted. It has been revealed that solubility is just as important as antioxidant functionality when considering the design of new antioxidant macromolecules.

3.4 Experimental

Reagents and solvents were purchased from Sigma Aldrich or Fisher Scientific and used without further purification with the exception of 3-(3,5-di-*tert*-butyl-4-hydroxyphenyl)-propionic acid which was purchased from Alfa Aesar. Dichloromethane was distilled under a nitrogen atmosphere from calcium hydride. All further purification and characterisation was carried out as described in **Chapter 2**.

Preparation of propane-1,2,3-triyl tris(3-(3,5-di-*tert*-butyl-4-hydroxyphenyl)propanoate) (3.1**) and general esterification procedure.**

Glycerol (1.00 g, 10.86 mmols), 3-(3,5-di-*tert*-butyl-4-hydroxyphenyl)propionic acid (9.70 g, 34.75 mmols) and DPTS (60%) were dissolved in dry dichloromethane (60 mL) and stirred at room temperature for 30 minutes. To the solution, DCC (7.21 g, 34.75

mmols) dissolved in dry dichloromethane (40 mL) was added over 15 minutes. The reaction was left overnight at room temperature under a nitrogen atmosphere. The reaction mixture was filtered to remove the white DCU precipitate and the filtrate was concentrated. The residue was purified by flash column chromatography on silica eluting with hexane/ethyl acetate (90:10) ($R_f = 0.30$) to afford 6.64 g (70%) of **3.1** as a highly viscous yellow oil. IR (ATR) ν/cm^{-1} : 3641, 2954, 1739, 1435, 1138. ^1H NMR (400 MHz/ CDCl_3)/ppm, $\delta = 1.42(\text{s}, 54\text{H}, \text{CH}_3 \text{ tert-butyl})$, $2.61(\text{t}, 6\text{H}, J=8 \text{ Hz}, \text{Ar-CH}_2\text{CH}_2\text{-COO})$, $2.86(\text{t}, 6\text{H}, J=8 \text{ Hz}, \text{Ar-CH}_2\text{CH}_2\text{-COO})$, $4.15(\text{m}, 2\text{H}, \text{-CH}_2)$, $4.28(\text{m}, 2\text{H}, \text{-CH}_2)$, $5.07(\text{s}, 3\text{H}, \text{-OH})$, $5.28(\text{m}, 1\text{H}, \text{-CH})$, $6.98(\text{s}, 6\text{H}, \text{ArH})$. ^{13}C NMR (100 MHz/ CDCl_3)/ppm, $\delta = 30.3, 30.9, 34.3, 36.2, 62.2, 69.0, 124.8, 130.8, 136.0, 152.2, 172.3, 172.7$. Found $[\text{M}+\text{Na}]^+$ ($\text{C}_{54}\text{H}_{80}\text{O}_9$) $m/z = 895.5697$ (Calc. 895.5792).

Preparation of 2-(3,5-di-*tert*-butyl-4-hydroxyphenyl)propanoate) (3.3)

Glycerol (1.00 g, 10.86 mmol), 3-(3,5-di-*tert*-butyl-4-hydroxyphenyl)propionic acid (6.05 g, 21.72 mmol), DPTS (60%) and DCC (5.15 g, 24.98 mmol) were allowed to react according to the general esterification procedure. The crude product was purified by flash column chromatography on silica eluting with hexane/ethyl acetate (80:20) ($R_f = 0.27$) to afford 2.96 g (45%) of **3.3** as a pale yellow oil. IR (ATR) ν/cm^{-1} : 3580, 3503, 2954, 1722, 1434. ^1H NMR (400 MHz/ CDCl_3)/ppm, $\delta = 1.43(\text{s}, 36\text{H}, \text{CH}_3 \text{ tert-butyl})$, $2.65(\text{t}, 4\text{H}, J=8 \text{ Hz}, \text{Ar-CH}_2\text{CH}_2\text{-COO})$, $2.88(\text{t}, 4\text{H}, J=8 \text{ Hz}, \text{Ar-CH}_2\text{CH}_2\text{-COO})$, $4.00(\text{m}, 1\text{H}, \text{-OH})$, $4.08(\text{m}, 2\text{H}, \text{-CH}_2)$, $4.13(\text{m}, 2\text{H}, \text{-CH}_2)$, $5.09(\text{s}, 2\text{H}, \text{ArOH})$, $6.99(\text{s}, 4\text{H}, \text{ArH})$. ^{13}C NMR (100 MHz/ CDCl_3)/ppm, $\delta = 30.3, 30.9, 34.3, 36.2, 65.2, 68.3, 124.8, 130.8, 136.0, 152.3, 173.2$. Found $[\text{M}+\text{Na}]^+$ ($\text{C}_{37}\text{H}_{56}\text{O}_7$) $m/z = 635.3922$ (Calc. 635.4026).

Preparation of 2-((2-ethylhexanoyl)oxy)propane-1,3-diyl bis(3-(3,5-di-*tert*-butyl-4-hydroxyphenyl)propanoate) (3.2)

The diester **3.3** (0.5 g, 0.82 mmol), 2-ethylhexanoic acid (0.13 mL, 0.82 mmol), DPTS (60%) and DCC (0.22 g, 1.06 mmol) were allowed to react according to the general esterification procedure. The crude product was purified by flash column chromatography on silica eluting with hexane/ethyl acetate (80:20) ($R_f = 0.33$) to afford 0.47 g (76%) of **3.2** as a colourless oil. IR (ATR) ν/cm^{-1} : 3283, 2935, 1727, 1463, 1118. ^1H NMR (400 MHz/ CDCl_3)/ppm, $\delta = 0.88(\text{m}, 6\text{H}, \text{-CH}_3)$, $1.27(\text{m}, 4\text{H}, \text{-CH}_2)$, $1.45(\text{s}, 36\text{H}, \text{CH}_3$

tert-butyl), 1.50-1.65(m, 4H, -CH₂), 2.30(m, 1H, -CH), 2.60(t, 6H, J=8 Hz, Ar-CH₂CH₂-COO), 2.86(t, 6H, J=8 Hz, Ar-CH₂CH₂-COO), 4.14(m, 2H, -CH₂), 4.30(m, 2H, -CH₂), 5.08(s, 2H, -OH), 5.33(m, 1H, -CH), 6.98(s, 4H, ArH).¹³C NMR (100 MHz/CDCl₃)/ppm, δ = 11.8, 13.9, 22.6, 25.5, 29.5, 30.2, 30.8, 31.7, 34.3, 36.2, 47.3, 62.5, 68.6, 124.7, 130.8, 135.9, 152.2, 172.6, 175.5. Found [M+Na]⁺ (C₄₅H₇₀O₈) m/z = 761.4958 (Calc. 761.5071).

Preparation of 2-hydroxypropane-1,3-diyl bis(2-ethylhexanoate) (3.4)

Glycerol (1.00 g, 10.86 mmol), 2-ethylhexanoic acid (3.47 mL, 21.72 mmol), DPTS (60%) and DCC (5.15 g, 24.98 mmol) were allowed to react according to the general esterification procedure. The crude product was purified by flash column chromatography on silica eluting with hexane/ethyl acetate (90:10) (R_f = 0.25) to afford 1.12 g (30%) of **3.4** as a colourless oil. IR (ATR) ν/cm⁻¹: 3457, 2935, 1736, 1166. ¹H NMR (400 MHz/CDCl₃)/ppm, δ = 0.90(m, 12H, -CH₃), 1.20-1.34(m, 8H, -CH₂), 1.45-1.67(m, 8H, -CH₂), 2.32(m, 2H, -CH), 2.58(m, 1H, -OH), 4.10(m, 1H, -CH), 4.18(m, 4H, -CH₂).¹³C NMR (100 MHz/CDCl₃)/ppm, δ = 11.8, 13.9, 22.6, 25.4, 29.6, 31.7, 47.2, 64.8, 68.5, 176.6. Found [M+Na]⁺ (C₁₉H₃₆O₅) m/z = 367.2341 (Calc. 367.2563).

Preparation of 2-((3-(3,5-di-*tert*-butyl-4-hydroxyphenyl)propanoyl)oxy)propane-1,3-diyl bis(2-ethylhexanoate) (3.5)

The diester **3.4** (0.3 g, 0.81 mmol), 3-(3,5-di-*tert*-butyl-4-hydroxyphenyl)propionic acid (0.34 g, 1.21 mmol), DPTS (60%) and DCC (0.25 g, 1.21 mmol) were allowed to react according to the general esterification procedure. The crude product was purified by flash column chromatography on silica eluting with hexane/ethyl acetate (90:10) (R_f = 0.34) to afford 0.38 g (75%) of **3.5** as a colourless oil. IR (ATR) ν/cm⁻¹: 3638, 2959, 1737, 1136. ¹H NMR (400 MHz/CDCl₃)/ppm, δ = 0.89(m, 12H, -CH₃), 1.20-1.33(m, 8H, -CH₂), 1.43(s, 18H, CH₃ *tert*-butyl), 1.47-1.69(m, 8H, -CH₂), 2.28(m, 2H, -CH), 2.60(t, 2H, J=8 Hz, Ar-CH₂CH₂-COO), 2.86(t, 2H, J=8 Hz, Ar-CH₂CH₂-COO), 4.16(m, 2H, -CH₂), 4.36(m, 2H, -CH₂), 5.09(s, 1H, ArOH), 5.29(m, 1H, -CH), 6.98(s, 2H, ArH).¹³C NMR (100 MHz/CDCl₃)/ppm, δ = 11.8, 13.9, 22.6, 25.4, 29.6, 30.3, 30.9, 31.6, 34.3, 36.4, 47.2, 61.7, 69.2, 124.7, 130.8, 135.9, 152.2, 172.2, 175.8. Found [M+Na]⁺ (C₃₆H₆₀O₇) m/z = 627.4231 (Calc. 627.4339).

Preparation of nitrilotris(ethane-2,1-diyl) tris(3-(3,5-di-*tert*-butyl-4-hydroxyphenyl)propanoate) (3.6)

Triethanolamine (1.0 mL, 7.52 mmol), 3-(3,5-di-*tert*-butyl-4-hydroxyphenyl)propionic acid (8.79 g, 31.58 mmol), DPTS (60%) and DCC (6.52 g, 31.58 mmol) were allowed to react according to the general esterification procedure. The crude product was purified by flash column chromatography on silica eluting with hexane/ethyl acetate (90:10) ($R_f = 0.28$) to afford 4.53 g (65%) of **3.6** as a white powder. IR (ATR) ν/cm^{-1} : 3625, 2954, 1725, 1434, 1149. ^1H NMR (400 MHz/ CDCl_3)/ppm, $\delta = 1.42(\text{s}, 54\text{H}, \text{CH}_3 \text{ tert-butyl})$, 2.59(t, 6H, $J=8$ Hz, $-\text{CH}_2$), 2.82(m, 12H, $-\text{CH}_2$), 4.12(t, 6H, $J=8$ Hz, $-\text{CH}_2$), 5.07(s, 3H, $-\text{OH}$), 6.98(s, 6H, ArH). ^{13}C NMR (100 MHz/ CDCl_3)/ppm, $\delta = 30.3, 31.0, 34.3, 36.5, 53.3, 62.6, 124.8, 131.0, 135.9, 152.2, 173.1$. Found $[\text{M}+\text{H}]^+$ ($\text{C}_{57}\text{H}_{87}\text{NO}_9$) $m/z = 930.6458$ (Calc. 930.6381).

Preparation of nitrilotris(propane-1,2-diyl) tris(3-(3,5-di-*tert*-butyl-4-hydroxyphenyl) propanoate) (3.7)

Triisopropanolamine (0.85 g, 4.49 mmol), 3-(3,5-di-*tert*-butyl-4-hydroxyphenyl) propionic acid (5.00 g, 17.96 mmol), DPTS (60%) and DCC (3.71 g, 17.96 mmol) were allowed to react according to the general esterification procedure. The crude product was purified by flash column chromatography on silica eluting with hexane/ethyl acetate (90:10) ($R_f = 0.29$) to afford 2.80 g (62%) of **3.7** as a highly viscous yellow oil. IR (ATR) ν/cm^{-1} : 3645, 2954, 1726, 1435, 1164, 755. ^1H NMR (400 MHz/ CDCl_3)/ppm, $\delta = 1.17(\text{m}, 9\text{H}, -\text{CH}_3)$, 1.42(s, 54H, $\text{CH}_3 \text{ tert-butyl}$), 2.45-2.72(m, 12H, $-\text{CH}_2$), 2.85 (t, 6H, $J=8$ Hz, $-\text{CH}_2$), 4.96(m, 3H, $-\text{CH}$), 5.07(s, 3H, $-\text{OH}$), 6.99(s, 6H, ArH). ^{13}C NMR (100 MHz/ CDCl_3)/ppm, $\delta = 18.2, 30.3, 31.0, 34.3, 36.8, 60.1, 69.0, 124.8, 131.1, 135.9, 152.2, 172.7$. Found $[\text{M}+\text{H}]^+$ ($\text{C}_{60}\text{H}_{93}\text{NO}_9$) $m/z = 972.6924$ (Calc. 972.6850).

Preparation of 2,2'-((2-ethylhexyl)azanediyl)bis(ethan-1-ol) (3.8)

2-Ethylhexyl bromide (3.40 mL, 19 mmols) was added to diethanolamine (2.00 g, 19.00 mmols) and sodium carbonate (2.42 g, 23.00 mmols) in acetonitrile. The reaction was heated under reflux for 48 hours. Upon completion, the reaction was cooled to room temperature, filtered and the solvent was removed *in vacuo*. The crude product was purified by flash column chromatography on silica eluting with chloroform/methanol (80:20) ($R_f = 0.17$) to afford 1.89 g (46%) of **3.8** as a yellow oil. IR (ATR) ν/cm^{-1} : 3320, 2922, 1456, 1036. ^1H NMR (400 MHz/ CDCl_3)/ppm, $\delta = 0.88(\text{m}, 6\text{H}, \text{CH}_3)$, 1.26-1.46(m, 9H,

-CH,-CH₂), 2.33(m, 2H, -CH₂), 2.59-2.67,(m, 4H, CH₂) 2.85(s, 2H, -OH), 3.61(t, 4H, J=4 Hz, -CH₂).¹³C NMR (100 MHz/CDCl₃)/ppm, δ = 10.6, 14.1, 23.2, 24.2, 28.8, 31.1, 37.3, 56.8, 59.6, 59.7. Found [M+H]⁺ (C₁₂H₂₇NO₂) m/z = 218.2113 (Calc. 218.2042).

Preparation of ((2-ethylhexyl)azanediyl)bis(ethane-2,1-diyl) bis(3-(3,5-di-*tert*-butyl-4-hydroxyphenyl)propanoate) (3.9)

The diol **3.8** (0.5 g, 2.30 mmol), 3-(3,5-di-*tert*-butyl-4-hydroxyphenyl)propionic acid (1.48 g, 5.30 mmol), DPTS (60%) and DCC (1.09 g, 5.30 mmol) were allowed to react according to the general esterification procedure. The crude product was purified by flash column chromatography on silica eluting with hexane/ethyl acetate (90:10) (R_f = 0.35) to afford 1.24 g (73%) of **3.9** as a viscous yellow oil. IR (ATR) ν /cm⁻¹: 3642, 2960, 1730, 1433, 1157, 765. ¹H NMR (400 MHz/CDCl₃)/ppm, δ = 0.86(m, 6H, -CH₃), 1.23-1.32(m, 9H, -CH, -CH₂), 1.42(s, 36H, -CH₃ *tert*-butyl), 2.33(m, 2H, -CH₂), 2.59(t, 4H, J=8 Hz, -CH₂), 2.72(t, 4H, J=8 Hz, -CH₂), 2.86(t, 4H, J=8 Hz, -CH₂), 4.12(t, 4H, J=8 Hz, -CH₂), 5.07(s, 2H, -OH), 6.99(s, 4H, ArH).¹³C NMR (100 MHz/CDCl₃)/ppm, δ = 10.7, 14.2, 22.2, 24.1, 28.8, 30.3, 30.9, 31.0, 34.3, 36.5, 37.6, 53.3, 59.7, 62.6, 124.8, 131.1, 135.9, 152.2, 173.1. Found [M+H]⁺ (C₄₆H₇₅NO₆) m/z = 738.5670 (Calc. 738.5594).

Preparation of 1,1'-((2-ethylhexyl)azanediyl)bis(propan-2-ol) (3.10)

2-Ethylhexyl bromide (2.67 mL, 15.00 mmols) was added to diisopropanolamine (2.00 g, 15.00 mmols) and sodium carbonate (1.91 g, 18.00 mmols) in acetonitrile. The reaction was heated under reflux for 48 hours. Upon completion, the reaction was cooled to room temperature, filtered and the solvent was removed *in vacuo*. The crude product was purified by flash column chromatography on silica eluting with chloroform/methanol (90:10) (R_f = 0.24) to afford 1.29 g (35%) of **3.10** as a pale yellow oil. IR (ATR) ν /cm⁻¹: 3348, 2960, 1457, 1054. ¹H NMR (400 MHz/CDCl₃)/ppm, δ = 0.88(m, 6H, CH₃), 1.14(m, 6H, -CH₃), 1.26-1.46(m, 9H, -CH,-CH₂), 2.28-2.48,(m, 6H, -CH₂) 2.82(s, 2H, -OH), 3.81(m, 2H, -CH).¹³C NMR (100 MHz/CDCl₃)/ppm, δ = 10.12, 10.6, 14.1, 20.2, 20.6, 23.1, 24.1, 24.3, 24.5, 28.4, 28.7, 29.0, 31.0, 31.1, 31.3, 36.9, 37.3, 37.5, 59.9, 60.3, 61.1, 63.3, 63.5, 63.9, 64.0, 64.7, 65.5, 65.6. Found [M+H]⁺ (C₁₄H₃₁NO₂) m/z = 246.2428 (Calc. 246.2355).

Preparation of ((2-ethylhexyl)azanediyl)bis(propane-1,2-diyl) bis(3-(3,5-di-*tert*-butyl-4-hydroxyphenyl)propanoate) (3.11)

The diol **3.10** (0.5 g, 2.04 mmol), 3-(3,5-di-*tert*-butyl-4-hydroxyphenyl)propionic acid (1.31 g, 4.69 mmol), DPTS (60%) and DCC (0.96 g, 4.69 mmol) were allowed to react according to the general esterification procedure. The crude product was purified by flash column chromatography on silica eluting with hexane/ethyl acetate (90:10) ($R_f = 0.37$) to afford 1.01 g (62%) of **3.11** as a viscous yellow oil. IR (ATR) ν/cm^{-1} : 3643, 2960, 1727, 1434, 1054, 767. ^1H NMR (400 MHz/ CDCl_3)/ppm, $\delta = 0.88(\text{m}, 6\text{H}, -\text{CH}_3)$, $1.18(\text{m}, 6\text{H}, -\text{CH}_3)$, $1.22\text{-}1.37(\text{m}, 9\text{H}, -\text{CH}, -\text{CH}_2)$, $1.42(\text{s}, 36\text{H}, -\text{CH}_3 \text{ tert-butyl})$, $2.25\text{-}2.62(\text{m}, 10\text{H}, -\text{CH}_2)$, $2.85(\text{t}, 4\text{H}, J=8 \text{ Hz}, -\text{CH}_2)$, $4.96(\text{m}, 2\text{H}, -\text{CH})$, $5.06(\text{s}, 2\text{H}, -\text{OH})$, $6.99(\text{s}, 4\text{H}, \text{ArH})$. ^{13}C NMR (100 MHz/ CDCl_3)/ppm, $\delta = 10.7, 10.8, 14.2, 18.4, 18.5, 23.3, 20.0, 28.9, 30.3, 30.9, 31.0, 34.3, 36.8, 37.5, 60.0, 60.1, 60.2, 60.3, 68.9, 69.0, 69.1, 69.2, 124.8, 131.1, 135.9, 152.1, 172.7$. Found $[\text{M}+\text{H}]^+$ ($\text{C}_{48}\text{H}_{79}\text{NO}_6$) $m/z = 766.5983$ (Calc. 766.5907).

3.5 References

- 1 A. Carlmark, E. Malmström and M. Malkoch, *Chem. Soc. Rev.*, 2013, **42**, 5858–5879.
- 2 S. García-Gallego, A. M. Nyström and M. Malkoch, *Prog. Polym. Sci.*, 2015, **48**, 85–110.
- 3 M. Pagliaro, R. Ciriminna, H. Kimura, M. Rossi and C. Della Pina, *Angew. Chem. Int. Ed.*, 2007, **46**, 4434–4440.
- 4 F. Yang, M. A. Hanna and R. Sun, *Biotechnol. Biofuels*, 2012, **5**, 13.
- 5 R. Haag and F. Vögtle, *Angew. Chem. Int. Ed. Engl.*, 2004, **43**, 272–273.
- 6 H. Frey and R. Haag, *Rev. Mol. Biotechnol.*, 2002, **90**, 257–267.
- 7 M. M. K. Boysen, K. Elsner, O. Sperling and T. K. Lindhorst, *European J. Org. Chem.*, 2003, **2003**, 4376–4386.
- 8 E. R. Gillies and J. M. J. Fréchet, *Drug Discov. Today*, 2005, **10**, 35–43.
- 9 D. A. Tomalia, H. Baker, J. Dewald, M. Hall, G. Kallos, S. Martin, J. Roeck, J. Ryder and P. Smith, *Polym. J.*, 1985, **17**, 117–132.
- 10 R. Esfand and D. A. Tomalia, *Drug Discov. Today*, 2001, **6**, 427–436.
- 11 D. A. Tomalia, *Mater. Today*, 2005, **8**, 34–46.
- 12 A. W. Bosman, H. M. Janssen and E. W. Meijer, *Chem. Rev.*, 1999, **99**, 1665–1688.
- 13 J. Wu, J. Zhou, F. Qu, P. Bao, Y. Zhang and L. Peng, *Chem. Commun.*, 2005, 313.
- 14 X. Liu, J. Wu, M. Yammine, J. Zhou, P. Posocco, S. Viel, C. Liu, F. Ziarelli, M. Fermeglia, S. Pricl, G. Victorero, C. Nguyen, P. Erbacher, J.-P. Behr and L. Peng, *Bioconjug. Chem.*, 2011, **22**, 2461–2473.
- 15 M. F. Ottaviani, M. Changiotti, A. Fattori, C. Coppola, P. Posocco, E. Laurini, X. Liu, C. Liu, M. Fermeglia, L. Peng and S. Pricl, *Phys. Chem. Chem. Phys.*, 2014, **16**, 685–694.
- 16 B. Sen and R. L. Dotson, *J. Inorg. Nucl. Chem.*, 1970, **32**, 2707–2716.
- 17 K. H. Whitmire, J. C. Hutchison, A. Gardberg and C. Edwards, *Inorganica Chim. Acta*, 1999, **294**, 153–162.
- 18 A. Karadag, V. T. Yilmaz and C. Thoene, *Polyhedron*, 2001, **20**, 635–641.
- 19 G. Aguilar, G. Mazzamaro and M. Rasberger, in *Chemistry and Technology of Lubricants*, eds. R. Mortier, M. Fox and S. Orszulik, Springer Science and Business Media, London, 3rd edn., 2010.

- 20 J. Dong and C. A. Migdal, in *Lubricant Additives Chemistry and Applications*, ed. L. R. Rudnick, CRC Press Taylor and Francis, London, 2nd edn., 2009, pp. 4–50.
- 21 T. Colclough, *Ind. Eng. Chem. Res.*, 1987, **26**, 1888 –1895.

Chapter 4

Investigating the synergy between diphenylamine derivatives and hindered phenolic antioxidants.

Abstract

Diphenylamines and hindered phenols have been shown to exhibit a synergistic antioxidant effect when both are present in a material. For this synergism to be effective, both compounds have to be in close proximity which is a diffusion controlled process. It was therefore hypothesised that if both diphenylamine and phenolic functionalities were incorporated into the same compound the synergistic effect would be enhanced. Three series of diphenylamine derivatives were synthesised utilising the palladium catalysed Buchwald-Hartwig amination. The diphenylamine derivatives were designed to possess carboxylic acid functionalities in either the *ortho*, *meta* or *para* position with respect to the secondary amine. Methyl or ethyl spacers were also incorporated between the carboxylic acid and the aromatic ring to further investigate structure-activity relationships. The first generation *bis*(MPA)-based diol linker (**Chapter 2**) was selectively reacted with 3-(3,5-di-*tert*-butyl-4-hydroxyphenyl)propionic acid to yield a first generation mono-phenolic linker with one free hydroxyl to which the diphenylamine derivatives were attached. The antioxidant ability of the first generation mixed amine-phenols was evaluated using differential scanning calorimetry (DSC) and when blended into a lubricant base oil, at 0.5% w/w, an increase in antioxidant performance was observed. The antioxidant performance was compared to the current industry antioxidants Irganox L135 and Irganox L57 as both individual components and as a synergistic blend together. Excellent oxidative stability was observed from **Series 3** whereby an ethyl spacer was introduced between the diphenylamine the carboxylic acid in the *meta* or *para* position with respect to the secondary amine functionality. An impressive 52% increase in the oxidation induction time was observed in comparison to the current synergistic blend of Irganox L135 and Irganox L57.

4.1 Introduction

The first chapters of this thesis introduced the concept of autoxidation in organic materials and how, through the inclusion of stabilising additives, the rate of the degradation process can be reduced. Phenolic antioxidants (**Chapter 2 and 3**) are widely reported in the literature and are recognised across many industries as efficient radical scavengers, however this chapter introduces another common radical scavenger in the form of diphenylamines, examples of which are shown in **Figure 4.1**.

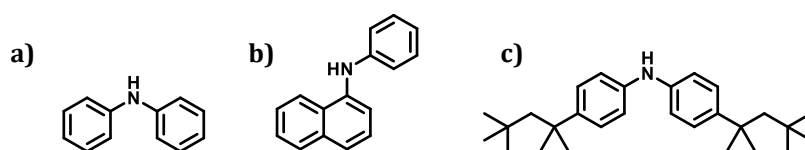
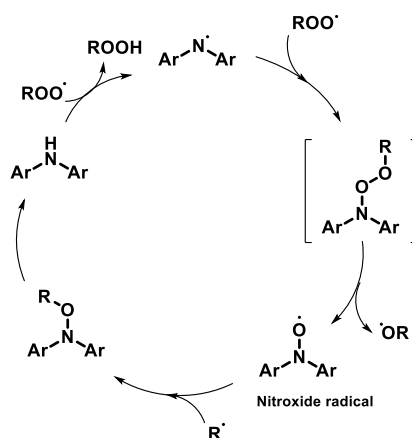


Figure 4.1 Example structures of some common arylamine antioxidants **a)** diphenylamine, **b)** *N*-phenyl-1-naphthylamine and **c)** bis(4-(1,1,3,3-tetramethylbutyl) phenyl)amine.

The scavenging behaviour of diphenylamines is comparable to that of phenols. A similar hydrogen abstraction pathway to phenolic antioxidants has been reported where at 50 °C, they can trap two peroxy radicals through donation of a hydrogen atom from their NH group to a peroxy radical.^[1-3] A unique characteristic of diphenylamines, however, is that at temperatures >100 °C, their stoichiometric factors increase.^[4] An example of which was reported in 1978 when an unbelievable stoichiometry of $n = 41$ was revealed from the diphenylamine inhibited oxidation of paraffin oil at 130 °C.^[5] After much debate, this dramatic observation was later attributed by Korcek and co-workers to a cyclical scavenging pathway involving the regeneration of the original amine (**Scheme 4.1**).^[6]



Scheme 4.1 Proposed mechanism of catalytic activity of diphenylamine radical scavengers.^[6]

The regeneration was found to be part of a catalytic cycle which relied upon the formation of the corresponding nitroxide. The nitroxide was an intermediate that had been proposed much earlier on by Thomas and co-workers,^[7-9] however the proof of the reduction of diarylnitroxides to regenerate the corresponding diamines provided an explanation for the high stoichiometric values at temperatures >100 °C.^[6] A survey of the literature does not reveal any disagreement of this proposed mechanism, however, it has been noted that there is still much to learn about the kinetics and mechanisms surrounding the radical scavenging pathways of diphenylamines.^[4,10] While data has been reported on improving the individual antioxidant capabilities of hindered phenols and diphenylamines through structural variations, very little research, has been reported on the inclusion of both functional groups within the same compound. The closest example found of a mixed phenol and amine derivative was reported by Valgimigli and co-workers who found by introducing nitrogen into the aromatic ring of the phenol, radical scavenging ability was improved.^[11-13] In addition, a couple of current industrial antioxidants have also made use of introducing nitrogen containing functionalities (**Figure 4.2**), however diphenylamine structures have not been described on the same compound with a sterically hindered phenol.

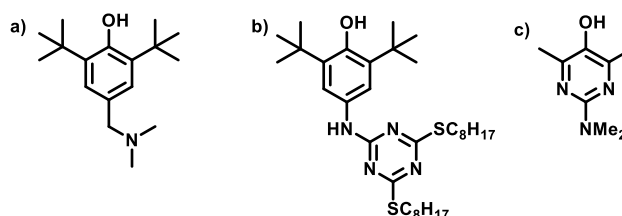


Figure 4.2 Example structures of some nitrogen containing antioxidants **a)** Ethanox 703, **b)** Irganox 565 and **c)** a pyrimidinal structure developed by the collaboration between the Valgimigli and Porter groups.^[11-13]

It is well-known, particularly in lubricant chemistry, that phenols and diphenylamines, when in the presence of each other, show a synergistic effect and greater antioxidant capabilities are observed.^[10] The term ‘synergism’ refers to the cooperative action of two or more additive species in such a way that the total effect is greater than the sum of the individual effects taken independently.^[14] Scott, in 1965, expressed this idea in terms of the molar ratio of each antioxidant whereby the replacement of a molar percentage of an antioxidant A by an antioxidant B would be predictable by the ideal straight line a’-b’ (**Figure 4.3**).^[15] In reality, the result is generally better or worse than predicted, if better

this is termed 'synergism' and is a practical advantage. If the result is worse, it is termed 'antagonism' and that ratio would have to be avoided.^[15]

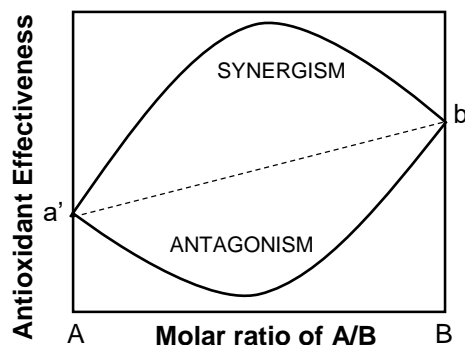
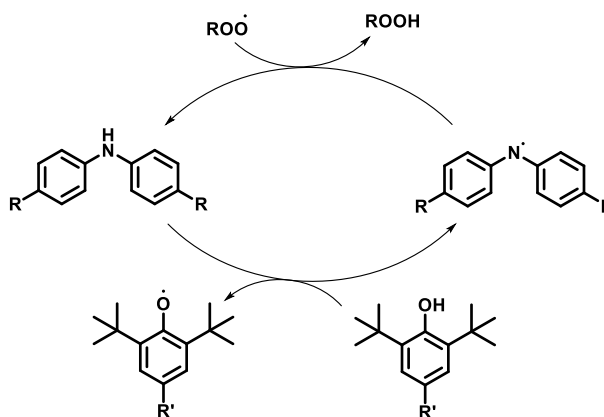


Figure 4.3 Synergism and antagonism expressed as a function of the molar ratio of antioxidant A and B.^[15]

Synergism can also be expressed mathematically by stating that synergism is obtained when $T_{1,2} > T_1 + T_2$ where T_1 and T_2 are the induction periods for each antioxidant and $T_{1,2}$ is the induction period under the action of both.^[14] The synergism between phenols and diphenylamines was reported by Meskina and co-workers in the late 1960s^[16-18] and some noteworthy combination effects have been observed over the years. The success of this combination is attributed to the regeneration of the diphenylamine by the sterically hindered phenol.^[19,20] Diphenylamines react sacrificially in the scavenging process, in comparison to sterically hindered phenols, as a result of their higher rate constants associated with the reaction of peroxy radicals (ROO^\cdot). The less efficient phenolic serves as a hydrogen donor for the aminyl radical hence allowing the parent amine to be regenerated (**Scheme 4.2**).^[21-23]



Scheme 4.2 Mechanism of synergism between a diphenylamine and a sterically hindered phenol.^[23]

The formed phenoxy radicals (ArO^\cdot) are irreversibly consumed through reaction with subsequent peroxy radicals (ROO^\cdot). The diphenylamine only starts to be consumed after the disappearance of all of the phenolic component.^[21-23] The subsequent development of synergistic packages has been one of the major developments of stabilisation technology most notably in the stabilisation of polymers, fuels and lubricants.^[15] This chapter outlines the synthesis of a series of diphenylamine derivatives which have been appended to a mono-phenolic linker to derive a series of novel mixed amine-phenol antioxidants. It was hypothesised that while synergistic effects have been found for blending separate components together there must undoubtedly be significant limitations to the process. If the literature is correct in stating that the amine antioxidant is regenerated by the phenol then the two compounds would have to be within a contact distance which is assumed to be diffusion controlled. This could potentially be hindered by the relative antioxidant concentrations within the hydrocarbon medium and also by the large array of other chemical species within the formulation not only from other additive components but also from degradation products. To alleviate these limitations it was proposed that by incorporating both functional groups on the same compound, synergism could be targeted in a more controlled manner. Herein, the synthesis of a series of mixed amine-phenol derivatives is reported where, when blended into a lubricant base oil, enhanced synergistic and antioxidant capabilities were revealed.

4.2 Results and Discussion

4.2.1 Synthesis, Characterisation and Testing – Series 1

An initial diphenylamine **4.1** was designed whereby the ester functionality was initially placed in the *meta* position (**Figure 4.4**) with respect to the secondary amine as this was believed to be the favoured position for enhanced antioxidant performance, in comparison to *ortho* or *para*.

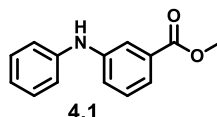
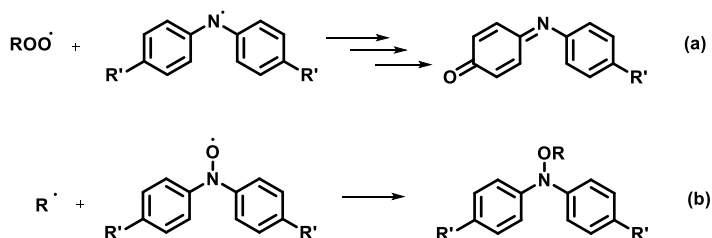


Figure 4.4 Structure of initial diphenylamine **4.1**.

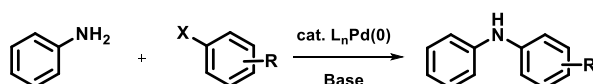
Side reactions in the radical scavenging pathway of diphenylamines results in termination of the catalytic cycle which explains the large but not infinite radical scavenging stoichiometries (**Scheme 4.3**).^[10] It has been reported that both the aminyl

radical and its nitroxide have significant spin density at the *ortho* and *para* positions of their aromatic rings allowing these side reactions to occur.^[10,24]



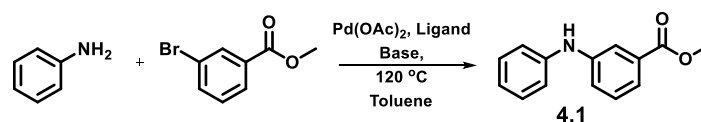
Scheme 4.3 Examples of radical scavenging termination reactions of a) aminyl radical and b) nitroxide radical substituted in the *para* position.^[10]

Palladium catalysed Buchwald-Hartwig amination was used to synthesise the diphenylamine whereby an aryl halide or sulfonate was coupled to a primary amine (**Scheme 4.4**). Buchwald and Hartwig independently developed the palladium catalysed N-arylation methodology using suitable diamine or phosphine ligands in the 1990s.^[25-28] Significant progress has since been made in improving the efficiency and applicability of palladium catalysed C-N cross-coupling reactions and numerous palladium species, ligands and reaction conditions have been reviewed in the literature.^[29-32]



Scheme 4.4 General scheme for the coupling of aniline and an aromatic halide where X represents Cl, Br, I or Ts and R, in the case of this chapter, represents a methyl ester (CO₂Me) at a position *ortho*, *meta* or *para* to the halide on the aromatic ring.

For the scope of this chapter, focus was drawn to research carried out by Csuk and co-workers which revealed the successful coupling of ester bearing arylamines, using Buchwald-Hartwig methodology, of which excellent yields of >85% were reported.^[33] Based on the findings of Csuk and co-workers, optimised reaction conditions were derived through a series of model reactions using methyl 3-bromobenzoate and aniline as the reactants (**Scheme 4.5**). Palladium acetate (Pd(OAc)₂) was chosen as the catalyst, which has been described as the most versatile palladium species, from an industrial perspective, with toluene used as the solvent.^[31]



Scheme 4.5 General synthesis of the diphenylamine **4.1**.

Two diphosphine ligands (\pm)-2,2'-bis(diphenylphosphino)-1-1'-binaphthalene (*rac.* BINAP) and bis[(2-diphenylphosphino)phenyl]ether (DPE-Phos) (**Figure 4.5**) were investigated initially using cesium carbonate (Cs_2CO_3) as the base for functional group compatibility.

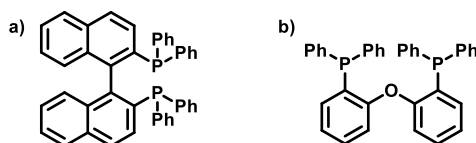


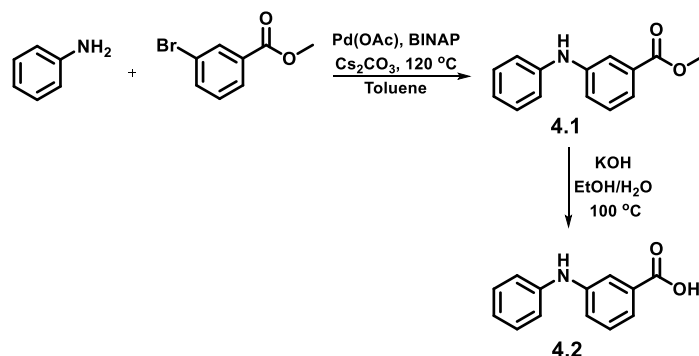
Figure 4.5 Structures of two diphosphine ligands **a)** *rac.* BINAP and **b)** DPE-Phos

The highest yield of the diphenylamine **4.1** was achieved using *rac.* BINAP (>60%) in comparison to DPE-Phos which yielded less than 15% of the target compound. Therefore, *rac.* BINAP was chosen as the ligand. A range of bases were also investigated in an attempt to increase the yield (**Table 4.1**), however, Cs_2CO_3 remained the most successful. Sodium *tert*-butoxide (NaO^tBu) is used commonly in C-N coupling reactions, however, it caused hydrolysis of the ester moiety of methyl 3-bromobenzoate and the desired compound was not observed. It was also found that de-gassing of the solvent and the pre-mixing of $\text{Pd}(\text{OAc})_2$ with the diphosphine ligand was a requirement for optimisation. These practical observations were in agreement with that reported by Csuk.^[33]

Catalyst	Ligand	Solvent	Base	Yield of (3.1)
$\text{Pd}(\text{OAc})_2$	BINAP	Toluene	Cs_2CO_3	60%
$\text{Pd}(\text{OAc})_2$	DPE-Phos	Toluene	Cs_2CO_3	<15%
$\text{Pd}(\text{OAc})_2$	BINAP	Toluene	K_2CO_3	18%
$\text{Pd}(\text{OAc})_2$	BINAP	Toluene	Triethylamine	-
$\text{Pd}(\text{OAc})_2$	BINAP	Toluene	NaO^tBu	- (Ester hydrolysis)

Table 4.1 Effect of the ligand and base on the generation of **4.1**.

The aim of this research was to introduce the diphenylamine derivatives into a compound already bearing a phenolic functionality with the hypothesis that greater synergistic effects would be revealed. Hence, a carboxylic acid functionality was targeted, *via* ester hydrolysis, to allow simple attachment of the diphenylamine to a suitable linker. The optimised synthetic procedure used to reach the initial target compound is detailed in **Scheme 4.6**.



Scheme 4.6 Synthesis of series 1 diphenylamine carboxylic acid (**4.2**).

Successful coupling of methyl 3-bromobenzoate to aniline to form **4.1** was achieved and synthesis was confirmed using ^1H NMR spectroscopic analysis where an upfield shift was observed for the aromatic H_A proton resonance from 8.17 ppm in methyl 3-bromobenzoate, to 7.72 ppm in the diphenylamine **4.1** (**Figure 4.6**). This change in chemical shift was associated with the loss of the strongly electron-withdrawing bromine and replacement with an electron donating nitrogen moiety. In addition, when the secondary amine proton resonance was integrated with respect to the methyl ester proton resonance at 3.90 ppm an integral of one was revealed indicating conversion from a primary to a secondary amine. The carboxylic acid **4.2** was yielded *via* the base catalysed ester hydrolysis of the methyl ester **4.1**. Cleavage of the methyl moiety was confirmed by ^{13}C NMR spectroscopic analysis whereby the methyl resonance at 52.2 ppm was no longer evident. In addition, a slight downfield shift was observed for the carbonyl ^{13}C resonance from 167 ppm, associated with the ester moiety, to 172 ppm for the newly formed carboxylic acid. FTIR spectroscopic analysis also revealed a broad absorbance from *ca.* 2400-2900 cm^{-1} which is characteristic of a carboxylic acid hydroxyl stretch.

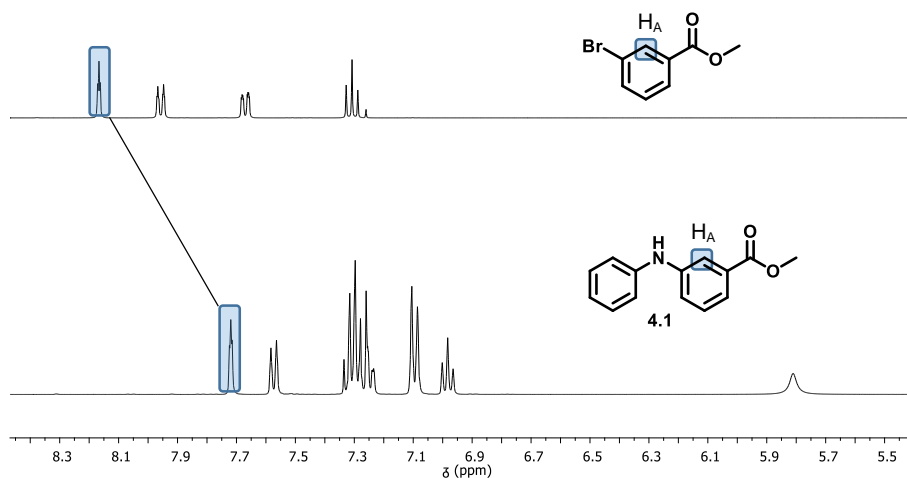
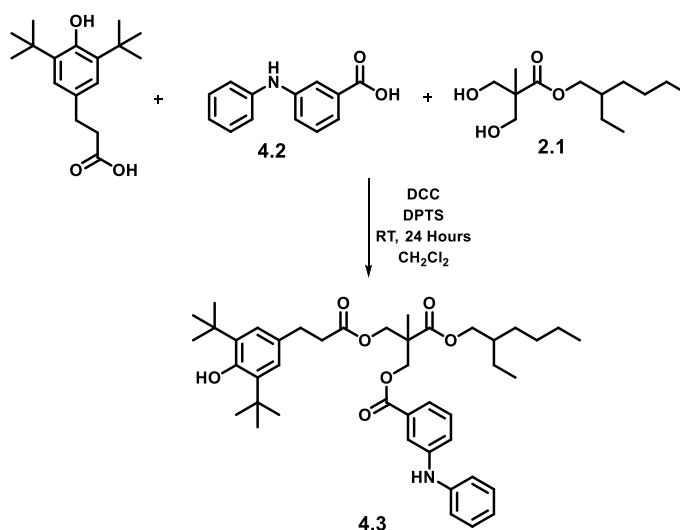


Figure 4.6 Overlay of ^1H NMR spectra to show the upfield shift of the H_A proton at 8.17 ppm from methyl 3-bromobenzoate to 7.72 ppm upon coupling to aniline.

In **Chapter 2**, a first generation hydroxyl linker was synthesised and successfully functionalised with phenolic end groups to provide antioxidant activity. The first generation hydroxyl linker was therefore used to introduce both the amine and phenol functionalities. Two synthetic procedures were targeted, both utilising *N,N'*-dicyclohexylcarbodiimide (DCC) mediated coupling. The first, shown in **Scheme 4.7**, was a statistical reaction whereby the diphenylamine **4.2**, the hindered phenol 3-(3,5-di-*tert*-butyl-4-hydroxyphenyl)propionic acid and the first generation hydroxyl linker **2.1** were reacted in a ratio of 1:1:1.



Scheme 4.7 The statistical reaction between 3-(3,5-di-*tert*-butyl-4-hydroxyphenyl)propionic acid, **4.2** and **2.1** to yield the mixed amine-phenol **4.3**.

The statistical reaction successfully yielded the desired compound **4.3**, however, competing by-products, shown in **Figure 4.7**, resulted in a yield of *ca.* 30%. Even though this yield was low, it was statistically the maximum yield that could be obtained from this reaction. Upon separation of the crude reaction mixture using flash column chromatography it was revealed that both the by-products **2.9** and **4.4** were recovered in *ca.* 30% yield. This reaction was successful in as far as the expected yields were achieved, however the scope of this work required a more controlled synthetic approach to ensure a good yield of **4.3** to enable detailed antioxidant analysis. The statistical approach may be beneficial in industry because even though compounds **2.9** and **4.4** are inevitably synthesised as by-products, they can be utilised independently as antioxidants.

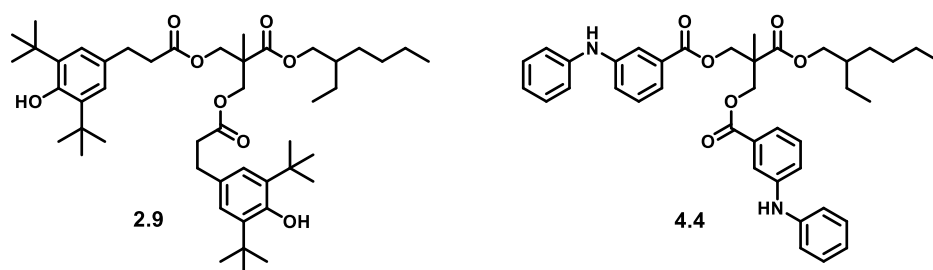
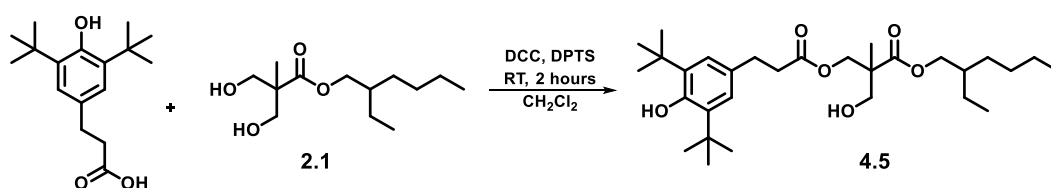


Figure 4.7 Potential products from the statistical reaction shown in **Scheme 4.7**.

An alternative dilution method was therefore utilised where a mono-phenolic hydroxyl linker was synthesised from the reaction of a single hydroxyl functionality with 3-(3,5-di-*tert*-butyl-4-hydroxyphenyl)propionic acid (**Scheme 4.8**).



Scheme 4.8 Synthesis of the mono-phenolic hydroxyl linker (**4.5**) using the first generation hydroxyl linker (**2.1**) and 3-(3,5-di-*tert*-butyl-4-hydroxyphenyl)propionic acid.

A five-fold excess of the first generation hydroxyl linker was dissolved in dichloromethane along with DCC and 4-(dimethylamino)pyridinium-4-toluenesulfonate (DPTS). The 3,5-di-*tert*-butyl-4-hydroxyphenylpropionic acid was added slowly to the reaction and the progress was monitored closely by thin layer chromatography which indicated when the reaction was complete. An excellent yield of *ca.* 90% was achieved using this methodology. Synthesis of the mono-phenol hydroxyl linker **4.5** was confirmed

by ^1H NMR spectroscopic analysis. Mono protection of the terminal hydroxyl moiety was ascertained by integrating the methylene protons adjacent to the ester linkage of the solubilising alkyl chain (a multiplet at 4.06 ppm, 2 protons) with respect to the protons of the *tert*-butyl groups of the antioxidant terminal unit (a singlet at 1.43 ppm, 18 protons). In addition, a downfield shift of the doublet resonances, associated with the methylene protons adjacent to the newly formed ester linkage, was observed from 3.70 and 3.88 ppm to 4.22 and 4.32 ppm. An upfield shift from 3.07 ppm to 2.53 ppm was observed for the remaining hydroxyl proton and the adjacent methylene protons were represented by a broad singlet at 3.57 ppm. ^1H - ^1H COSY NMR spectroscopic analysis (**Figure 4.8**) also confirmed the assignment by showing a correlation between the methylene resonance at 3.57 ppm and the hydroxyl resonance at 2.53 ppm whereas the methylene doublet resonances at 4.34 and 4.21 ppm did not reveal a coupling to the hydroxyl resonance indicating they were instead appended to the newly formed ester functionality.

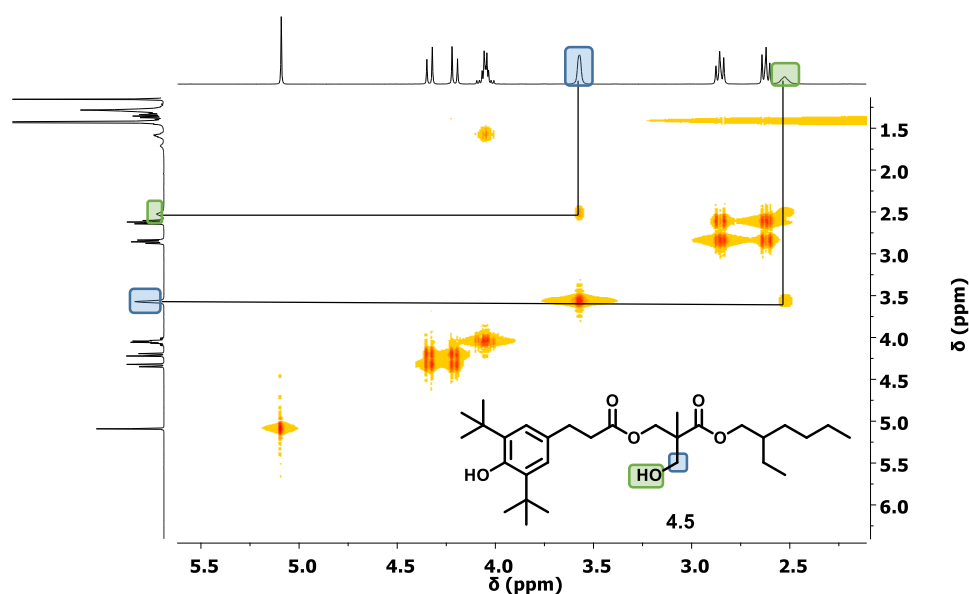
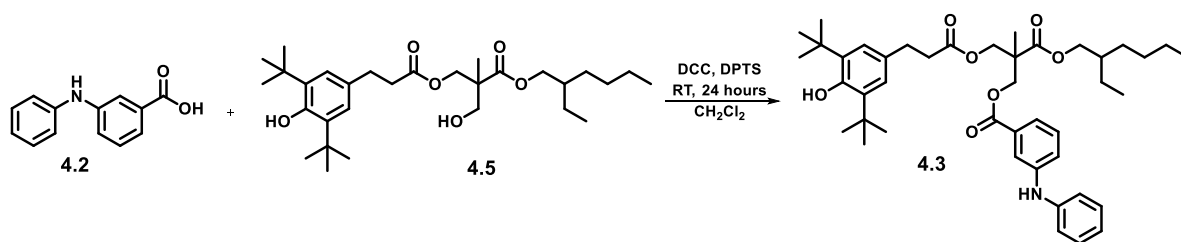


Figure 4.8 ^1H - ^1H COSY NMR spectroscopic analysis to confirm the structure of the mono-phenol hydroxyl linker (**4.5**)

The remaining hydroxyl moiety on the mono-phenol hydroxyl linker (**4.5**) was then functionalised with the diphenylamine (**4.2**) *via* DCC mediated coupling (**Scheme 4.9**). The mixed amine-phenol **4.3** was successfully synthesised with an improved yield of *ca.* 70%. The overall yield for the two-step synthetic approach was therefore *ca.* 80%.



Scheme 4.9 Synthesis of the mixed amine-phenol **4.3** via the mono-phenol hydroxyl linker **4.5**.

Mass spectrometric analysis confirmed the expected molecular weight $[M+Na]^+$ ($C_{43}H_{59}NO_7$) $m/z = 724.4184$ (Calc. 724.419). In addition, 1H NMR spectroscopic analysis revealed a 1:1 ratio of amine to phenol proton resonances at 5.86 ppm and 5.07 ppm, respectively. The loss of the hydroxyl proton resonance at 2.53 ppm was observed and a downfield shift of the adjacent methylene resonance was seen at 4.43 ppm as a result of the newly formed ester linkage to the diphenylamine (**Figure 4.9**).

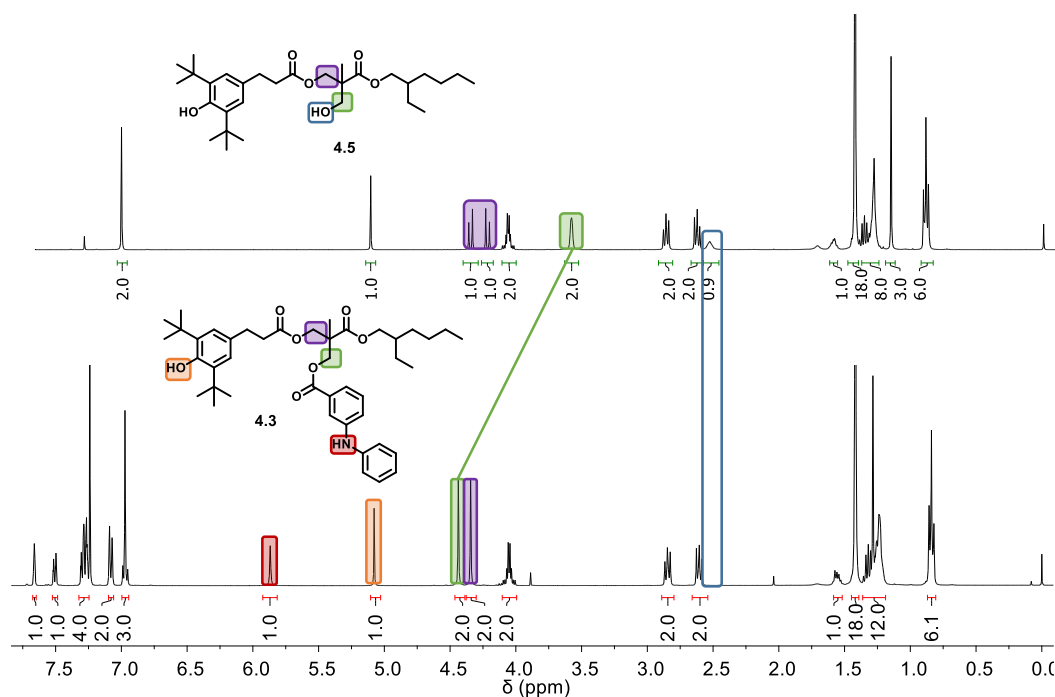
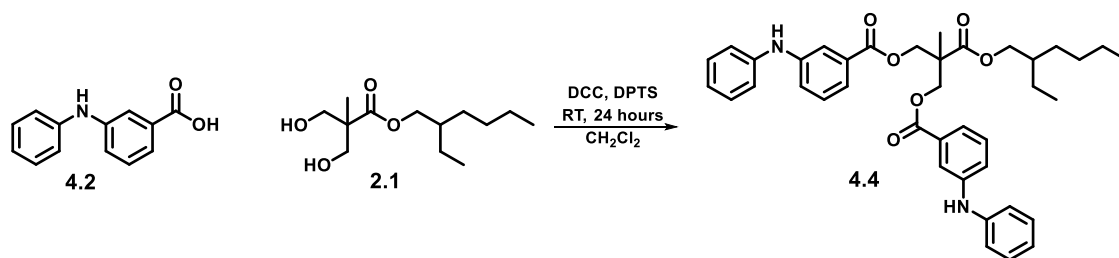


Figure 4.9 1H NMR spectra displaying the coupling of the diphenylamine **4.2** to the mono-phenolic hydroxyl linker **4.5**.

To investigate structure-activity relationships of the novel mixed amine-phenol, the *bis*(diphenylamine) **4.4** was also synthesised, as shown in **Scheme 4.10**.



Scheme 4.10 Synthesis of first generation bis(diphenylamine) **4.4**.

Synthesis of the *bis*(diphenylamine) **4.4** was confirmed using FTIR spectroscopic analysis where the loss of the broad hydroxyl absorbance at 3400 cm^{-1} was evident and a distinct absorbance at 3357 cm^{-1} characteristic of a secondary amine was revealed. Absorbances were also evident at 1516 and 1596 cm^{-1} which are characteristic of C-C aromatic stretches in addition to absorbances at 692 and 745 cm^{-1} corresponding to the C-H out of plane bends on the aromatic rings.

The *para* substituted diphenylamine, shown in **Figure 4.10**, was provided by BP Technology Centre, Pangbourne for incorporation into this study. A structural difference was that there was a methylene spacer between the carboxylic acid and the aromatic ring which diminished the deactivating effect of the ester moiety, hence improving the antioxidant capability of the amine. This carboxylic acid was attached to the mono-phenolic linker **4.5** and the first generation hydroxyl linker to yield both the mixed amine-phenol (**4.6**) and the *bis*(diphenylamine) (**4.7**) (**Table 4.2**).

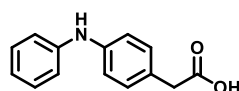


Figure 4.10 Structure of the *para* substituted diphenylamine provided by BP Technology Centre, Pangbourne.

The structures of the four potential antioxidant compounds are shown in **Table 4.2**. To further assess the antioxidant potential of the novel compounds, they were blended into the synthetic lubricant base oil, Durasyn 164, at 0.5% w/w as described in **Chapter 2**.

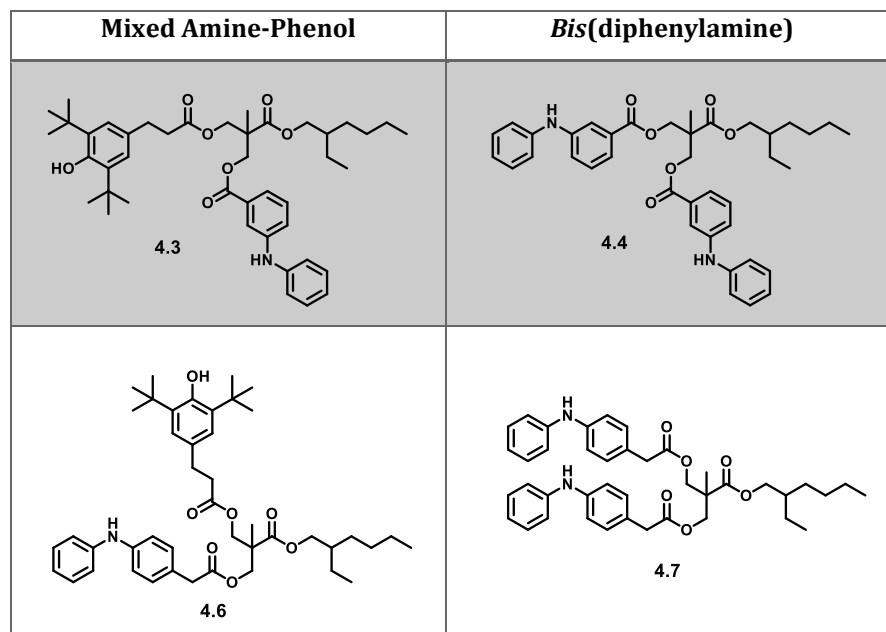


Table 4.2 Structure of the *meta* substituted amine-phenol (**4.3**) and *bis*(diphenylamine) (**4.4**) for comparison against the *para* substituted amine-phenol (**4.6**) and *bis*(diphenylamine) (**4.7**).

Current commercial antioxidants were used as a comparison, where Irganox L135 is a phenolic antioxidant and Irganox L57 is an aromatic amine antioxidant (**Figure 4.11**). The blends were analysed using pressurised differential scanning calorimetry.

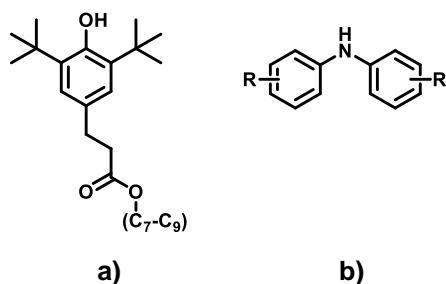


Figure 4.11 Commercial antioxidants a) Irganox L135 and b) L57.

Oxidation induction time (OIT) and oxidation onset temperature (OOT) were the two methods used. The miscibility of the *bis*(diphenylamines) **4.4** and **4.7** in the lubricant base oil was poor and full dissolution was only evident at high temperatures. When the blends were left to stand at room temperature, the *bis*(diphenylamines) precipitated out of solution and aggregated on the side of the sample container hence analysis was not possible. In comparison, the mixed amine-phenols remained in solution even though an extended heating period was required to ensure full dissolution. The results for the OIT of each oil blend are shown in **Figure 4.12**.

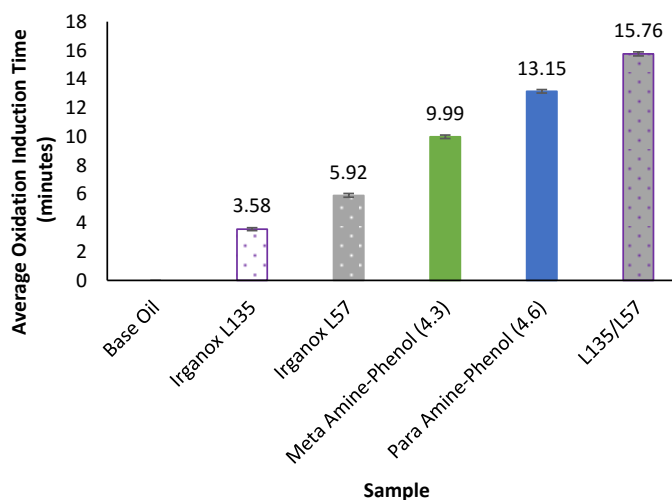


Figure 4.12 Average Oxidation induction time of 0.5% w/w antioxidant-base oil samples (tested in duplicate).

Oxidation induction time analysis revealed that the presence of **4.3** and **4.6** in the base oil has increased the oxidative stability (**Figure 4.12**). The induction time has been increased from <3 minutes for the unblended base oil to *ca.* 10-13 minutes for the blended samples. In addition, **4.3** and **4.6** have shown superiority to both of the commercial antioxidants, Irganox L135 and Irganox L57. However, the synergistic effect of having both functionalities on the same compound did not outweigh the effect of blending both together as evident in the L135/L57 blend. The methylene spacer in the mixed amine-phenol **4.6** appeared to have a positive effect on the antioxidant capabilities, showing an induction time of *ca.* 3 minutes longer than **4.3**. Oxidation onset temperature analysis was also performed and the results for each oil blend are shown in **Figure 4.13** where again, a significant increase in temperature was observed when **4.3** and **4.6** were incorporated into the blend when compared to the base oil in isolation.

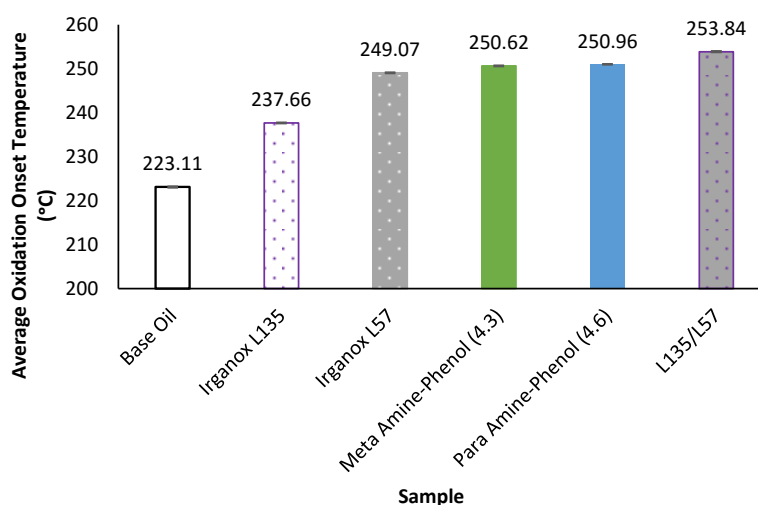
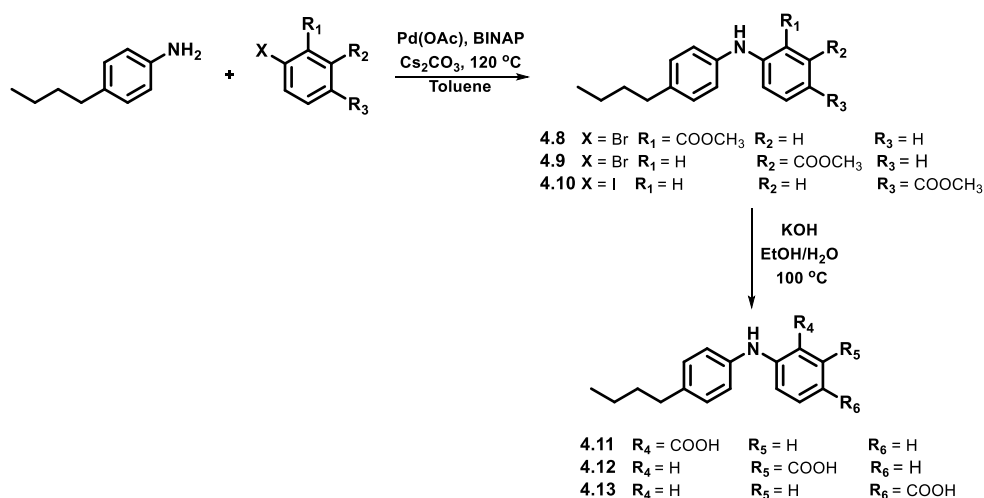


Figure 4.13 Average Oxidation onset temperature of 0.5% w/w antioxidant-base oil samples (tested in duplicate).

The results revealed these compounds do have antioxidant capabilities but physical properties such as solubility was not yet optimised. To further refine the structure of the mixed amine-phenols, two additional series of derivatives were generated.

4.2.2 Synthesis, Characterisation and Testing – Series 2

The first issue to address was the poor solubility observed for both the *bis*(diphenylamines) and the mixed amine-phenols in **Series 1**. An alkyl chain was therefore introduced by using 4-butylaniline as the starting material. The most effective position to link the diphenylamine to the hydroxyl linker was also investigated and *ortho*, *meta* and *para* carboxylic acid substituted diphenylamines were synthesised *via* the Buchwald-Hartwig amination methodology developed in **Series 1**. The esters **4.8** (*ortho*), **4.9** (*meta*) and **4.10** (*para*) were generated first, followed by base hydrolysis to yield the carboxylic acids **4.11**, **4.12** and **4.13**. The general synthesis of this series of compounds is shown in **Scheme 4.11**.



Scheme 4.11 General scheme for the synthesis of Series 2 diphenylamine derivatives.

Successful coupling of 4-butylaniline to methyl 3-bromobenzoate and methyl 4-bromobenzoate was achieved to yield the *meta* and *para* diphenylamines **4.9** and **4.10**, respectively (*ca.* 50%). The synthesis of **4.8**, using methyl 2-bromobenzoate, proved more challenging where a low yield of only *ca.* 25% was achieved. It was believed this low yield was attributed to the combination of steric hindrance surrounding the bromine from the ester moiety in the *ortho* position and through use of the bulky base Cs₂CO₃. In an attempt to improve the yield K₂CO₃ was used instead and an increase in yield to 53% was observed. The synthesis of **4.8** was confirmed using ¹H NMR spectroscopic analysis

where a dramatic downfield shift of the amine proton resonance was revealed from 3.5 ppm in 4-butylaniline (starting material) to 9.4 ppm in the diphenylamine **4.8**. This shift was associated with intramolecular hydrogen bonding between the secondary amine and the ester carbonyl as shown in **Figure 4.14**. A slight downfield shift of the amine proton resonance in **4.9** and **4.10** was observed at *ca.* 5.6 ppm.

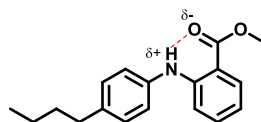


Figure 4.14 Intramolecular hydrogen bonding in the diphenylamine **4.8**.

The diphenylamine **4.8** also exhibited a characteristic *ortho* substitution proton splitting pattern as observed by ^1H NMR spectroscopic analysis (**Figure 4.15**). Consultation of the 2D NMR spectroscopic analyses, HMBC revealed a long range coupling between the apparent doublet, H_A , at 7.95 ppm and the ester carbonyl carbon at 170 ppm. Subsequent assignments were determined using ^1H - ^1H COSY NMR spectroscopic analysis which revealed proton coupling between H_A at 7.95 ppm and the apparent triplet, H_B , at 6.68 ppm. H_B also revealed coupling to the apparent triplet H_C at 7.29 ppm. The four protons associated with the 4-butylaniline ring coalesced into a single resonance at 7.17 ppm which partially masked the resonance for proton H_B .

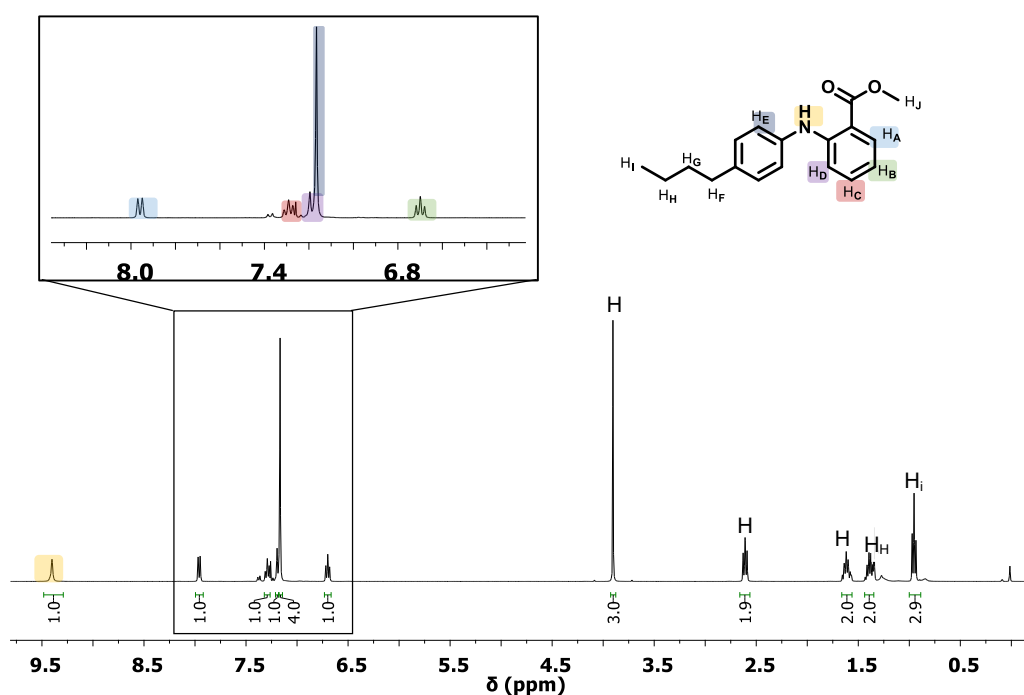


Figure 4.15 ^1H NMR spectroscopic analysis of diphenylamine **4.8**.

Subsequent ester hydrolysis yielded **4.11**, **4.12** and **4.13** in good yield (>80%). The loss of the methyl moiety was observed using ^{13}C NMR spectroscopic analysis whereby the methyl resonance at *ca.* 52 ppm, in all three compounds, was not observed. The mono-phenol hydroxyl linker (**4.5**) was functionalised with all three carboxylic acid diphenylamine derivatives (**4.11**, **4.12** and **4.13**) to yield a series of mixed amine-phenols (**4.14-16**) shown in **Table 3.3**. In addition, the *bis*(diphenylamines) were also generated from reaction with the first generation diol linker **2.1**. Synthesis of the mixed amine-phenols was confirmed using ^1H NMR spectroscopic analysis. The hydroxyl proton resonance at 2.53 ppm, of the mono-phenolic linker, was not observed for each of **4.14**, **4.15** and **4.16**.

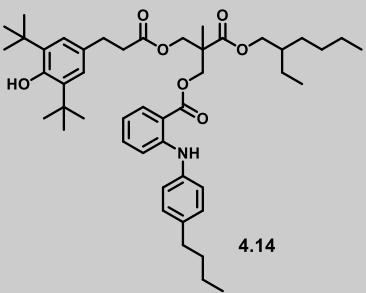
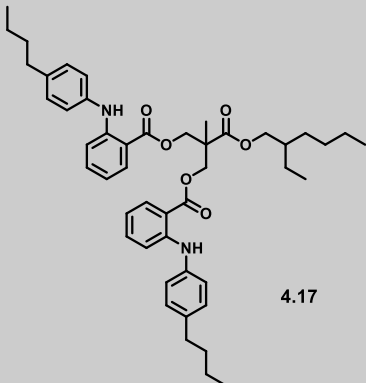
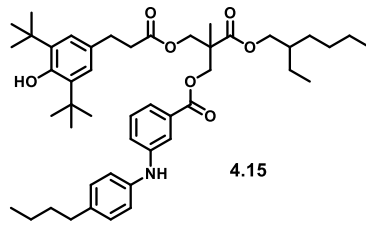
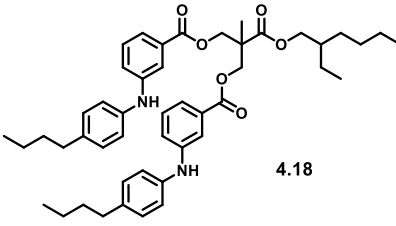
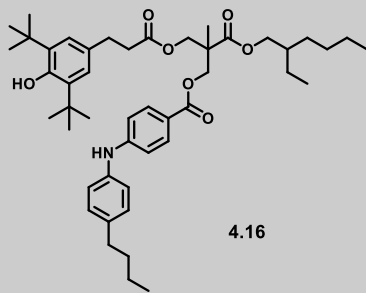
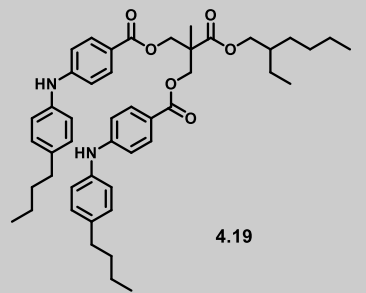
Mixed Amine-Phenol	<i>Bis</i> (diphenylamine)
 <p style="text-align: right;">4.14</p>	 <p style="text-align: right;">4.17</p>
 <p style="text-align: right;">4.15</p>	 <p style="text-align: right;">4.18</p>
 <p style="text-align: right;">4.16</p>	 <p style="text-align: right;">4.19</p>

Table 4.3 Structure of the *ortho*, *meta* and *para* substituted amine-phenols (**4.14**, **4.15** and **4.16**) and the *bis*(diphenylamines) (**4.17**, **4.18** and **4.19**) for comparison.

Full characterisation of **4.16** revealed the expected proton splitting pattern resulting from the symmetry associated with the diphenylamine in an AA'XX' system (**Figure 4.16**). The protons associated with the 4-butylaniline ring, were observed at 7.08 and 7.15 ppm as apparent doublets. This was in contrast to the observed singlet for the *ortho* substituted diphenylamine **4.8** which was caused by the change in electronics associated with the intramolecular hydrogen bonding. The apparent doublets at 7.84 ppm were attributed to the protons closest to the electron withdrawing ester moiety, hence a more downfield shift was observed when compared to the apparent doublets at 6.91 ppm which corresponded to the protons adjacent to the secondary amine.

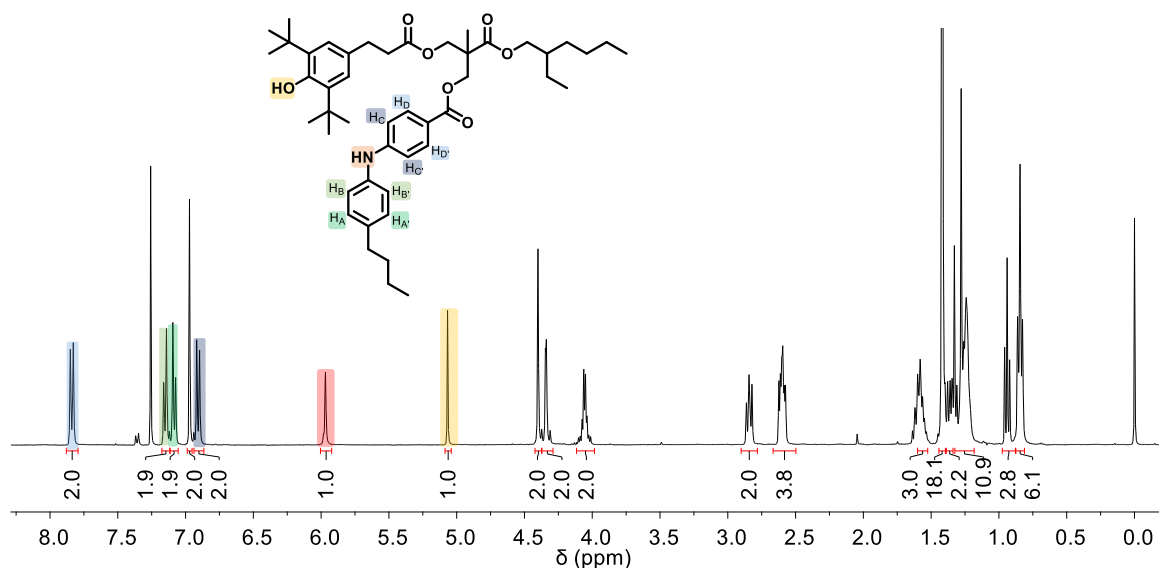


Figure 4.16 ¹H NMR spectroscopic analysis of mixed amine-phenol **4.16**.

Synthesis of the *bis*(diphenylamines) (**4.17-19**) was once again confirmed using FTIR spectroscopic analysis where the loss of the broad hydroxyl absorbance at 3400 cm⁻¹ was evident and a distinct absorbance at 3376 cm⁻¹ characteristic of a secondary amine was revealed. Mass spectrometric analysis confirmed the expected molecular weights and provided additional structural information whereby the presence of dimers was revealed for all three *bis*(diphenylamines) (**Figure 4.17**).

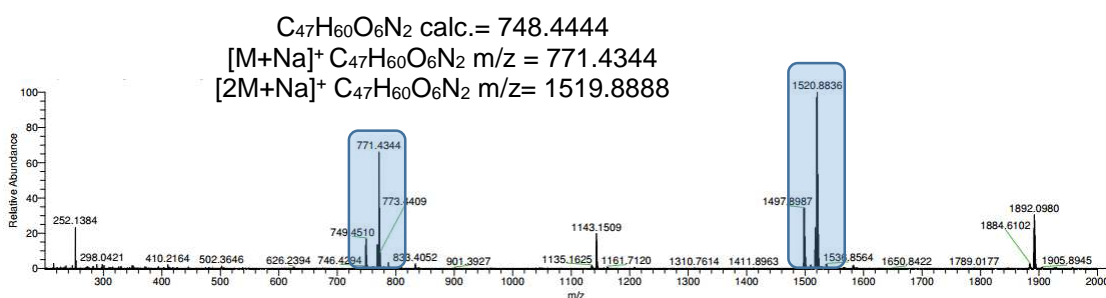


Figure 4.17 Mass spectrometric analysis of **4.17**, **4.18** and **4.19** to reveal dimer formation.

The mass spectrometry data suggested that there was some degree of intermolecular interaction between the *bis*(diphenylamines). Scrutiny of the structures revealed that these compounds would lend themselves to Π - Π stacking of the aromatic functionalities in addition to intermolecular interactions between the straight chain butyl moieties. The implications of these structural characteristics on solubility was revealed in the oxidation analysis.

Both the mixed amine-phenols and the *bis*(diphenylamines) were blended into the lubricant base oil Durasyn 164 at 0.5% w/w. Oxidation induction time analysis of **4.14**-**4.16** revealed a difference in the antioxidant capabilities of each compound (**Figure 4.18**). This demonstrated that there was clearly a favoured substitution position on the ring for enhanced antioxidant properties.

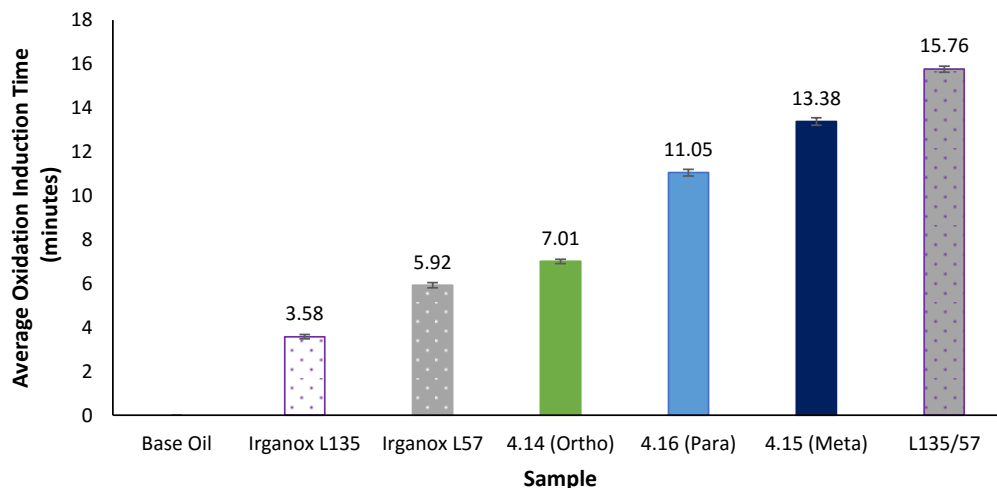


Figure 4.18 Average Oxidation induction time of Series 2, mixed amine-phenol base oil samples (tested in duplicate).

The mixed amine-phenol **4.14** exhibited the quickest oxidation induction time in comparison to **4.15** and **4.16**. The poor performance of the mixed amine-phenol **4.14** was attributed to the *ortho* substitution which allowed intramolecular hydrogen bonding between the aromatic amine proton and the carbonyl oxygen from the ester moiety. It

was proposed that the intramolecular hydrogen bonding stabilised the secondary amine to such an extent that the initial step of hydrogen abstraction required a higher energy of activation hence the rate of reaction with peroxy radicals was reduced. The success of an antioxidant can be determined by how well it competes with the substrate (in this case the base oil) for the reaction with peroxy radicals. The potential presence of an intramolecular hydrogen bond in the mixed amine-phenol **4.14** was confirmed using computational analysis (Cerius2®) to generate an energy minimised conformation (**Figure 4.19**). The computational analysis revealed a twisting of both the amine and phenolic branches towards each other. A distance of 2.013 Å was predicted between the secondary amine proton and the carbonyl oxygen, which equates to typical hydrogen bonding parameters.

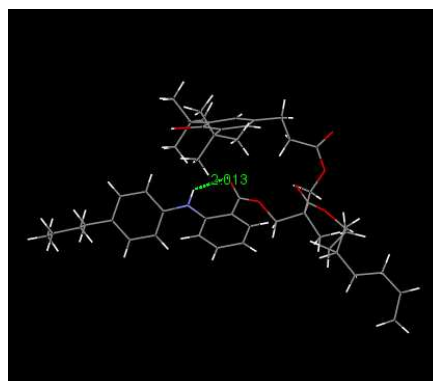
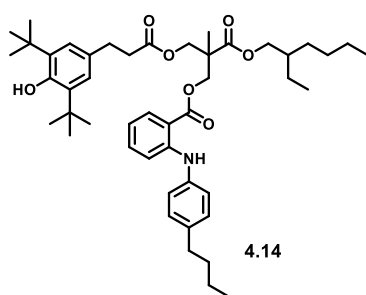


Figure 4.19 Energy minimised computational model of the mixed amine-phenol **4.14**, revealing presence of a potential intramolecular hydrogen bond.

In comparison, the mixed-amine phenol **4.15**, which was substituted in the *meta* position, revealed the best oxidation induction time of 13.4 minutes. Interestingly, this result still was not greater than a simple 1:1 (0.25% w/w of each of Irganox L135 and Irganox L57) blend of the two current antioxidants Irganox L135 and Irganox L57, however some improvement had been observed from **Series 1**. A direct comparison was made between the oxidation induction times from **Series 1** and **2** to determine the structural characteristics that were contributing to an increase in induction time (**Figure 4.20**).

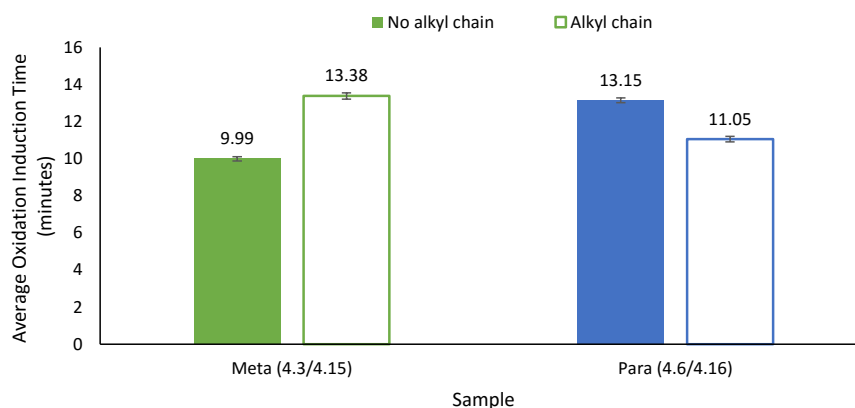


Figure 4.20 Comparison of oxidation induction time analysis from Series 1 and 2.

Comparison of the *meta* substituted mixed amine-phenols **4.3** and **4.15** (from **Series 1** and **2**, respectively) revealed that through the addition of an alkyl chain, oxidation induction time increased. It was proposed that this increase was associated with an improved solubility in the lubricant base oil and hence better diffusion within the medium was achieved. Additionally, comparison of the *para* substituted mixed amine-phenols **4.6** and **4.16** revealed that incorporation of a methylene spacer between the aromatic ring and the ester moiety had an even greater effect on the oxidation induction time than just the addition of a solubilising group. This was believed to be a result of a change in the electronics of the system. Instead of the strongly electron-withdrawing ester moiety, the methyl spacer provided some electron-donating capacity to the aromatic ring. Greater electron donation into the aromatic ring provided an increased stability to the aminyl radical hence reducing the bond dissociation energy of the N-H and in turn the rate of reaction with peroxy radicals is increased.

Oxidation onset temperature was also analysed and revealed the same trend of increasing oxidative stability from **4.14** (*ortho*) to **4.16** (*para*) to **4.15** (*meta*) (**Figure 4.21**).

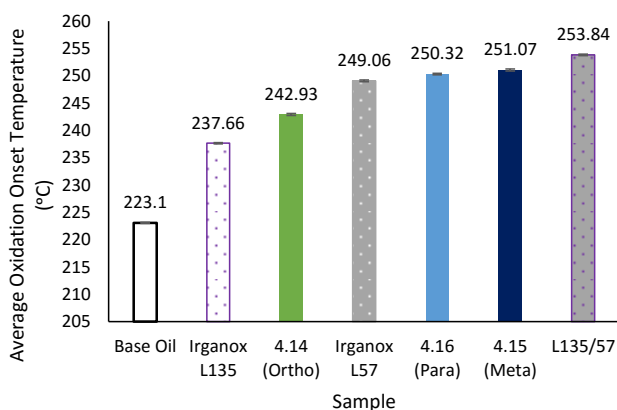


Figure 4.21 Oxidation onset temperature analysis of Series 2, mixed amine-phenol base oil samples.

The *ortho* substituted mixed amine-phenol **4.14** revealed an oxidation onset temperature that was significantly less than that observed for the diphenylamine **Irganox L57**. The *para* and *meta* substituted mixed amine-phenols (**4.16** and **4.15**, respectively), however, revealed the ability to perform in the higher temperature region associated with diphenylamines.

Oxidative stability analysis of the *bis*(diphenylamines) proved more challenging as the solubility in the lubricant base oil remained an issue even with the additional butyl chain. Better dispersion was achieved instead of the complete aggregation of the additive, as seen for **Series 1**, however, a hazy precipitation was noted. Oxidation induction time analysis revealed very poor results for the series of *bis*(diphenylamines) whereby only **4.18** was able to stabilise the base oil for more than 3 minutes.

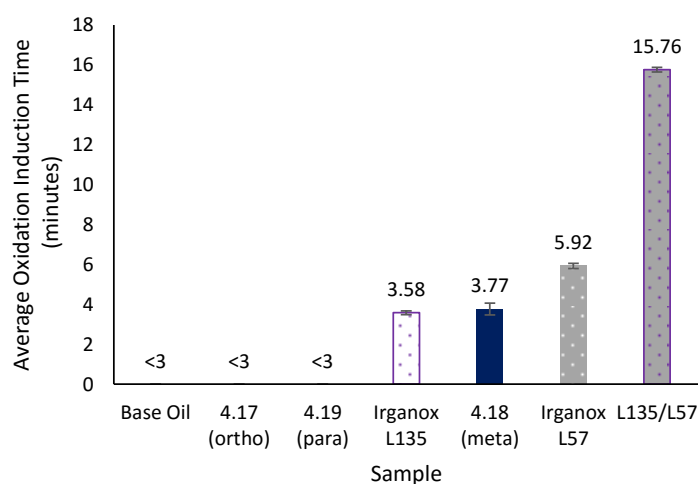


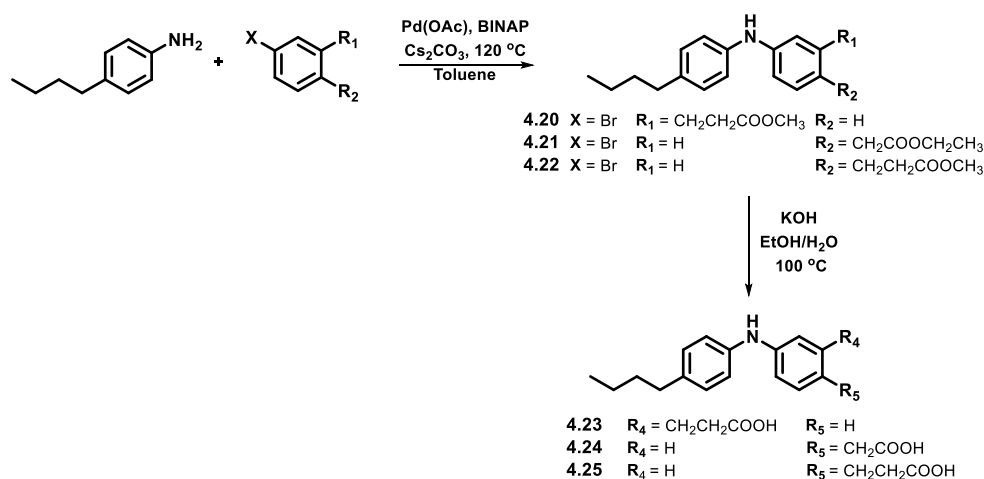
Figure 4.22 Oxidation induction time analysis of *bis*(diphenylamines) **4.17-4.19**.

Oxidation onset temperature analysis also revealed the same trend where **4.18** provided the best stabilisation out of the series, however it was noted that none of the new species were able to perform better than Irganox L57. This was unexpected as this series of *bis*(diphenylamines) possessed an additional diphenylamine in comparison to Irganox L57 which theoretically gave them a greater radical scavenging capacity.

The poor dispersion within the lubricant oil significantly hindered the radical scavenging ability of this series of *bis*(diphenylamines). It was proposed that a branched alkyl unit would need to be incorporated, for example 2-ethylhexanol, to disrupt the ordered structures and hence improve solubility. These results did, however, give confirmation that there was a synergistic effect occurring in the mixed phenol-amines where both induction time and onset temperature were significantly increased through incorporation of a phenolic moiety.

4.2.3 Synthesis, Characterisation and Testing – Series 3

Oxidative stability analysis of the mixed amine-phenols from **Series 1** (**4.3** and **4.6**) revealed an improvement in antioxidant performance when a methylene spacer was introduced between the aromatic ring and the ester moiety. Further development in **Series 2** revealed that, with the addition of a butyl chain to enhance solubility, *meta* and *para* substitution provided the greatest stability to the lubricant base oil and so were the focus of this series. The inclusion of a methyl or ethyl spacer at these positions was investigated. The esters **4.20** (*meta* -CH₂CH₂-), **4.21** (*para* -CH₂-) and **4.22** (*para* -CH₂CH₂-) were generated first, followed by ester hydrolysis to yield the carboxylic acids **4.23**, **4.24** and **4.25**. The general synthesis of this series of compounds is shown in **Scheme 4.12**.



Scheme 4.12 General scheme for the synthesis of series 3 diphenylamine derivatives.

Successful coupling of 4-butylaniline to the respective bromobenzoate was achieved to yield the diphenylamines **4.20**, **4.21** and **4.22** in reasonable yield (*ca.* 60%). Ester hydrolysis generated **4.23**, **4.24** and **4.25** in good yield of *ca.* 80%. The mono-phenol

hydroxyl linker (**4.5**) was functionalised with the carboxylic acid diphenylamine derivatives (**4.23**, **4.24** and **4.25**) to yield a series of mixed amine-phenols (**4.26-28**) shown in **Table 4.4**. In addition, the *bis*(diphenylamines) (**4.29-31**) were also generated by reaction of the carboxylic acid diphenylamine derivatives with the first generation diol linker (**2.1**).

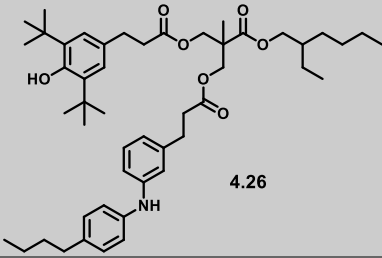
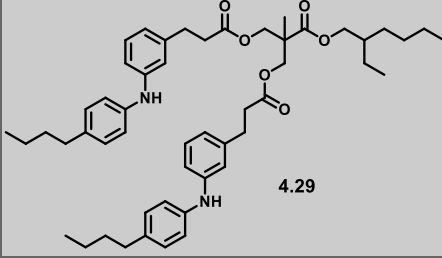
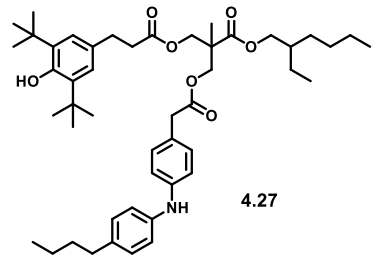
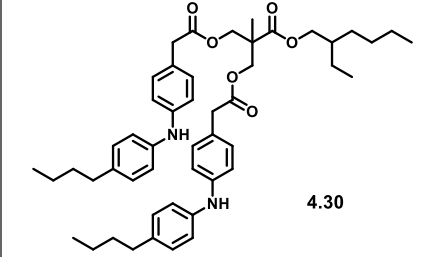
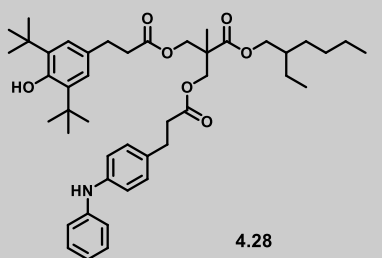
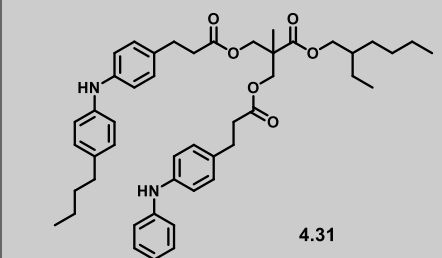
Mixed Amine-Phenol	<i>Bis</i> (diphenylamine)
 <p style="text-align: right;">4.26</p>	 <p style="text-align: right;">4.29</p>
 <p style="text-align: right;">4.27</p>	 <p style="text-align: right;">4.30</p>
 <p style="text-align: right;">4.28</p>	 <p style="text-align: right;">4.31</p>

Table 4.4 Structure of the mixed amine-phenols (**4.26**, **4.27** and **4.28**) and the *bis*(diphenylamines) (**4.29**, **4.30** and **4.31**) for comparison

Full characterisation of the mixed amine-phenol **4.26** was carried out using NMR spectroscopic analysis. Interpretation of the ^1H NMR spectrum for **4.26**, detailed in **Figure 4.23**, revealed the complex splitting pattern associated with *meta* substitution. The aromatic protons associated with the 4-butylaniline ring, were observed at 7.00 and 7.08 ppm as apparent doublets. The apparent triplet at 7.14 ppm was assigned to the proton H_C. This was confirmed using ^1H - ^1H COSY NMR spectroscopic analysis whereby both the apparent doublets H_B and H_D revealed a direct *ortho* coupling to H_C with J values

of *ca.* 8.0 Hz. The apparent singlet at 6.82 ppm represented the proton H_A where no strong coupling to the protons H_B-H_D was observed. The complex multiplet observed in the range of 2.54-2.64 ppm encompassed the 6 methylene protons highlighted in red, which again was confirmed using 2D NMR techniques.

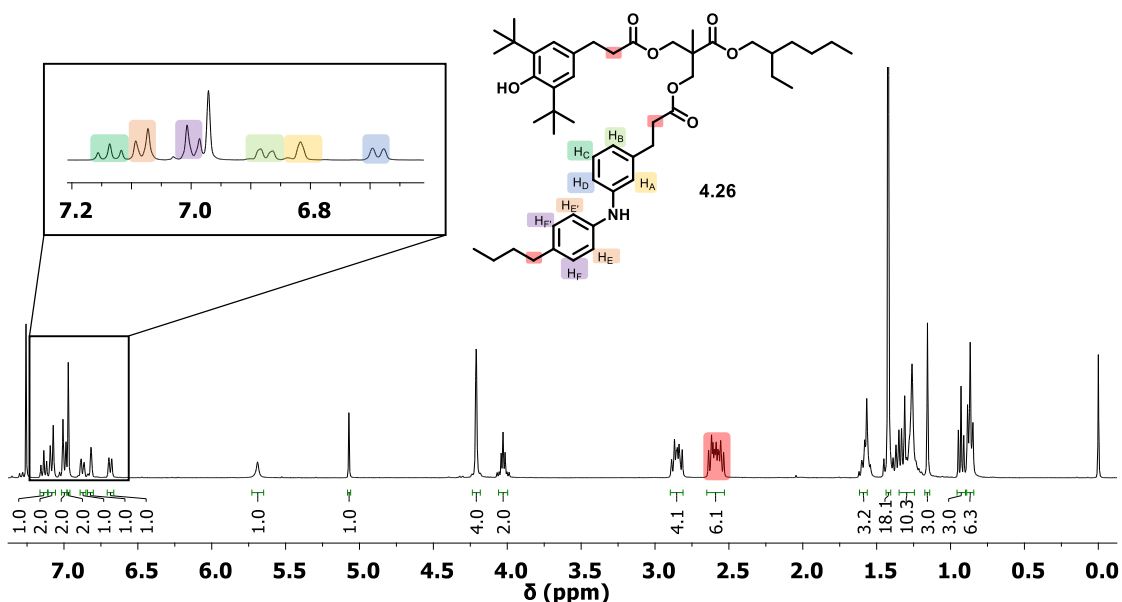


Figure 4.23 ¹H NMR spectroscopic analysis of the mixed amine-phenol **4.26**.

Additional confirmation of successful synthesis was revealed by the correct proton ratio of the singlets at 5.07 and 5.69 ppm representing the phenolic and secondary amine protons, respectively.

The mixed amine-phenols (**4.26**, **4.27** and **4.28**) and the *bis*(diphenylamines) (**4.29**, **4.30** and **4.31**) were blended into the lubricant base oil Durasyn 164 at 0.5% w/w. Oxidation induction time analysis of **4.26-4.28** revealed a dramatic increase in the stabilisation capabilities of all three compounds where the induction time for each exceeded that of the Irganox L135/57 1:1 blend.

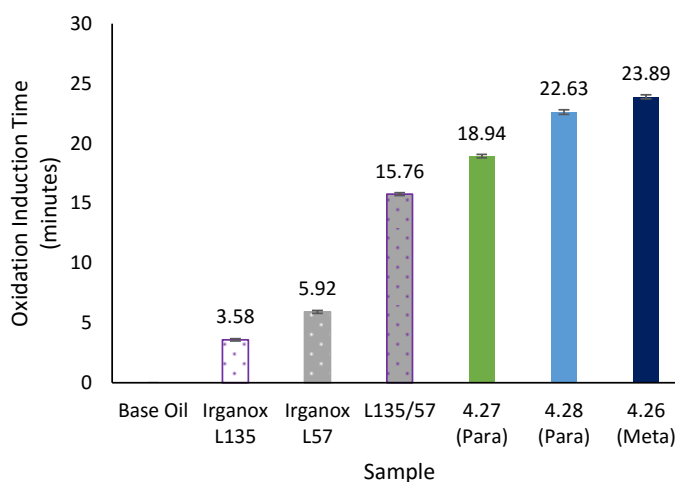


Figure 4.24 Oxidation induction time analysis of Series 3, mixed amine-phenol base oil samples.

The greatest induction time was revealed for the mixed amine-phenol **4.26** where an increase of *ca.* 8 minutes from the L135/57 blend was observed. The mixed amine-phenol **4.26** possessed an ethyl spacer between the aromatic ring and the ester moiety, which directed electron density towards the aromatic ring. An increase of *ca.* 4 minutes was observed from **4.27** to **4.28** where an additional methylene unit was introduced. This result indicated that stabilisation of the secondary amine, through electron donation, was a significant factor in increasing the antioxidant capabilities of these compounds. It was also proposed that the ethyl spacers provided the ideal contact distance between the diphenylamine and the phenol, therefore potentially increasing the ability of amine regeneration. This proposal was supported by using computational analysis (Cerius2[®]) to generate an energy minimised conformation (**Figure 4.25 a**). A stabilised structure was revealed, with an energy of -807 Kcal, whereby the amine and the phenol were within 2.39 Å of each other. In comparison, minimisation of the mixed amine-phenol **4.15** was carried out to determine a favoured conformation without the ethyl spacer (**Figure 4.25 b**).

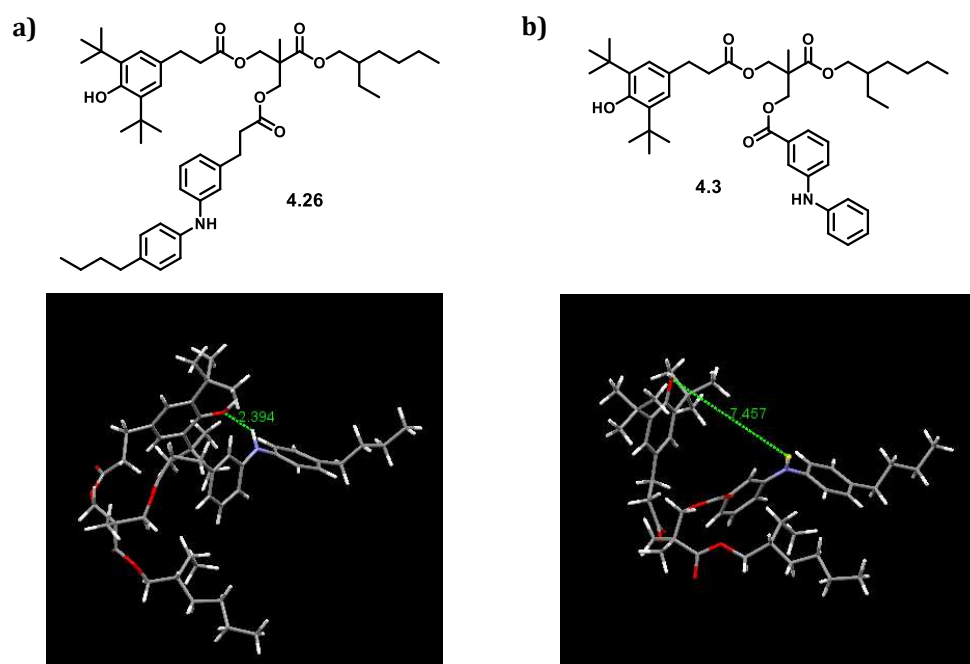


Figure 4.25 Energy minimised computational model of a) the mixed amine-phenol **4.26**, revealing a close contact distance (2.39 Å) between the phenol and the secondary amine and b) the mixed amine-phenol **4.15** revealing a larger intramolecular distance (7.46 Å).

The computational analysis revealed the energy of **4.15** was reduced the further away the amine and phenol became which was opposite to that found for **4.26**. A stabilised structure with an energy of -665 Kcal revealed a much larger distance of 7.46 Å between the secondary amine and the phenol. This reinforced the proposal that the ethyl spacer promotes a closer contact distance between the two functionalities potentially promoting amine regeneration. A direct comparison of the *meta* substituted compounds (**4.3**, **4.15** and **4.26**) from the three series revealed the increase in induction time associated with each of the structural developments (**Figure 4.26**). This highlighted the significance of enhanced solubility through the inclusion of an alkyl chain which increased the induction time by *ca.* 3 minutes (**4.15**). In addition, inclusion of electron donating substituents as opposed to electron withdrawing substituents increased the oxidation induction time by a further *ca.* 10 minutes (**4.26**).

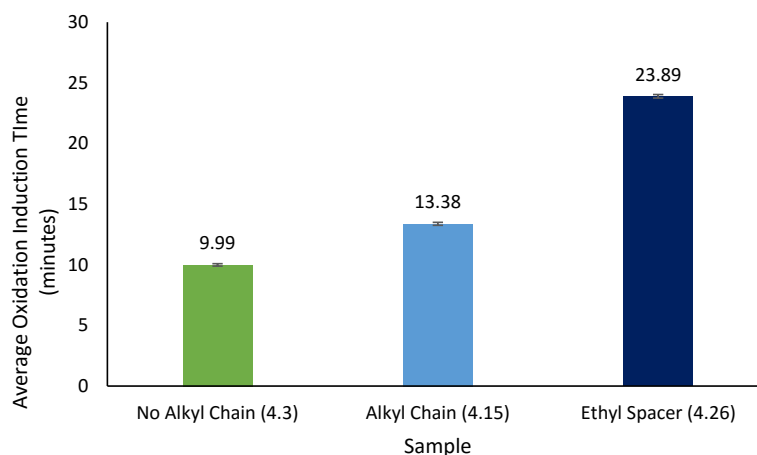


Figure 4.26 Comparison of average oxidation induction time analysis from Series 1 (4.3), series 2 (4.15) and series 3 (4.26).

Oxidation onset temperature analysis also revealed excellent stability properties from the mixed amine-phenols where 4.26, 4.27 and 4.28 all performed in the same temperature region as the L135/57 blend. (Figure 4.27).

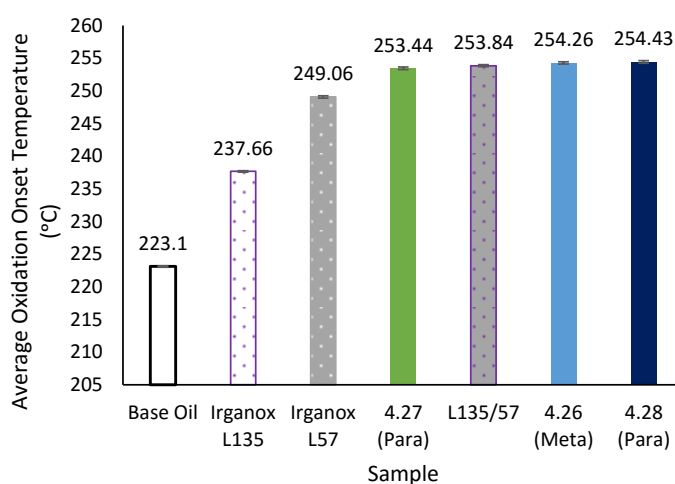


Figure 4.27 Average Oxidation onset temperature analysis of Series 2, mixed amine-phenol base oil samples (tested in duplicate).

The *bis*(diphenylamines) 4.29-4.31 also revealed similar solubility issues as seen in **Series 2**. Oxidation induction times did not exceed that of the aromatic amine Irganox L57 hence reinforcing further still the excellent synergistic effects of combining both diphenylamines and sterically hindered phenols within the same compound.

4.3 Conclusions

In conclusion, three series of first generation mixed amine-phenols and *bis*(diphenylamines) were successfully synthesised, blended into the lubricant base oil Durasyn 164 and analysed for their oxidative stability properties, highlighting interesting structure-activity relationships. The mixed amine-phenols were all soluble in the lubricant base oil at 0.5% w/w which was further improved through the introduction of a butyl chain on the aniline ring. Even with the additional alkyl chain, all derivatives of the *bis*(diphenylamines) revealed poor solubility and hence oxidation induction times and oxidation onset temperatures were all lower than the current diphenylamine antioxidant Irganox L57. **Series 2** of the mixed amine-phenols revealed that *meta* (**4.15**) and *para* (**4.16**) substitution provided the best oxidative stability properties. These properties were further enhanced in **Series 3** through the inclusion of methyl or ethyl spacers between the diphenylamine and the ester moiety from the attachment to the mono-phenol linker. It was observed that *meta* substitution with an ethyl spacer (**4.26**) provided the longest oxidation induction time of *ca.* 23 minutes, which was *ca.* 8 minutes longer than the current 1:1 synergistic blend of Irganox L135 and Irganox L57. It was proposed that electron donation into the aromatic ring was potentially allowing better stabilisation of the aminyl radical, generated from the initial hydrogen abstraction. Additionally, computational modelling revealed that the combination of *meta* substitution and an ethyl spacer allowed close contact of both amine and phenol functionalities suggesting the regeneration of the diphenylamine by the phenol could be enhanced using these structural combinations.

4.4 Experimental

Reagents and solvents were purchased from Sigma Aldrich or Fisher Scientific and used without further purification with the exception of 3-(3,5-di-*tert*-butyl-4-hydroxyphenyl)-propionic acid which was purchased from Alfa Aesar and methyl (3-(4-bromophenyl)propanoate which was purchased from TCI Chemicals. Dichloromethane was distilled under a nitrogen atmosphere from calcium hydride. All further purification and characterisation was carried out as described in **Chapter 2**.

Series 1 and general procedures:

Preparation of methyl 3-(phenylamino)benzoate (4.1) and general procedure for Buchwald-Hartwig amination reactions

In a 25 mL round-bottomed flask, toluene (10 mL) was degassed with argon for 20 minutes. Under a flow of argon, Pd(OAc)₂, BINAP and Cs₂CO₃ were added and left to stir for a further 20 minutes. To the mixture, methyl (3-bromobenzoate) and aniline were added. The reaction was stirred at 120 °C and monitored by thin layer chromatography (TLC) for 24 hours. Upon completion, the reaction was cooled to room temperature and filtered through Celite®, with hexane as the eluent, followed by concentration under reduced pressure. The residue was purified by flash column chromatography on silica eluting with hexane/ethyl acetate (90:10) (R_f = 0.23) to afford 0.87 g (82%) of **4.1** as a pale yellow solid. M.p 110-112 °C. IR (ATR) ν/cm^{-1} : 3358, 3030, 1694, 1578, 1294, 744. ¹H NMR (400 MHz/CDCl₃)/ppm, δ = 3.90(s, 3H, -COOCH₃), 5.81(s, 1H, -NH), 6.98 (*app. t*, 1H, *app J*=8 Hz, CH_{para}C₄H₄-NH), 7.09(*app. d*, 2H, CH_{para}C₂H₂metaC₂H₂ortho-NH), 7.23 (m, 1H, HN-CH-C(COOCH₃)-CHCHCH-), 7.29(m, 3H, C₂H₂ortho-HN-CH-C(COOCH₃)-CHCHCH-), 7.57(*app. d*, 1H, HN-CH-C(COOCH₃)-CH), 7.72(m, 1H, HN-CH-C(COOCH₃)); ¹³C NMR (100 MHz/CDCl₃)/ppm, δ = 52.2, 118.2, 118.4, 121.5, 121.77, 121.80, 129.4, 129.3, 131.4, 142.4, 143.6, 167.1. Found [M+H]⁺ (C₁₄H₁₃NO₂) m/z = 228.1019 (Calc. 228.0946).

Preparation of 3-(phenylamino)benzoic acid (4.2) and general procedure for base catalysed ester hydrolysis reactions

To a solution of **4.1** (0.5 g, 2.2 mmol) in ethanol (10 mL), aqueous potassium hydroxide (0.25 g, 4.4 mmol) was added at room temperature. The mixture was then allowed to stir at 100 °C for a minimum of 1 hour and was monitored closely by TLC until consumption of **4.1** was observed. Upon completion, the reaction was allowed to cool and the ethanol was removed *in vacuo*. The remaining solution was cooled to 0 °C and acidified to pH 2 with 2M HCl. The resulting precipitate was collected *via* vacuum filtration and washed with water (15 ml). The precipitate was then dissolved in chloroform (20 mL) and washed with brine (20 mL). The organic layer was dried over MgSO₄, filtered and the solvent removed *in vacuo* to yield 0.38 g (81 %) of **4.2** as a white solid. M.p 140-142 °C. IR (ATR) ν/cm^{-1} : 3398, 2992-2540 (br), 1682, 1584, 1464, 1294, 748. ¹H NMR (400 MHz/CDCl₃)/ppm, δ = 6.99 (*app. t*, 1H, *app J*=8 Hz, CH_{para}C₄H₄-NH), 7.10(*app. d*, 2H,

$\text{CH}_{para}\text{C}_2\text{H}_2\text{meta}\text{C}_2\text{H}_2\text{ortho-NH}$), 7.30(m, 4H, $\text{C}_2\text{H}_2\text{ortho-HN-CH-C(COOH)-CHCHCH-}$), 7.64(*app.* d, 1H, HN-CH-C(COOH)-CH), 7.77(m, 1H, $\text{HN-CH-C(COOCH}_3\text{)}$); ^{13}C NMR (100 MHz/ CDCl_3)/ppm, δ = 118.5, 118.6, 122.0, 122.2, 129.5, 129.6, 130.5, 142.2, 143.8, 172.2. Found $[\text{M}+\text{H}]^+$ ($\text{C}_{13}\text{H}_{11}\text{NO}_2$) m/z = 214.0863 (Calc. 214.0868).

Preparation of the mono-phenolic linker (4.5)

The first generation hydroxyl linker (**2.3**) (5 g, 22.30 mmol), *N,N'*-dicyclohexylcarbodiimide (DCC) (0.92 g, 4.46 mmol) and DPTS (60%) were dissolved in dry dichloromethane (50 mL) and cooled to 0 °C. To this, a solution of 3-(3,5-di-*tert*-butyl-4-hydroxy-phenyl)-propionic acid (1.24 g, 4.46 mmol) in dry dichloromethane (20 mL) was added dropwise to the solution. The reaction was left to stir at room temperature and was monitored closely by TLC (90:10 hexane/ethyl acetate) until any small formation of the diphenol was observed (R_f = 0.38). The reaction mixture was filtered to remove the white *N,N'*-dicyclohexylurea (DCU) precipitate and the filtrate was concentrated *in vacuo*. The crude product was immediately subjected to flash column chromatography on silica eluting with hexane/ethyl acetate (80:20) (R_f = 0.24) to afford 2.15 g (95%) of **4.5** as a colourless oil. IR (ATR) ν/cm^{-1} : 3528, 2960, 1726, 1140, 1042. ^1H NMR (400 MHz/ CDCl_3)/ppm, δ = 0.89(t, 6H, $-\text{CH}_2\text{CH}_3$), 1.15(s, 3H, $-\text{CH}_3$), 1.28-1.37(m, 8H, $\text{COO-CH}_2\text{-CH}(\text{CH}_2\text{CH}_3)\text{-CH}_2\text{CH}_2\text{CH}_2\text{CH}_3$), 1.43(s, 18H, CH_3 *tert*-butyl), 1.59(m, 1H, $\text{COO-CH}_2\text{-CH}(\text{CH}_2\text{CH}_3)\text{-C}_4\text{H}_9$), 2.53(s(br), 1H, $-\text{OH}$), 2.62(t, 2H, $\text{Ar-CH}_2\text{CH}_2\text{-COO-}$), 2.86(t, 2H, $\text{Ar-CH}_2\text{CH}_2\text{-COO-}$), 3.57(m, 2H, $\text{HO-CH}_2\text{-C,}$), 4.05(m, 2H, $\text{COO-CH}_2\text{-CH}(\text{CH}_2\text{CH}_3)\text{-C}_4\text{H}_9$), 4.20(d, 1H, $\text{COO-CH-C equatorial}$), 4.33(d, 1H, COO-CH-C axial), 5.09(s, 1H, Ar-OH), 6.98(s, 2H, Ar-CH); ^{13}C NMR (100 MHz/ CDCl_3)/ppm, δ = 11.0, 14.1, 17.6, 23.0, 23.8, 28.9, 30.4, 30.9, 34.3, 36.3, 38.7, 48.3, 64.9, 65.7, 67.3, 124.7, 130.7, 136.0, 152.3, 173.4, 174.6. Found $[\text{M}+\text{Na}]^+$ ($\text{C}_{30}\text{H}_{50}\text{O}_6$) m/z = 529.3500 (Calc. 529.3505).

Preparation of the mixed amine-phenol (4.3) and general procedure

The mono-phenolic linker (**4.5**) (0.34 g, 0.67 mmol), 3-(phenylamino)benzoic acid (**3.2**) (0.16 g, 0.74 mmol) and DPTS (60%) were dissolved in dry dichloromethane (10 mL) and stirred at room temperature for 30 minutes. To the solution, DCC (0.15 g, 0.74 mmol) dissolved in dry dichloromethane (10 mL) was added over 15 minutes. The reaction was left overnight at room temperature under a nitrogen atmosphere. The reaction mixture was filtered to remove the white DCU precipitate and the filtrate was concentrated. The

residue was purified by flash column chromatography on silica eluting with hexane/ethyl acetate (80:20) ($R_f = 0.32$) to afford 0.31 g (46%) of **4.3** as a viscous yellow oil. IR (ATR) ν/cm^{-1} : 3641, 3385, 2960, 1731, 1517, 1132, 749. ^1H NMR (400 MHz/ CDCl_3)/ppm, $\delta = 0.84(\text{t}, 6\text{H}, -\text{CH}_2\text{CH}_3)$, 1.23-1.36(m, 12H, alkyl $-\text{CH}_2$, $-\text{CH}_3$), 1.42(s, 18H, CH_3 *tert*-butyl), 1.56(m, 1H, $-\text{CH}$), 2.60(t, 2H, Ar- $\text{CH}_2\text{CH}_2\text{-COO}$), 2.85(t, 2H, Ar- $\text{CH}_2\text{CH}_2\text{-COO}$), 4.04(m, 2H, $\text{COO-CH}_2\text{-CH}(\text{CH}_2\text{CH}_3)\text{-C}_4\text{H}_9$), 4.34(s, 2H, Ar- $\text{COO-CH}_2\text{-C}$), 4.44(s, 2H, Ar- $\text{COO-CH}_2\text{-C}$), 5.08(s, 1H, $-\text{OH}$), 5.87(s, 1H, $-\text{NH}$), 6.97(m, 3H, Ar $\text{CH}_{para}\text{C}_4\text{H}_4\text{-NH}$ and Ph- CH), 7.09(*app. d*, 2H, Ar $\text{CH}_{para}\text{C}_2\text{H}_2\text{metaC}_2\text{H}_2\text{ortho-NH}$), 7.30(m, 4H, Ar $\text{C}_2\text{H}_2\text{ortho-HN-ArCH-C(COOH)-CHCHCH-}$), 7.50(*app. d*, 1H, HN-Ar CH-C(COOH)-CH), 7.67(m, 1H, HN-Ar $\text{CH-C(COOCH}_3\text{)}$). ^{13}C NMR (100 MHz/ CDCl_3)/ppm, $\delta = 11.0, 14.1, 18.0, 22.9, 23.7, 28.9, 30.3, 30.9, 34.3, 36.2, 38.7, 46.6, 65.6, 66.1, 67.5, 118.0, 118.5, 121.5, 121.7, 121.9, 124.7, 129.4, 129.5, 130.8, 136.0, 142.2, 143.7, 152.2, 166.0, 172.7, 172.9$. Found $[\text{M}+\text{Na}]^+$ ($\text{C}_{43}\text{H}_{59}\text{NO}_7$) $m/z = 724.4184$ (Calc. 724.4292).

Preparation of the bis(diphenylamine) (**4.4**) and general procedure

The first generation hydroxyl linker (**2.3**) (0.28 g, 1.12 mmol), 3-(phenylamino)benzoic acid (**3.2**) (0.5 g, 2.34 mmol) and DPTS (60%) were dissolved in dry dichloromethane (20 mL). To the solution, DCC (0.48 g, 2.34 mmol) dissolved in dry dichloromethane (10 mL) was added over 15 minutes. The reaction was left overnight at room temperature under a nitrogen atmosphere. The reaction mixture was filtered to remove the white DCU precipitate and the filtrate was concentrated. The crude product was purified by flash column chromatography on silica eluting with hexane/ethyl acetate (80:20) ($R_f = 0.4$) to afford 0.47 g (66%) of **4.4** as a viscous orange oil. IR (ATR) ν/cm^{-1} : 3380, 2960, 1714, 1590, 1494, 1204, 1104, 746. ^1H NMR (400 MHz/ CDCl_3)/ppm, $\delta = 0.81(\text{m}, 6\text{H}, -\text{CH}_2\text{CH}_3)$, 1.20-1.33(m, 8H, alkyl $-\text{CH}_2$), 1.41(s, 3H, $-\text{CH}_3$), 1.54(m, 1H, $-\text{CH}$), 4.06(m, 2H, $\text{COO-CH}_2\text{-CH}(\text{CH}_2\text{CH}_3)\text{-C}_4\text{H}_9$), 4.55(s, 4H, Ar- $\text{COO-CH}_2\text{-C}$), 5.79(s(br), 2H, $-\text{NH}$), 6.97(*app. t*, 2H, *app. J*=8 Hz, $\text{CH}_{para}\text{C}_4\text{H}_4\text{-NH}$), 7.08(*app. d*, 4H, *app. J*=8 Hz, $\text{CH}_{para}\text{C}_2\text{H}_2\text{metaC}_2\text{H}_2\text{ortho-NH}$), 7.29(m, 8H, $\text{C}_2\text{H}_2\text{ortho-HN-CH-C(COOCH}_3\text{)-CHCHCH-}$), 7.51(*app. d*, 2H, *app. J*=4 Hz, HN- $\text{CH-C(COOCH}_3\text{)-CH}$), 7.65(*app. s*, 2H, HN- $\text{CH-C(COOCH}_3\text{)}$). ^{13}C NMR (100 MHz/ CDCl_3)/ppm, $\delta = 10.9, 14.0, 18.1, 22.9, 23.7, 28.9, 30.3, 38.7, 46.8, 66.3, 67.5, 118.1, 118.5, 121.4, 121.7, 121.9, 129.5, 130.8, 142.2, 146.7, 166.0, 172.9$. Found $[\text{M}+\text{H}]^+$ ($\text{C}_{39}\text{H}_{44}\text{N}_2\text{O}_6$) $m/z = 637.3272$ (Calc. 637.3199).

Preparation of mixed amine-phenol (4.6)

The mono-phenolic linker (**4.5**) (0.74 g, 1.46 mmol), 2-(4-(phenylamino)phenyl)acetic acid (0.5 g, 2.20 mmol), DPTS (60%) and DCC (0.45 g, 2.2 mmol) were allowed to react according to the general mixed amine-phenol procedure. The crude product was purified by flash column chromatography on silica eluting with hexane/ethyl acetate (80:20) ($R_f = 0.31$) to afford 0.75 g (72%) of **4.6** as a viscous pale yellow oil. IR (ATR) ν/cm^{-1} : 3641, 3385, 2960, 1731, 1517, 1132, 749. ^1H NMR (400 MHz/ CDCl_3)/ppm, $\delta = 0.87(\text{m}, 6\text{H}, -\text{CH}_2\text{CH}_3)$, 1.16(s, 3H, $-\text{CH}_3$), 1.31-1.36(m, 8H, alkyl $-\text{CH}_2$), 1.42(s, 18H, CH_3 *tert*-butyl), 1.54(m, 1H, $-\text{CH}$), 2.57(t, 2H, $J=8$ Hz, Ar- $\text{CH}_2\text{CH}_2\text{-COO}$), 2.83(t, 2H, $J=8$ Hz, Ar- $\text{CH}_2\text{CH}_2\text{-COO}$), 3.54(s, 2H, Ar- $\text{CH}_2\text{-COO}$), 4.01(m, 2H, $\text{COO-CH}_2\text{-CH}(\text{CH}_2\text{CH}_3)\text{-C}_4\text{H}_9$), 4.22(m, 4H, $\text{CH}_2\text{-COO-CH}_2\text{-C}$), 5.07(s, 1H, ArOH), 5.68(s, 1H, $-\text{NH}$), 6.92(*app. t*, 1H, *app. J*=8 Hz, $\text{CH}_{\text{para}}\text{C}_4\text{H}_4\text{-NH}$), 6.97(s, 2H, Ph-CH), 7.03(m, 4H, Ar $\text{CH}_{\text{ortho}}\text{-NH-ArCH}_{\text{ortho}}$), 7.14(*app. d*, 2H, $J=12$ Hz, NH-Ar $\text{CHCH-C}(\text{CH}_2\text{COO-})$), 7.25(*app. t*, 2H, $J=8$ Hz, Ar $\text{CH}_{\text{para}}\text{CH}_{\text{meta}}\text{CH}_{\text{ortho}}\text{-NH}$). ^{13}C NMR (100 MHz/ CDCl_3)/ppm, $\delta = 10.9, 14.0, 17.8, 22.9, 23.7, 28.9, 30.3, 30.8, 34.3, 36.2, 38.7, 40.5, 46.4, 65.4, 65.8, 67.4, 117.8, 121.0, 124.7, 126.0, 129.3, 130.2, 130.8, 136.0, 142.2, 143.0, 152.2, 171.3, 172.6, 172.8$. Found $[\text{M}+\text{H}]^+$ ($\text{C}_{44}\text{H}_{61}\text{NO}_7$) $m/z = 716.4524$ (Calc. 716.4448).

Preparation of bis(diphenylamine) (4.7)

The first generation hydroxyl linker (**2.3**) (0.43 g, 1.91 mmol), 2-(4-(phenylamino)phenyl)acetic acid (1 g, 4.40 mmol), DPTS (60%) and DCC (0.91 g, 4.4 mmol) were allowed to react according to the general bis(diphenylamine) procedure. The crude product was purified by flash column chromatography on silica eluting with hexane/ethyl acetate (80:20) ($R_f = 0.43$) to afford 0.98 g (77%) of **4.7** as a viscous dark red oil. IR (ATR) ν/cm^{-1} : 3385, 2960, 1727, 1596, 1516, 1132, 746. ^1H NMR (400 MHz/ CDCl_3)/ppm, $\delta = 0.86(\text{m}, 6\text{H}, -\text{CH}_2\text{CH}_3)$, 1.16(s, 3H, $-\text{CH}_3$), 1.25-1.35(m, 8H, alkyl $-\text{CH}_2$), 1.54(m, 1H, $-\text{CH}$), 3.52(s, 4H, Ar- $\text{CH}_2\text{-COO}$), 3.98(m, 2H, $\text{COO-CH}_2\text{-CH}(\text{CH}_2\text{CH}_3)\text{-C}_4\text{H}_9$), 4.17(d, 2H, $J=8$ Hz, Ar- $\text{COO-CH}_2\text{-C}$), 4.24(d, 2H, $J=12$ Hz, Ar- $\text{COO-CH}_2\text{-C}$), 5.67(s, 2H, $-\text{NH}$), 6.92(*app. t*, 2H, *app. J*=8 Hz, $\text{CH}_{\text{para}}\text{C}_4\text{H}_4\text{-NH}$), 6.99(*app. d*, 4H, *app. J*=8 Hz, NH- $\text{CHCH}(\text{CH}_2\text{COO-})$), 7.04(*app. d*, 4H, *app. J*=8 Hz, Ar $\text{CH}_{\text{para}}\text{CH}_{\text{meta}}\text{CH}_{\text{ortho}}\text{-NH}$), 7.10(*app. d*, 4H, *app. J*=8 Hz, NH- $\text{CHCH}(\text{CH}_2\text{COO-})$), 7.25(*app. t*, 4H, *app. J*=8 Hz, Ar $\text{CH}_{\text{para}}\text{CH}_{\text{meta}}\text{CH}_{\text{ortho}}\text{-NH}$). ^{13}C NMR (100 MHz/ CDCl_3)/ppm, $\delta = 10.9, 14.1, 17.9, 22.9, 23.7, 28.8, 30.3, 38.6, 40.4,$

46.3, 65.6, 67.4, 117.9, 121.0, 126.0, 129.3, 130.2, 142.2, 143.0, 171.3, 172.8. Found $[M+H]^+$ ($C_{41}H_{48}N_2O_6$) $m/z = 665.3585$ (Calc. 665.3512).

Series 2

Preparation of methyl 2-((4-butylphenyl)amino)benzoate (4.8)

Methyl (2-bromobenzoate) (1.00 g, 4.65 mmol) and 4-butylaniline (0.88 mL, 5.58 mmol) were added to $Pd(OAc)_2$ (21 mg, 0.09 mmol), BINAP (116 mg, 0.18 mmol) and K_2CO_3 (0.90 g, 6.51 mmol) and were allowed to react according to the general Buchwald-Hartwig amination procedure. The crude residue was purified by flash column chromatography on silica eluting with hexane/ethyl acetate (80:20) ($R_f = 0.38$) to afford 0.70 g (53%) of **4.8** as a white solid. M.p 135 °C. IR (ATR) ν/cm^{-1} : 3321, 2928, 1684, 1514, 1230, 1082, 746. 1H NMR (400 MHz/ $CDCl_3$)/ppm, $\delta = 0.95$ (t, 3H, $J = 8$ Hz, $-CH_3CH_2CH_2CH_2Ar$), 1.39(*sex.*, 2H, $J = 8$ Hz, $-CH_3CH_2CH_2CH_2Ar$), 1.61(*quin.*, 2H, $J = 8$ Hz, $-CH_3CH_2CH_2CH_2Ar$), 2.61(t, 2H, $J = 8$ Hz, $-CH_3CH_2CH_2CH_2Ar$), 3.91(s, 3H, $-COOCH_3$), 6.70(*app. t*, 1H, *app. J* = 8 Hz, $H_3COOC-CHCHCHCH-NH$), 7.17(*app. s*, 4H, C_4H_9-ArCH), 7.20 (*app. d*, 1H, $H_3COOC-CHCHCHCH-NH$), 7.29(*app. t*, 1H, $H_3COOC-CHCHCHCH-NH$), 7.96(*app. d*, 1H, $H_3COOC-CHCHCHCH-NH$), 9.40(s, 1H, $-NH$); ^{13}C NMR (100 MHz/ $CDCl_3$)/ppm, $\delta = 14.0, 22.4, 33.8, 35.1, 51.7, 111.4, 113.8, 116.6, 122.6, 123.1, 126.2, 129.3, 131.6, 134.1, 138.2, 138.6, 148.6, 169.0$. Found $[M+H]^+$ ($C_{18}H_{21}NO_2$) $m/z = 284.1645$ (Calc. 284.1572).

Preparation of methyl 3-((4-butylphenyl)amino)benzoate (4.9)

Methyl (3-bromobenzoate) (0.5 g, 2.33 mmol) and 4-butylaniline (0.44 mL, 2.79 mmol) were added to $Pd(OAc)_2$ (17 mg, 0.08 mmol), BINAP (95 mg, 0.16 mmol) and Cs_2CO_3 (1.06 g, 3.26 mmol) and were allowed to react according to the general Buchwald-Hartwig amination procedure. The crude residue was purified by flash column chromatography on silica eluting with hexane/ethyl acetate (80:20) ($R_f = 0.36$) to afford 0.35 g (55%) of **4.9** as a pale yellow solid. M.p 121-123 °C. IR (ATR) ν/cm^{-1} : 3364, 2927, 1700, 1288, 1217, 750. 1H NMR (400 MHz/ $CDCl_3$)/ppm, $\delta = 0.93$ (t, 3H, $J = 8$ Hz, $-CH_3CH_2CH_2CH_2Ar$), 1.36(*sex.*, 2H, $J = 8$ Hz, $-CH_3CH_2CH_2CH_2Ar$), 1.59(*quin.*, 2H, $J = 8$ Hz, $-CH_3CH_2CH_2CH_2Ar$), 2.57(t, 2H, $J = 8$ Hz, $-CH_3CH_2CH_2CH_2Ar$), 3.89(s, 3H, $-COOCH_3$), 5.72(s, 1H, $-NH$), 7.03(*app. d*, 2H, *app. J* = 8 Hz, $HN-ArCHCH$), 7.11(*app. d*, 2H, *app. J* = 8 Hz, $C_4H_9-ArCHCH$), 7.19 (*app. d*, 1H, *app. J* = 8 Hz, $HN-CH-C(COOCH_3)-CHCHCH-NH$), 7.28(*app. t*, 1H, $J = 8$ Hz, $HN-CH-C(COOCH_3)-CHCHCH-NH$), 7.52(*app. d*, 1H, $J = 8$ Hz, $HN-CH-C(COOCH_3)-$

CHCHCH-NH), 7.66(*app. s*, 1H, *HN-CH-C(COOCH₃)*); ¹³C NMR (100 MHz/CDCl₃)/ppm, δ = 14.0, 22.4, 33.8, 35.0, 52.1, 117.4, 119.3, 120.7, 121.1, 129.3, 129.4, 131.3, 136.9, 139.7, 144.3, 167.2. Found [M+H]⁺ (C₁₈H₂₁NO₂) m/z = 284.1646 (Calc. 284.1572).

Preparation of methyl 4-((4-butylphenyl)amino)benzoate (4.10)

Methyl (4-iodobenzoate) (1 g, 3.82 mmol) and 4-butylaniline (0.72 mL, 4.58 mmol) were added to Pd(OAc)₂ (18 mg, 0.08 mmol), BINAP (100 mg, 0.16 mmol) and Cs₂CO₃ (1.74 g, 5.35 mmol) and were allowed to react according to the general Buchwald-Hartwig amination procedure. The crude residue was purified by flash column chromatography on silica eluting with hexane/ethyl acetate (80:20) (R_f = 0.36) to afford 0.54 g (50 %) of **4.10** as a waxy brown solid. M.p 51 °C. IR (ATR) ν /cm⁻¹: 3340, 2922, 1689, 1591, 1435, 1285, 754. ¹H NMR (400 MHz/CDCl₃)/ppm, δ = 0.94(*t*, 3H, J = 8 Hz, -CH₃CH₂CH₂CH₂Ar), 1.38(*sex.*, 2H, J = 8 Hz, -CH₃CH₂CH₂CH₂Ar), 1.61(*quin.*, 2H, J = 8 Hz, -CH₃CH₂CH₂CH₂Ar), 2.59(*t*, 2H, J = 8 Hz, -CH₃CH₂CH₂CH₂Ar), 3.87(*s*, 3H, -COOCH₃), 5.94(*s*, 1H, -NH), 6.93(*app. d*, 2H, *app. J* = 12 Hz, *HN-ArCHCH-CHCH-C(COOCH₃)*), 7.09(*app. d*, 2H, *app. J* = 8 Hz, *HN-ArCHCH*), 7.15(*app. d*, 1H, *app. J* = 8 Hz, C₄H₉-ArCHCH), 7.89(*app. d*, 2H, J = 8 Hz, ArCHCH-C(COOCH₃)); ¹³C NMR (100 MHz/CDCl₃)/ppm, δ = 14.0, 22.4, 33.7, 35.1, 51.7, 114.0, 120.6, 121.2, 129.4, 131.5, 138.2, 138.3, 148.7, 167.0. Found [M+H]⁺ (C₁₈H₂₁NO₂) m/z = 284.1645 (Calc. 284.1572).

Preparation of 2-((4-butylphenyl)amino)benzoic acid (4.11)

Aqueous potassium hydroxide (36 mL, 7.27 mmol) was added to **4.8** (1.03 g, 3.63 mmol) in ethanol (20 mL) at room temperature and allowed to react according to the general ester hydrolysis procedure to yield 0.90 g (92 %) of **4.11** as a pale yellow solid. M.p 147-148 °C. IR (ATR) ν /cm⁻¹: 3333, 3000-2480 (*br*), 2922, 1650, 1574, 1514, 1441, 1256, 746. ¹H NMR (400 MHz/CDCl₃)/ppm, δ = 0.95(*t*, 3H, J = 8 Hz, -CH₃CH₂CH₂CH₂Ar), 1.39(*sex.*, 2H, J = 8 Hz, -CH₃CH₂CH₂CH₂Ar), 1.61(*quin.*, 2H, J = 8 Hz, -CH₃CH₂CH₂CH₂Ar), 2.61(*t*, 2H, J = 8 Hz, -CH₃CH₂CH₂CH₂Ar), 6.72(*app. t*, 1H, *app. J* = 8 Hz, HOOC-CHCHCHCHC-NH), 7.15 (*app. d*, 1H, HOOC-CHCHCHCHC-NH), 7.18(*app. s*, 4H, C₄H₉-ArCH), 7.33 (*app. t*, 1H, HOOC-CHCHCHCHC-NH), 8.01(*app. d*, 1H, HOOC-CHCHCHCHC-NH), 9.25(*s*, 1H, -NH); ¹³C NMR (100 MHz/CDCl₃)/ppm, δ = 14.0, 22.4, 33.7, 35.1, 109.9, 113.9, 116.7, 123.1, 123.7, 126.3,

129.4, 132.5, 135.2, 137.8, 139.1, 149.5, 173.2. Found $[M+H]^+$ ($C_{17}H_{21}NO_2$) $m/z = 270.1490$ (Calc. 270.1416).

Preparation of 3-((4-butylphenyl)amino)benzoic acid (4.12)

Aqueous potassium hydroxide (14 mL, 2.76 mmol) was added to **4.9** (0.39 g, 1.38 mmol) in ethanol (7 mL) at room temperature and allowed to react according to the general ester hydrolysis procedure to yield 0.3 g (81 %) of **4.12** as a pale yellow solid. M.p 79-80 °C. IR (ATR) ν/cm^{-1} : 3386, 3000-2500 (br), 2928, 1687, 1520, 1288, 746. 1H NMR (400 MHz/ $CDCl_3$)/ppm, $\delta = 0.94$ (t, 3H, $J = 8$ Hz, $-CH_3CH_2CH_2CH_2Ar$), 1.38(*sex.*, 2H, $J = 8$ Hz, $-CH_3CH_2CH_2CH_2Ar$), 1.60(*quin.*, 2H, $J = 8$ Hz, $-CH_3CH_2CH_2CH_2Ar$), 2.58(t, 2H, $J = 8$ Hz, $-CH_3CH_2CH_2CH_2Ar$), 7.04(*app. d.*, 2H, *app. J* = 8 Hz, HN-Ar*CHCH*), 7.13(*app. d.*, 2H, *app. J* = 8 Hz, C_4H_9 -Ar*CHCH*), 7.23 (*app. d.*, 1H, *app. J* = 8 Hz, HN-CH-C(COOH)-*CHCHCH*-NH), 7.32(*app. t.*, 1H, $J = 8$ Hz, HN-CH-C(COOH)-*CHCHCH*-NH), 7.60(*app. d.*, 1H, $J = 8$ Hz, HN-CH-C(COOH)-*CHCHCH*-NH), 7.72(*app. s.*, 1H, HN-*CH*-C(COOH)-*CHCHCH*-NH); ^{13}C NMR (100 MHz/ $CDCl_3$)/ppm, $\delta = 14.0, 22.4, 33.8, 35.0, 117.6, 119.5, 121.4, 121.7, 129.4, 129.5, 130.4, 137.1, 139.5, 144.5, 172.0$. Found $[M+H]^+$ ($C_{17}H_{21}NO_2$) $m/z = 270.1489$ (Calc. 270.1416).

Preparation of 4-((4-butylphenyl)amino)benzoic acid (4.13)

Aqueous potassium hydroxide (18 mL, 3.53 mmol) was added to **4.10** (0.5 g, 1.76 mmol) in ethanol (9 mL) at room temperature and allowed to react according to the general ester hydrolysis procedure to yield 0.41 g (86%) of **4.13** as a white solid. M.p 138 °C IR (ATR) ν/cm^{-1} : 3406, 3070-2545 (br), 2921, 1663, 1598, 1513, 1288, 1175, 755. 1H NMR (400 MHz/ $CDCl_3$)/ppm, $\delta = 0.94$ (t, 3H, $J = 8$ Hz, $-CH_3CH_2CH_2CH_2Ar$), 1.39(*sex.*, 2H, $J = 8$ Hz, $-CH_3CH_2CH_2CH_2Ar$), 1.61(*quin.*, 2H, $J = 8$ Hz, $-CH_3CH_2CH_2CH_2Ar$), 2.60(t, 2H, $J = 8$ Hz, $-CH_3CH_2CH_2CH_2Ar$), 6.00(s, 1H, -NH), 6.94(*app. d.*, 2H, *app. J* = 12 Hz, HN-Ar*CHCH*-*CHCH*-C(COOH));), 7.11(*app. d.*, 2H, *app. J* = 8 Hz, HN-Ar*CHCH*), 7.17(*app. d.*, 1H, *app. J* = 8 Hz, C_4H_9 -Ar*CHCH*), 7.96(*app. d.*, 2H, $J = 8$ Hz, Ar*CHCH*-C(COOH)); ^{13}C NMR (100 MHz/ $CDCl_3$)/ppm, $\delta = 14.0, 22.4, 33.7, 35.1, 113.9, 119.4, 121.6, 129.4, 132.3, 137.9, 138.6, 149.5, 171.5$. Found $[M+H]^+$ ($C_{17}H_{21}NO_2$) $m/z = 270.1489$ (Calc. 270.1416).

Preparation of mixed amine-phenol (4.14)

The mono-phenolic linker (**4.5**) (0.21 g, 0.40 mmol), 2-((4-butylphenyl)amino)benzoic acid (**4.11**) (0.4 g, 1.49 mmol), DPTS (60%) and DCC (0.31 g, 1.49 mmol) were allowed to

react according to the general mixed amine-phenol procedure. The crude product was purified by flash column chromatography on silica eluting with hexane/ethyl acetate (90:10) ($R_f=0.25$) to afford 0.25 g (82%) of **4.14** as a yellow oil. IR (ATR) ν/cm^{-1} : 3636, 3324, 2960, 1731, 1516, 1225, 1134, 748. ^1H NMR (400 MHz/ CDCl_3)/ppm, δ = 0.85(m, 6H, $-\text{CH}_2\text{CH}_3$), 0.94(t, 3H, $J=8$ Hz, $-\text{CH}_3\text{CH}_2\text{CH}_2\text{CH}_2\text{Ar}$), 1.25-1.38(m, 13H, $-\text{CH}_2\text{CH}_3$, $-\text{CH}_3$ and $\text{CH}_3\text{CH}_2\text{CH}_2\text{CH}_2\text{Ar}$), 1.42(s, 18H, CH_3 *tert*-butyl), 1.60(m, 3H, $-\text{CH}_3\text{CH}_2\text{CH}_2\text{CH}_2\text{Ar}$ and $-\text{CH}(\text{CH}_2\text{CH}_3)$), 2.61(m, 4H, Ph- $\text{CH}_2\text{CH}_2\text{-COO-}$ and $-\text{C}_3\text{H}_7\text{CH}_2\text{Ar}$), 2.85(t, 2H, $J=8$ Hz, Ph- $\text{CH}_2\text{CH}_2\text{-COO-}$), 4.08(m, 2H, $\text{COO-CH}_2\text{-CH}(\text{CH}_2\text{CH}_3)\text{-C}_4\text{H}_9$), 4.37(s, 2H, $\text{COO-CH}_2\text{-C}$), 4.42(s, 2H, $\text{COO-CH}_2\text{-C}$), 5.07(s, 1H, -OH) 6.67(*app. t*, 1H, $-\text{OOC-CHCHCHCHC-NH}$), 6.97(s, 2H, Ph- CH), 7.15(m, 5H, $\text{C}_4\text{H}_9\text{-ArCH}$ and $-\text{OOC-CHCHCHCHC-NH}$), 7.29(*app. d*, 1H, $J=8$ Hz, $-\text{OOC-CHCHCHCHC-NH}$), 7.85(*app. d*, 1H, $J=8$ Hz, $-\text{OOC-CHCHCHCHC-NH}$), 9.31(s, 1H, -NH); ^{13}C NMR (100 MHz/ CDCl_3)/ppm, δ = 10.9, 14.0, 18.0, 22.4, 22.9, 23.7, 28.9, 30.3, 30.9, 33.7, 34.3, 35.1, 36.2, 38.7, 46.6, 65.8, 67.5, 110.7, 113.8, 116.7, 123.3, 124.7, 129.3, 130.8, 131.4, 135.9, 137.9, 138.8, 148.8, 152.2, 167.8, 172.7, 173.0. Found $[\text{M}+\text{Na}]^+$ ($\text{C}_{47}\text{H}_{67}\text{NO}_7$) $m/z = 780.4810$ (Calc. 780.4918).

Preparation of mixed amine-phenol (4.15)

The mono-phenolic linker (**4.5**) (0.61 g, 1.20 mmol), 3-((4-butylphenyl)amino)benzoic acid (**4.12**) (0.48 g, 1.80 mmol), DPTS (60%) and DCC (0.37 g, 1.80 mmol) were allowed to react according to the general mixed amine-phenol procedure. The crude product was purified by flash column chromatography on silica eluting with hexane/ethyl acetate (90:10) ($R_f=0.23$) to afford 0.75 g (82%) of **4.15** as a dark yellow oil. IR (ATR) ν/cm^{-1} : 3633, 3381, 2955, 1725, 1213, 749. ^1H NMR (400 MHz/ CDCl_3)/ppm, δ = 0.84(m, 6H, $-\text{CH}_2\text{CH}_3$), 0.93(t, 3H, $J=8$ Hz, $-\text{CH}_3\text{CH}_2\text{CH}_2\text{CH}_2\text{Ar}$), 1.23-1.39(m, 13H, $-\text{CH}_2\text{CH}_3$, $-\text{CH}_3$ and $\text{CH}_3\text{CH}_2\text{CH}_2\text{CH}_2\text{Ar}$), 1.42(s, 18H, CH_3 *tert*-butyl), 1.57(m, 3H, $-\text{CH}_3\text{CH}_2\text{CH}_2\text{CH}_2\text{Ar}$ and $-\text{CH}(\text{CH}_2\text{CH}_3)$), 2.59(m, 4H, Ph- $\text{CH}_2\text{CH}_2\text{-COO-}$ and $-\text{C}_3\text{H}_7\text{CH}_2\text{Ar}$), 2.84(t, 2H, $J=8$ Hz, Ph- $\text{CH}_2\text{CH}_2\text{-COO-}$), 4.05(m, 2H, $\text{COO-CH}_2\text{-CH}(\text{CH}_2\text{CH}_3)\text{-C}_4\text{H}_9$), 4.34(s, 2H, $\text{COO-CH}_2\text{-C}$), 4.43(s, 2H, $\text{COO-CH}_2\text{-C}$), 5.07(s, 1H, -OH), 5.75(s, 1H, -NH), 6.97(s, 2H, Ph- CH), 7.02(*app. d*, 1H, *app. J*=8 Hz, $\text{ArCH-C}(\text{C}_4\text{H}_9)$), 7.11(*app. d*, 2H, *app. J*=8 Hz, ArCH-CN), 7.21(*app. d*, 2H, *app. J*=8 Hz, $\text{HN-CH-C}(\text{COO-})\text{-CHCHCH-}$), 7.28(m, 1H, $\text{HN-CH-C}(\text{COO-})\text{-CHCHCH-}$), 7.46(*app. d*, 1H, $J=8$ Hz, $\text{HN-CH-C}(\text{COO-})\text{-CHCHCH-}$), 7.60(m, 1H, $\text{HN-CH-C}(\text{COO-})$); ^{13}C NMR (100 MHz/ CDCl_3)/ppm, δ = 11.0, 14.0, 17.9, 22.4, 22.9, 23.7, 28.9, 30.3, 30.9, 33.8, 34.3, 35.0,

36.2, 38.7, 46.6, 65.7, 66.1, 67.4, 117.3, 119.4, 120.7, 121.0, 124.7, 129.4, 130.8, 130.9, 136.0, 144.4, 152.2, 166.1, 172.7, 172.9. Found $[M+H]^+$ ($C_{47}H_{67}NO_7$) $m/z = 758.4961$ (Calc. 758.4918).

Preparation of mixed amine-phenol (4.16)

The mono-phenolic linker (4.5) (0.50 g, 0.99 mmol), 4-((4-butylphenyl)amino)benzoic acid (4.13) (0.4 g, 1.49 mmol), DPTS (60%) and DCC (0.31 g, 1.49 mmol) were allowed to react according to the general mixed amine-phenol procedure. The crude product was purified by flash column chromatography on silica eluting with hexane/ethyl acetate (80:20) ($R_f = 0.33$) to afford 0.65 g (86%) of 4.16 as a an orange oil. IR (ATR) ν/cm^{-1} : 3636, 3361, 2960, 1715, 1598, 1517, 1170, 754. 1H NMR (400 MHz/ $CDCl_3$)/ppm, $\delta = 0.84$ (m, 6H, $-CH_2CH_3$), 0.94(t, 3H, $J=8$ Hz, $-CH_3CH_2CH_2CH_2Ar$), 1.24-1.21(m, 11H, $-CH_2CH_3$, $-CH_3$), 1.36(m, 2H, $CH_3CH_2CH_2CH_2Ar$), 1.42(s, 18H, CH_3 *tert*-butyl), 1.58(m, 3H, $-CH_3CH_2CH_2CH_2Ar$ and $-CH(CH_2CH_3)$), 2.60(m, 4H, Ph- $CH_2CH_2-COO^-$ and $-C_3H_7CH_2Ar$), 2.84(t, 2H, $J=8$ Hz, Ph- $CH_2CH_2-COO^-$), 4.06(m, 2H, $COO-CH_2-CH(CH_2CH_3)-C_4H_9$), 4.34(s, 2H, $COO-CH_2-C$), 4.40(s, 2H, $COO-CH_2-C$), 5.07(s, 1H, $-OH$), 5.97(s, 1H, $-NH$), 6.91(*app. d*, 2H, *app. J*=8 Hz, $NH-ArC-CH$), 6.97(s, 2H, Ph- CH), 7.06(*app. d*, 2H, *app. J*=8 Hz, $ArCH-C(C_4H_9)$), 7.15(*app. d*, 2H, *app. J*=8 Hz, $ArCH-CN$), 7.84(*app. d*, 2H, *app. J*=8 Hz, $ArCH-C(COO^-)$); ^{13}C NMR (100 MHz/ $CDCl_3$)/ppm, $\delta = 11.0, 14.0, 14.1, 17.9, 22.3, 22.9, 23.7, 28.9, 30.3, 30.9, 33.7, 34.3, 35.0, 36.2, 38.7, 46.7, 65.6, 65.7, 67.4, 114.0, 119.9, 121.3, 124.7, 129.4, 130.9, 131.6, 135.9, 138.1, 138.4, 149.0, 152.2, 165.9, 172.8, 173.1$. Found $[M+Na]^+$ ($C_{47}H_{67}NO_7$) $m/z = 780.4810$ (Calc. 780.4918).

Preparation of bis(diphenylamine) (4.17)

The first generation hydroxyl linker (2.3) (0.20 g, 0.91 mmol), 2-((4-butylphenyl)amino)benzoic acid (4.11) (0.56 g, 2.09 mmol), DPTS (60%) and DCC (0.43 g, 2.09 mmol) were allowed to react according to the general bis(diphenylamine) procedure. The crude product was purified by flash column chromatography on silica eluting with chloroform/hexane (70:30) ($R_f = 0.56$) to afford 0.56 g (82%) of 4.17 as a yellow oil. IR (ATR) ν/cm^{-1} : 3320, 2960, 1683, 1514, 1216, 1074, 745. 1H NMR (400 MHz/ $CDCl_3$)/ppm, $\delta = 0.83$ (m, 6H, $-CH_2CH_3$), 0.92(t, 6H, $J=8$ Hz, $-CH_3CH_2CH_2CH_2Ar$), 1.21-1.40(m, 12H, $-CH_2CH_3$ and $CH_3CH_2CH_2CH_2Ar$), 1.46(s, 3H, $-CH_3$), 1.60(m, 5H, $-CH_3CH_2CH_2CH_2Ar$ and $-CH(CH_2CH_3)$), 2.59(t, 4H, $J=8$ Hz, $-CH_3CH_2CH_2CH_2Ar$), 4.10(m, 2H,

COO-CH₂-CH(CH₂CH₃)-C₄H₉), 4.56(s, 4H, COO-CH₂-C), 6.66(*app. t*, 2H, *app. J*=8 Hz, -OOC-CHCHCHCHC-NH), 7.15(m, 10H, C₄H₉-ArCH and -OOC-CHCHCHCHC-NH), 7.30(m, 2H, -OOC-CHCHCHCHC-NH), 7.88(*app. d*, 2H, *app. J*=8 Hz, -OOC-CHCHCHCHC-NH), 9.32(s, 2H, -NH); ¹³C NMR (100 MHz/CDCl₃)/ppm, δ = 10.9, 14.0, 22.4, 22.9, 23.7, 28.9, 30.3, 33.7, 35.1, 46.9, 66.0, 67.6, 110.7, 113.8, 116.6, 123.3, 126.2, 129.3, 131.4, 134.4, 138.0, 138.7, 148.8, 167.8, 173.1. Found [M+Na]⁺ (C₄₇H₆₀N₂O₆) m/z = 771.4344 (Calc. 771.4451).

Preparation of bis(diphenylamine) (4.18)

The first generation hydroxyl linker (**2.3**) (0.17 g, 0.74 mmol), 3-((4-butylphenyl)amino)benzoic acid (**4.12**) (0.46 g, 1.70 mmol), DPTS (60%) and DCC (0.35 g, 1.70 mmol) were allowed to react according to the general bis(diphenylamine) procedure. The crude product was purified by flash column chromatography on silica eluting with hexane/ethyl acetate (80:20) (R_f = 0.50) to afford 0.42 g (75%) of **4.18** as a pale yellow oil. IR (ATR) ν/cm⁻¹: 3376, 2960, 1721, 1515, 1208, 1103, 747. ¹H NMR (400 MHz/CDCl₃)/ppm, δ = 0.80(m, 6H, -CH₂CH₃), 0.93(t, 6H, *J*=8 Hz, -CH₃CH₂CH₂CH₂Ar), 1.19-1.37(m, 12H, -CH₂CH₃ and CH₃CH₂CH₂CH₂Ar), 1.40(s, 3H, -CH₃), 1.58(m, 5H, -CH₃CH₂CH₂CH₂Ar and -CH(CH₂CH₃)), 2.56(t, 4H, *J*=8 Hz, -C₃H₇CH₂Ar), 4.05(m, 2H, COO-CH₂-CH(CH₂CH₃)-C₄H₉), 4.55(s, 4H, COO-CH₂-C), 5.74(s, 2H, -NH), 7.00(*app. d*, 4H, *app. J*=8 Hz, ArCH-C(C₄H₉)), 7.10(*app. d*, 4H, *app. J*=8 Hz, ArCH-CN₂H), 7.18(m, 2H, HN-CH-C(COO-)-CHCHCH-), 7.25(m, 2H, HN-CH-C(COO-)-CHCHCH-), 7.46(*app. d*, 2H, *app. J*=8 Hz, HN-CH-C(COO-)-CHCHCH-), 7.60(m, 2H, HN-CH-C(COO-)); ¹³C NMR (100 MHz/CDCl₃)/ppm, δ = 11.0, 14.0, 18.1, 22.3, 22.9, 23.7, 28.9, 30.3, 33.8, 35.0, 38.7, 46.8, 66.3, 67.5, 117.3, 118.9, 119.4, 120.6, 121.0, 126.3, 129.3, 130.8, 136.9, 139.6, 144.4, 166.1, 172.9. Found [M+Na]⁺ (C₄₇H₆₀N₂O₆) m/z = 771.4343 (Calc. 771.4451).

Preparation of bis(diphenylamine) (4.19)

The first generation hydroxyl linker (**2.3**) (0.15 g, 0.65 mmol), 4-((4-butylphenyl)amino)benzoic acid (**4.13**) (0.4 g, 1.49 mmol), DPTS (60%) and DCC (0.31 g, 1.49 mmol) were allowed to react according to the general bis(diphenylamine) procedure. The crude product was purified by flash column chromatography on silica eluting with hexane/ethyl acetate (80:20) (R_f = 0.53) to afford 0.44 g (90%) of **4.19** as a pale orange oil. IR (ATR) ν/cm⁻¹: 3345, 2960, 1696, 1596, 1514, 1265, 1168, 1100, 755. ¹H NMR (400 MHz/CDCl₃)/ppm, δ = 0.82(m, 6H, -CH₂CH₃), 0.94(t, 6H, *J*=8

Hz, $-CH_3CH_2CH_2CH_2Ar$), 1.20-1.38(m, 15H, $-CH_2CH_3$, $-CH_3$, and $CH_3CH_2CH_2CH_2Ar$), 1.61(m, 5H, $-CH_3CH_2CH_2CH_2Ar$ and $-CH(CH_2CH_3)$), 2.59(t, 4H, $J=8$ Hz, $-CH_3CH_2CH_2CH_2Ar$), 4.08(m, 2H, $COO-CH_2-CH(CH_2CH_3)-C_4H_9$), 4.52(s, 4H, $COO-CH_2-C$), 5.96(s, 2H, $-NH$), 6.90(*app. d.*, 4H, *app. J*=8 Hz, $ArCH-CN$), 7.08(*app. d.*, 4H, *app. J*=8 Hz, $ArCH-C(C_4H_9)$), 7.15(*app. d.*, 4H, *app. J*=8 Hz, $ArCH-CN$), 7.85(*app. d.*, 4H, *app. J*=8 Hz $ArCH-C(COO-)$); ^{13}C NMR (100 MHz/ $CDCl_3$)/ppm, δ = 10.9, 14.0, 18.1, 22.3, 22.9, 23.7, 28.9, 30.3, 33.7, 35.0, 38.7, 47.0, 65.9, 67.4, 114.0, 120.0, 121.2, 129.4, 131.6, 138.1, 138.1, 148.9, 165.9, 173.2. Found $[M+Na]^+$ ($C_{47}H_{60}N_2O_6$) m/z = 771.4344 (Calc. 771.4451).

Series 3

Preparation of methyl 3-(3-((4-butylphenyl)amino)phenyl)propanoate (4.20)

Methyl 3-(3-bromophenyl)propanoate (1 g, 4.11 mmol) and 4-butylaniline (0.78 mL, 4.93 mmol) were added to $Pd(OAc)_2$ (18 mg, 0.08 mmol), BINAP (100 mg, 0.16 mmol) and Cs_2CO_3 (1.87 g, 5.75 mmol) and were allowed to react according to the general Buchwald-Hartwig amination procedure. The crude residue was purified by flash column chromatography on silica eluting with hexane/ethyl acetate (80:20) (R_f = 0.41) to afford 0.43 g (34%) of **4.20** as an orange oil. IR (ATR) ν/cm^{-1} : 3380, 2925, 1725, 1591, 1514, 1166, 778. 1H NMR (400 MHz/ $CDCl_3$)/ppm, δ = 0.93(t, 3H, $J=8$ Hz, $-CH_3CH_2CH_2CH_2Ar$), 1.36(*sex.*, 2H, $J=8$ Hz, $-CH_3CH_2CH_2CH_2Ar$), 1.58(*quin.*, 2H, $J=8$ Hz, $-CH_3CH_2CH_2CH_2Ar$), 2.56(t, 2H, $J=8$ Hz, $-CH_3CH_2CH_2CH_2Ar$), 2.61(t, 2H, $J=8$ Hz, $ArC-CH_2CH_2-COOCH_3$), 2.89(t, 2H, $J=8$ Hz, $ArC-CH_2CH_2-COOCH_3$), 3.67(s, 3H, $-COOCH_3$), 5.60(s, 1H, $-NH$), 6.71(*app. d.*, *app. J*=8 Hz, 2H, $HN-CH-C(CH_2CH_2(COOCH_3))-CHCHCH-$), 6.86(*app. d.*, *app. J*=8 Hz, 2H, $HN-CH-C(CH_2CH_2(COOCH_3))-CHCHCH-$), 7.00(*app. d.*, 2H, *app. J*=8 Hz, $HN-ArCHCH$), 7.09(*app. d.*, 2H, *app. J*=8 Hz, $C_4H_9-ArCHCH$), 7.14 (*app. d.*, 1H, *app. J*=8 Hz, $HN-CH-C(COOCH_3)-CHCHCH-NH$); ^{13}C NMR (100 MHz/ $CDCl_3$)/ppm, δ = 14.0, 22.4, 31.0, 33.8, 35.0, 35.7, 51.7, 114.8, 116.7, 118.8, 120.2, 129.2, 129.4, 136.1, 140.4, 141.8, 144.1, 173.4. Found $[M+H]^+$ ($C_{20}H_{25}NO_2$) m/z = 312.1958 (Calc. 312.1885).

Preparation of ethyl 2-(4-((4-butylphenyl)amino)phenyl)acetate (4.21)

Ethyl 2-(4-(bromophenyl)acetate (0.5 g, 2.06 mmol) and 4-butylaniline (0.39 mL, 2.47 mmol) were added to $Pd(OAc)_2$ (9 mg, 0.04 mmol), BINAP (50 mg, 0.08 mmol) and Cs_2CO_3 (0.94 g, 2.88 mmol) and were allowed to react according to the general Buchwald-Hartwig amination procedure. The crude residue was purified by flash column

chromatography on silica eluting with hexane/ethyl acetate (85:15) ($R_f = 0.33$) to afford 0.43 g (67%) of **4.21** as an orange oil. IR (ATR) ν/cm^{-1} : 3385, 2928, 1725, 1608, 1514, 1308, 1140, 750 ^1H NMR (400 MHz/ CDCl_3)/ppm, $\delta = 0.92(\text{t}, 3\text{H}, J=8 \text{ Hz}, -\text{CH}_3\text{CH}_2\text{CH}_2\text{CH}_2\text{Ar})$, $1.25(\text{t}, 3\text{H}, J=8 \text{ Hz}, \text{ArC}-\text{CH}_2-\text{COOCH}_2\text{CH}_3)$, $1.35(\text{sex.}, 2\text{H}, J=8 \text{ Hz}, -\text{CH}_3\text{CH}_2\text{CH}_2\text{CH}_2\text{Ar})$, $1.57(\text{quin}, 2\text{H}, J=8 \text{ Hz}, -\text{CH}_3\text{CH}_2\text{CH}_2\text{CH}_2\text{Ar})$, $2.55(\text{t}, 2\text{H}, J=8 \text{ Hz}, -\text{CH}_3\text{CH}_2\text{CH}_2\text{CH}_2\text{Ar})$, $3.53(\text{s}, 2\text{H}, \text{ArC}-\text{CH}_2-\text{COOCH}_2\text{CH}_3)$, $4.14(\text{q}, 2\text{H}, J=8 \text{ Hz}, \text{ArC}-\text{CH}_2-\text{COOCH}_2\text{CH}_3)$, $5.62(\text{s}, 1\text{H}, -\text{NH})$, $6.97(\text{m}, 4\text{H}, \text{HN}-\text{ArCH}_4-\text{CH}_2(\text{COOCH}_2\text{CH}_3))$, $7.00(\text{app. d}, 2\text{H}, \text{app. } J=8 \text{ Hz}, \text{HN}-\text{ArCHCH})$, $7.07(\text{app. d}, 2\text{H}, \text{app. } J=8 \text{ Hz}, \text{C}_4\text{H}_9-\text{ArCHCH})$; ^{13}C NMR (100 MHz/ CDCl_3)/ppm, $\delta = 14.0, 14.3, 22.4, 33.9, 35.0, 40.7, 60.8, 117.1, 118.6, 125.8, 129.2, 130.1, 136.0, 140.6, 142.9, 172.1$. Found $[\text{M}+\text{H}]^+$ ($\text{C}_{20}\text{H}_{25}\text{NO}_2$) $m/z = 312.1958$ (Calc. 312.1885).

Preparation of methyl 3-(4-((4-butylphenyl)amino)phenyl)propanoate (**4.22**)

Methyl 3-(4-(bromophenyl)propanoate (1 g, 4.11 mmol) and 4-butylaniline (0.78 mL, 4.93 mmol) were added to $\text{Pd}(\text{OAc})_2$ (18 mg, 0.08 mmol), BINAP (100 mg, 0.16 mmol) and Cs_2CO_3 (1.87 g, 5.75 mmol) and were allowed to react according to the general Buchwald-Hartwig amination procedure. The crude residue was purified by flash column chromatography on silica eluting with hexane/ethyl acetate (80:20) ($R_f = 0.37$) to afford 1.61 g (91%) of **4.22** as a waxy yellow solid. M.p 48 °C. IR (ATR) ν/cm^{-1} : 3384, 2960, 1726, 1514, 1191, 823. ^1H NMR (400 MHz/ CDCl_3)/ppm, $\delta = 0.93(\text{t}, 3\text{H}, J=8 \text{ Hz}, -\text{CH}_3\text{CH}_2\text{CH}_2\text{CH}_2\text{Ar})$, $1.36(\text{sex.}, 2\text{H}, J=8 \text{ Hz}, -\text{CH}_3\text{CH}_2\text{CH}_2\text{CH}_2\text{Ar})$, $1.57(\text{quin}, 2\text{H}, J=8 \text{ Hz}, -\text{CH}_3\text{CH}_2\text{CH}_2\text{CH}_2\text{Ar})$, $2.55(\text{t}, 2\text{H}, J=8 \text{ Hz}, -\text{CH}_3\text{CH}_2\text{CH}_2\text{CH}_2\text{Ar})$, $2.61(\text{t}, 2\text{H}, \text{Ar}-\text{CH}_2\text{CH}_2-(\text{COOCH}_3))$, $2.89(\text{t}, 2\text{H}, \text{Ar}-\text{CH}_2\text{CH}_2-(\text{COOCH}_3))$, $3.67(\text{s}, 3\text{H}, -\text{COOCH}_3)$, $5.56(\text{s}, 1\text{H}, -\text{NH})$, $6.97(\text{m}, 4\text{H}, \text{HN}-\text{ArCH}_4-\text{CH}_2(\text{COOCH}_2\text{CH}_3))$, $7.07(\text{app. d}, 2\text{H}, \text{app. } J=8 \text{ Hz}, \text{C}_4\text{H}_9-\text{ArCH}_4)$; ^{13}C NMR (100 MHz/ CDCl_3)/ppm, $\delta = 14.0, 22.4, 30.2, 33.9, 34.9, 36.0, 51.6, 117.5, 118.2, 129.1, 129.2, 132.5, 135.7, 140.8, 142.0, 173.5$. Found $[\text{M}+\text{H}]^+$ ($\text{C}_{20}\text{H}_{25}\text{NO}_2$) $m/z = 312.1958$ (Calc. 312.1885)

Preparation of 3-(3-((4-butylphenyl)amino)phenyl)propanoic acid (**4.23**)

Aqueous potassium hydroxide (11 mL, 2.24 mmol) was added to **4.20** (0.35 g, 1.12 mmol) in ethanol (6 mL) at room temperature and allowed to react according to the general ester hydrolysis procedure to yield 0.25 g (70%) of **4.23** as a waxy red solid. M.p 45 °C. IR (ATR)

ν/cm^{-1} : 3407, 3102-2601 (br), 2960, 1687, 1605, 1519, 1303, 792. ^1H NMR (400 MHz/ CDCl_3)/ppm, δ = 0.93(t, 3H, J = 8 Hz, $-\text{CH}_3\text{CH}_2\text{CH}_2\text{CH}_2\text{Ar}$), 1.38(*sex.*, 2H, J = 8 Hz, $-\text{CH}_3\text{CH}_2\text{CH}_2\text{CH}_2\text{Ar}$), 1.58(*quin.*, 2H, J = 8 Hz, $-\text{CH}_3\text{CH}_2\text{CH}_2\text{CH}_2\text{Ar}$), 2.56(t, 2H, J = 8 Hz, $-\text{CH}_3\text{CH}_2\text{CH}_2\text{CH}_2\text{Ar}$), 2.67(t, 2H, J = 8 Hz, $\text{ArC}-\text{CH}_2\text{CH}_2-\text{COOCH}_3$), 2.89(t, 2H, J = 8 Hz, $\text{ArC}-\text{CH}_2\text{CH}_2-\text{COOCH}_3$), 6.72(*app. d.*, 1H, $\text{HN}-\text{CH}-\text{C}(\text{CH}_2\text{CH}_2(\text{COOH}))-\text{CHCHCH}$), 6.86 (m, 2H, $\text{HN}-\text{CH}-\text{C}(\text{CH}_2\text{CH}_2(\text{COOH}))-\text{CHCHCH}$), 7.00(*app. d.*, 2H, *app. J* = 8 Hz, $\text{HN}-\text{ArCHCH}$), 7.09(*app. d.*, 1H, *app. J* = 8 Hz, $\text{C}_4\text{H}_9-\text{ArCHCH}$), 7.16(*app. t.*, 2H, J = 8 Hz, $\text{HN}-\text{CH}-\text{C}(\text{CH}_2\text{CH}_2(\text{COOH}))-\text{CHCHCH}$); ^{13}C NMR (100 MHz/ CDCl_3)/ppm, δ = 14.0, 22.4, 30.6, 33.8, 34.9, 35.5, 114.8, 116.6, 118.9, 120.1, 129.2, 129.5, 136.2, 140.3, 141.4, 144.1, 178.8. Found $[\text{M}+\text{Na}]^+$ ($\text{C}_{19}\text{H}_{23}\text{NO}_2$) m/z = 320.1622 (Calc. 320.1729).

Preparation of 2-(4-((4-butylphenyl)amino)phenyl)acetic acid (4.24)

Aqueous potassium hydroxide (41 mL, 8.16 mmol) was added to **4.21** (1.27 g, 4.08 mmol) in ethanol (20 mL) at room temperature and allowed to react according to the general ester hydrolysis procedure to yield 0.73 g (63%) of **4.24** as a pale orange solid. M.p 105-108 °C IR (ATR) ν/cm^{-1} : 3374, 3088-2535 (br), 2923, 1696, 1611, 1515, 1177, 803. ^1H NMR (400 MHz/ CDCl_3)/ppm, δ = 0.93(t, 3H, J = 8 Hz, $-\text{CH}_3\text{CH}_2\text{CH}_2\text{CH}_2\text{Ar}$), 1.38(*sex.*, 2H, J = 8 Hz, $-\text{CH}_3\text{CH}_2\text{CH}_2\text{CH}_2\text{Ar}$), 1.58(*quin.*, 2H, J = 8 Hz, $-\text{CH}_3\text{CH}_2\text{CH}_2\text{CH}_2\text{Ar}$), 2.56(t, 2H, J = 8 Hz, $-\text{CH}_3\text{CH}_2\text{CH}_2\text{CH}_2\text{Ar}$), 3.58(s, 2H, $\text{ArC}-\text{CH}_2-\text{COOH}$), 6.99(m, 4H, $\text{HN}-\text{ArCH}_4-\text{CH}_2(\text{COOCH})$), 7.08(*app. d.*, 2H, *app. J* = 8 Hz, $\text{HN}-\text{ArCHCH}$), 7.14(*app. d.*, 2H, *app. J* = 8 Hz, $\text{C}_4\text{H}_9-\text{ArCHCH}$); ^{13}C NMR (100 MHz/ CDCl_3)/ppm, δ = 14.0, 22.4, 33.8, 34.9, 40.2, 117.0, 118.8, 124.8, 129.2, 130.3, 136.2, 140.3, 143.2, 177.4. Found $[\text{M}+\text{H}]^+$ ($\text{C}_{18}\text{H}_{21}\text{NO}_2$) m/z = 284.1645 (Calc. 284.1572).

Preparation of 3-(4-((4-butylphenyl)amino)phenyl)propanoic acid (4.25)

Aqueous potassium hydroxide (32 mL, 6.42 mmol) was added to **4.22** (1.0 g, 3.21 mmol) in ethanol (16 mL) at room temperature and allowed to react according to the general ester hydrolysis procedure to yield 0.91 g (95%) of **4.25** as a pale orange solid. M.p 118-120 °C. IR (ATR) ν/cm^{-1} : 3402, 3090-2607 (br), 2920, 1689, 1514, 1305, 818. ^1H NMR (400 MHz/ CDCl_3)/ppm, δ = 0.93(t, 3H, J = 8 Hz, $-\text{CH}_3\text{CH}_2\text{CH}_2\text{CH}_2\text{Ar}$), 1.39(*sex.*, 2H, J = 8 Hz, $-\text{CH}_3\text{CH}_2\text{CH}_2\text{CH}_2\text{Ar}$), 1.58(*quin.*, 2H, J = 8 Hz, $-\text{CH}_3\text{CH}_2\text{CH}_2\text{CH}_2\text{Ar}$), 2.55(t, 2H, J = 8 Hz, $-\text{CH}_3\text{CH}_2\text{CH}_2\text{CH}_2\text{Ar}$), 2.66(t, 2H, $\text{Ar}-\text{CH}_2\text{CH}_2-(\text{COOCH}_3)$), 2.90(t, 2H, $\text{Ar}-\text{CH}_2\text{CH}_2-(\text{COOCH}_3)$), 6.97(m, 4H, $\text{HN}-\text{ArCH}_4-\text{CH}_2(\text{COOCH}_2\text{CH}_3)$), 7.08(m, 4H, $\text{C}_4\text{H}_9-\text{ArCH}_4$); ^{13}C NMR

(100 MHz/CDCl₃)/ppm, δ = 14.0, 22.4, 30.0, 33.8, 34.9, 35.8, 117.4, 118.3, 129.1, 129.2, 132.1, 135.8, 140.7, 142.2, 178.5. Found [M+Na]⁺ (C₁₉H₂₃NO₂) m/z = 320.1622 (Calc. 320.1729).

Preparation of mixed amine-phenol (4.26)

The mono-phenolic linker (4.5) (0.40 g, 0.79 mmol), 3-(3-((4-butylphenyl)amino)phenyl)propanoic acid (4.23) (0.35 g, 1.18 mmol), DPTS (60%) and DCC (0.24 g, 1.18 mmol) were allowed to react according to the general mixed amine-phenol procedure. The crude product was purified by flash column chromatography on silica eluting with hexane/ethyl acetate (80:20) (R_f = 0.39) to afford 0.52 g (84%) of 4.26 as a dark orange oil. IR (ATR) ν /cm⁻¹: 3634, 3380, 2960, 1731, 1515, 1135, 752. ¹H NMR (400 MHz/CDCl₃)/ppm, δ = 0.87(m, 6H, -CH₂CH₃), 0.93(t, 3H, J=8 Hz, -CH₃CH₂CH₂CH₂Ar), 1.16(s, 3H, -CH₃), 1.26-1.35(m, 10H, -CH₂CH₃), 1.42(s, 18H, -CH₃ *tert*-butyl), 1.58(m, 3H, -CH₃CH₂CH₂CH₂Ar and -CH(CH₂CH₃)), 2.59(m, 6H, Ph-CH₂CH₂-COO-, -C₃H₇CH₂Ar, ArC-CH₂CH₂-COO), 2.85(m, 4H, Ph-CH₂CH₂-COO-, ArC-CH₂CH₂-COO), 4.03(m, 2H, COO-CH₂-CH(CH₂CH₃)-C₄H₉), 4.21(s, 4H, COO-CH₂-C), 5.07(s, 1H, -OH), 5.69(s, 1H, -NH), 6.69(*app. d*, 1H, HN-ArCH²-C(CH₂CH₃COO-)-CH⁴CH⁵CH⁶-), 6.82(*app. s*, 1H, HN-ArCH²-C(CH₂CH₃COO-)), 6.87(*app. d*, 1H, HN-ArCH²-C(CH₂CH₃COO-)-CH⁴CH⁵CH⁶-), 6.97(s, 2H, Ph-CH), 7.00(*app. d*, 2H, ArCHCH-NH), 7.08(*app. d*, 2H, C₄H₉-ArCHCH), 7.14(*app. t*, 1H, HN-ArCH²-C(CH₂CH₃COO-)-CH⁴CH⁵CH⁶-); ¹³C NMR (100 MHz/CDCl₃)/ppm, δ = 11.0, 14.0, 17.8, 22.4, 22.9, 23.7, 28.9, 30.2, 30.3, 30.8, 33.8, 34.3, 34.9, 36.2, 38.7, 46.4, 65.4, 65.6, 67.4, 114.6, 116.7, 118.7, 124.7, 126.1, 129.2, 129.4, 130.8, 135.9, 136.0, 140.4, 141.5, 144.1, 152.2, 172.4, 172.7, 172.9. Found [M+H]⁺ (C₄₉H₇₁NO₇) m/z = 786.5303 (Calc. 786.5231).

Preparation of mixed amine-phenol (4.27)

The mono-phenolic linker (4.5) (0.51 g, 1.01 mmol), 2-(4-((4-butylphenyl)amino)phenyl)acetic acid (4.24) (0.43 g, 1.52 mmol), DPTS (60%) and DCC (0.31 g, 1.52 mmol) were allowed to react according to the general mixed amine-phenol procedure. The crude product was purified by flash column chromatography on silica eluting with hexane/ethyl acetate (85:15) (R_f = 0.33) to afford 0.42 g (54%) of 4.27 as an orange oil. IR (ATR) ν /cm⁻¹: 3632, 3382, 2960, 1730, 1514, 1132, 753. ¹H NMR (400 MHz/CDCl₃)/ppm, δ = 0.87(m, 6H, -CH₂CH₃), 0.93(t, 3H, J=8 Hz, -CH₃CH₂CH₂CH₂Ar),

1.16(s, 3H, -CH₃), 1.26-1.36(m, 10H, -CH₂CH₃), 1.42(s, 18H, -CH₃ *tert*-butyl), 1.57(m, 3H, -CH₃CH₂CH₂CH₂Ar and -CH(CH₂CH₃)), 2.56(m, 4H, Ph-CH₂CH₂-COO- and -C₃H₇CH₂Ar), 2.82(t, 2H, J=8 Hz, Ph-CH₂CH₂-COO-), 3.53(s, 2H, ArC-CH₂-COO), 4.00(m, 2H, COO-CH₂-CH(CH₂CH₃)-C₄H₉), 4.21(m, 4H, COO-CH₂-C), 5.07(s, 1H, -OH), 5.60(s, 1H, -NH), 6.97(m, 6H, Ph-CH and ArCH-CN), 7.10(m, 4H, ArCH-CCH₂); ¹³C NMR (100 MHz/CDCl₃)/ppm, δ = 11.0, 14.0, 14.1, 17.8, 22.4, 22.9, 23.7, 28.9, 30.3, 30.8, 33.8, 34.3, 34.9, 36.2, 38.7, 40.4, 46.4, 65.4, 65.8, 67.4, 117.0, 118.6, 124.7, 125.3, 129.2, 130.1, 130.8, 135.9, 136.1, 140.4, 143.0, 152.2, 171.4, 172.6, 172.8. Found [M+H]⁺(C₄₈H₆₉NO₇) m/z = 772.5147 (Calc. 772.5074).

Preparation of mixed amine-phenol (4.28)

The mono-phenolic linker (4.5) (0.46 g, 0.90 mmol), 3-(4-((4-butylphenyl)amino)phenyl)propanoic acid (4.25) (0.4 g, 1.34 mmol), DPTS (60%) and DCC (0.28 g, 1.34 mmol) were allowed to react according to the general mixed amine-phenol procedure. The crude product was purified by flash column chromatography on silica eluting with hexane/ethyl acetate (80:20) (R_f = 0.37) to afford 0.64 g (90%) of 4.28 as a purple oil. IR (ATR) ν /cm⁻¹: 3633, 3384, 2960, 1731, 1514, 1136, 753. ¹H NMR (400 MHz/CDCl₃)/ppm, δ = 0.87(m, 6H, -CH₂CH₃), 0.93(t, 3H, J=8 Hz, -CH₃CH₂CH₂CH₂Ar), 1.16(s, 3H, -CH₃), 1.27-1.36(m, 10H, -CH₂CH₃), 1.42(s, 18H, -CH₃ *tert*-butyl), 1.57(m, 3H, -CH₃CH₂CH₂CH₂Ar and -CH(CH₂CH₃)), 2.59(m, 6H, Ph-CH₂CH₂-COO-, -C₃H₇CH₂Ar, ArC-CH₂CH₂-COO), 2.85(m, 4H, Ph-CH₂CH₂-COO-, ArC-CH₂CH₂-COO), 4.03(m, 2H, COO-CH₂-CH(CH₂CH₃)-C₄H₉), 4.21(s, 4H, COO-CH₂-C), 5.07(s, 1H, -OH), 5.56(s, 1H, -NH), 6.96(m, 6H, Ph-CH and ArCH-CN), 7.06(m, 4H, ArCH-CCH₂); ¹³C NMR (100 MHz/CDCl₃)/ppm, δ = 11.0, 14.0, 17.8, 22.4, 22.9, 23.7, 28.9, 30.3, 30.8, 33.8, 34.3, 34.9, 35.9, 36.2, 38.7, 46.4, 65.5, 67.3, 117.5, 118.2, 124.7, 126.1, 129.0, 129.2, 130.8, 132.2, 135.7, 136.0, 140.8, 142.1, 152.2, 172.5, 172.7, 172.9. Found [M+H]⁺(C₄₉H₇₁NO₇) m/z = 786.5303 (Calc. 786.5231).

Preparation of bis(diphenylamine) (4.29)

The first generation hydroxyl linker (2.3) (0.08 g, 0.35 mmol), 3-(3-((4-butylphenyl)amino)phenyl)propanoic acid (4.23) (0.24 g, 0.81 mmol), DPTS (60%) and DCC (0.17 g, 0.81 mmol) were allowed to react according to the general bis(diphenylamine) procedure. The crude product was purified by flash column

chromatography on silica eluting with hexane/ethyl acetate (80:20) ($R_f = 0.38$) to afford 0.21 g (75%) of **4.29** as a pale orange oil. IR (ATR) ν/cm^{-1} : 3382, 2960, 1730, 1514, 1134, 776. ^1H NMR (400 MHz/ CDCl_3)/ppm, $\delta = 0.86(\text{m}, 6\text{H}, -\text{CH}_2\text{CH}_3)$, $0.93(\text{t}, 6\text{H}, \text{J}=8\text{ Hz}, -\text{CH}_3\text{CH}_2\text{CH}_2\text{CH}_2\text{Ar})$, $1.15(\text{s}, 3\text{H}, -\text{CH}_3)$, $1.26\text{-}1.39(\text{m}, 12\text{H}, -\text{CH}_2\text{CH}_3)$, $1.58(\text{m}, 5\text{H}, -\text{CH}_3\text{CH}_2\text{CH}_2\text{CH}_2\text{Ar}$ and $-\text{CH}(\text{CH}_2\text{CH}_3)$), $2.55(\text{t}, 4\text{H}, \text{J}=8\text{ Hz}, -\text{C}_3\text{H}_7\text{CH}_2\text{Ar})$, $2.60(\text{t}, 4\text{H}, \text{J}=8\text{ Hz}, \text{ArC}-\text{CH}_2\text{CH}_2\text{-COO})$, $2.86(\text{t}, 4\text{H}, \text{J}=8\text{ Hz}, \text{ArC}-\text{CH}_2\text{CH}_2\text{-COO})$, $4.02(\text{m}, 2\text{H}, \text{COO}-\text{CH}_2\text{-CH}(\text{CH}_2\text{CH}_3)\text{-C}_4\text{H}_9)$, $4.19(\text{m}, 4\text{H}, \text{COO}-\text{CH}_2\text{-C})$, $5.67(\text{s}, 2\text{H}, \text{-NH})$, $6.68(\text{app. d}, 2\text{H}, \text{J}=8\text{ Hz}, \text{HN-ArCH}^2\text{-C}(\text{CH}_2\text{CH}_3\text{COO-})\text{-CH}^4\text{CH}^5\text{CH}^6\text{-})$, $6.80(\text{m}, 2\text{H}, \text{HN-ArCH}^2\text{-C}(\text{CH}_2\text{CH}_3\text{COO-}))$, $6.87(\text{m}, 2\text{H}, \text{HN-ArCH}^2\text{-C}(\text{CH}_2\text{CH}_3\text{COO-})\text{-CH}^4\text{CH}^5\text{CH}^6\text{-})$, $6.99(\text{app. d}, 4\text{H}, \text{app. J}=8\text{ Hz}, \text{ArCHCHC-NH})$, $7.10(\text{app. d}, 4\text{H}, \text{app. J}=8\text{ Hz}, \text{C}_4\text{H}_9\text{-ArCHCH})$, $7.13(\text{app. t}, 2\text{H}, \text{app. J}=8\text{ Hz}, \text{HN-ArCH}^2\text{-C}(\text{CH}_2\text{CH}_3\text{COO-})\text{-CH}^4\text{CH}^5\text{CH}^6\text{-})$; ^{13}C NMR (100 MHz/ CDCl_3)/ppm, $\delta = 11.0, 14.0, 17.8, 22.4, 22.9, 23.7, 28.9, 30.3, 30.8, 31.5, 33.8, 34.9, 35.5, 38.7, 46.3, 65.5, 67.4, 114.6, 116.8, 118.7, 120.1, 129.2, 129.4, 136.0, 140.4, 141.5, 144.1, 172.4, 172.9$. Found $[\text{M}+\text{H}]^+(\text{C}_{51}\text{H}_{68}\text{N}_2\text{O}_6)$ $m/z = 805.5155$ (Calc. 805.5077).

Preparation of bis(diphenylamine) (**4.30**)

The first generation hydroxyl linker (**2.3**) (0.19 g, 0.86 mmol), 2-(4-((4-butylphenyl)amino)phenyl)acetic acid (**4.24**) (0.56 g, 1.98 mmol), DPTS (60%) and DCC (0.41 g, 1.98 mmol) were allowed to react according to the general bis(diphenylamine) procedure. The crude product was purified by flash column chromatography on silica eluting with hexane/ethyl acetate (80:20) ($R_f = 0.41$) to afford 0.46 g (68%) of **4.30** as a dark red oil. IR (ATR) ν/cm^{-1} : 3379, 2960, 1730, 1607, 1514, 1131. ^1H NMR (400 MHz/ CDCl_3)/ppm, $\delta = 0.87(\text{m}, 6\text{H}, -\text{CH}_2\text{CH}_3)$, $0.93(\text{t}, 6\text{H}, \text{J}=8\text{ Hz}, -\text{CH}_3\text{CH}_2\text{CH}_2\text{CH}_2\text{Ar})$, $1.15(\text{s}, 3\text{H}, -\text{CH}_3)$, $1.25\text{-}1.30(\text{m}, 8\text{H}, -\text{CH}_2\text{CH}_3)$, $1.36(\text{m}, 4\text{H}, -\text{CH}_3\text{CH}_2\text{CH}_2\text{CH}_2\text{Ar})$, $1.58(\text{m}, 5\text{H}, -\text{CH}_3\text{CH}_2\text{CH}_2\text{CH}_2\text{Ar}$ and $-\text{CH}(\text{CH}_2\text{CH}_3)$), $2.55(\text{t}, 4\text{H}, \text{J}=8\text{ Hz}, -\text{CH}_3\text{CH}_2\text{CH}_2\text{CH}_2\text{Ar})$, $3.50(\text{s}, 4\text{H}, \text{ArC}-\text{CH}_2\text{-COO-})$, $3.98(\text{m}, 2\text{H}, \text{COO}-\text{CH}_2\text{-CH}(\text{CH}_2\text{CH}_3)\text{-C}_4\text{H}_9)$, $4.16(\text{d}, 2\text{H}, \text{J}=12\text{ Hz}, \text{COO}-\text{CH}_2\text{-C})$, $4.22(\text{d}, 2\text{H}, \text{J}=12\text{ Hz}, \text{COO}-\text{CH}_2\text{-C})$, $5.59(\text{s}, 2\text{H}, \text{-NH})$, $6.94(\text{app. d}, 4\text{H}, \text{ArCH-CN})$, $6.98(\text{app. d}, 4\text{H}, \text{ArCH-CN})$, $7.07(\text{m}, 8\text{H}, \text{ArCH-CCH}_2)$; ^{13}C NMR (100 MHz/ CDCl_3)/ppm, $\delta = 10.9, 14.0, 17.9, 22.4, 23.0, 28.9, 30.3, 31.5, 33.8, 34.9, 38.6, 40.4, 46.3, 65.6, 67.4, 117.1, 118.6, 125.3, 129.2, 130.1, 136.0, 140.4, 142.9, 171.4, 172.8$. Found $[\text{M}+\text{H}]^+(\text{C}_{49}\text{H}_{64}\text{N}_2\text{O}_6)$ $m/z = 777.4839$ (Calc. 777.4764).

Preparation of bis(diphenylamine) (4.31)

The first generation hydroxyl linker (**2.3**) (0.13 g, 0.58 mmol), 3-(4-((4-butylphenyl)amino)phenyl)propanoic acid (**4.25**) (0.4 g, 1.34 mmol), DPTS (60%) and DCC (0.28 g, 1.34 mmol) were allowed to react according to the general bis(diphenylamine) procedure. The crude product was purified by flash column chromatography on silica eluting with hexane/ethyl acetate (80:20) ($R_f = 0.42$) to afford 0.45 g (96%) of **4.31** as a pale yellow oil. IR (ATR) ν/cm^{-1} : 3384, 2960, 1730, 1514, 1137, 752. ^1H NMR (400 MHz/ CDCl_3)/ppm, $\delta = 0.87(\text{m}, 6\text{H}, -\text{CH}_2\text{CH}_3)$, $0.92(\text{t}, 6\text{H}, J=8\text{ Hz}, -\text{CH}_3\text{CH}_2\text{CH}_2\text{CH}_2\text{Ar})$, $1.17(\text{s}, 3\text{H}, -\text{CH}_3)$, $1.27\text{-}1.38(\text{m}, 12\text{H}, -\text{CH}_2\text{CH}_3$ and $-\text{CH}_3\text{CH}_2\text{CH}_2\text{CH}_2\text{Ar})$, $1.57(\text{m}, 8\text{H}, -\text{CH}_3\text{CH}_2\text{CH}_2\text{CH}_2\text{Ar}$ and $-\text{CH}(\text{CH}_2\text{CH}_3)$), $2.57(\text{m}, 8\text{H}, -\text{CH}_3\text{CH}_2\text{CH}_2\text{CH}_2\text{Ar}$ and $\text{Ar}-\text{CH}_2\text{CH}_2-(\text{COO}-)$), $2.85(\text{t}, 4\text{H}, J=8\text{ Hz}, \text{Ar}-\text{CH}_2\text{CH}_2-(\text{COOCH}_3))$, $4.03(\text{m}, 2\text{H}, \text{COO}-\text{CH}_2-\text{CH}(\text{CH}_2\text{CH}_3)-\text{C}_4\text{H}_9)$, $4.19(\text{s}, 4\text{H}, \text{COO}-\text{CH}_2-\text{C})$, $5.55(\text{s}, 2\text{H}, -\text{NH})$, $6.95(\text{m}, 8\text{H}, \text{ArCH}-\text{CCH}_2)$, $7.05(\text{m}, 8\text{H}, \text{ArCH}-\text{CNH})$; ^{13}C NMR (100 MHz/ CDCl_3)/ppm, $\delta = 11.0, 14.0, 17.8, 22.4, 22.9, 23.7, 28.9, 30.1, 30.3, 33.8, 34.9, 35.9, 38.7, 46.3, 65.5, 67.4, 117.5, 118.2, 129.0, 129.2, 132.2, 135.7, 140.8, 142.0, 172.5, 172.9$. Found $[\text{M}+\text{H}]^+(\text{C}_{51}\text{H}_{68}\text{N}_2\text{O}_6)$ $m/z = 805.5150$ (Calc. 805.5077).

4.5 References

- 1 M. Lucarini, P. Pedrielli, G. F. Pedulli, L. Valgimigli, D. Gigmes and P. Tordo, *J. Am. Chem. Soc.*, 1999, **121**, 11546–11553.
- 2 E. T. Denisov and I. V. Khudyakov, *Chem. Rev.*, 1987, **87**, 1313–1357.
- 3 C. Boozer, G. Hammond, C. Hamilton and J. Sen, *J. Am. Chem. Soc.*, 1955, **77**, 3233–3237.
- 4 E. A. Haidasz, R. Shah and D. A. Pratt, *J Am Chem Soc*, 2014, **136**, 16643–16650.
- 5 T. A. B. M. Bolsman, A. P. Blok and J. H. G. Frijns, *J. R. Netherlands Chem. Soc.*, 1978, **97**, 310–312.
- 6 R. K. Jenson, S. Korcek, M. Zinbo and J. L. Gerlock, *J. Org. Chem.*, 1995, **60**, 5396–5400.
- 7 J. R. Thomas, *J Am Chem Soc*, 1960, **82**, 5955–5956.
- 8 J. R. Thomas and C. A. Tolman, *J Am Chem Soc*, 1962, **84**, 2930–2935.
- 9 K. Adamic, M. Dunn and K. U. Ingold, *Can. J. Chem.*, 1969, **47**, 287–294.
- 10 K. U. Ingold and D. A. Pratt, *Chem. Rev.*, 2014, **114**, 9022–9046.
- 11 D. A. Pratt, G. A. DiLabio, G. Brigati, G. F. Pedulli and L. Valgimigli, *J. Am. Chem. Soc.*, 2001, **123**, 4625–4626.
- 12 M. Wijtmans, D. A. Pratt, J. Brinkhorst, R. Serwa, L. Valgimigli, G. F. Pedulli and N. A. Porter, *J. Org. Chem*, 2004, **69**, 9215–9223.
- 13 L. Valgimigli, G. Brigati, G. F. Pedulli, G. A. DiLabio, M. Mastragostino, C. Arbizzani and D. A. Pratt, *Chem. - A Eur. J.*, 2003, **9**, 4997–5010.
- 14 T. S. Chao, D. A. Hutchison and M. Kjonaas, *Ind. Eng. Chem. Prod. Res. Dev.*, 1984, **23**, 21–27.
- 15 G. Scott, *Synergism and Antagonism*, Elsevier, New York, 1965.
- 16 M. Meskina, G. Karpukhina and Z. Maizus, *Pet. Chem. U.S.S.R.*, 1972, **12**, 178–184.
- 17 G. Karpukhina, Z. Maizus and N. Emanuel, *Pet. Chem. U.S.S.R.*, 1966, **5**, 149–154.
- 18 G. Karpukhina, Z. Maizus and L. Matiyenko, *Pet. Chem. U.S.S.R.*, 1966, **6**, 195–200.

- 19 J. Barret, P. Gijsman, J. Swagten and R. F. M. Lange, *Polym. Degrad. Stab.*, 2002, **75**, 367–374.
- 20 J. Barret, P. Gijsman, J. Swagten and R. F. M. Lange, *Polym. Degrad. Stab.*, 2002, **76**, 441–448.
- 21 J. Pospisil, in *Advances in Polymer Science*, 1995, vol. 124, pp. 87–190.
- 22 T. Mang and W. Dresel, *Lubricants and Lubrication*, Wiley-VCH, Weinheim, 2nd edn., 2007.
- 23 J. Dong and C. A. Migdal, in *Lubricant Additives Chemistry and Applications*, ed. L. R. Rudnick, CRC Press Taylor and Francis, London, 2nd edn., 2009, pp. 4–50.
- 24 M. S. Davis, K. Morokuma and R. W. Kreilick, *J. Am. Chem. Soc.*, 1972, **94**, 5588–5592.
- 25 J. Louie and J. F. Hartwig, *Tetrahedron Lett.*, 1995, **36**, 3609–3612.
- 26 M. S. Driver and J. F. Hartwig, *J. Am. Chem. Soc.*, 1996, **118**, 7217–7218.
- 27 A. S. Guram, R. A. Rennels and S. L. Buchwald, *Angew. Chemie Int. Ed.*, 1995, **34**, 1348.
- 28 J. P. Wolfe, S. Wagaw and S. L. Buchwald, *J. Am. Chem. Soc.*, 1966, **118**, 7215–7216.
- 29 D. S. Surry and S. L. Buchwald, *Chem. Sci.*, 2011, **2**, 27–50.
- 30 V. P. Mehta and E. V. Van der Eycken, *Chem. Soc. Rev.*, 2011, **40**, 9283–9303.
- 31 B. Schlummer and U. Scholz, *Adv. Synth. Catal.*, 2004, **346**, 1599–1626.
- 32 A. R. Muci and S. L. Buchwald, in *Cross-Coupling Reactions*, ed. N. Miyaura, Springer Berlin Heidelberg, 2002, vol. 219, pp. 131–209.
- 33 R. Csuk, A. Barthel and C. Raschke, *Tetrahedron*, 2004, **60**, 5737–5750.

Chapter 5

From food to petroleum analysis: The development of a screening assay for new antioxidants using the stable radical DPPH

Abstract

By taking inspiration from the food industry, an assay was investigated as a potential screening tool to test the efficiency of new phenolic antioxidants. The method was based on the spectrophotometric measurement of the stable free radical 1,1-diphenyl-2-picryl-hydrazyl (DPPH) which, in its radical form, has an absorption maxima at 515 nm. The disappearance of this absorption band, upon reaction with an antioxidant, was monitored to reveal the kinetic pathway of the reaction which was defined simply as either fast, medium or slow. Adaptation of the assay was attempted for application to fuel and lubricants whereby the effect of polar and non-polar solvents on the kinetics of the reaction was investigated. In addition, the stoichiometry of the radical scavenging reaction was also analysed to give an insight into the structure-activity relationships of phenolic antioxidants.

5.1 Introduction

Oxidation is not only attributed to the oil and automotive industry but is also a prominent issue in the food industry where the oxidation of lipids is responsible for changes in the colour, flavour, nutritional quality, safety and texture of foods.^[1,2] In addition, the consumption of radical species in foodstuffs has been found to contribute to the aging process of human tissues and to the development of various pathological diseases.^[2-4] It is therefore necessary for this industry to protect food lipids and human tissues against free radicals by introducing antioxidants from a natural or synthetic origin, in a similar fashion to the stabilisation of hydrocarbon base oils, which has been discussed in the previous chapters of this thesis. Natural antioxidants, particularly those derived from fruit and vegetable extracts, have gained increasing interest among the scientific community because epidemiological studies have indicated that frequent intake of natural antioxidants is associated with a lower risk of cardiovascular disease and cancer.^[5-7] Furthermore, there is a widespread agreement that some commonly used

synthetic antioxidants such as 2-*tert*-butyl-4-hydroxyanisole (BHA) and 2,6-di-*tert*-butyl-4-methylphenol (BHT) (**Figure 5.1**) need to be replaced with natural antioxidants because of their potential health risks and toxicity.^[8,9] Hence, in recent years an increase in the use of methods for estimating the radical scavenging efficiency of large quantities of natural products has been observed.^[10-12]

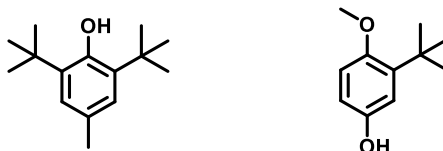


Figure 5.1 Structures of the synthetic antioxidants BHT and BHA.

A wide range of spectrophotometric assays have been adopted with convenient methodologies which allow quick and simple quantification of antioxidant capacities which lend themselves to high-throughput analysis.^[13-17] Free radical scavenging is one of the known mechanisms by which antioxidants inhibit oxidation and consequently the most popular assays utilise generated or stable radical species such as 2,2'-azino-bis-3-ethylbenzthiazoline-6-sulfonic acid (ABTS) and 1,1-diphenyl-2-picryl-hydrazyl (DPPH) (**Figure 5.2**).^[12,18,19]

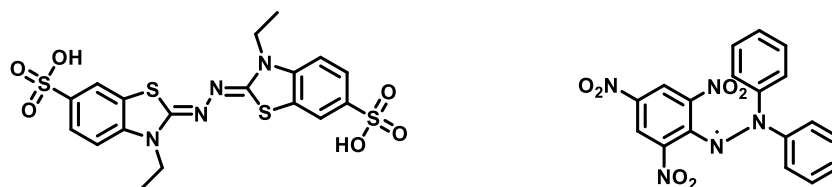
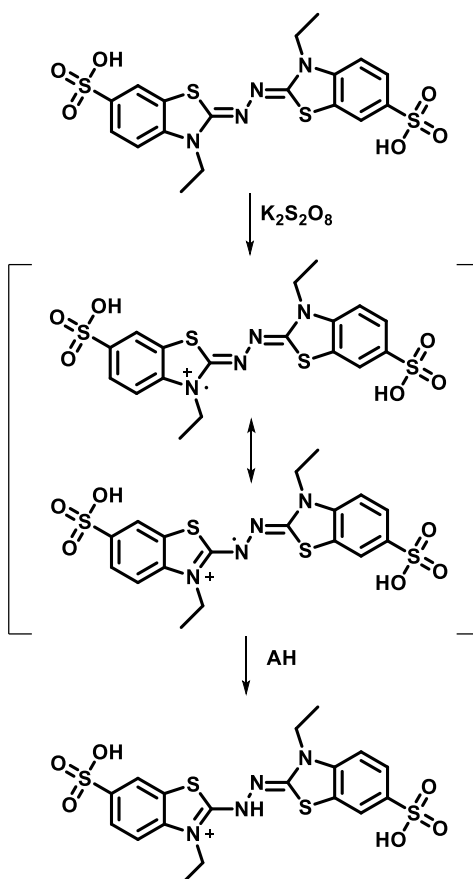


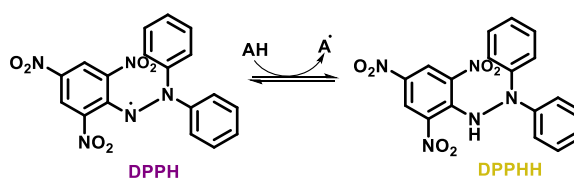
Figure 5.2 Structures of the spectrophotometer assay species ABTS and DPPH.

Both assays are based on an electron transfer process and involve the reduction of a coloured oxidant which can be monitored easily by a spectrophotometer. More recent developments of the ABTS assay are based on the generation of a blue/green ABTS^{•+} chromophore through an initial reaction with potassium persulfate (K₂S₂O₈).^[20] This is a relatively long-lived radical species and can subsequently be reduced by an antioxidant or hydrogen donor (**Scheme 5.1**).^[10] This process can be monitored by use of UV-Vis spectroscopy with multiple absorbance intensities reported at 415, 645, 734 and 815 nm.^[20-22] An advantage of this assay is that it is suitable for strongly coloured samples as the absorbance can be measured outside the visible spectral range using the 734 or 815 nm absorbance.^[10] Moreover, this species is water soluble which is of particular importance when analysing biological systems.



Scheme 5.1 Generation of the blue/green $ABTS^{\bullet+}$ radical cation and subsequent reduction by an antioxidant, AH, to the colourless $ABTS^{\bullet}$.

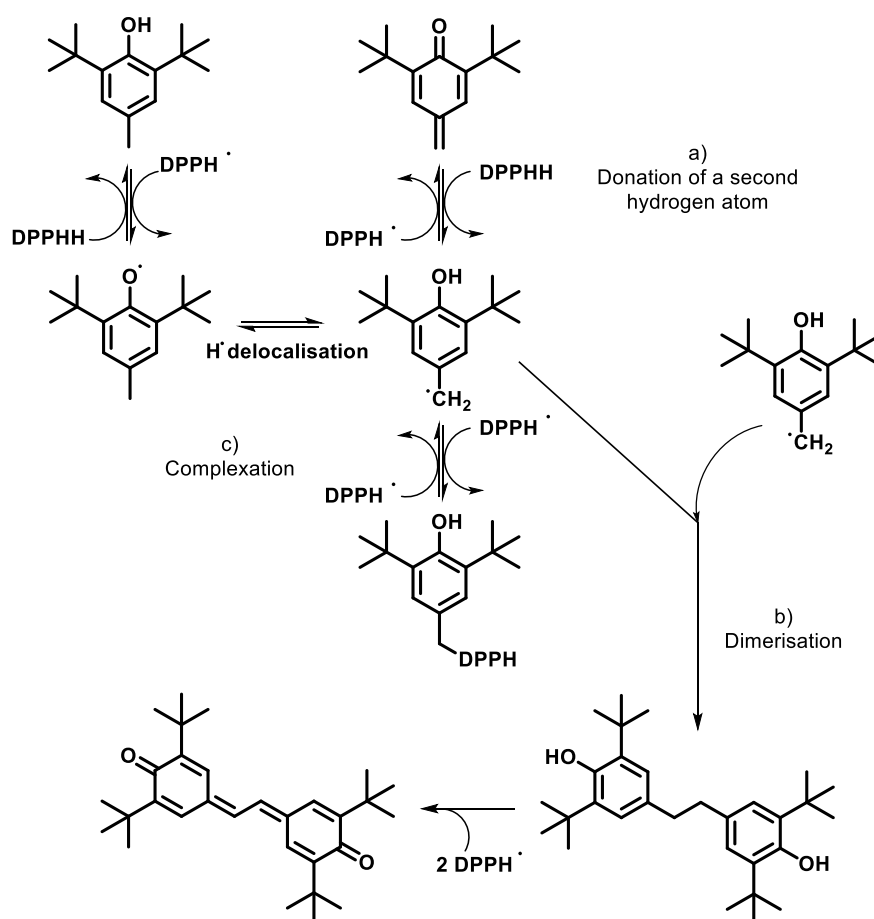
In contrast, the DPPH assay is based on the reduction of the commercially available, stable radical DPPH to 1,1-diphenyl-2-picrylhydrazine (DPPHH) (**Scheme 5.2**). The DPPH assay was first reported^[23] by Blois in 1958 and the reaction conveniently shows a colour change from deep purple to pale yellow. This colour change can be monitored by UV-Vis spectroscopy by noting the decrease in intensity of the characteristic absorbance maxima at 515 nm.



Scheme 5.2 Reduction of DPPH free radical by an antioxidant AH to DPPHH.

Even though both assays are convenient in their application, the DPPH assay has an advantage in that the stable radical is commercially available and the initial generation

step of the photoactive indicator is not required. An improvement on the original method by Blois was introduced by Brand-Williams and co-workers who found that the radical scavenging reaction was more complex than originally thought and three possible pathways for the reaction between antioxidants and the DPPH radical were proposed (Scheme 5.3).^[24]



Scheme 5.3 Proposed mechanism for BHT/DPPH reaction showing three possible radical scavenging pathways a) donation of a second hydrogen atom, b) dimerisation and c) complexation.

This method has been implemented by many research groups to analyse a number of sample types for their antioxidant properties including fruits, herbs, leaves, spices and vegetables.^[25-29] There are, however, significant limitations arising from the inconsistency of the conditions used across each research group. This makes it difficult to compare results and examples of such inconsistencies include different starting concentrations of DPPH, incubation times, solvents and temperatures.^[30-40] A consistent set of parameters needs to be determined for this assay to be used and compared within

an industry. These assays were originally designed with the aim of simple, high-throughput analysis, however the need for careful consideration of the kinetics and mechanisms of the reactions between radical species and phenolic antioxidants needs to be emphasised.

Even though these assays may have limitations regarding a biological application, there is, however, an opportunity for the methods to be applied to other industries. Currently, in fuel and lubricant technology, the performance of new antioxidants is measured by blending antioxidant chemistries into a hydrocarbon base oil or fuel and accelerated oxidative conditions are used to assess the hydrocarbons' resistance to oxidation.^[41] Exposure to typical conditions found in an engine is important, however these methods often require relatively large amounts of the antioxidant and significant blend volumes which is not always practical. Oxidative stability tests also require the use of specialised and expensive instrumentation whereby standard analysis techniques include pressurised differential scanning calorimetry, rancimat analysis and bespoke oxidation tests which often have lengthy testing procedures.^[41] Through the exploitation of the DPPH assay it was proposed that a suitable screening method to evaluate the performance of potential antioxidants as radical scavengers could be developed and applied to fuel and lubricant technology. The DPPH assay has a greater advantage over the ABTS assay in that the radical species is acquired directly therefore eliminating the need to introduce more chemical species into the reaction medium. The DPPH assay could provide a convenient analysis of potential new antioxidants by giving an estimation of which candidates possess radical scavenging capabilities while also probing key antioxidant structure-activity relationships.

5.2 Results and Discussion

The stable free radical DPPH (**Figure 5.2**) was employed to determine the antioxidant efficiency of a series of phenolic compounds designed for use in lubricant base oils. The stability of the DPPH radical occurs from the delocalisation of the unpaired electron over the molecule as a whole, hence dimerisation does not take place. The delocalisation within the DPPH molecule gives rise to a deep purple colour with a characteristic absorption maxima at 515 nm. When DPPH is exposed to a substance that can donate a hydrogen atom, such as an antioxidant, it is reduced to DPPHH (**Scheme 5.2**) and a colour change is observed from deep purple to pale yellow. A typical trace showing the decrease

in the absorbance maxima at 515 nm corresponding to the consumption of the radical is shown in **Figure 5.3**.

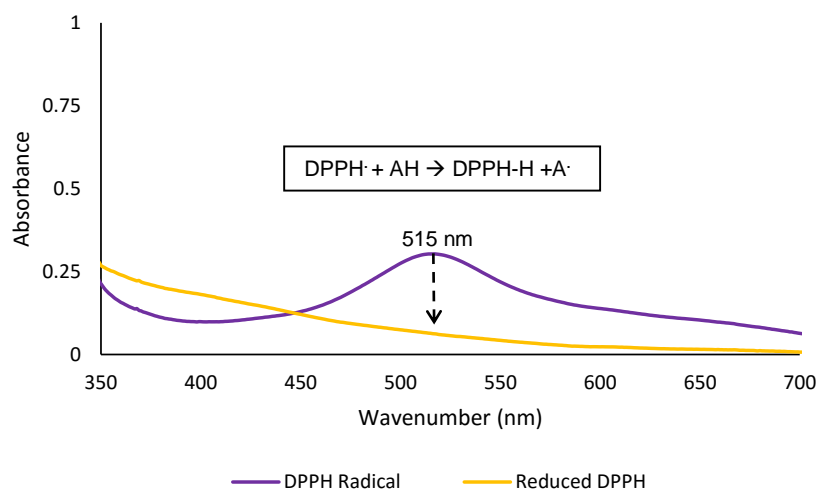


Figure 5.3 UV-Vis spectroscopic analysis shows the reduction in the absorbance maxima at 515 nm when the DPPH radical is reduced by reaction with an antioxidant (AH).

The most common solvent system used for analysing plant and food extracts was found to be methanol and hence was investigated first to use as a comparison against literature values.

5.2.1 Radical scavenging analysis using alcoholic solvents.

UV-Vis spectroscopic analysis was used to monitor the reaction between the antioxidants and the DPPH radical. The range of accuracy for spectrophotometric measurements falls within an absorbance range of 0.221-0.698 according to Ayres *et al.*,^[42] however, a number of researchers in the literature have used DPPH concentrations far beyond the spectrophotometric accuracy. For this assay, a calibration of varying concentrations of the DPPH radical, in methanol, was achieved successfully (**Figure 5.4**) with absorbances obeying the Beer-Lambert law within the range of accuracy.

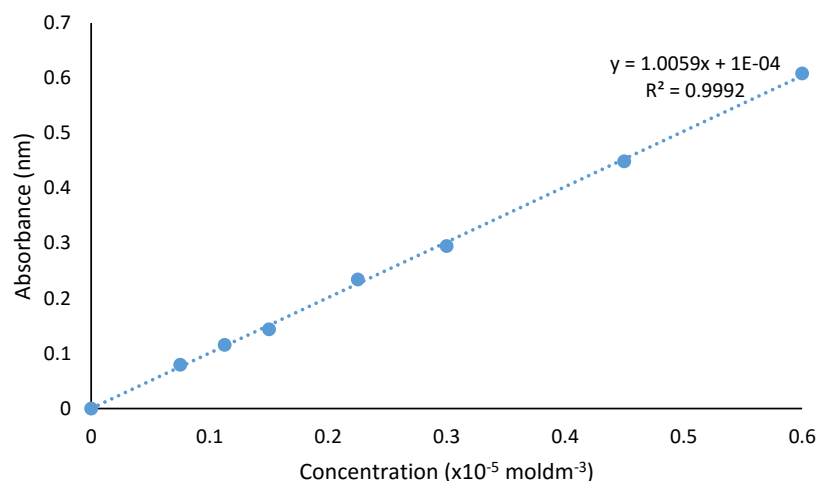


Figure 5.4 Calibration of the DPPH radical in methanol.

The first generation (**2.9**) and second generation (**2.10**) polyphenols (**Figure 5.5**), as synthesised in Chapter 2, were analysed and compared to the phenolic antioxidant BHT. Equimolar solutions of each antioxidant were prepared in methanol.

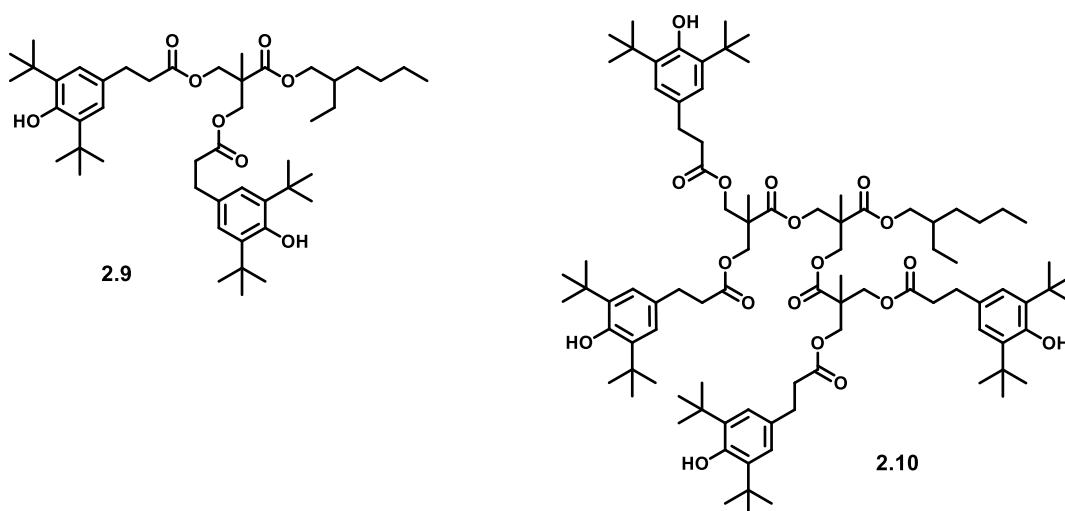


Figure 5.5 Structure of first generation (**2.9**) and second generation (**2.10**) polyester dendrons.

In a 3 mL quartz cuvette, 1.5 mL of the methanolic DPPH solution was added to 1.5 mL of the methanolic antioxidant solution hence producing a 1:1 reaction medium. The temperature was maintained at 25 °C and the decrease in absorbance was determined at 515 nm by taking readings at intervals from 0 minutes to 180 minutes whereby a steady state was observed. The percentage of DPPH radical remaining was calculated by converting the absorbance to concentration (mol dm⁻³) using **Equation 1**, derived from

the calibration in **Figure 5.4**. The percentage was subsequently calculated using **Equation 2** and plotted against time to produce the ‘time-scavenging’ graph shown in **Figure 5.6**.

$$Abs_{515nm} = 1.0059[DPPH] + 1 \times 10^{-4}$$

Equation 1

$$\% \text{ of DPPH remaining} = \frac{[DPPH]_{t=x}}{[DPPH]_{t=0}} \times 100$$

Equation 2

The time-scavenging graph shows the successful reduction of the DPPH radical by all three antioxidants (**Figure 5.6**). The kinetic profile for BHT shows what is described in the literature as a ‘slow’ reaction with DPPH. The time taken to reach a steady state is greater than one hour and this finding corresponds well to that reported by Brand-Williams and co-workers.^[24]

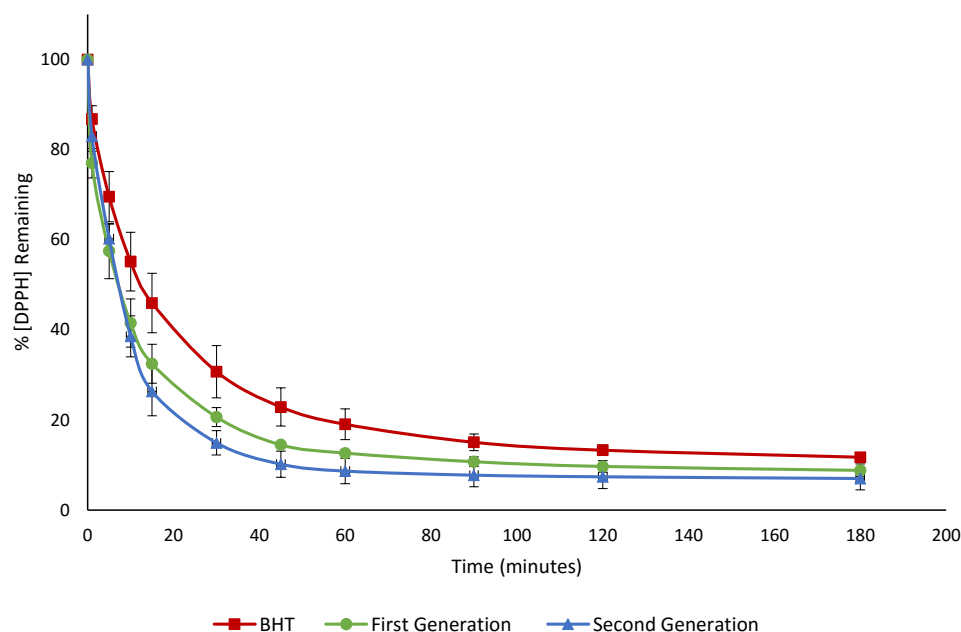
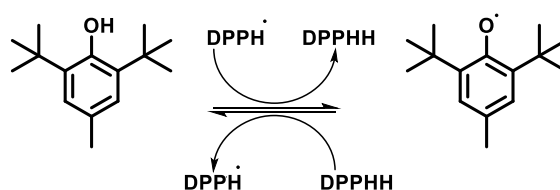


Figure 5.6 Radical scavenging analysis of equimolar solutions of BHT and the first generation (2.9) and second generation (2.10) polyphenols.

Structural analysis of each antioxidant suggested that the second generation (2.10), which possessed four active phenolic alcohols, would show the best radical scavenging capabilities followed by the first generation (2.9) with two active phenolic alcohols and finally BHT with one active phenolic alcohol. The results shown in **Figure 5.6** confirmed

this by showing the second generation (**2.10**) had the most efficient radical scavenging profile by scavenging a higher percentage of DPPH radicals in a shorter time than the first generation (**2.9**) and BHT. An observation to note was once the steady state was reached *ca.* 10% of the DPPH radical still remained. The first generation (**2.9**) and the second generation (**2.10**) were expected to scavenge all of the DPPH radicals as there was an excess of radical scavenging sites compared to the number of moles of DPPH radicals. It was postulated that the system, under these experimental conditions, could reach the equilibrium suggested in **Scheme 5.4**.



Scheme 5.4 Proposed equilibrium of radical scavenging between an antioxidant, BHT, and a radical where R• represents the DPPH radical.

This equilibrium agreed with the mechanistic pathways suggested by Brand-Williams and co-workers, shown in **Figure 5.3**. The presence of an equilibrium highlighted a limitation with using the data to analyse antioxidant potentials as it was not possible to quantitate the amount of radical scavenged by each antioxidant by reporting the end point of the reaction alone. This method did, however, give a good indication of the kinetic pathways and an alternative method to quantify radical scavenging capabilities is discussed later in this chapter.

With a significant drive for renewable and more environmentally friendly fuels, biofuel production and use is increasing. In Europe, ethanol is currently blended into gasoline at a minimum of 10% while in other parts of the world, like Brazil, up to 85% is used.^[43] To achieve an improved understanding of how antioxidants may behave in a biofuel the assay was repeated using ethanol as the solvent with the aim of moving closer to a typical fuel or lubricant medium. As before, a calibration of DPPH was carried out with an excellent R^2 value of 0.9998. Equimolar solutions of BHT, first generation (**2.9**) and second generation (**2.10**) polyphenols were analysed for their radical scavenging properties. In addition, a typical lubricant antioxidant, Irganox L135, was also analysed for an industrial comparison (**Figure 5.7**).

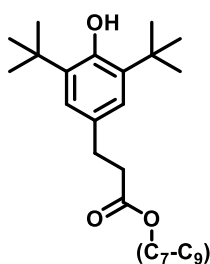


Figure 5.7 Structure of the lubricant phenolic antioxidant Irganox L135.

A steady-state was observed after 3 hours and again a percentage of the DPPH remained at the end of the 3 hour test in all of the four compounds tested (**Figure 5.8**).

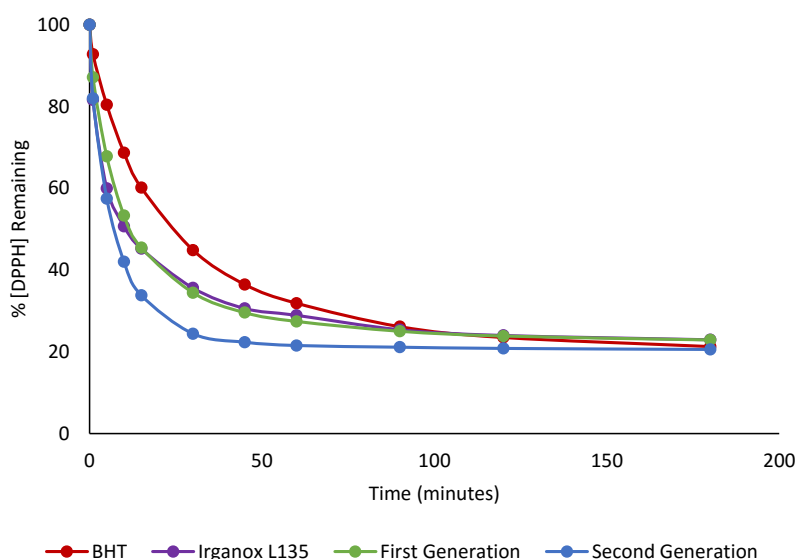


Figure 5.8: Radical scavenging analysis of equimolar solutions of BHT, Irganox L135, first generation (**2.9**) and second generation (**2.10**) in ethanol.

From the 'time-scavenging' profile, shown in **Figure 5.8**, it was observed that Irganox L135, which possessed one phenolic hydroxyl, was scavenging radicals at a very similar rate to the first generation (**2.9**) which had two phenolic hydroxyls. In addition, Irganox L135 scavenged radicals faster than the structurally similar mono-phenol, BHT. The longer alkyl chain and the ester functionality in Irganox L135 may have contributed a greater stabilising effect than the methyl moiety on BHT therefore allowing a more efficient scavenging pathway. Polyphenols can be described as having a higher antioxidant potential than mono-phenols on the basis that there are more phenolic

hydroxyls which are available for hydrogen donation to a radical species. It was therefore expected that the first generation (**2.9**) would reveal a greater radical scavenging ability than Irganox L135, however this was not observed. The first generation (**2.9**) had a more bulky end group from the 2,2-*bis*(hydroxymethyl)propionic acid (*bis*-(MPA)) branching unit compared to Irganox L135 which had an unbranched alkyl chain. Furthermore, the additional *tert*-butyl groups surrounding the phenolic hydroxyls on the first generation (**2.9**) may have caused a greater steric effect hence impeding access to the bulky DPPH radical. It was suggested by Brand-Williams and co-workers that antioxidants which followed a 'slow' kinetic profile, as revealed in **Figure 5.8**, presented a stoichiometry that was more difficult to interpret. As proposed previously, further analysis was needed to determine the true stoichiometry of these reactions.

5.2.2 Radical scavenging analysis using hydrocarbon reaction mediums.

In an effort to represent a more typical reaction medium in which the antioxidants would be utilised, the liquid alkane 2,6,10,15,19,23-hexamethyltetracosane, commercially known as squalane, was used. Squalane is a saturated branched hydrocarbon with the structure shown in **Figure 5.9**. It is described as a viscous oil (*ca.* 0.0361 kg m s⁻¹ at 293 K, in comparison to ethanol which is reported as *ca.* 0.0012 kg m s⁻¹)^[44] which is characteristic of a typical lubricant formulation.

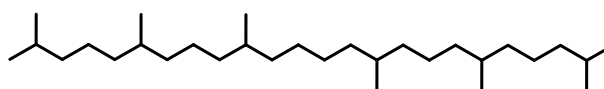


Figure 5.9 Structure of the branched hydrocarbon, squalane

Generation of an accurate DPPH calibration using squalane proved to be more challenging. A drawback of using viscous solutions is that accurate dispensing is not always possible with a small volume of oil residue unavoidably left in the pipette tip. Nevertheless, a satisfactory calibration was achieved with an R² value of 0.9962. BHT was analysed first and a different kinetic profile was observed (**Figure 5.10**). In ethanol, the kinetics were described as 'slow' whereas in squalane it was described as 'intermediate' where a steady state was reached between *ca.* 5 and 10 minutes. A 'fast' kinetic profile would be described as reaching a steady state in less than 1 minute.

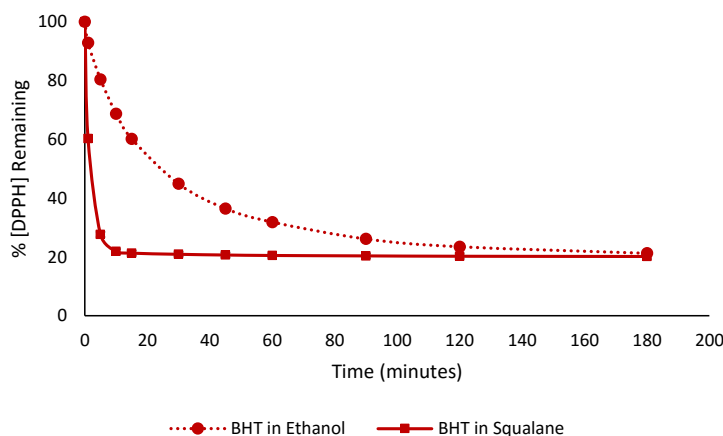


Figure 5.10 Overlay of the time-scavenging profiles for BHT in ethanol and in squalane to show the differences in reaction kinetics between the two solvents.

From this data it was hypothesised that when the antioxidants were solvated in an alcoholic solution, such as methanol or ethanol, there was a potential for hydrogen bonding to occur between the alcoholic hydroxyl and the phenolic hydroxyl shown in **Figure 5.11**. This intermolecular association could potentially decrease the rate of reaction in comparison to an apolar hydrocarbon based solvent where hydrogen bonding would not occur.

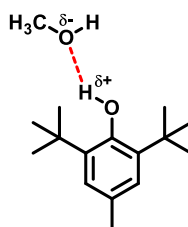


Figure 5.11 Proposed hydrogen bonding interaction between the methanolic hydroxyl and the phenolic hydroxyl of BHT.

Since 1958 the use of the DPPH assay to assess the total antioxidant potential of food and plant products has gained increasing popularity. Interestingly, in parallel to these studies, independent research into the kinetics of the DPPH/phenol reactions also began around the same time. A number of studies, in particular over the last 15 years, have highlighted the significant impact that different solvent systems have on the rate of reaction between a radical species and phenol derivatives.^[44-53] Primarily, these reports disagree with the theory of solvent-phenol hydrogen bonding. Other solvents such as acetonitrile and ethyl acetate were also shown to hydrogen bond to phenolic compounds, however, alcohols, such as methanol and ethanol, produced unexpected kinetic data.^[53-55] A controversial

paper by Thavasi and co-workers reported that intermolecular hydrogen bonding between methanol solvent molecules actually prevented the interaction between methanol and the phenolic hydroxyl moieties (**Figure 5.12**).^[45] This scenario ensured that more phenolic hydroxyl groups were available for scavenging the free radical hence a faster kinetic profile would be expected in alcoholic type solvent mediums.

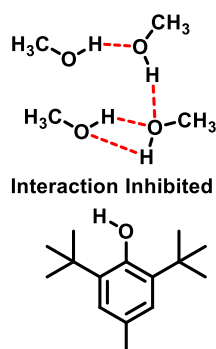


Figure 5.12 Proposed intermolecular hydrogen bonding between methanol solvent molecules.^[45]

Litwinienko and Ingold reported that BHT had the fastest rate of H-atom abstraction in the alkane heptane when compared to a number of alcohols including ethanol.^[49] To probe radical scavenging in an alkane further, the first generation (**2.9**) and second generation (**2.10**) polyphenols and Irganox L135 were also analysed in squalane (**Figure 5.13**).

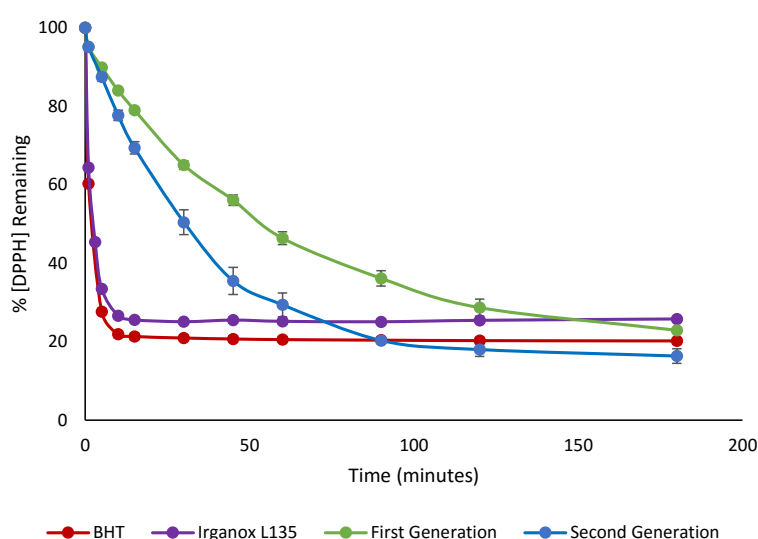


Figure 5.13 Radical scavenging analysis of equimolar solutions of BHT, Irganox L135, first generation (**2.9**) and second generation (**2.10**) in squalane.

The analysis revealed that BHT and Irganox L135 both followed the same ‘intermediate’ kinetic profile whereas the first (2.9) and second (2.10) generation displayed a ‘slow’ kinetic profile similar to that seen in ethanol. This data suggested that the cause of the differences could be ascribed to the solubility of the antioxidants, their ability to diffuse within the oil matrix and also their capacity to react with a bulky radical such as DPPH. The first (2.9) and second (2.10) generations are both bulky antioxidants and it would be sensible to suggest that diffusion within the oil would be reduced when compared to the smaller, more soluble Irganox L135 and BHT. The first and second generation proposal agrees with the literature findings where the rate of reaction was observed to decrease as the viscosity of the solvent increased.^[54] The anomaly of BHT and Irganox L135 could be attributed to a preferred solvency in the hydrocarbon over an alcohol, however, viscous solvent mediums have not been reported widely hence a direct comparison of the data is difficult. An evaluation of the kinetic pathways in ethanol and squalane for the first generation (2.9) is shown in **Figure 5.14**, which reinforces the unexpected literature proposal that alcoholic solvents give rise to a faster kinetic profile in comparison to an alkane.

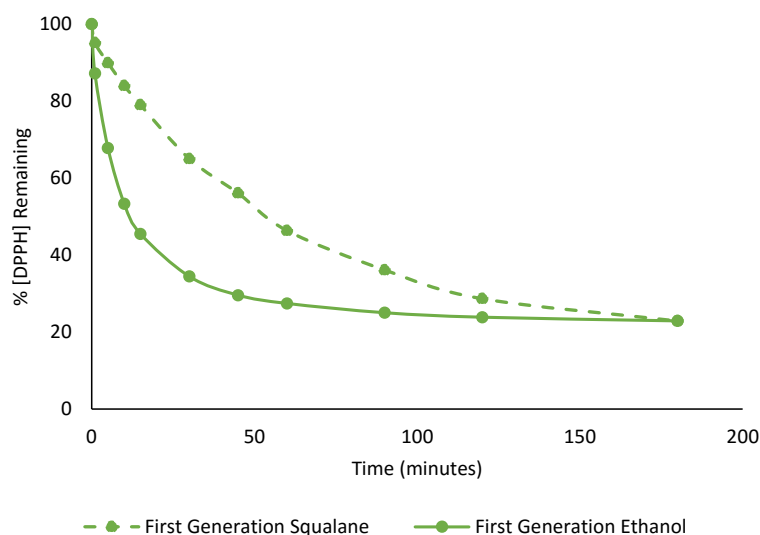
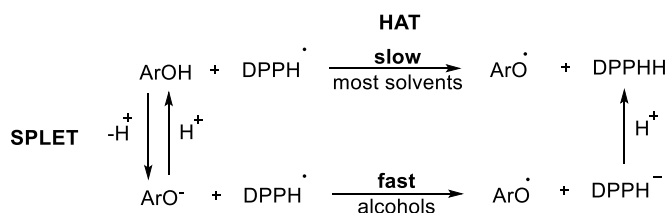


Figure 5.14 Comparison of the kinetic profile of the first generation (2.9) in ethanol and squalane.

The solvent effects on the kinetics of hydrogen abstraction are significantly more complex than hydrogen bonding alone and it has been reported that alcohols reveal unusual kinetic behaviours. Extensive research has found that there are two main mechanisms regarding phenolic hydrogen atom transfer by radicals.^[47-50,53] The first is hydrogen atom

transfer (HAT) and the second is sequential proton-loss electron-transfer (SPLET) (Scheme 5.5).



Scheme 5.5 Representation of the two key mechanistic pathways of hydrogen abstraction from a phenol.^[48]

HAT is generally favoured in alkanes or hydrogen bond acceptor (HBA) solvent types such as ethyl acetate. SPLET, in contrast, becomes the dominant mechanism in solvents that support ionisation such as methanol. Ionisation of the phenol generates a phenoxide anion which is highly reactive towards radical species such as DPPH, hence a higher than expected reaction rate is observed.^[48,50] The SPLET mechanism is favoured for phenols with low pK_a values which is typical of stronger acids. Therefore, dissociation into the counter ions is more favourable and the formation of the phenoxide anion would be preferred. Solvents with a low dielectric constant cause an increase in pK_a value for example ethanol has a dielectric constant of *ca.* 24.6 and hexane has a dielectric constant of *ca.* 1.9.^[56] Formation of the phenoxide anion is hence unfavourable in alkanes and further confirms the reasoning behind the presence of the two hydrogen abstraction mechanistic pathways.

Additional studies have shown that the addition of base increases the rate of the SPLET mechanism whereas the addition of acid causes a decrease in rate.^[49,52] This is worth considering when analysing the lifecycle of an oil formulation. A typical oil formulation is basic in nature as a result of the performance enhancing additives and during oxidation, various chemical species are generated including acids. This change from a basic environment to an acidic environment could have a significant effect on the type of mechanism by which the antioxidants function. An additional consideration is that the oxidation process continues to occur within the oil even after the engine has stopped. This assay therefore potentially gives an insight into antioxidant behaviour during resting conditions within the oil sump. The slower kinetics of the first generation (2.9) and second generation (2.10) could be beneficial as it would suggest that the antioxidants

are present in the oil for longer whereas in the case of BHT and Irganox L135 they are both consumed quickly once exposed to radical species.

From the 'time-scavenging' analysis in two different solvent types it was clear that this analysis alone was not enough to determine antioxidant efficiency. Not only were there significant differences between solvent systems but the number of radicals scavenged could not be quantitated as a result of complex mechanistic pathways attributed to each individual antioxidant and solvent. In an attempt to overcome these limitations and to standardise a method, an alternative analysis procedure known as the Efficient Concentration (EC_{50}) was assessed.

5.2.3 Efficient Concentration (EC_{50}) analysis.

Anti-radical activity can be defined as the amount of antioxidant necessary to decrease the initial concentration of the DPPH radical by 50%. This is termed as the 'efficient concentration' or EC_{50} value. The advantage of using this method of analysis over the 'time-scavenging' procedure was that numerical values were obtained as a function of the molar ratio of antioxidant to radical. This analysis eliminated any issues with incomplete scavenging as a result of an equilibrium between the antioxidant and the radical. Initially, EC_{50} analysis was carried out for BHT, Irganox L135, first generation (**2.9**) and second generation (**2.10**) in ethanol. Ethanol was chosen so that comparisons could be made to current literature in addition to ease of handling, low cost and low toxicity. Solutions of different molar ratios of antioxidant to DPPH radical were prepared and allowed to stand in the dark at room temperature for 3 hours to ensure a steady state was reached. The absorbance of each solution was measured at 515 nm and converted to the percentage of DPPH radical remaining using **Equation 1** and **2**. The EC_{50} value was then determined graphically by finding the molar ratio when the remaining DPPH concentration was equal to 50%. The graphical analysis for BHT is shown in **Figure 5.15**.

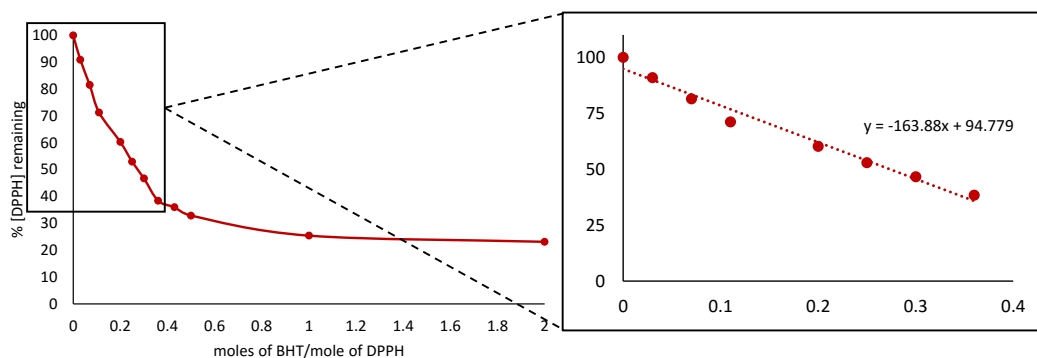


Figure 5.15 Graphical analysis of the EC₅₀ value for BHT.

Using the EC₅₀ value a number of other parameters were calculated. The anti-radical power (ARP) was calculated as the inverse of EC₅₀ whereby the larger the ARP the more efficient the antioxidant. The stoichiometry was calculated by multiplying the EC₅₀ value by two. This gave the theoretical efficient concentration of antioxidant needed to reduce 100% of the DPPH radicals. The number of reduced DPPH radicals per mole of antioxidant was calculated subsequently by the inverse of the stoichiometry ($1/2 \times \text{EC}_{50}$). The results for the numerical analysis of each antioxidant are shown in **Table 1**.

Compound	Number of -OH	EC ₅₀	Antiradical Power (ARP, $1/\text{EC}_{50}$)	Stoichiometric Value ($2 \times \text{EC}_{50}$)	Number of reduced DPPH radicals
BHT	1	0.27	3.70	0.54	1.85
Irganox L135	1	0.49	2.05	0.98	1.02
First Generation (2.9)	2	0.22	4.55	0.44	2.27
Second Generation (2.10)	4	0.06	16.67	0.12	8.33

Table 5.1: EC₅₀ analysis of BHT, Irganox L135, first generation (2.9) and second generation (2.10).

The EC₅₀ value shown in **Table 5.1** agreed well with the reported radical scavenging pathway (**Figure 5.16**), suggesting that BHT can scavenge 1.85 DPPH radicals per molecule.

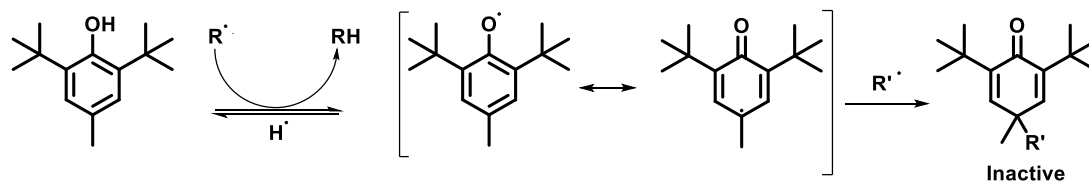


Figure 5.16 Radical scavenging pathway of BHT.

Referring back to the structures of the first generation (**2.9**) and second generation (**2.10**) polyphenols (**Figure 5.17**), and comparing to the radical scavenging pathway of BHT, it was sensible to propose that there are four and eight active scavenging sites for the first generation (**2.9**) and second generation (**2.10**), respectively.

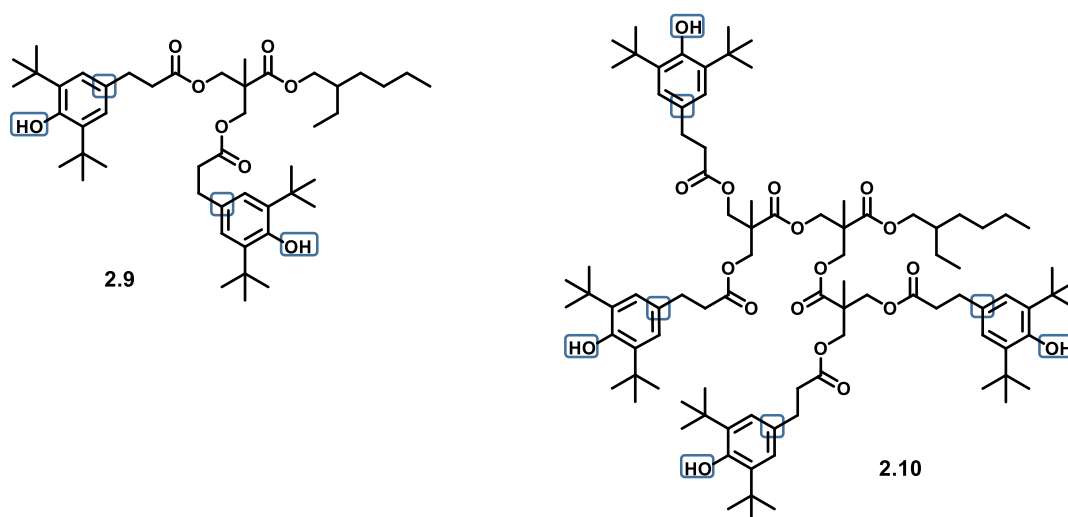


Figure 5.17 Structures of first generation (**2.9**) and second generation (**2.10**) with potential radical scavenging sites highlighted.

The results from the EC_{50} analysis revealed that this was true for the second generation (**2.10**) but not for the first generation (**2.9**). Initial considerations were that the second generation (**2.10**) was a much larger molecule compared to the first generation and it was surprising that the results revealed such a high scavenging efficiency for a bulky radical like DPPH. The additional *bis*(MPA) branching units in the second generation may have allowed a more disperse structure compared to the first generation where a more sterically hindered conformation may have been observed. Computational analysis, using Cerius2[®] modelling software, confirmed this hypothesis and revealed the energy minimised structures for the first (**2.9**) and second (**2.10**) generation to have different preferred spatial arrangements (see **Figures 5.18** and **5.19**). Analysis of the first

generation revealed an energetically minimised structure where both phenolic end-groups were in close proximity (**Figure 5.18, a**). In particular, the phenolic hydroxyl of one aromatic ring was aligned with the second scavenging site, in the *para* position, on the second aromatic ring. This led to the proposal that maybe hydrogen abstraction was occurring intramolecularly, from one phenolic ring to the other, hence rendering two scavenging sites inactive and resulting in a scavenging stoichiometry of 2 radicals per mole of antioxidant. This hypothesis was supported by analysing the energy minimised structure after intramolecular hydrogen abstraction (**Figure 5.18, b**), which again revealed a stabilised conformation suggesting that this pathway could be possible.

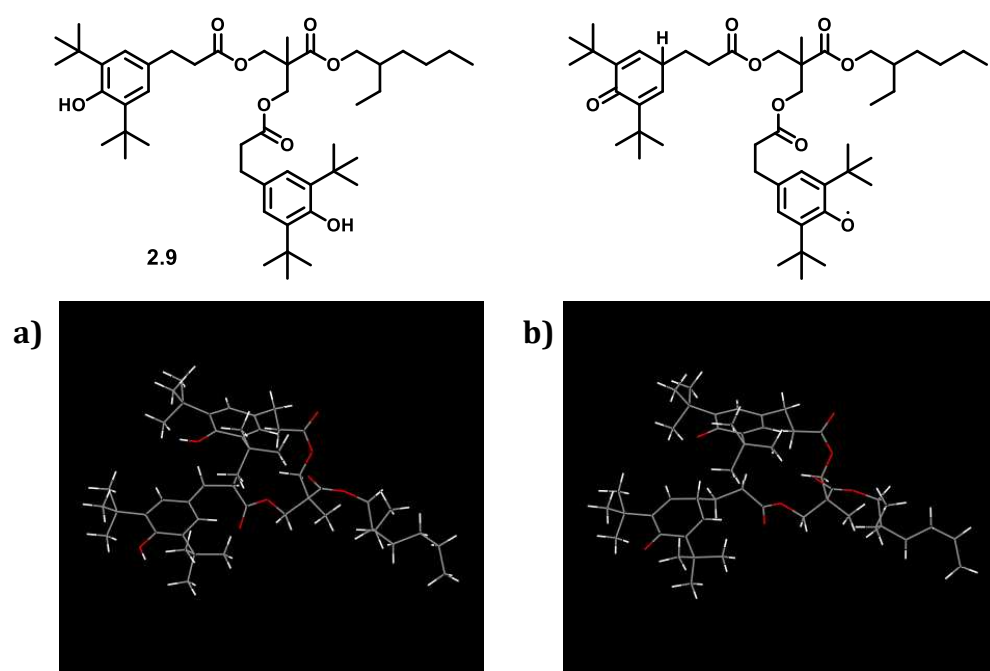


Figure 5.18 Energy minimised computational models of the first generation polyphenol (**2.9**) where **a**) revealed the close proximity of both aromatic rings, suggesting steric hindrance plays a role in the lower than expected radical scavenging stoichiometry and **b**) revealed the possibility of proton transfer between aromatic rings rendering one ring inactive to radical scavenging.

Computational analysis of the second generation revealed an energetically favourable disperse conformation (**Figure 5.19, a**) with an energy of 216 Kcal. This indicated that there would be little steric hindrance interfering with the radical scavenging pathway.

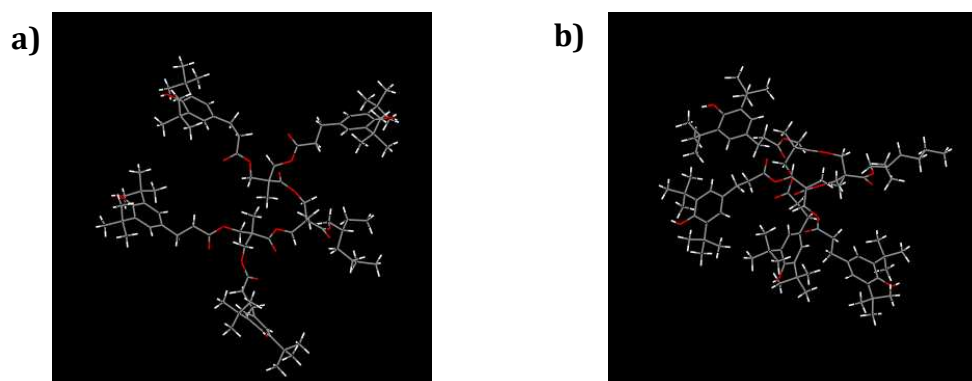
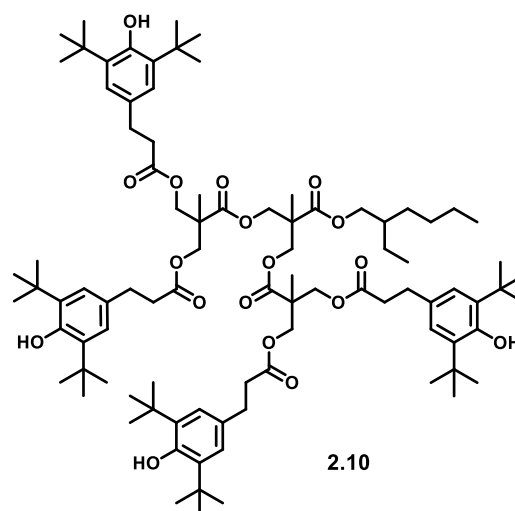


Figure 5.19 Energy minimised computational models of the second generation polyphenol (**2.10**) where **a)** revealed an energetically stabilised disperse structure and **b)** revealed a further energetically stabilised conformation whereby one branch intersects the other to again prevent close contact between the phenolic end-groups.

Further minimisation of the conformation revealed a more favourable structure with a reduced energy of 144 Kcal. Interestingly, the geometries of the phenolic end-groups meant that an intersection of one diphenol branch through the middle of the second diphenol branch was revealed. This intersection prevented close contact of the phenolic end-groups therefore making the intramolecular hydrogen abstraction, hypothesised for the first generation, unlikely. All potential radical scavenging sites would thus be retained hence a scavenging stoichiometry of 8 radicals per mole of antioxidant would be expected.

An additional series of potential phenolic antioxidants, shown in **Table 5.2**, were also analysed for their EC_{50} values to gather more of an understanding on structure-activity relationships.

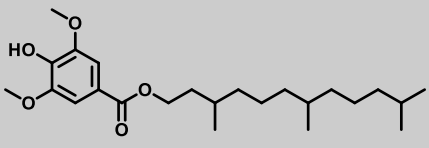
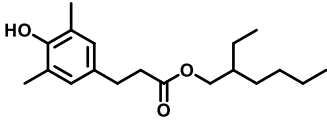
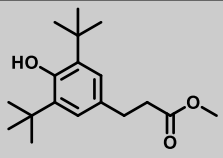
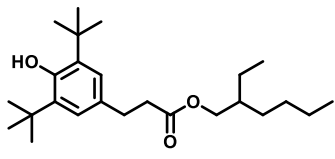
Structure	Code
	A01
	A02
	5.1
	5.2

Table 5.2 Structures of potential phenolic antioxidants **A01** and **A02** (provided by BP Technology Centre, Pangbourne) and **5.1** and **5.2** (synthesised at the University of Reading).

The antioxidants **A01** and **A02** were potential antioxidant candidates and were provided as research samples by the BP Technology Centre, Pangbourne. The EC₅₀ results are presented in **Table 5.3**.

Compound	Number of -OH	EC ₅₀	Antiradical Power (ARP, 1/EC ₅₀)	Stoichiometric Value (2xEC ₅₀)	Number of reduced DPPH radicals
A01	1	-	-	-	-
A02	1	0.22	4.55	0.44	2.27
5.1	1	0.43	2.32	0.86	1.16
5.2	1	0.55	1.82	1.10	0.91

Table 5.3 EC₅₀ analysis of **A01**, **A02**, **5.1** and **5.2**.

The mono-phenol **A01** showed very little radical scavenging activity and even at the higher molar ratio 2:1, a 50% scavenging was not reached (**Figure 5.20**). The poor scavenging capability could be attributed to the methoxy moieties positioned *ortho* to the phenolic hydroxyl. These moieties could have hydrogen bonding interactions with not

only the phenolic hydroxyl but also the ethanol molecules. In addition, the ester moiety linking the alkyl chain to the aromatic ring, is directly appended at the *para* position. This direct attachment was also seen to have a negative effect on antioxidant capability in the structures discussed previously in **Chapter 4**.

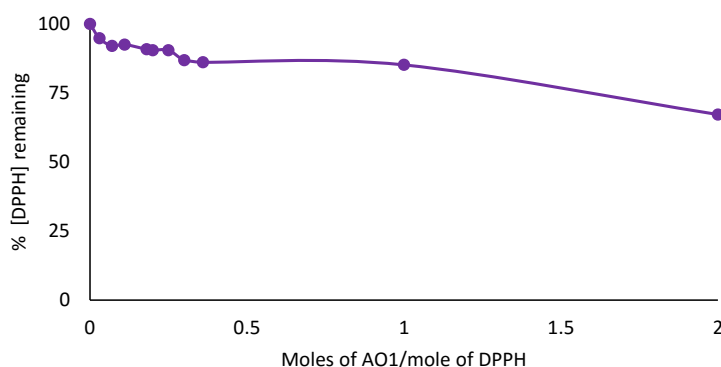


Figure 5.20 EC_{50} radical scavenging analysis of **A01**.

The antioxidant **A02** showed good radical scavenging of *ca.* 2 DPPH radicals per mole of antioxidant. By possessing only methyl groups at the 2 and 6 position of the ring it is less sterically hindered when compared to the *tert*-butyl groups of BHT, however, it was hypothesised that this antioxidant would not perform well in high temperature conditions with the stability of the antioxidant radical being negatively affected. Subsequently, the antioxidants **5.1** and **5.2** were both synthesised to investigate the effect of different structural features on the radical scavenging ability. A direct comparison between **A02** and **5.2** revealed the impact of steric hindrance on the radical scavenging process and confirmed a significant limitation of the assay. The DPPH radical is bulky and does not represent the typical radical species that would be found in the oil matrix during oxidation as small species, such as alkyl and peroxy radicals, are more typical. However, Avila and co-workers reported that the rate of hydrogen abstraction was independent of the nature of the radical species.^[57] This implies that hydrogen abstraction is not the rate determining step in this process but rather other scavenging pathways such as dimerization and complexation, as described in **Scheme 5.3**, are determining the antioxidant capability.

A final series of antioxidants were investigated (**Figure 5.21**) using this method and the results are shown in **Table 5.4**. Aromatic amines are known to exhibit antioxidant characteristics at higher temperatures within the lubricant and typically show a synergistic effect when blended with phenolic antioxidants (**Chapter 4**). It was thought that this spectroscopic assay may be able to determine synergistic capabilities.

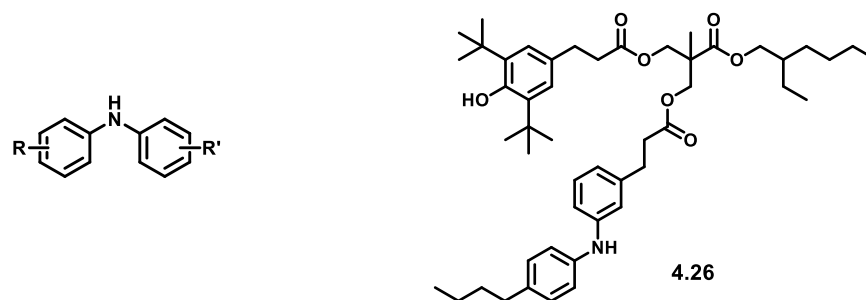


Figure 5.21 Structures of Irganox L57, where R and R' are typically octyl or *tert*-butyl, and mixed amine-phenol **4.26**.

Compound	Number of -NH	EC ₅₀	Antiradical Power (ARP, 1/EC ₅₀)	Stoichiometric Value (2xEC ₅₀)	Number of reduced DPPH radicals
Irganox L57	1	-	-	-	-
Irganox L135/L57	1	0.60	1.67	1.2	0.83
4.26	1	0.38	2.63	0.76	1.31

Table 5.4 EC₅₀ analysis of Irganox L57, a blend of Irganox L135 and L57 and **4.26**.

Differential scanning calorimetry analysis, discussed in **Chapter 4**, revealed that the mixed amine-phenol **4.26** exhibited better antioxidant activity than a combination of L135 and L57 when blended into a hydrocarbon base oil and subjected to oxidative conditions. In the case of this assay the result was also true, however it was expected that the number of reduced DPPH radicals per mole of antioxidant would be much greater. It is known from the literature that aromatic amines and phenolic antioxidants show a synergistic effect when in the presence of each other whereby one can be regenerated from the other. An additional limitation was revealed from the analysis of Irganox L57 where a similar profile to **AO1** was observed. Less than 50% of the DPPH radicals were scavenged even at the higher ratio of antioxidant to radical. It was proposed that the activation energy of the initial hydrogen abstraction from the secondary amine was not being reached at

25 °C. To investigate this further, the time-scavenging profile for Irganox L57 was analysed at a higher temperature (**Figure 5.22**).

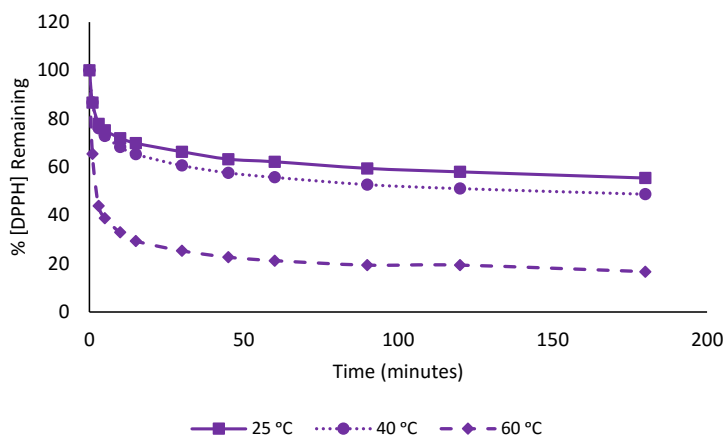


Figure 5.22 Time-scavenging analysis of Irganox L57 in ethanol at 25 °C, 40 °C and 60 °C.

The time-scavenging analysis revealed there was an increase in the percentage of DPPH radicals scavenged by increasing the temperature to 60 °C. It can therefore be concluded from this analysis that the DPPH assay, at room temperature, would not be suitable for testing the performance or synergistic properties of amine-based antioxidants.

In summary, from these preliminary studies, it was concluded that this assay would not be suitable for the analysis of antioxidant compounds in hydrophobic environments. The limitations of complex mechanistic pathways and solvent effects have been revealed which prevents the development of a standardised method. Further in depth kinetic studies would need to be carried out for each individual antioxidant for a reliable data set to be generated regarding radical scavenging capabilities. This would in turn defeat the object of the work which was to develop a simple, high-throughput analysis of new phenolic antioxidants.

5.3 Conclusions

A series of antioxidants were analysed for their radical scavenging properties using the stable free radical DPPH. Using this assay, both the kinetic profiles and stoichiometry of the radical scavenging reactions were investigated. The radical scavenging reactions in ethanol revealed a 'slow' kinetic profile for BHT, Irganox L135, first generation (**2.9**) and second generation (**2.10**) phenolic antioxidants which was in agreement with data originally reported by Brand-Williams and co-workers. When the solvent system was

changed from ethanol to squalane, a significant shift in the kinetic profile of the mono-phenols BHT and Irganox L135 was observed whereby a steady state was achieved in less than 10 minutes when compared to over 60 minutes in ethanol. The kinetic profiles of the first generation (2.9) and second generation (2.10) polyphenols were revealed to be slower in squalane than in ethanol. Analysis of the literature highlighted an alternative mechanistic pathway for hydrogen abstraction when alcoholic solvents were used which resulted in a faster than predicted rate of reaction. Additional factors were considered when analysing the polyphenolic antioxidants such as increased bulkiness and steric hindrance surrounding the radical scavenging sites within the molecules. A quantitative analysis, termed EC₅₀, was carried out to determine the stoichiometry of the reaction between the antioxidants and the radicals. The number of DPPH radicals scavenged per mole of antioxidant was calculated for a series of phenolic and aminic antioxidants and an overriding limitation of using a bulky radical was revealed. Antioxidants known to perform well in typical lubricant oxidation tests exhibited poor radical scavenging capabilities in this assay. In addition, aromatic amine chemistries were not suitable for this test as a result of the activation energy required for the radical scavenging reaction to occur. The time-scavenging profile for the aromatic amine Irganox L57 revealed, at 25 °C, less than 50% scavenging was achieved whereas at higher temperatures this percentage was increased. The overall outcome of the development of this assay was that there were too many limitations regarding mechanistic pathways and solvent effects for it to be used as a reliable study for new antioxidants. If the results are interpreted with caution and in conjunction with more in depth kinetic studies, mechanistic pathways of phenolic antioxidants could be determined with the potential to guide a more directed design of new antioxidants.

5.4 Experimental

Reagents and solvents were purchased from Sigma Aldrich and used without further purification with the exception of 3-(3,5-di-*tert*-butyl-4-hydroxy-phenyl)-propionic acid which was purchased from Alfa Aesar. Dichloromethane was distilled under a nitrogen atmosphere from calcium hydride. All further purification and characterisation was carried out as described in **Chapter 2**.

All radical scavenging assays were analysed using a Varian Cary 300 UV-Visible Spectrometer. The wavelength was set to a range of 200-800 nm and 3 mL quartz

cuvettes were used with a 1 cm path length. The temperature was maintained at 25 °C unless otherwise stated.

Time-Scavenging: In a 3 mL quartz cuvette, 1.5 mL of DPPH solution (6×10^{-4} mol dm⁻³) was added to 1.5 mL of the antioxidant solution (6×10^{-4} mol dm⁻³). The temperature was maintained at 25 °C and the decrease in absorbance was determined at 515 nm by taking readings at intervals from 0 minutes to 180 minutes whereby a steady state was observed. For the time-scavenging analysis of Irganox L57 the same procedure was followed with the exception that the temperature was raised to either 40 °C or 60 °C using the variable temperature setting available on the Varian Cary 300 UV-Visible Spectrometer.

EC₅₀: In a 3 mL quartz cuvette, varying volumes of DPPH solution (6×10^{-4} mol dm⁻³) to antioxidant solution (6×10^{-4} mol dm⁻³) were added. For example 0.9 mL of antioxidant and 2.1 mL of DPPH produced a 1:2.3 ratio of antioxidant to DPPH radical. Twelve ratios were prepared for each antioxidant and samples were allowed to stand in the dark at room temperature for 3 hours. A set of references were prepared using DPPH solutions containing no antioxidant. The absorbance of each sample was measured at 515 nm and recorded.

Computational modelling was carried out on a Silicon Graphics O2 workstation using Cerius2® (version 3.5, Accelrys San Diego) software. The force-field used for the calculations (molecular mechanics with charge equilibration) was Dreiding 2.21, developed by the Goddard group at The California Institute of Technology.^[58]

Preparation methyl 3-(3,5-di-*tert*-butyl-4-hydroxyphenyl)propanoate (5.1)

3-(3,5-Di-*tert*-butyl-4-hydroxy-phenyl)-propionic acid (2.00 g, 7.18 mmol) was dissolved in methanol (100 mL) and cooled to 0 °C. To the solution, thionyl chloride (2.08 mL, 28.72 mmol) was added dropwise. The reaction was allowed to warm to room temperature and was stirred overnight. Upon completion, the solvent was removed *in vacuo*. The resulting residue was diluted with ethyl acetate (40 mL) and washed with 1M aqueous NaOH (3 x 20 mL). The organic phase was dried over MgSO₄, filtered and the solvent was removed *in vacuo* to afford 1.99 g (95%) of **5.2** as a pale orange oil. IR (ATR) ν/cm^{-1} : 3609, 2960, 1716, 1433, ¹H NMR (400 MHz/CDCl₃)/ppm, δ = 1.43 (s, 18H, -CH₃ *tert*-butyl), 2.60 (t, 2H, J=8 Hz, -CH₂), 2.87 (t, 2H, J=8 Hz, -CH₂), 3.69 (s, 3H, -CH₃), 5.08 (s,

1H, -OH), 6.99 (s, 2H, -CH aromatic); ¹³C NMR (100 MHz/CDCl₃)/ppm, δ = 30.3, 31.0, 34.3, 36.4, 51.6, 124.8, 131.1, 135.9, 152.2, 173.7. Found [M+H]⁺ (C₁₈H₂₈O₃) m/z = 293.2121 (Calc. 293.2117).

Preparation 2-ethylhexyl 3-(3,5-di-*tert*-butyl-4-hydroxyphenyl)propanoate (5.2)

3-(3,5-Di-*tert*-butyl-4-hydroxy-phenyl)-propionic acid (1.00 g, 3.60 mmol), 2-ethylhexan-1-ol (0.56 mL, 3.60 mmol) and DPTS (60%) were dissolved in dry dichloromethane (15 mL). The solution was stirred at room temperature for 30 minutes. To the solution, *N,N'*-dicyclohexylcarbodiimide (DCC) (0.74 g, 3.60 mmol) dissolved in dry dichloromethane (10 mL) was added over 15 minutes. The reaction was left overnight at room temperature under a nitrogen atmosphere. The reaction mixture was filtered to remove the white *N,N'*-dicyclohexylurea (DCU) precipitate and the filtrate was concentrated. The crude product was dissolved in dichloromethane (40 mL) and washed sequentially with 0.5M HCl (40 mL) and saturated NaHCO₃ (40 mL). The organic phase was dried over MgSO₄, filtered and the solvent was removed *in vacuo* to yield a pale yellow oil. Hexane was added to the crude product and the resulting white precipitate was filtered off. The solvent was once again removed *in vacuo* and the resulting oil was purified by flash column chromatography on silica eluting with hexane/ethyl acetate (95:5) (R_f = 0.18) to afford 1.13 g (80%) of **5.1** as a pale yellow oil. IR (ATR) ν/cm⁻¹: 3611, 2960, 1716, 1433, ¹H NMR (400 MHz/CDCl₃)/ppm, δ = 0.89 (m, 6H, -CH₃), 1.28-1.35 (m, 8H, -CH₂), 1.43 (s, 18H, -CH₃ *tert*-butyl), 1.57 (m, 1H, -CH), 2.61 (t, 2H, J=8.0 Hz, -CH₂), 2.87 (t, 2H, J=8.0 Hz, -CH₂), 4.00 (m, 2H, -CH₂), 5.07 (s, 1H, -OH), 6.99 (s, 2H, -CH aromatic); ¹³C NMR (100 MHz/CDCl₃)/ppm, δ = 11.0, 14.1, 23.0, 23.8, 28.9, 30.3, 30.4, 31.0, 34.3, 36.5, 38.7, 66.9, 124.8, 131.2, 135.9, 152.2, 173.5. Found [M+H]⁺ (C₂₅H₄₂O₃) m/z = 391.3211 (Calc. 391.3213).

5.5 References

- 1 F. Shahidi and P. K. Wanasundara, *Crit. Rev. Food Sci. Nutr.*, 1992, **32**, 67–103.
- 2 E. N. Frankel, *Prog. Lipid Res.*, 1984, **23**, 197–221.
- 3 J. Lee, N. Koo and D. B. Min, *Compr. Rev. Food Sci. Food Saf.*, 2004, **3**, 21–33.
- 4 W. Dröge, *Physiol. Rev.*, 2002, **82**, 47–95.
- 5 E. Bright-See, *Semin. Oncol.*, 1983, **10**, 294–298.
- 6 G. Block, *Nutr. Rev.*, 1992, **50**, 207–213.
- 7 M. G. Bourassa and J. Tardif, *Antioxidants and Cardiovascular Disease*, Springer, New York, 2nd edn., 2006.
- 8 R. Kahl and H. Kappus, *Z. Leb. Unters Forsch*, 1993, **196**, 329–338.
- 9 S. Dudonne, X. Vitrac, P. Coutiere, M. Woillez and J.-M. Merillon, *J. Agric. Food Chem.*, 2009, **57**, 1768–1774.
- 10 S. De Oliveira, G. A. De Souza, C. R. Eckert, T. A. Silva, E. S. Sobral, O. A. Fávero, M. J. P. Ferreira, P. Romoff and W. J. Baader, *Quim. Nova*, 2014, **37**, 497–503.
- 11 P. Molyneux, *Songklanakarini J. Sci. Technol.*, 2004, **26**, 211–219.
- 12 A. Floegel, D. O. Kim, S. J. Chung, S. I. Koo and O. K. Chun, *J. Food Compos. Anal.*, 2011, **24**, 1043–1048.
- 13 D. Huang, B. Ou, M. Hampsch-Woodill, J. A. Flanagan and R. L. Prior, *J. Agric. Food Chem.*, 2002, **50**, 4437–4444.
- 14 K. K. Adom and H. L. Rui, *J. Agric. Food Chem.*, 2005, **53**, 6572–6580.
- 15 R. Prior, X. Wu and K. Schaich, *J. Agric. Food Chem.*, 2005, 4290–4302.
- 16 J. Moore, J. J. Yin and L. Yu, *J. Agric. Food Chem.*, 2006, **54**, 617–626.
- 17 Z. Cheng, J. Moore and L. Yu, *J. Agric. Food Chem.*, 2006, **54**, 7429–7436.
- 18 M. Antolovich, P. D. Prenzler, E. Patsalides, S. McDonald and K. Robards, *Analyst*, 2002, **127**, 183–198.
- 19 M. B. Arnao, *Trends Food Sci. Technol.*, 2001, **11**, 419–421.
- 20 R. Re, N. Pellegrini, A. Proteggente, A. Pannala, M. Yang and C. Rice-Evans, *Free Radic. Biol. Med.*, 1999, **26**, 1231–1237.

- 21 N. J. Miller, C. Rice-Evans, M. Davies, V. Gopinathan and A. Milner, *Clin. Sci.*, 1993, **84**, 407–412.
- 22 B. S. Wolfenden and R. L. Willson, *J. Chem. Soc. Perkin Trans. II*, 1982, 805–812.
- 23 M. Blois, *Nature*, 1958, **181**, 1199–1200.
- 24 W. Brand-Williams, M. E. Cuvelier and C. Berset, *LWT - Food Sci. Technol.*, 1995, **28**, 25–30.
- 25 K. Shimada, K. Fujikawa, K. Yahara and T. Nakamura, *J. Agric. Food Chem.*, 1992, **40**, 945–948.
- 26 G. C. Yen and P. D. Duh, *J. Agric. Food Chem.*, 1994, **42**, 629–632.
- 27 Y. Chen, M. Wang, R. T. Rosen and C. Ho, *J. Agric. Food Chem.*, 1999, **47**, 2226–2228.
- 28 A. Von Gadow, E. Joubert and C. F. Hansmann, *J. Agric. Food Chem.*, 1997, **45**, 632–638.
- 29 C. Sánchez-Moreno, J. A. Larrauri and F. Saura-Calixto, *Food Res. Int.*, 1999, **32**, 407–412.
- 30 O. P. Sharma and T. K. Bhat, *Food Chem.*, 2009, **113**, 1202–1205.
- 31 N. Mimica-Dukic, B. Bozin, M. Sokovic and N. Simin, *J. Agric. Food Chem.*, 2004, **52**, 2485–2489.
- 32 A. Karioti, D. Hadjipavlou-Litina, M. L. K. Mensah, T. C. Fleischer and H. Skaltsa, *J. Agric. Food Chem.*, 2004, **52**, 8094–8098.
- 33 P. C. Eklund, O. K. Långvik, J. P. Wärnå, T. O. Salmi, S. M. Willför and R. E. Sjöholm, *Org. Biomol. Chem.*, 2005, **3**, 3336–3347.
- 34 Y. Chen, Y. Sugiyama, N. Abe, R. Kuruto-Niwa, R. Nozawa and A. Hirota, *Biosci. Biotechnol. Biochem.*, 2005, **69**, 999–1006.
- 35 R. Govindarajan, S. Rastogi, M. Vijayakumar, A. Shirwaikar, A. K. S. Rawat, S. Mehrotra and P. Pushpangadan, *Biol. Pharm. Bull.*, 2003, **26**, 1424–1427.
- 36 M. Kano, T. Takayanagi, K. Harada, K. Makino and F. Ishikawa, *Biosci. Biotechnol. Biochem.*, 2005, **69**, 979–988.
- 37 S. Saito, Y. Okamoto and J. Kawabata, *Biosci. Biotechnol. Biochem.*, 2004, **68**, 1221–1227.
- 38 B. Tepe, M. Sokmen, H. Askin Akpulat and A. Sokmen, *Food Chem.*, 2005, **90**, 685–689.

- 39 M. H. Alma, A. Mavi, A. Yildirim, M. Digrak and T. Hirata, *Biol. Pharm. Bull.*, 2003, **26**, 1725–1729.
- 40 H. Kim, F. Chen, C. Wu, X. Wang, H. Y. Chung and Z. Jin, *J. Agric. Food Chem.*, 2004, **52**, 2849–2854.
- 41 G. Cochrac and S. Rizvi, in *Fuels and Lubricants Handbook: Technology, properties, performance and testing.*, eds. S. Westbrook and R. Shah, ASTM International, 2003, pp. 787–824.
- 42 G. H. Ayres, *Anal. Chem.*, 1949, **21**, 652–657.
- 43 E. Martinot, *Renewables 2005 Global Status Report*, Worldwatch Institute, REN21 Renewable Energy Policy Network 2005, Washington DC, 2005.
- 44 M. J. P. Comuñas, X. Paredes, F. M. Gaciño, J. Fernández, J. P. Bazile, C. Boned, J. L. Daridon, G. Galliero, J. Pauly, K. R. Harris, M. J. Assael and S. K. Mylona, *J. Phys. Chem. Ref. Data*, 2013, **42**, 1–6.
- 45 V. Thavasi, R. Phillip, A. Bettens and L. P. Leong, *J. Phys. Chem.*, 2009, **113**, 3068–3077.
- 46 P. MacFaul, K. U. Ingold and J. Luszytk, *J. Org. Chem.*, 1996, **61**, 1316–1321.
- 47 G. Litwinienko and K. U. Ingold, *Acc. Chem. Res.*, 2007, **40**, 222–230.
- 48 G. Litwinienko and K. U. Ingold, *J. Org. Chem.*, 2004, **69**, 5888–5896.
- 49 G. Litwinienko and K. U. Ingold, *J. Org. Chem.*, 2003, **68**, 3433–3438.
- 50 M. Musialik and G. Litwinienko, *Org. Lett.*, 2005, **7**, 4951–4954.
- 51 K. I. Priyadarsini, D. K. Maity, G. H. Naik, M. S. Kumar, M. K. Unnikrishnan, J. G. Satav and H. Mohan, *Free Radic. Biol. Med.*, 2003, **35**, 475–484.
- 52 M. Foti, C. Daquino and C. Geraci, *J. Org. Chem.*, 2004, 2309–2314.
- 53 M. C. Foti, L. R. C. Barclay and K. U. Ingold, *J. Am. Chem. Soc.*, 2002, **124**, 12881–12888.
- 54 L. Valgimigli, J. T. Banks, K. U. Ingold and J. Luszytk, *J. Am. Chem. Soc.*, 1995, **117**, 9966–9971.
- 55 L. Valgimigli, J. T. Banks, J. Luszytk and K. U. Ingold, *J. Org. Chem.*, 1999, **64**, 3381–3383.
- 56 D. D. Perrin, B. Dempsey and B. D. Serjeant, *pKa Prediction for Organic Acids and Bases*, Chapman and Hall, Netherlands, 1981.

- 57 D. Avila, K. U. Ingold and J. Lusztyk, *J. Am. Chem. Soc.*, 1995, **117**, 2929–2930.
- 58 S. L. Mayo, B. D. Olafson and W. A. Goddard III, *J. Phys. Chem.*, 1990, **94**, 8897–8909.

Chapter 6

Conclusions and Future Perspectives

6.1 Conclusions

Oxidation is a detrimental process which has a profound effect on hydrocarbon based materials. This is particularly problematic in the automotive industry where fuels and lubricants are subjected to harsh conditions which accelerate the oxidative pathways leading to ineffective combustion and engine protection. Antioxidants, such as sterically hindered phenols and diphenylamine derivatives, are known to interrupt oxidation processes by predominantly reacting with radical species. Numerous small molecule antioxidants have been reported in the literature (see **Chapter 1**), however, these are susceptible to volatilisation as a result of the high temperatures experienced within an engine environment. Antioxidant immobilisation has hence emerged as a suitable route to introducing higher molecular weights and improve thermal stabilities. This study focussed on the use of dendritic architectures with the aim of achieving high molecular weights with a high degree of functionality while also maintaining good solubility within the hydrocarbon based material.

The first series of dendritic architectures saw the use of the AB₂ monomer *bis*(MPA) to synthesise a series of antioxidant functionalised polyester dendrons. The first and second generation polyester dendrons (**2.9** and **2.10**) were synthesised with molecular weights of 767 and 1520 with four and eight phenolic peripheral functionalities, respectively. Thermogravimetric analysis of **2.9** and **2.10** revealed thermal stabilities that were far superior (by an improvement of greater than 200 °C) to the industrial standard BHT which has a molecular weight of 220 with only one phenolic functionality. The incorporation of a 2-ethylhexanol solubilising unit also promoted good solubility of the polyester dendrons **2.9** and **2.10** in a base oil. When blended into the base oil at 0.5% w/w an impressive 229% increase in oxidative stability was observed in comparison to two current commercial antioxidants, Irganox L135 and Irganox L57. Once again, these commercial antioxidants possessed low molecular weights with only one active functionality. It was therefore revealed that dendritic macromolecules are suitable for

use in antioxidant immobilisation whereby the thermal and oxidative stabilities were improved dramatically while still maintaining good solubility in the base oil.

Alternative functional core monomers to *bis*(MPA) were investigated with a focus on low cost and commercial availability. Hence, glycerol and triethanolamine (TREN) were targeted and subsequently functionalised with antioxidant moieties and solubilising alkyl chains to yield a further series of first generation polyester antioxidants. The series of glycerol-based antioxidants revealed some interesting structure-activity relationships and highlighted the need to consider a balance between both solubility and functionality when designing new antioxidant macromolecules. A series of nitrogen core monomers, based on triethanolamine, were also investigated and some excellent oxidation induction times in the region of *ca.* 12-15 minutes were revealed, however solubility in the lubricant base oil proved to be an issue. To overcome the solubility issues, a solubilising unit was introduced and the diphenols **3.9** and **3.11** were synthesised and again revealed oxidation times in the region of *ca.* 10-12 minutes. It has been revealed that solubility is just as important as antioxidant functionality when considering the design of new antioxidant macromolecules. In addition, the oxidation induction times were within the same region whether the central core was *bis*(MPA), glycerol or a triethanolamine derivative. It was therefore concluded that the central core monomer does not necessarily contribute to the antioxidant capabilities but is instead a facilitator to increase the molecular weight through branching and hence achieve reduced volatility.

The hindered phenolic polyester dendrons revealed some excellent thermal and oxidative stabilities, however it was proposed that more enhanced properties could be targeted by considering the synergistic relationship between hindered phenols and diphenylamines. It was envisaged that by incorporating a diphenylamine derivative into the same branching unit as the hindered phenol, synergistic antioxidant properties could be achieved. While data has been reported on improving the individual antioxidant capabilities of hindered phenols and diphenylamines through structural variations, very little research, if any, has been reported on the inclusion of both functional groups within the same compound. This study was therefore the first of its kind and a series of novel mixed amine-phenolic antioxidants were synthesised and analysed for their oxidative stability properties. The relationship between the location of the antioxidant amine residue and the link to the branching unit proved to be crucial in these studies. It was

revealed that *meta* and *para* substitution on the diphenylamine provided the best oxidative stability properties and these properties were further enhanced through the inclusion of methyl or ethyl spacers between the diphenylamine and the bis(MPA) central core. It was observed that *meta* substitution with an ethyl spacer provided the longest oxidation induction time of *ca.* 23 minutes, which was *ca.* 8 minutes longer than the 1:1 blend of Irganox L135 and Irganox L57. It was proposed that electron donation into the aromatic ring was potentially allowing better stabilisation of the aminyl radical, generated from the initial hydrogen abstraction. Computational modelling also revealed that the combination of *meta* substitution and an ethyl spacer allowed close contact of both amine and phenol functionalities suggesting that the regeneration of the diphenylamine by the phenol could be enhanced using these structural combinations.

With the synthesis of new phenolic antioxidants comes the need for an understanding of the structural and functional characteristics to allow successful development of new antioxidants in the future. The literature has highlighted numerous studies into the properties of hindered phenols, however the analysis procedures reported do not often correlate hence comparison of results is problematic. A radical scavenging assay, using the stable free radical DPPH, was therefore investigated with the aim to understand structure-activity relationships of new sterically hindered phenolic antioxidants. Using this assay, both the kinetic profiles and stoichiometry of the radical scavenging reactions of sterically hindered phenols were investigated. The radical scavenging reactions in ethanol revealed a 'slow' kinetic profile for the following antioxidants: BHT, Irganox L135, first generation (2.9) and second generation (2.10) phenols. This kinetic data is in agreement with the report of Brand-Williams and co-workers. When the solvent system was changed from ethanol to squalane, a significant shift in the kinetic profile of the mono-phenols BHT and Irganox L135 was observed whereby a steady state was achieved in less than 10 minutes when compared to over 60 minutes in ethanol. The kinetic profiles of the first generation (2.9) and second generation (2.10) polyphenols were revealed to be slower in squalane than in ethanol. Analysis of the literature highlighted an alternative mechanistic pathway for hydrogen abstraction when alcoholic solvents were used which resulted in a faster than predicted rate of reaction. Additional factors were considered when analysing the polyphenolic antioxidants such as increased bulkiness and steric hindrance surrounding the radical scavenging sites within the molecules. A quantitative analysis, termed EC₅₀, was carried out to determine the stoichiometry of the reaction

between the antioxidants and the radicals. The number of DPPH radicals scavenged per mole of antioxidant was calculated for a series of phenolic and aminic antioxidants and an overriding limitation of using a bulky radical was revealed. Antioxidants known to perform well in typical lubricant oxidation tests exhibited poor radical scavenging capabilities in this assay. In addition, aromatic amine chemistries were not suitable for this test as a result of the activation energy required for the radical scavenging reaction to occur. The time-scavenging profile for the aromatic amine Irganox L57 revealed, at 25 °C, less than 50% scavenging was achieved whereas at higher temperatures this percentage was increased. The overall outcome of the development of this assay was that there were too many limitations regarding mechanistic pathways coupled with complex solvent effects for it to be used as a reliable study for new antioxidants. If the results are interpreted with caution and in conjunction with more in depth kinetic studies, mechanistic pathways of phenolic antioxidants could be determined with the potential to guide a more directed design of new antioxidants.

In summary, a series of novel dendritic antioxidants have been synthesised and excellent thermal and oxidative stabilities were revealed. In addition, structure-activity relationships have been probed and the use of a radical scavenging assay revealed the complexity of the mechanisms involved in antioxidant chemistry. Further studies could be carried out in the future to improve upon the results revealed in this research.

6.2 Future Perspectives

Whilst advances have been made in the development of dendritic antioxidants, this still remains a relatively 'young' area of research and there are considerable opportunities for further improvements. Within the scope of this thesis, the first area to address would be to further improve on the solubility of the branched structures described. It was revealed that the third generation polyester dendron in **Chapter 2** was not soluble in the hydrocarbon medium and it was proposed that a larger ratio of solubilising units to antioxidant functionality would be required. In addition, it was revealed that even though an antioxidant may be soluble in the base oil it may not be completely disperse, hence, the oxidative stability was affected. This was observed in particular for the glycerol series of first generation polyesters in **Chapter 3** whereby the diphenol with one solubilising unit revealed a greater oxidation induction time than the triphenol without a solubilising unit. Therefore, it was proposed that the polyester dendrons would further benefit from

a greater number of solubilising units. With a focus on the first and second generation polyester dendrons of **Chapter 2**, there are two possible approaches to improved solubility that could be effective. The first is to introduce a longer, branched hydrocarbon chain such as a squalane-based unit. It was revealed in **Chapter 4** that the lack of branching from the butyl chain on the diphenylamine actually promoted stacking and hence solubility was effected. Alternatively, a second approach would be to investigate heterofunctional dendrimers whereby the number of solubilising units can match the number of active phenolic functionalities. The polyester structure shown in **Figure 6.1** could be a sensible starting structure.

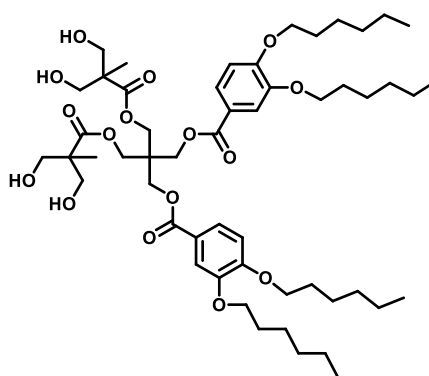


Figure 6.1 Example of a 'Janus' dendrimer reported by Rissanen and co-workers bearing bis(MPA) and 3,4-bis-hexyloxybenzoic ester terminal groups.^[1,2]

An example of this approach has been observed for dendritic macromolecules which are used in drug delivery. Typically, the solubility of these macromolecules in aqueous media has often hindered their ability to perform in this complex area of chemistry. The literature has revealed a number of adapted dendritic structures which have incorporated hydrophilic solubilising units such as polyethylene glycol or charged chain ends.^[3-5] The enhanced solubility of the dendritic macromolecules has allowed these structures to be a viable option for targeted drug delivery and many advances in this area have been observed in recent years.^[6] It is therefore proposed that if the solubility of the first, second and third generation polyphenols from this project was improved, superior performance characteristics may be achieved. It would also be interesting to observe whether there is a benefit for having a greater number of phenolic functionalities on the same compound because the results from **Chapter 2** have indicated that there was not a large increase in oxidation induction time between the first and second generation.

Another area of research would be to investigate the optimum synergistic ratio between hindered phenols and diphenylamines. In the present study a ratio of 1:1 was investigated, however it is known from the literature that during the radical scavenging process the diphenylamine is regenerated by the phenol and is only consumed once the phenol functionalities are also expended. It is therefore expected that the optimum synergistic ratio would be to have a greater number of phenolic functionalities in comparison to diphenylamine functionalities. This could be achieved through extending the structure from the first generation to the second or third as revealed in **Figure 6.2**.

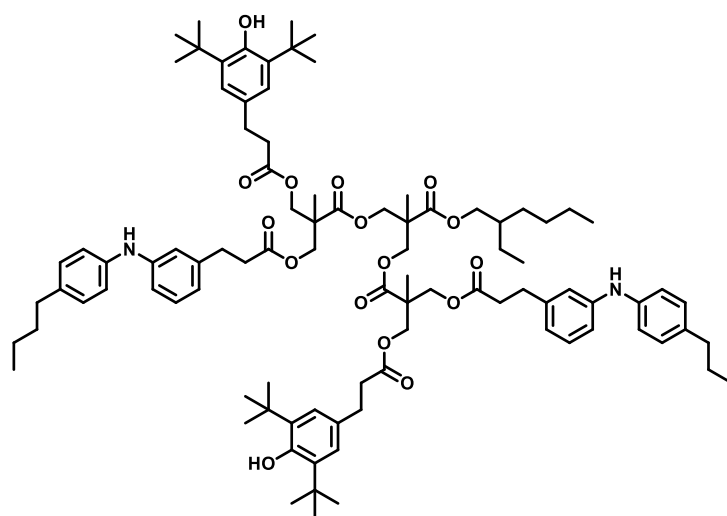


Figure 6.2 Example of a second generation mixed amine-phenol polyester dendron.

Alternatively, heterofunctional dendrimers could also be used and it would be interesting to see whether having phenolic functionalities on one side of the core and diphenylamines on the other has any improved effect. Considering the results so far, however, it would be proposed that the separation of the active functionalities onto opposite sides of the core would potentially not show any improved effect as the contact distances would be too great.

Finally, **Chapter 5** revealed the complexity of the radical scavenging mechanism and it was found that the DPPH radical scavenging assay did not provide enough information to fully understand the structure-activity relationships of phenolic antioxidants. Instead a number of assays and data points would need to be considered to reach a conclusion over structure-activity relationships. It would therefore appear to be beneficial to attempt to correlate the data obtained from a range of studies and assays to build a multidisciplinary database of phenolic antioxidant properties. Much like in the area of drug design, a library

of data could be searched to find a 'hit' for a particular function. For example, you may require a phenolic antioxidant with a high molecular weight that is suitable for use in lipids and can perform at high temperatures. These parameters could be searched and a series of possible phenolic antioxidants would be returned or a set of structural characteristics could be suggested to guide the design of a new phenolic antioxidant. Many iterations of phenolic antioxidants can be generated, however, targeted design cannot be achieved without a solid understanding of structure-activity relationships and the mechanisms of action.

6.3 References

- 1 T. Tuuttila, M. Lahtinen, N. Kuuloja, J. Huuskonen and K. Rissanen, *Thermochim. Acta*, 2010, **497**, 101–108.
- 2 T. Tuuttila, M. Lahtinen, J. Huuskonen and K. Rissanen, *Thermochim. Acta*, 2010, **497**, 109–116.
- 3 A. K. Patri, I. J. Majoros and J. R. Baker, *Curr. Opin. Chem. Biol.*, 2002, **6**, 466–471.
- 4 M. Liu and J. M. J. Fréchet, *Pharm. Sci. Technolo. Today*, 1999, **2**, 393–401.
- 5 E. R. Gillies and J. M. J. Fréchet, *Drug Discov. Today*, 2005, **10**, 35–43.
- 6 J. Bugno, H. Hsu and S. Hong, *Biomater. Sci.*, 2015, **3**, 1025–1034.